The Control and Manipulation of Angiogenesis in the Primate Corpus Luteum

Sarah Dickson
BSc (Hons) MSc

Doctor of Philosophy
University of Edinburgh
October 2000

Declaration

I hereby declare that this thesis has been composed by myself and is my own work. Any contribution of others has been fully acknowledged. The work described in this thesis has not been submitted in full or in part for any other degree, diploma or professional qualification.

Sarah Dickson
October 2000

Dedication

For Mama,

Thanks for your support and encouragement.

Contents

Figures and Tables

Chapter 4

Chapter 5

Chapter 6

Chapter 7

Chapter 8

Abbreviations

3β HSD	3β-hydroxysteroid dehydrogenase
α-SMA	α-smooth muscle actin
ABC	avidin biotin complex
Ang-1	angiopoietin-1
Ang-2	angiopoietn-2
ANOVA	analysis of variance
ANSA	8-anilino-1-naptha-lenesulfonic-acid
APAAP	alkaline phosphatase-anti-alkaline phosphatase
aFGF	acidic fibroblastic growth factor
bFGF	basic fibroblastic growth factor
bp	base pair
BrdU	bromodeoxyuridine
BSA	bovine serum albumin
CAM	chorio-allantoic membrane
CG	chorionic gonadotropin
cpm	counts per minute
cAMP	cyclic adenosine monophosphate
cDNA	complementary deoxyribonucleic acid
CD31	cluster differentiation factor 31
CD34	cluster differentiation factor 34
Cx	connexin
DAB	diaminobenzadine
DEPC	diethyl pyrocarbonate
DNA	deoxyribonucleic acid
DNase	deoxyribonuclease
DTT	dithiothreitol
ECM	extracellular matrix
FAM	6-carboxyfluoroscein
FITC	fluorescein isothyocyanate
Flt-1	*fms*-like tyrosin kinase-1
FSH	follicle stimulating hormone
GnRH	gonadotropin releasing hormone
hCG	human chorionic gonadotropin
H and E	haematoxylin and eosin
HDL	high density lipoprotein
HRP	horse radish peroxidase

i.m.	intramuscular
i.v.	intravenous
IGF	insulin-like growth factor
IGFBP	insulin-like growth factor binding protein
IgG	immunoglobulin G
kDa	kilodalton
KDR	kinase insert domain receptor
HUVEC	human umbilical vein endothelial cells
LDL	low density lipoprotein
LH	luteinising hormone
LMP	last menstrual period
MMP	matrix metalloproteinase
MRC HRSU	Medical Research Council Human Reproductive Sciences Unit
mRNA	messenger ribonucleic acid
NBT	nitro blue tetrazolium
NGS	normal goat serum
NRS	normal rabbit serum
NSS	normal swine serum
rNTP	ribonucleotide triphosphate
$P450_{arom}$	cytochrome P450, aromatase
$P450_{c17}$	cytochrome P450, 17α-hydroxylase/C_{17-20} lyase
$P450_{scc}$	cytochrome P450, side chain cleavage
PBS	phosphate-buffered saline
PCNA	proliferating cell nuclear antigen
PCR	polymerase chain reaction
PDGF	platelet derived growth factor
PECAM-1	platelet endothelial cell adhesion molecule-1
PFA	paraformaldehyde
PG	prostaglandin
PI	proliferation index
PlGF	placental growth factor
PLSD	protected least significant difference
PMS	post-menopausal serum
PMSG	pregnant mares serum gonadotropin
rATP	riboadenosine triphosphate
rCTP	ribocytosine triphosphate
rGTP	riboguanine triphosphate

RIA	radioimmunoassay
RNA	ribonucleic acid
RNase	ribonuclease
ROX	6-caroboxy X rhodamine
RT	reverse transcription
S phase	DNA synthesis phase
SEM	standard error of the mean
StAR	steroidogenic acute regulatory protein
TBS	tris-buffered saline
TEA	triethanolamine
TGFβ	transforming growth factor β
Tie	tyrosine kinase with immunoglobulin and epidermal growth factor homology domains
TIMP	tissue inhibitor of metalloproteinases
TRITC	tetra rhodamine isothyocyanate
UTP	uridine 5`triphosphate
UV	ultra violet
VEGF	vascular endothelial growth factor
von Willebrand factor	von Willebrand factor VIII-related antigen

Publications and Presentations Relating to this Thesis

Publications in peer reviewed journals

Fraser, HM., **Dickson, SE.,** Morris, KD., Erickson, GF. and Lunn, SF. (1999) The effect of the angiogenesis inhibitor TNP-470 on luteal establishment and function in the primate. *Hum Reprod,* 14: 2054-2060

Fraser, HM., **Dickson, SE.,** Lunn, SF., Wulff, C., Morris, KD., Carroll, V. and Bicknell, R. (2000) Suppression of luteal angiogenesis in the primate after neutralisation of vascular endothelial cell growth factor. *Endocrinology*, 141: 995-1000

Dickson, SE. and Fraser, HM. (2000) Inhibition of early luteal angiogenesis by gonadotropin-releasing hormone antagonist treatment in the primate. *J Clin Endocrinol Metab*, 85: 2339-2344

Dickson, SE., Bicknell, R. and Fraser, HM. (2001) Mid-luteal angiogenesis and function in the primate is dependent on VEGF. *J Endocrino*l, 168: 409-416

Wulff, C, **Dickson, SE.,** Duncan, WC and Fraser, HF. (2001) Angiogenesis in the human corpus luteum: Simulated early pregnancy by hCG treatment is associated with both angiogenesis and vessel stabilisation. Submitted to Human Reproduction.

Oral presentations

Dickson, SE. and Fraser, HM (July-August, 1999*)* Manipulation of angiogenesis in the primate corpus luteum. *32nd Annual Meeting for the Society for the Study of Reproduction,* Washington State University, Washington, USA.

Fraser, HM., **Dickson, SE.,** Lunn, SF., Wulff, C. and Bicknell, R. (March, 2000) Angiogenesis in the Ovary. Symposium Lecture at *19th Joint Meeting of the British Endocrine Society,* Birmingham, UK.

Poster presentations

Fraser, HM., **Dickson, SE.** and Lunn, SF., (April, 1998) The effect of the anti-angiogenic agent TNP-470 on luteal establishment and function in the macaque and marmoset. *International Business Communications,* Boston, USA.

Fraser, HM., **Dickson, SE.,** Morris, KD., Lunn, SF., Carroll, V. and Bicknell, R. (June, 1999) Suppression of luteal angiogenesis and pregnancy by neutralisation of VEGF: new prospects for manipulation of fertility. *81st Annual Meeting of the Endocrine Society*, San Diego, USA.

Fraser, HM., **Dickson, SE.,** Lunn, SF., Wulff, C. and Bicknell, R. (March, 2000) Manipulation of physiological angiogenesis: targeting the reproductive system in primates. *Keystone Symposia*, Experimental and Clinical Regulation of Angiogenesis, Salt Lake City, Utah, USA.

Acknowledgements

Dr Hamish Fraser warrants a special acknowledgement and thank you for all his help over the last three years. His expertise in the primate corpus luteum and *in vivo* experimentation is second to none, and has made this work possible. I am most grateful for his continual input and ideas for the thesis, which I couldn't have completed without him. Other members of the group have also been invaluable. Pawlina Largue taught me all the laboratory techniques used in this thesis and offered her assistance even after she'd left the group. Helen Wilson and Dr Christine Wulff have helped me considerably with their expertise in *in situ* hybridisation and immunocytochemistry, especially when time was running out. Also, Dr Christine Wulff and Dr Steve Lunn with their extensive knowledge of the primate corpus luteum have made numerous intellectual contributions.

The work of Keith Morris and the rest of the staff at the Primate Centre has been exceptional. Without them, for the general care of the marmoset colony, the administration of treatments and collection of tissue, this project could not have taken place. Their work has been paramount to the smooth running of this project and I thank them. Also, the expertise of Ian Swantson and Fiona Pitt in the assay lab has been invaluable for monitoring marmoset ovulatory cycles and the accurate dating of tissue.

Mike Miller and Sheila McPherson in the Histology department have been wonderful, undertaking all tissue processing, assisting with immunocytochemistry and image analysis, and giving their continual support throughout the last three years, thank you. Also, Dr Julie Brooks and Sheila Boddy deserve a special mention for their assistance with the Real Time quantitative RT-PCR technique, and Julie for her help with statistical analysis.

I also acknowledge Tom McFetters and Ted Pinner for the preparation of slides and assistance with graphics, which have always been of the highest quality and completed at such short notice. Similarly, the work done by the administration department has been invaluable. In particular Carol Adam and Jane Grindley have been very efficient in getting the job done, especially when it comes to understanding the financial hardships of a PhD student.

On a more personal level, I would like to acknowledge Pawlina again, not only for her technical assistance, but for being a very special friend and helping me through the last three years, it would have been impossible without you, thanks P. Also, Pawlina, Sheila, Julie and Rodney for the interesting coffee room banter which made the time slip by, 20 minutes was never long enough. Annette, Bev and Miriam, have been great, making the SSR conference in the States such a laugh and very interesting indeed, for being complete party animals and for their friendship over the last three years. Cheers

guys. Also to everyone else who I socialised with from work, especially Gillian, back in the days when we could drink 5 pints on an empty stomach and feel fine the next day. It was great to spend the last three years with such similar minded alcoholics!

Finally, a very special mention goes to Ruth, for being such a close friend, for introducing me to tequila and for being there nursing me through the breakdowns in the difficult early times. Breakfast cereal in bed never fails. Cheers Ruth. And last but not least to Stan, who has been an absolute star, giving his loving support (and financial help) throughout. Thank you.

Abstract of Thesis

The corpus luteum is formed from the preovulatory follicle after ovulation and its main function is the secretion of progesterone which is essential for the establishment of pregnancy. Growth of the corpus luteum is associated with extensive vascular remodelling, so that by the mid-luteal phase every steroidogenic cell is adjacent to a capillary for optimal synthesis and secretion of progesterone. In the non-fertile cycle luteal vascular regression takes place and progesterone production falls. If conception occurs the corpus luteum is rescued and continues to produce progesterone. The corpus luteum provides a unique example of tightly controlled physiological angiogenesis. Little is known about the effect of inhibition of physiological angiogenesis that occurs in female reproductive tissues. Elucidation of the process of luteal angiogenesis may provide new insights into tumour therapy and treatment of infertility, and offer a novel approach to contraception research. Previous research focused on angiogenesis in the non-primate ovary but the mechanisms that regulate luteal function in primates are markedly different, therefore the marmoset monkey, supplemented with archived human corpora lutea, was used for the research described in this thesis.

Angiogenesis is a dynamic process of endothelial cell proliferation and capillary tubule formation, controlled primarily by vascular endothelial cell growth factor (VEGF); and capillary stabilisation by the association of pericytes. *In vivo* luteal angiogenesis was assessed by measuring these parameters in luteal sections by quantitative immunocytochemistry. It was established that 1) quantification of cell proliferation by bromodeoxyuridine administration to label DNA during the S phase of the cell cycle was a robust and reproducible technique; 2) over 80% of proliferating cells in marmoset corpora lutea were endothelial cells; and 3) quantification of these parameters in one luteal section reflected the angiogenic activity of the whole corpus luteum. In the primate, early luteal development was associated with intense angiogenesis, expression of VEGF and the growth of a stable microvascular network. In the mid-luteal mature gland angiogenesis was ongoing but at a reduced level, VEGF expression remained high and a full microvascular network had been established containing both stable microvessels and small immature capillaries, optimal for maximal progesterone production and secretion. In the late corpus luteum, endothelial cell proliferation and VEGF expression declined, there were signs of immature vessel regression and progesterone levels decreased markedly. Human chorionic gonadotropin administered to women from the mid-luteal phase to rescue the corpus luteum, was associated with increased angiogenesis and VEGF production, and stabilisation of newly formed vessels.

In the marmoset luteal angiogenesis was manipulated by the administration of various putative angiogenesis inhibitors specifically targeting the intense angiogenesis in the early luteal phase and mid-luteal ongoing angiogenesis. Luteal function was assessed by measuring plasma progesterone. Firstly, in two studies marmosets were treated with a GnRH antagonist to analyse the control of luteal angiogenesis by the major luteotropic factor, LH in the early and mid-luteal phases. Withdrawal of LH had a marked inhibitory effect on the high level of endothelial cell proliferation in the early luteal phase but did not disturb the ongoing mid-luteal phase angiogenesis. Lutein cell morphology was severely disrupted after treatment at both stages, preventing the production and secretion of progesterone. Secondly, the effects of the angiogenesis inhibitor, TNP-470, shown to inhibit pregnancy in the mouse, was examined. This failed to affect endothelial cell proliferation or development of the microvasculature, which was confirmed by normal plasma progesterone concentrations, emphasising the need for caution in extrapolating results from the rodent. Finally, VEGF was immunoneutralised in three separate regimes of treatment, in the early, from early to mid-, and specifically in the mid-luteal phase. Treatment suppressed proliferation in the early luteal phase and subsequently prevented formation of the mid-luteal microvascular network. The ongoing angiogenesis of the mid-corpus luteum was shown to be VEGF dependent, and VEGF withdrawal affected pericyte recruitment at all stages.

To explore the molecular control of luteal angiogenesis, expression of the angiopoietins and their receptor, Tie 2 were analysed in association with expression of VEGF and its receptors in the human, using quantitative RT-PCR. The early luteal phase was associated with peak expression of all factors with slight increases in mRNAs for Ang-2 in the late corpus luteum and VEGF in the rescued.

This study highlights the importance of researching reproductive angiogenesis *in vivo* in the primate. It demonstrates that luteal angiogenesis is dependent upon LH stimulation of the lutein cells during the early luteal phase. The specific angiogenic factor having a major role in stimulating luteal angiogenesis has been demonstrated to be VEGF. Suppression of VEGF and luteal angiogenesis results in profound inhibitory effects on luteal function *in vivo*. Since physiological angiogenesis occurs exclusively in reproductive tissues in the healthy adult, manipulation of angiogenesis may have important clinical implications in the treatment of infertility, in which angiogenesis is lacking, or for the development of a new approach to post-ovulatory fertility control based upon suppression of angiogenesis.

Chapter 1

Introduction

1.1 Overview

Angiogenesis is a process of new blood vessel growth that depends on the sprouting and proliferation of capillaries from pre-existing vessels. In the adult, capillary growth occurs rarely and is largely associated with repair of damaged tissues and pathological conditions such as tumour growth, diabetic retinopathy, psoriasis and rheumatoid arthritis. Physiological angiogenesis is almost unique to the female reproductive system, the ovary, uterus and placenta. In the ovary, cyclic angiogenesis occurs in relation to follicular development and corpus luteum formation. It is the regulation of angiogenesis in the primate corpus luteum that is the subject of this thesis.

The corpus luteum is formed from the dominant follicle after ovulation of the oocyte. Its predominant role is in the production of progesterone which alters the morphology and function of the uterine endometrium, preparing it for implantation of the developing blastocyst. The luteal phase of the cycle is the time at which the corpus luteum is functionally active. The corpus luteum has a functional lifespan or luteal phase of approximately 14 days (human), or 20 days (marmoset monkey), and the synthetic capacity of the corpus luteum changes during this period. Progesterone secretion rises in the early luteal phase to reach a maximum in the mid-luteal phase, and in the late luteal phase the functional integrity of the corpus luteum is lost and progesterone production falls. Withdrawal of progesterone results in endometrial destabilisation and menstruation in the human.

During corpus luteum formation, the avascular granulosa cell layer of the follicle becomes vascularised and the corpus luteum is transformed into a highly vascularised endocrine gland. Extensive angiogenesis occurs throughout development culminating in the formation of the large, solid, orange-red gland, typical of the mid-corpus luteum, with its high blood supply and lipid content. In the late luteal phase, in a process known as luteolysis, the newly formed vasculature regresses and progesterone production decreases resulting in the formation of a small relatively avascular, fibrous mass which may be apparent in subsequent cycles. In the presence of an implanting blastocyst, luteolysis is prevented by exposure to chorionic gonadotropin synthesised by the trophoblast of the developing pregnancy. The continued presence of progesterone maintains the uterine environment and prevents menstruation, allowing implantation and

early embryonic development. In a conceptual cycle, the corpus luteum is 'rescued' from luteolysis which is paramount for the establishment of pregnancy.

The factors potentially involved in the regulation of the intense vascularisation seen in the corpus luteum have been predicted largely from the effects of gene knock-out studies on embryonic vascular development in transgenic mice, from tumour angiogenesis analysis, and *in vitro* culture studies. However, direct research relating to *in vivo* luteal angiogenesis in the primate is lacking. It was proposed that since the corpus luteum is so dynamic, it has the potential to provide a unique model for studying the regulation of angiogenesis during the processes of growth, differentiation and regression of luteal tissue and vasculature. Such angiogenesis must be tightly regulated, being switched on and off over a brief time schedule measured in days. The understanding of the regulation of physiological angiogenesis in the corpus luteum is clinically relevant. Inadequate luteal function may be associated with decreased luteal vascularisation. Tumour growth and metastasis is highly dependent on angiogenic activity. Also, the ability to manipulate luteal angiogenesis and consequently luteal function could lead to novel approaches in post-ovulatory fertility control.

This chapter reviews the current understanding of 1) the control of the functional and structural lifespan of the corpus luteum and 2) the angiogenic process. It begins by discussing the ovarian cycle: the gonadotropin control of follicular growth, the mechanisms of ovulation, formation of the corpus luteum, luteolysis and the maternal recognition of pregnancy, emphasising the functional relevance of ovarian vascularisation. The control of angiogenesis is then discussed. This outlines the molecular mechanisms involved in the regulation of angiogenesis and highlights areas for further study. Finally, the clinical relevance of the study of *in vivo* angiogenesis in the primate corpus luteum will be discussed. This chapter serves as an introduction to the following experimental chapters which report studies of the quantification of luteal *in vivo* angiogenesis, its manipulation and molecular control in the primate.

1.2 Folliculogenesis

The corpus luteum is formed from ovulation of the preovulatory follicle, and developmental events that transpire during the follicular phase of the cycle are essential for the appropriate functioning of the corpus luteum, so any discussion concerning the corpus luteum must first consider follicular development. Similarly, the control of follicular development and corpus luteum function are dependent on gonadotropins from the anterior pituitary gland. The control of the secretion of these gonadotropins will be discussed at this stage. It is also worth noting that the majority of research into folliculogenesis and luteal function has been carried out in rodent and domestic livestock species. This review emphasises findings in women and primates and extrapolates from other species where necessary, however, the control of ovarian function between these species is likely to differ and caution is needed when extrapolating such research.

Folliculogenesis is the growth of ovarian follicles from primordial to preovulatory stages of development, in preparation for ovulation of the maturing oocyte. Primordial growth is not dependent upon pituitary gonadotropins. Further development becomes increasingly dependent on gonadotropin support and preovulatory follicular development occurs solely under the influence of cyclical levels of these hormones (reviewed by Zeleznik and Hillier, 1996). Morphologically, the primordial follicle has a single layer of epithelial cells surrounding a single oocyte (Block, 1951; Koering, 1969). At the preovulatory stage these cells have differentiated into cuboidal granulosa cells and divided numerous times forming multiple layers around the oocyte; a fluid-filled antrum has formed from granulosa cell secretions; and elongated theca cells, differentiated from stromal progenitor cells, become fully vascularised surrounding the avascular granulosa cell layer, separated by a basement membrane (Block, 1951; Koering, 1969). This is a highly sophisticated structure, the theca and granulosa cells of which co-ordinate to synthesise oestrogen, and, at the expense of other less mature follicles the preovulatory follicle directs its own survival. The process of folliculogenesis is outlined in Figure 1.1.

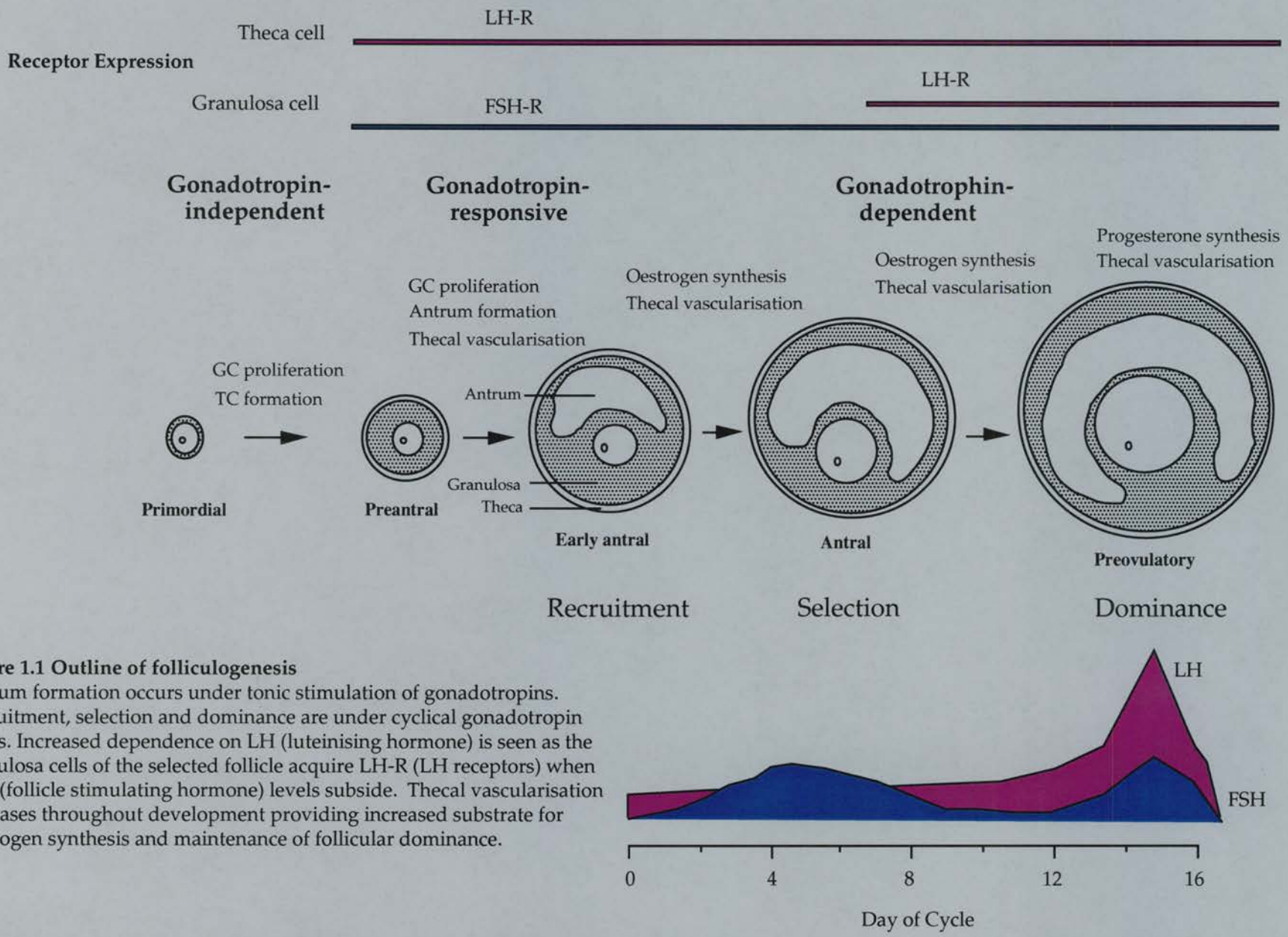

Figure 1.1 Outline of folliculogenesis
Antrum formation occurs under tonic stimulation of gonadotropins. Recruitment, selection and dominance are under cyclical gonadotropin levels. Increased dependence on LH (luteinising hormone) is seen as the granulosa cells of the selected follicle acquire LH-R (LH receptors) when FSH (follicle stimulating hormone) levels subside. Thecal vascularisation increases throughout development providing increased substrate for oestrogen synthesis and maintenance of follicular dominance.

1.2.1 Pituitary gonadotropin secretion

Pituitary gonadotropin synthesis and release is controlled by binding of gonadotropin releasing hormone (GnRH) to its receptor on anterior pituitary gonadotrope cells and the activation of protein kinase C. The gonadotropins luteinising hormone (LH) and follicle stimulating hormone (FSH) are heterodimeric polypeptides comprising a common α-subunit and a unique, structurally related β-subunit that confers biological specificity. GnRH is released in a pulsatile manner, from the synaptic terminals of the GnRH neurones in the hypothalamus into the hypophysial portal vessels, which connect a primary capillary bed in the median eminence to a secondary capillary bed in the anterior pituitary gland (reviewed by Clarke, 1996). The GnRH receptor is the crucial regulatory molecule that transduces the action of GnRH to stimulate gonadotropin synthesis and release. Occupation of the receptor by GnRH triggers a rapid increase in intracellular calcium levels and activation of protein kinase C, both of which may lead to the exocytosis of secretory granules and enhanced biosynthesis of gonadotropin subunits. The maintenance of both α- and β-subunit mRNA (messenger ribonucleic acid) levels is reliant upon GnRH input. They are regulated by changes in the frequency and amplitude of the GnRH pulses (Marshall *et al.*, 1991), as is the exocytosis of LH and FSH hormones. Binding of a GnRH antagonist to the receptor does not induce activation, and leads to a rapid decline in gonadotropin subunit mRNA synthesis and prevents gonadotropin release. GnRH action is also subject to control by gonadal hormones such as oestrogen, progesterone and inhibin (reviewed by Clarke, 1996).

1.2.2 Pre-antral and early antral development

Folliculogenesis begins with the transition of primordial follicles which were generated during fetal life. The transition is characterised by the expansion of the epithelial-like granulosa cells to a cuboidal appearance, the initiation of cellular replication of granulosa cells, and the initiation of growth of the oocyte. When the follicle has acquired 3-6 layers of granulosa cells, some stromal cells align in a parallel fashion around the primary follicle. These cells eventually differentiate into theca cell layers capable of steroidogenesis (reviewed by Zeleznik and Benyo, 1994). Following formation of 6-7 layers of granulosa cells the antral cavity begins to form, and a specific group of

granulosa cells surrounding the oocyte form the cumulus (reviewed by Gougeon, 1996). This process takes approximately 85 days (Gougeon, 1986). Pre-antral and early antral follicles are found in hypophysectomised and pre-pubertal monkeys, indicating that the early stages of follicular development, up to and including the formation of early antral follicles are independent of the secretion of the pituitary gonadotropins LH and FSH (Goldenberg *et al.*, 1976; Knobil *et al.*, 1959; Peters *et al.*, 1975; van Wagenen and Simpson, 1973). Granulosa cells are responsive to FSH as demonstrated by the production of oestrogen following prolonged incubation of granulosa cells from early antral follicles with FSH and androgen substrate. They are however, not responsive to LH. This follows because only cell surface receptors for FSH, and not LH are present on granulosa cells at this time (Zeleznik *et al.*, 1981). Early antral follicles are present throughout the cycle as a result of the continuous entry of primordial follicles into the pool of developing follicles, and so it is generally accepted that the process of pre-antral follicular development serves to provide a constantly suitable source of maturing follicles for further development when provided with appropriate gonadotropin support (Zeleznik and Benyo, 1994).

1.2.3 Antral follicular development

The maturation of follicles beyond the early antral stage is under obligatory gonadotropic control. Since early antral follicles possess only FSH receptors it is this gonadotropin which is responsible for further development and the associated biochemical changes within the follicle that accompany this process. Binding of FSH to its granulosa cell surface receptor activates adenylyl cyclase and cAMP (cyclic adenosine monophosphate)-dependent protein kinases, leading to altered expression of multiple genes crucial to cytoproliferation and differentiation (Richards, 1994). Granulosa cell genes that are responsive to FSH include: aromatase ($P450_{arom}$) the steroidogenic cytochrome P450 crucial to oestrogen synthesis; cholesterol side-chain cleavage ($P450_{scc}$), rate limiting in progesterone synthesis; the LH receptor; and polypeptide growth factors and binding proteins such as insulin-like growth factors (IGFs) and their binding proteins (reviewed by Zeleznik and Hillier, 1996). The mitogenic action of FSH is facilitated by locally produced growth factors, production

and/or action of which may be modified by FSH (Skinner and Parrott, 1994). Tonic stimulation by FSH is sufficient to sustain the development of small antral follicles, however cyclic levels of FSH are required for further development, and so before puberty all follicles that survive to this stage become atretic. When sufficiently high levels of FSH are present during the reproductive life of a female, follicles at such an intermediate stage are rescued from atresia and preovulatory development begins.

1.2.4 Preovulatory follicular recruitment

At the beginning of the follicular phase of the cycle pituitary secretion of FSH increases due to withdrawal of the negative feedback of action of oestradiol, progesterone and inhibin produced by the corpus luteum of the previous cycle (Baird *et al.*, 1984; Goodman and Hodgen, 1983; Le Nestour *et al.*, 1993). The rise in plasma FSH level causes multiple antral follicles to enter the stages of preovulatory development. Evidence from ovulation induction using exogenous FSH suggests that each follicle has a 'threshold' requirement for FSH beyond which it must be stimulated by FSH if it is to be protected from atresia and continue to develop (Brown, 1978; Goodman *et al.*, 1977). Small (10-30%) differences exist between individual follicles at this stage of development with respect to the threshold amount of FSH required to initiate preovulatory development, which explains why not all follicles recruited to begin preovulatory development mature fully and ovulate.

1.2.5 Preovulatory follicular selection

In mono-ovulatory species (e.g. human) only one of the follicles initially recruited to begin preovulatory development actually survives to secrete oestrogen in the late follicular phase. In other species such as rodents approximately 10 preovulatory follicles are ovulated, and in the marmoset monkey, the species used for the current research, 2-3 ovulations occur, reflecting the fact that marmosets give birth to 2-3 offspring at any one time. The number of follicles that develop to the preovulatory stage is dependent on the duration that FSH concentrations are maintained above the threshold (Zeleznik and Kubik, 1986). For simplicity this section discusses singular follicular selection and dominance. The ability of the follicle most rapidly to begin oestrogen synthesis is crucial

to its survival as the dominant follicle (Goodman *et al.*, 1977; Zeleznik, 1981). The hypothesis is that the maturing follicle inhibits the development of less mature follicles by suppressing FSH secretion by way of its production of oestrogen which has a negative feedback effect at the hypothalamic-pituitary axis, down regulating FSH secretion. In the follicular phase of the cycle the plasma FSH level rises, and $P450_{arom}$, responsible for oestrogen synthesis, is increasingly expressed in the granulosa cell layer of the dominant follicle. This activation of the aromatase system has been likened to a switch, which is turned on as the FSH threshold level is surpassed (Hillier, 1981). The first follicle to secrete oestradiol is the one with the greatest sensitivity to FSH (*i.e.* the lowest FSH threshold) (Zeleznik and Kubik, 1986). In addition FSH stimulates granulosa cell inhibin synthesis (Findlay, 1993), which also has a negative effect on pituitary FSH secretion (Groome *et al.*, 1995). Passive immunisation of rhesus monkeys with anti-oestradiol antibodies in the mid-late follicular phase of the cycle prevented the fall in FSH concentrations and caused the maturation of more than one preovulatory follicle (Zeleznik *et al.*, 1985). It is presumed that this effect of passive immunisation occurred in the presence of elevated inhibin secretion from the increased number of maturing follicles (McLachlan *et al.*, 1986), suggesting that in the absence of oestrogen-mediated suppression of FSH secretion, inhibin alone was not able to govern the development of a single preovulatory follicle (Zeleznik and Benyo, 1994). Thus, under the control of oestrogens, blood levels of FSH fall to insufficient concentrations to sustain the further development of other follicles within the cohort, and they undergo atresia.

Given that FSH is required for preovulatory growth and that the maturing follicle inhibits the development of other follicles by suppressing FSH secretion, how is it that the preovulatory follicle continues to develop in the presence of FSH concentrations that are unable to sustain the development of less mature follicles? It appears that, as a direct consequence of FSH stimulation, the preovulatory follicle undergoes maturation-dependent changes which further increase its sensitivity to gonadotropins (*i.e.* lowers its FSH threshold level) (Zeleznik and Hillier, 1996).

1.2.6 Responsiveness of dominant follicles to declining FSH concentrations

FSH and LH receptor levels

Increases in receptor numbers for FSH and LH should directly increase the sensitivity of the follicle to falling gonadotropin levels. In rats, the density of FSH receptors on granulosa cells increases during preovulatory follicular development (LaPolt *et al.*, 1992). In the primate, analysis of the dose-dependent relationship between FSH concentrations and oestrogen production by marmoset granulosa cells revealed that cells collected from preovulatory follicles were nearly four times more sensitive to FSH when compared with granulosa cells harvested from less mature follicles (Harlow *et al.*, 1988). In addition to changes in density of FSH receptors on granulosa cells, a hallmark of the action of FSH is the induction of receptors for LH (Zeleznik *et al.*, 1974). As both FSH and LH exert their actions via the stimulation of adenylyl cyclase and increase in intracellular cAMP concentrations, the presence of LH receptors on granulosa cells of the dominant follicle would protect it from the fall in FSH (Yong *et al.*, 1992a). Less mature follicles possess only FSH receptors and thus would be more susceptible to a fall in FSH secretion, while the selected follicle, as a result of the FSH-mediated increase in LH receptors, may survive the fall in FSH concentrations by developing the ability to respond to LH (Zeleznik and Hillier, 1996).

Vascularisation

In addition to increases in hormone responsiveness, preferential delivery of gonadotropins to the maturing follicle could protect it from the fall in FSH concentrations. Early investigators observed the heterogeneity in follicular vascularisation and suggested its importance in determining whether follicles remain healthy or become atretic (Clark, 1900; Anderson, 1926; Bassett, 1943; Burr and Davies, 1951). Subsequent work has supported the contention that maintenance of the follicular vasculature is important for maintaining follicular health. Early atretic ovine follicles will regenerate when placed *in vitro*, suggesting that decreased vascularity may limit access of atretic follicles to nutrients, substrates and tropic hormones *in vivo* (Moor and Seamark, 1986). In rhesus monkeys, the density of the capillary network that supplies the preovulatory follicle is at least three times greater than that supplying other less

mature follicles, and this increased density of capillaries results in a greater delivery of radiolabelled gonadotropin to the selected follicle (Zeleznik *et al.*, 1981). The findings that extracts of follicle cells or conditioned tissue culture medium from granulosa cells were able to stimulate the proliferation of endothelial cells *in vitro* suggested that the maturing follicle produces diffusible angiogenic factors that cause selective vascularisation of the theca (Koos, 1986).

Autocrine and paracrine agents

The actions of FSH and LH on the maturing follicle can be modified in a positive or negative manner by locally produced agents as demonstrated by *in vitro* studies (Hillier, 1991). Putative paracrine modulators of FSH action of granulosa cells are androgenic steroids and polypetides such as transforming growth factors produced by LH-stimulated theca cells (Magoffin and Erickson, 1994). This is based largely from studies in rodents and *in vitro* culture systems. FSH-stimulated granulosa cells can produce steroidal (e.g. oestradiol and progesterone) and non-steroidal (e.g. inhibin/activin and IGFs) substances that may influence theca responsiveness to LH (reviewed by Zeleznik and Hillier, 1996). In rats, IGF-1 contributes to this process by synergising the effects of FSH in the induction of aromatase activity (Hillier, 1991), however in humans the variable concentrations of IGFBPs (insulin like growth factor binding proteins) during follicular development are thought to have a greater role than *de novo* IGF production (San Roman and Magoffin, 1992). These and other factors may also exert autocrine regulation within the cells that produce them.

1.2.7 Follicular oestrogen synthesis

The onset of follicular oestrogen synthesis reflects a functional interplay between the two major steroidogenic cell types in the follicle, the granulosa and theca cells, regulated by FSH and LH (Zeleznik and Hillier, 1996), typical of the "two-cell, two-gonadotropin" model of oestrogen synthesis. Thus, both cell types and both gonadotropins are crucial to oestrogen synthesis (Armstrong *et al.*, 1979; Hillier *et al.*, 1994). Theca cells under LH stimulation produce C_{19} androgens (testosterone and principally androstenedione) because they abundantly express 17α-hydroxylase/C_{17-20}

lyase ($P450_{c17}$), needed for androgen synthesis, however, theca cells lack significant quantities of the aromatase enzyme and so cannot aromatise C_{19} androgens to oestrogens (Hillier, 1981). In contrast, granulosa cells lack the $P450_{c17}$ activities that are required to metabolise C_{21} steroids to C_{19} androgens but, under FSH stimulation, acquire the aromatase enzyme that converts C_{19} androgens to oestrogens, principally oestradiol (Hillier *et al.*, 1981). The theca interna is highly vascularised and so has direct access to blood-borne precursor cholesterol and theca cells contain the steroidogenic enzymes necessary to synthesise androgens from acetate and cholesterol (e.g. cholesterol side-chain cleavage, $P450_{scc}$). Within the preovulatory follicle the avascular granulosa cell layer is exposed to high concentrations of aromatisable androgen that reach it by diffusion from the theca interna. Cells on the outer (mural) granulosa cell layer are presumed to be particularly active sites of aromatisation, since they express more $P450_{arom}$ mRNA and LH receptors than do cells distal to the basement membrane (Amsterdam *et al.*, 1975; Whitelaw *et al.*, 1992). The theca vasculature is so well developed in the preovulatory follicle that murally located granulosa cells are effectively in contact with adjacent blood vessels. They are therefore well-placed to respond to changes in the circulating LH level which is important in the maintenance of follicular dominance, and the oestrogen they produce can be directly discharged into the venous effluent of the preovulatory follicle (Ravindranath *et al.*, 1992b).

1.2.8 Maintenance of follicular dominance

By the mid-follicular phase the dominant follicle is recognisably the largest follicle in the human ovary (Gougeon and Lefevre, 1983). At this time maintenance of its status becomes increasingly dependent on LH. Since LH receptors are constitutively expressed on theca cells and are induced on granulosa cells by FSH, the dominant follicle secretes increased amounts of androstenedione as well as oestradiol in response to stimulation by LH (McNatty *et al.*, 1976). Paracrine signalling (granulosa on theca) is thought to contribute to the selective enhancement of LH-responsive androgen synthesis that occurs in this follicle. *In vitro*, LH co-ordinately stimulates aromatse and inhibin synthesis in human granulosa cells from the dominant follicle (Hillier *et al.*, 1991), and inhibin potently stimulates LH-stimulated androgen synthesis (Hillier, 1991).

1.3 Ovulation

Ovulation is the central event in the ovarian cycle when the oocyte is released from the ovary and passes into the oviduct where it may be fertilised. Ovulation is stimulated by a surge in LH, it is the terminal step in the growth and differentiation of the follicle and marks the onset of the formation of the corpus luteum (reviewed by Zeleznik and Hillier, 1996).

1.3.1 The LH surge

As the oestrogenic production of the preovulatory follicle increases, its effect becomes increasingly stimulatory on pituitary LH production and secretion, in turn the frequency of pulsatile release of LH increases, culminating in what is termed the LH surge, which stimulates ovulation. Maturation of the oocyte is reactivated in response to the LH surge, as oocytes themselves do not express LH receptors this is presumably as a consequence of a decrease in exposure to inhibitory cAMP (Tsafriri and Dekel, 1994) from the breakdown in oocyte-granulosa cell connections (Albertini and Anderson, 1974). At the granulosa cell level, immediate responses to the LH surge are inhibition of mitosis, the cessation of follicular growth, and increased expression of $P450_{scc}$ (Yong *et al.*, 1992a; Yong *et al.*, 1994) and 3β-hydroxysteroid dehydrogenase (3β-HSD), the steroidogenic enzymes necessary for progesterone synthesis (Miller, 1988). This is known as granulosa cell luteinisation. Oestrogen synthesis declines due to inhibition of $P450_{c17}$ activity and the attendant lack of aromatase substrate (Hillier and Wickings, 1985). Thus as ovulation approaches the ovary increasingly secretes progesterone while oestrogen secretion temporarily declines.

1.3.2 Follicular rupture

The LH surge stimulates a proteolytic cascade within the preovulatory follicle, resulting in its rupture approximately 36 hours later. The biochemical nature of ovulation has been likened to an inflammatory response (Espey, 1980), which leads to ovarian hyperaemia and local increases in proteolytic enzyme activities that reduce the tensile strength of the apical wall. The follicular response to LH includes increased production of prostaglandins, platelet activating factor, plasminogen activators and matrix

metalloproteinases such as collagenases, gelatinases and stromelysins, which serve to digest the follicle wall (reviewed by Zeleznik and Hillier, 1996). Locally synthesised prostaglandins appear to be primarily responsible for the increase in vascular permeability which sustains positive intrafollicular pressure during the period when follicular fluid begins to leak through the partially digested wall (Zeleznik and Hillier, 1996). The gradual reduction in the tensile strength of the follicular wall eventually results in complete rupture and the release of the cumulus-enclosed oocyte in follicular fluid over many minutes.

A role for progesterone in follicular rupture has been proposed. Progesterone levels in follicular fluid rise markedly following the LH surge. Incubation of pieces of human follicular wall with progesterone *in vitro* decreases the formation of collagen (Tjugum *et al.*, 1984), and follicular steroids have been implicated in the regulation of plasminogen activator synthesis and the activation of collagenase, thereby facilitating breakdown of the follicular wall (Ohno and Mori, 1985). After follicular rupture the collapsing follicle becomes the corpus luteum.

1.4 The corpus luteum

The luteal phase of the ovulatory cycle is dominated by the corpus luteum which secretes large amounts of progesterone priming the endometrium for blastocyst implantation. In the non-fertile cycle, the corpus luteum grows, matures and regresses in 14 days in the human (Lenton and Woodward, 1988) and approximately 20 days in the marmoset (Hearn, 1983). If conception occurs the corpus luteum is rescued from regression which is essential for the establishment of pregnancy (Hartman and Corner, 1947; Csapo *et al.*, 1973).

1.4.1 Formation of the corpus luteum

The corpus luteum forms from the preovulatory follicle after ovulation. The basement membrane which separated the granulosa and theca cell layers, disintegrates (Corner, 1956). The blood-filled theca forms invaginations into the luteinising granulosa cell layer (Corner, 1956, Niswender and Nett, 1994) and both cell types invade the follicular

antrum. Blood vessels undergo extensive angiogenesis to form a microvascular network which serves each and every lutein cell in the structure (Redmer and Reynolds, 1996; Reynolds *et al.*, 1992). Luteinisation is the first stage in functional and structural luteal development. The hallmarks of luteinisation are evident directly after the LH surge, in the expression of enzymes critical for progesterone production (Yong *et al.*, 1992a; Yong *et al.*, 1994), and progesterone contributes to rupture of the follicle at ovulation (Ohno and Mori, 1985; Tjugum *et al.*, 1984). However, luteinisation is a gradual process which is completed 5-6 days into the luteal phase, when the characteristic morphological effects of lutein cells are fully evident (Adams and Hertig, 1969). This section discusses luteal formation in association with the acquired capacity for lutein cells to secrete progesterone and the structural changes which take place as the gland becomes fully functional.

1.4.1.1 Luteinisation and luteal steroidogenesis

The LH surge is the stimulus for luteinisation. Marmoset antral follicles spontaneously luteinise *in vitro* (Wehenberg and Rune, 2000), and so it appears *in vivo* that the LH surge removes the inhibitory effect of the preovulatory environment. Luteinisation involves the transformation of the granulosa and theca cells of the preovultory follicle to lutein cells of the corpus luteum. They terminally differentiate, and so granulosa cell proliferation ceases (Gougeon, 1981) and theca and granulosa lutein cells acquire the steroidogenic enzymes necessary to produce progesterone (Yong *et al.*, 1992a; Yong *et al.*, 1994). Progesterone becomes the major product of the corpus luteum. Although oestrogens are still produced by the primate corpus luteum, their synthesis is secondary to that of progesterone (reviewed by Zeleznik and Hillier, 1996).

Progesterone synthesis

Progesterone production by the corpus luteum relies on cholesterol as a substrate. Although luteal cells can manufacture cholesterol *de novo* from acetate, the corpus luteum relies extensively on serum low density (LDL) and high density lipoprotein (HDL)-cholesterol for use as a precursor for the synthesis of progesterone (Tureck and Strauss, 1982; Soto *et al.*, 1984). Uptake of LDL-cholesterol is via receptor-mediated

endocytosis (Brown and Goldstein, 1986), and HDL-cholesterol entrance to the cell is by receptor binding, but cholesterol is transported into the cell by an unknown mechanism which does not appear to be receptor-mediated endocytosis (reviewed by Niswender *et al.*, 2000). A rate limiting step in the steroidogenic pathway appears to be the transport of cholesterol from the outer to the inner mitochondrial membrane (Stevens *et al.*, 1993) which is dependent on the phosphorylation of the steroidogenic acute regulatory protein (StAR) (Lin *et al.*, 1995). Once transported to the mitochondrial matrix, $P450_{scc}$ cleaves the side chain from cholesterol to form pregnenolone, which is then transported to the closely associated smooth endoplasmic reticulum, where 3β-HSD converts pregnenolone to progesterone (reviewed by Niswender *et al.*, 2000).

Cellular levels of 3β-HSD and $P450_{scc}$ mRNA are highest shortly after ovulation, declining progressively throughout the luteal phase (Bassett *et al.*, 1991), whereas progesterone secretion is maximal during the mid-luteal phase. Dissociation of luteal steroidogenic secretion rate and biosynthetic potential may occur because the new corpus luteum is incompletely vascularised such that its access to precursor cholesterol in form of LDL is restricted (Carr *et al.*, 1982). When luteal vasculature becomes fully developed in the mid-luteal phase, precursor cholesterol no longer rate limits steroidogenesis. Thus the luteal progesterone secretion rate progressively increases during the early luteal phase in spite of the age related decline in steroidogenic potential at the cellular level (Zeleznik and Hillier, 1996).

Progesterone actions on the uterus

In the uterus, progesterone acts on the endometrium as a differentiation factor (Cummings and Yochim, 1984). During the follicular phase, oestrogens induce proliferation of cells of the endometrium, and elevated concentrations of progesterone during the luteal phase inhibit mitosis in the endometrium and down regulate receptors for oestradiol (reviewed by Niswender *et al.*, 2000), thereby blocking the mitogenic actions of oestrogens. Progesterone also induces stromal differentiation, stimulates glandular secretions and changes the pattern of proteins secreted by endometrial cells (Strinden and Shapiro, 1983; Maslar *et al.*, 1986). These uterine proteins provide an environment that supports early embryonic growth.

Oestradiol production

The luteal phase plasma oestradiol pattern mirrors progesterone in reaching a maximum at the mid-luteal phase when total aromatase activity is declining (Fisch *et al.*, 1989). Similar to granulosa cells in the preovulatory follicle, granulosa lutein cells in the corpus luteum cannot undertake oestradiol synthesis unless supplied with an aromatase substrate (reviewed by Zeleznik and Hillier, 1996). Theca lutein cells are presumed to provide precursor androgen for aromatisation by granulosa lutein cells in an extension of the "two-cell, two-gonadotropin" type mechanism of oestrogen synthesis that occurs in the preovulatory follicle. A high rate of C_{19} steroid synthesis in the theca depends on access to extracellular precursor cholesterol (Carr *et al.*, 1982). Presumably therefore androgen synthesis in the theca lutein cells, like progesterone synthesis in the granulosa lutein cells, benefits from the increased vascularisation of the corpus luteum that occurs during the first week after ovulation (Zeleznik and Hillier, 1996).

1.4.1.2 Structural formation of the corpus luteum

When the corpus luteum is fully formed it comprises a heterogeneous population of steroidogenic and non-steroidogenic cells (reviewed by Grazul-Bilska *et al.*, 1997). In the human, the two steroidogenic cell types, theca and granulosa derived cells, differ in their cellular origin and morphology, rate of progesterone production, response to LH, production of peptide hormones and angiogenic factors. Whereas in the marmoset, the origin of steroidogenic cells is unclear and both theca and granulosa cells are incorporated into the body of the corpus luteum (Webley *et al.*, 1990). The corpus luteum also contains other cell types including endothelial cells, pericytes, fibroblasts and immune cells. It is a dynamic gland in which the cellular morphology and relative contributions of each cell type change during its lifespan. The structure of a human mid-luteal phase corpus luteum is shown in Figure 1.2. Two morphologically distinct cell types are visible; large luteal cells of granulosa cell origin occupy much of the corpus luteum, and smaller luteal cells derived from follicular theca cells form a separate layer around the periphery with small indentations into the centre. In the mature marmoset corpus luteum (Figure 1.3b) the population of steroidogenic cells is more uniform and

heterogeneity arises from other luteal cell types such as endothelial cells, pericytes and fibroblasts.

During luteal formation, the increased steroidogenic capacity to secrete progesterone occurs in parallel with changes in the morphology of the granulosa lutein cells in the human and most primates, and both granulosa and theca derived cells in the marmoset. In the rhesus monkey, granulosa cells collected from the preovulatory follicles during the late follicular phase have a diameter of approximately 10μm, contain sparse amounts of endoplasmic reticulum, and possess mitochondria with lamelliform cristae. In contrast, lutein cells of newly formed corpora lutea have undergone hypertrophy, so measure approximately 25μm in diameter, and possess abundant smooth and rough endoplasmic reticulum and mitochondria with tubular cristae (Crisp and Channing, 1972), assuming the full morphological characteristics of steroid secretory endocrine cells. The structural remodelling of granulosa cells during luteinisation is dependent on LH secretion because granulosa cells collected from rhesus monkeys prior to the LH surge fail to produce substantial amounts of progesterone *in vitro* and failed to exhibit morphological signs of luteinisation (Channing, 1970).

The morphological events associated with luteinisation are not completed until 5-6 days post ovulation and so a marked difference in morphology and size of lutein cells are evident between the early and mid-luteal phases (Adams and Hertig, 1969). Figure 1.3 demonstrates the increase in lutein cell cytoplasmic volume associated with formation of the mature marmoset corpus luteum and the lutein cell shrinkage which begins in the mid-late luteal phase (Adams and Hertig, 1969), and is evident in the early regressing late luteal corpus luteum. Whilst lutein cells show degenerative changes during this time, this figure demonstrates that other cell types with little cytoplasm and densely staining nuclei, for example fibroblasts, become the major cell type in the regressed corpus luteum and there is little evidence of steroidogenic cell presence.

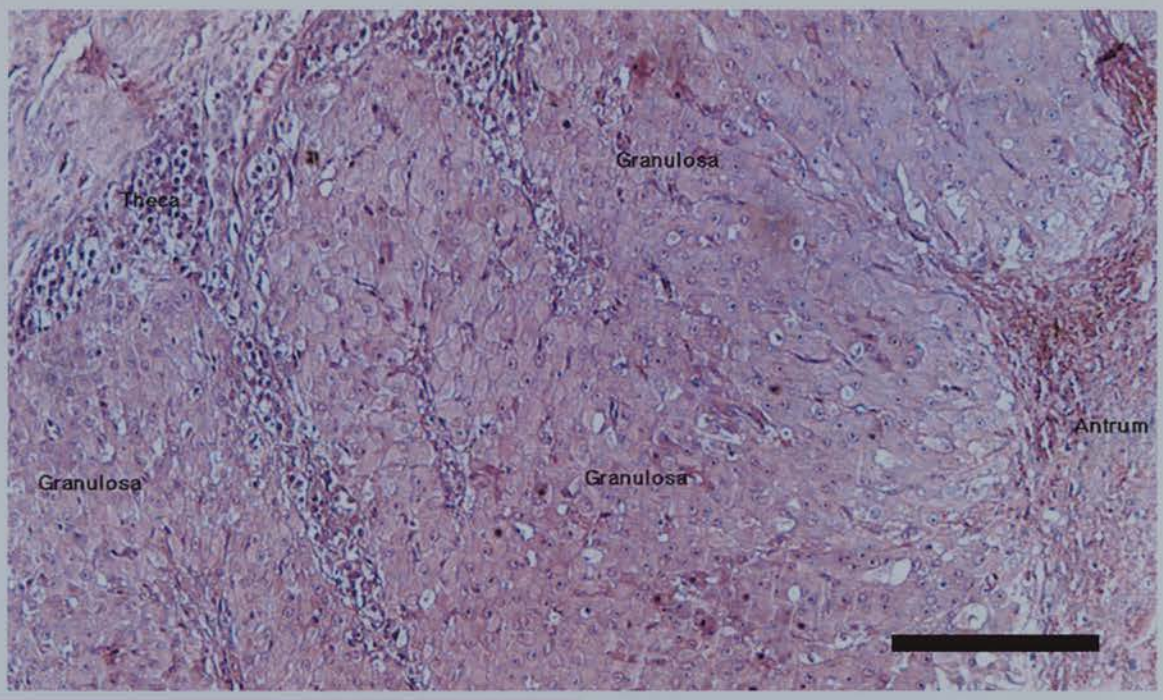

Figure 1.2 Morphology of the human corpus luteum
Haematoxylin and eosin staining of a mid luteal phase human corpus luteum. The theca and granulosa-derived lutein cells are present in two distinct compartments within the corpus luteum. The theca lutein cells are located on the outside of the structure and processes penetrate the granulosa lutein cells which make up the major part of the mature gland. The antrum of the preovulatory follicle forms the corpus luteum cavity which consists of blood, residual follicular fluid and connective tissue. Blood vessels are present in both the theca and granulosa-derived compartments after the extensive vascular remodelling which takes place during formation of the gland. Scale bar = 200μm.

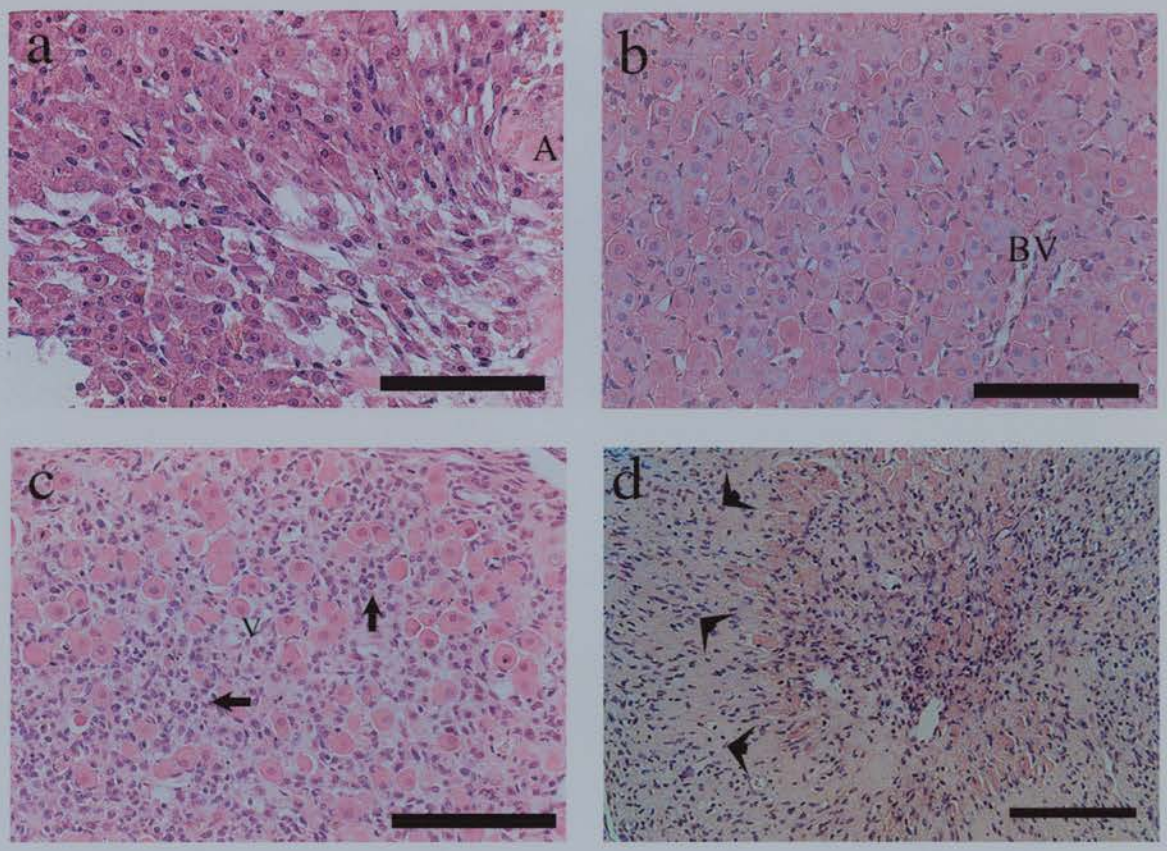

Figure 1.3 Morphology of the marmoset corpus luteum
Haemtoxylin and eosin staining of the marmoset corpus luteum at different stages of development. (a) An early luteal phase corpus luteum. Note that the lutein cells have similar morphology, the origins of which are not clear. Streaming of the lutein cells to fill the preovulatory antrum is taking place, and the residual follicular antrum (A) is still present at this stage. The morphology of the lutein cells reflects the early stage of development, and lutein cell hypertrophy is underway. (b) A mid-luteal phase corpus luteum. Luteinisation is complete and the lutein cells are fully mature, the appearance of which is consistent with active steroidogenic cells. They are large and spherical with central round nuclei and abundant cytoplasm. Note that the remodelling of the micro-vasculature is complete with the presence of many luminal blood vessels (BV). (c) A late luteal phase corpus luteum. Luteal degeneration is taking place, lutein cell death and vacuolation (V) are apparent, giving rise to a lower proportion of steroidogenic cells per unit area. Proliferation and infiltration of small cells with little cytoplasm has occurred as indicated by the arrows. These cells are probable fibroblasts and immune cells. (d) A regressed corpus luteum. This corpus luteum is mainly composed of connective tissue from the mass influx of fibroblasts which are indicated by the arrow heads. Few if any steroidogenic cells remain. Scale bars = 100µm.

In addition to alterations in cellular morphology, luteinisation is associated with terminal cellular differentiation. Studies in rats have convincingly demonstrated that corpora lutea do not incorporate tritiated thymidine in lutein cell nuclei, a measure of DNA synthesis, whereas such incorporation is readily apparent in follicular granulosa cells (Hirshfield, 1984). Analysis of human ovaries has indicated that the mitotic index of granulosa cells decreases dramatically after the LH surge (Gougeon, 1981), and mitotic figures in human corpora lutea are rare (Corner, 1956). The luteinising stimulus generated by the LH surge thus results in a co-ordinated series of responses of granulosa cells that include intracellular remodelling, enhanced gene expression, as well as modulation of the cell cycle (Zeleznik and Benyo, 1994), which have shown to be driven via the LH-induced massive increase in intracellular cAMP. Exposure of granulosa cells to maximal stimulatory concentration of LH *in vitro* resulted in increases in intracellular cAMP levels that were 15-fold greater than those induced by FSH (Yong *et al.*, 1992b). This suggests that during follicular development, FSH generated relatively low levels of cAMP within granulosa cells which favours DNA synthesis and the acquisition of steroidogenic capacity, whereas the LH surge, through generation of high intracellular concentrations of cAMP, arrests cell division and maximally stimulates the steroidogenic capacity of the luteinising granulosa cells (Zeleznik and Benyo, 1994).

Neovascularisation

In the preovulatory follicle, the granulosa cell layer is not vascularised; the capillary network that supplies the preovulatory follicles abruptly terminates at the basement membrane that separates the granulosa cell layer from the theca cell layer. Following ovulation, as the basement membrane loses integrity and the luteinising granulosa cell layer grows thicker, blood vessels infiltrate from the theca layer and form a network of capillaries that supplies every one of the lutein cells (Corner, 1943). The changes in vascularisation of the marmoset follicle and corpus luteum is shown in Figure 1.4. Within a few days after ovulation, endothelial cell proliferation is such that the corpus luteum becomes highly vascularised and on a tissue-weight basis, blood flow to the gland is among the greatest of any tissue in the body (Abdul-Karim and Bruce, 1973). The capillary network of the corpus luteum is so extensive that the majority of

steroidogenic cells are adjacent to one or more capillaries. This increased vascularity in addition to providing a conduit for the delivery of luteal steroids to the general circulation, is also necessary for the provision of cholesterol substrate in the form of LDL for progesterone biosynthesis (Carr *et al.*, 1982).

1.4.2 Trophic regulation of the corpus luteum

LH

Historically, the requirement for LH in the control of progesterone secretion and the functional lifespan of the corpus luteum has been the subject of numerous debates. Gemzell (1965) noted that induction of ovulation by hCG (human chorionic gonadotropin) in hypophysectomised women who had been treated with FSH to induce follicular growth was followed by luteal phases of normal duration, suggesting that, once formed, the human corpus luteum functioned independently of additional pituitary gonadotropin support. Subsequent studies by Vande Wiele *et al.*, (1970) demonstrated that the long half-life of hCG used to induce ovulation provided extended gonadotropin support to the corpus luteum; when LH was used to induce ovulation, the corpus luteum regressed after 5-6 days unless additional LH was given throughout the luteal phase. An obligatory requirement for LH in the maintenance of the corpus luteum was indicated when Moudgal *et al.*, (1971) passively immunised rhesus monkeys with antibodies against LH and found that treated animals exhibited premature luteal regression. Studies in rhesus monkeys in which pituitary gonadotropin secretion was controlled directly by pulsatile infusion of synthetic GnRH provided compelling evidence that pituitary secretion of gonadotropin was absolutely required for luteal function (Hutchison and Zeleznik, 1984), and others have shown that in both human and macaques that GnRH antagonist treatment rapidly suppresses luteal progesterone secretion and concomitantly evokes premature menses (Fraser *et al.*, 1986; Mais *et al.*, 1986).

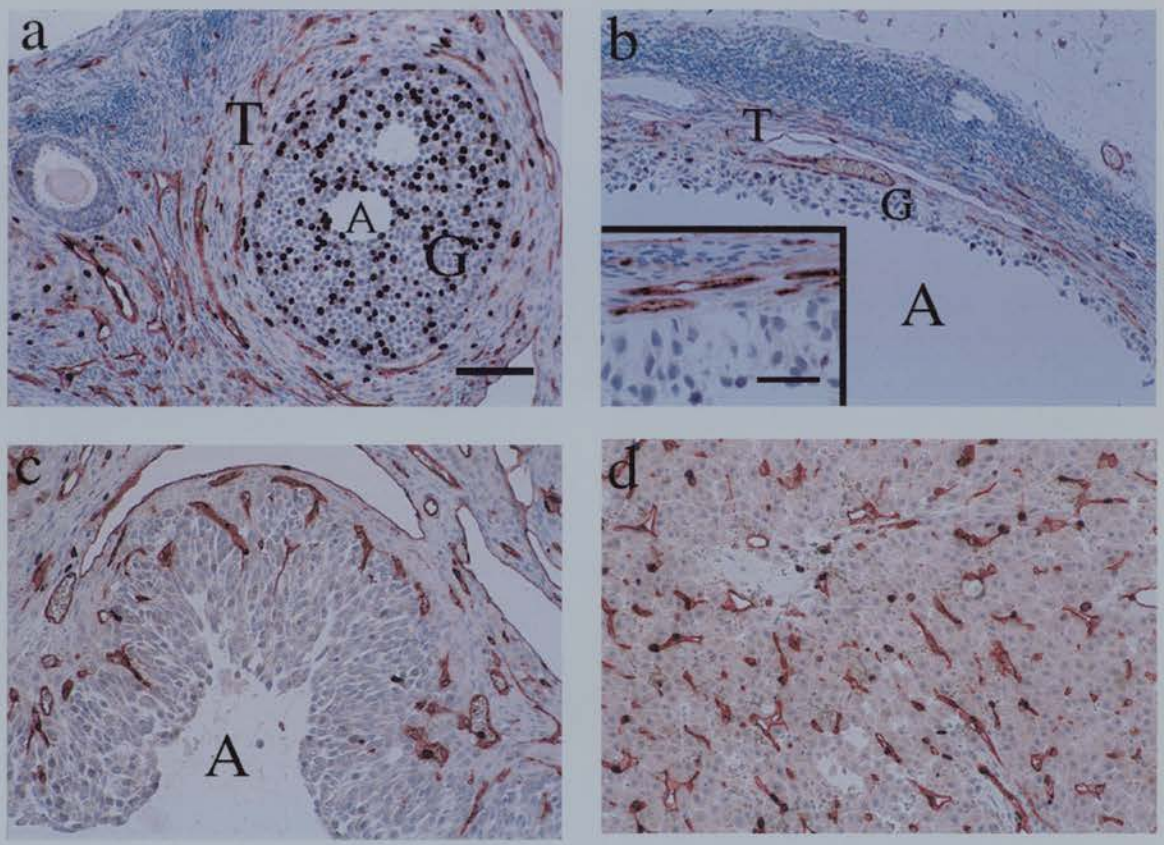

Figure 1.4 Cell proliferation and vascularisation of marmoset follicles and corpus luteum

Immunostaining for the endothelial cell marker, CD31, and the cell proliferation marker, bromodeoxyuridine. (a) An early antral follicle. The antrum (A) of this follicle is just beginning to develop and many granulosa cells (G) are proliferating (black nuclear staining). Blood vessels (red cell membrane staining) are restricted to the theca layer (T) and ovarian stroma, many endothelial cells of which are proliferating (dual stained cells). (b) A preovulatory follicle, the large antral cavity of which is clearly visible. Fewer granulosa cells (G) in this follicle are proliferating. The high power inset demonstrates that most thecal (T) cell proliferation is restricted to the vascular endothelium. (c) A corpus luteum approximately 12 hours after ovulation. Granulosa and theca cells are invading the antrum (A) of the preovulatory follicle, and granulosa and theca cell proliferation has almost ceased. The vessels from the theca layer now penetrate the granulosa lutein cells, the endothelial cells of which are actively dividing, as the basement membrane which separated the two is disintegrating. (d) An early luteal phase corpus luteum. The former follicular antrum has almost been filled and blood vessels have proliferated so that an extensive vascular network has been formed. Note also that most proliferating cells in the corpus luteum are endothelial cells. Scale bars = 100μm.

A close temporal association exists between secretory bursts of LH and episodes of progesterone production by the corpus luteum (Ellinwood *et al.*, 1984; Filicori *et al.*, 1984; Mais *et al.*, 1986). The speed of progesterone response to each pulse of LH implies an acute effect of LH on precursor cholesterol metabolism, such as StAR phosphorylation (reviewed by Niswender *et al.*, 2000), rather than increased production of steroidogenic enzymes *per se*, after the initial induction of expression by the LH surge (Zeleznik and Hillier, 1996). However, suppression of LH during the luteal phase with GnRH antagonist resulted in a decline in mRNA concentrations of $P450_{arom}$ and 3β-HSD to undetectable levels over a 3 day period (Ravindranath *et al.*, 1992b), thus LH is also required for the long term maintenance of steroidogenic capacity of the primate corpus luteum.

FSH

FSH receptors have been identified in the human corpus luteum (McNeilly *et al.*, 1980), but FSH does not stimulate progesterone secretion in either human or macaque corpora lutea *in vitro* (Stouffer *et al.*, 1977; Fisch *et al.*, 1989), and the sensitivity of human luteinised granulosa cells to LH with respect to both progesterone and oestrogen secretion is more than 10-fold greater than that of FSH (Zeleznik and Benyo, 1994). Furthermore, the observations that exogenous hCG and LH are able to maintain luteal function in hypophysectomised women indicate that FSH does not play an obligatory role in the regulation of the primate corpus luteum *in vivo* (Gemzell, 1965; Vande Wiele *et al.*, 1970).

Autocrine and paracrine regulation

Progesterone itself may represent a broader regulator of the lifespan and function of the corpus luteum in primates (Stouffer, 1996). Progesterone promotes the synthesis of both the LH receptor and luteotrophic prostaglandins (e.g. PGI_2 and PGE_2), which enhance luteal function in the bovine (reviewed by Stouffer, 1996). In the rhesus monkey, the progesterone receptor is driven by the LH peak. In luteinising granulosa cells from patients undergoing in vitro fertilisation, progestins induce cell differentiation and increased progesterone production (Stouffer, 1996). Moreover, the secretion of

progesterone itself during the early luteal phase is maintained by progesterone, as reported for the rat corpus luteum (Rothchild, 1981).

Insulin-like growth factor-1 mRNA is highly expressed in the ovary (Adashi *et al.*, 1991; Hernandez *et al.*, 1992), and it has been demonstrated that IGF-1 is produced in the ovaries of several non-primate species, and influences the steroidogenic activity of follicles in a paracrine and autocrine manner (Adashi *et al.*, 1991). This growth factor also stimulates oestradiol synthesis by human granulosa cells (Mason *et al.*, 1993). In the human, several observations indicate that IGF-1 regulates luteal steroidogenic function, eliciting a positive action on progesterone and oestradiol synthesis (reviewed by Vega and Devoto, 1997). For example IGF-1 and IGF-1 receptor mRNAs are expressed by the human corpus luteum and binding studies demonstrate functional receptors for IGF-1 in human luteal tissue (Johnson *et al.*, 1996).

Prostaglandins may also have a luteotrophic role in the corpus luteum. Prostacyclin (PGI_2) is a major product of endothelial cells and it plays an important role in vasodilation. Moreover, PGI_2 levels were demonstrated to be highest in the early luteal phase and that injection of a PGI_2 inhibitor during luteal development decreased progesterone production and luteal lifespan in the bovine (Milvae and Hansel, 1985; Milvae *et al.*, 1986), probably via restriction of blood flow and decreased availability of LDL-cholesterol. PGE_2 has also been demonstrated to stimulate progesterone secretion by lutein cells of many species (Hamberger *et al.*, 1987; Myamoto *et al.*, 1993).

Direct cell-cell contact

Interactions between certain luteal cell types based on the demonstration of gap junction-mediated intercellular communication between the different types of luteal cells, has been demonstrated in mature bovine and ovine corpora lutea, suggesting that gap junction communication may be an important mechanism for co-ordinating the growth, development, and differentiated function of the corpus luteum (Grazul-Bilska *et al.*, 1997). Connexins (Cxs) are a family of specific gap junctional proteins (reviewed by Grazul-Bilska *et al.*, 1997). The expression of Cx43 is localised exclusively between luteal cells in the bovine (Grazul-Bilska *et al.*, 1997), and the expression of Cx43 in luteal tissue is greatest during the early and mid-luteal phases and decreases during

luteal regression in the human and the baboon (Khan-Dawood *et al.*, 1996). LH appears to increase the rate of gap junctional intercellular communication between ovine or bovine luteal cell types (reviewed by Grazul-Bilska *et al.*, 1997) suggesting that the luteotropic effects of LH are also in controlling the luteal cell interactions. The phenomenon of direct intercellular communication by cell types in the corpus luteum has generated considerable interest but as yet the extent of such communication to the control of luteal function has still to be fully elucidated.

1.4.3 Luteolysis

The regression of the corpus luteum in the absence of conception is obligatory for the initiation of a new ovulatory cycle because its secretion of progesterone, oestradiol and inhibin (Burger, 1993) exert negative feedback at the hypothalamic-pituitary axis to prevent the rise of FSH and LH secretion that are essential for the development of a new preovulatory follicle (Baird *et al.*, 1975; Zeleznik and Resko, 1980). In many infra-primate species luteolysis is brought about by the luteolytic action of uterine $PGF_{2\alpha}$ on the corpus luteum. In primates however, hysterectomy does not result in prolonged luteal phases (Neil *et al.*, 1969; Beling *et al.*, 1970; Castracane *et al.*, 1979), and it is not completely clear if one such luteolysin is responsible. Normal luteolysis is associated with a loss of capacity to synthesise progesterone (McGuire *et al.*, 1994) followed by loss of lutein cells (Knickerbocker *et al.*, 1988).

Functional luteolysis

The increased progesterone production from the corpus luteum throughout the luteal phase exerts a negative feedback effect on the frequency of pulsatile LH secretion by the pituitary gland, which falls from approximately 1 pulse per hour during the early luteal phase to 1 pulse every 4-8 hours during the mid-luteal phase (Ellinwood *et al.*, 1984; Filicori *et al.*, 1984). However, this decline in pulse frequency cannot be the direct cause of luteal regression because setting the pulse frequency at 1 pulse per hour throughout the luteal phase does not prolong the lifespan of the corpus luteum (Knobil *et al.*, 1980; Leyendecker *et al.*, 1980). Similarly, premature reduction of the LH pulse frequency to 1 pulse every 8 hours during the early luteal phase does not cause premature luteal

regression (Hutchison *et al.*, 1986; Zelinski-Wooten *et al.*, 1992). The best explanation for luteal regression is that the corpus luteum undergoes an age-related reduction in sensitivity to LH, so that progressively more intense stimulation by LH is required to sustain luteal function. In other words the corpus luteum may regress not because of reduced exposure to LH, but due to its ever-decreasing ability to respond to the low plasma levels of LH that prevail throughout the luteal phase (Zeleznik and Hillier, 1996).

At the cellular level, factors thought to be involved in this decrease in LH responsiveness and the initiation of luteolysis include oestrogen, prostaglandins, oxytocin, reactive oxygen species, and various polypeptide growth factors and cytokines. In humans, direct injection of oestrogen into the ovary containing corpus luteum resulted in premature menstruation (Gore *et al.*, 1973; Karsch *et al.*, 1973) which led to a suggestion that internally produced oestrogen leads to the regression of the corpus luteum. This was supported by the findings that concentrations of oestradiol and oestrone in the macaque corpus luteum increase during the late luteal phase as progesterone declines. However, administration of oestrogen inhibitors to spontaneously cycling animals does not prolong the luteal phase (reviewed by Zeleznik and Benyo, 1994).

Although uterine prostaglandins are not responsible for luteal regression in the primate, numerous studies have shown that prostaglandins can affect luteal function. *In vivo*, infusions of $PGF_{2\alpha}$ directly into the corpus luteum have been shown to cause luteal regression (Auletta *et al.*, 1973; Auletta *et al.*, 1984; Auletta and Flint, 1988). Similarly, intramuscular injections of $PGF_{2\alpha}$ or analogue in the marmoset causes luteolysis (Summers *et al.*, 1985; Webley *et al.*, 1989). Considered with the fact that luteal cells themselves produce prostaglandins *in vitro* (reviewed by Zeleznik and Benyo, 1994) it is supposed that locally produced prostaglandin may exert luteolytic effects on the primate corpus luteum. Luteolytic actions of $PGF_{2\alpha}$ include the down regulation of adenylyl cyclase and LH receptor signal transduction (Agudo *et al.*, 1984; Garverick *et al.*, 1985), decreased transport of cholesterol across the mitochondrial membranes (Juengel *et al.*, 1995; Pescador *et al.*, 1996) and decreases in 3β-HSD mRNA (Hawkins *et al.*, 1993; Tian *et al.*, 1994). It has been suggested that many of the effects of $PGF_{2\alpha}$ on reducing

mRNA encoding StAR, and 3β-HSD in the bovine are mediated via the effect of $PGF_{2\alpha}$ on reducing luteal blood flow which would deprive the gland of nutrients, substrates and luteotrophic support (Pharriss *et al.*, 1970). Endothelial cells express $PGF_{2\alpha}$ receptors and $PGF_{2\alpha}$ has been shown to cause degeneration of luteal endothelial cells resulting in marked reduction in capillary density, thereby reducing blood flow to lutein cells (reviewed by Niswender *et al.*, 2000). Endothelin-1 has been implicated as a possible mediator of the effects of $PGF_{2\alpha}$ on luteal blood flow (Girsh *et al.*, 1996a; Girsh *et al.*, 1996b). Endothelin-1 is stimulated by $PGF_{2\alpha}$ *in vitro* (Girsh *et al.*, 1996b) and *in vivo* (Ohtani *et al.*, 1998), and can cause arteriole constriction (Ohtani *et al.*, 1998). In addition to its potent vasoconstrictive activity (reviewed by Huggins *et al.*, 1993), endothelin-1 also inhibits the steroidogenic activity of enriched populations of steroidogenic lutein cells (Girsh *et al.*, 1996b). This potential modulator of $PGF_{2\alpha}$ in the bovine corpus luteum may have such luteolytic effects in the primate.

Other factors produced locally in the corpus luteum such as oxytocin could also have a role in luteolysis. Oxytocin has an inhibitory effect on hCG-stimulated progesterone synthesis in bovine luteal cells (Tan *et al.*, 1982a; Tan *et al.*, 1982b), alters blood flow in many organs (Auletta and Flint, 1988), and is synthesised in the primate corpus luteum (Dawood and Khan-Dawood, 1986; Einspanier *et al.*, 1994) where receptors are present (Khan-Dawood *et al.*, 1993), so a role in primate luteal regression cannot be overlooked. In addition, prolactin receptors have been described in the human ovary and corpus luteum (McNeilly *et al.*, 1980; Bramley *et al.*, 1987), however, a role for prolactin in the demise of the corpus luteum has not been proven.

The immune system also appears to play a role in luteolysis. Leukocytes infiltrate the corpus luteum during luteolysis (reviewed by Murdoch *et al.*, 1988) and eosinophils and macrophages, accumulate in the regressing corpus luteum in response to chemotactic factors before the decline in serum levels of progesterone (Murdoch, 1987). Immune cells and cytokines are believed to perform three functions during luteolysis: 1) cytokine mediated inhibition of steroidogenesis, 2) stimulation of $PGF_{2\alpha}$ secretion by the corpus luteum. and 3) phagocytosis of degenerative luteal cells (reviewed by Niswender *et al.*, 2000).

Reactive oxygen compounds are integrally involved in luteolysis and apoptosis (Riley and Behrman, 1991; Carlson *et al.*, 1993). Superoxide anion radicals, hydroxyl radicals, and hydrogen peroxide are the primary reactive oxygen species generated by steroidogenic cells (Hornsby and Crivello, 1983a; Hornsby and Crivello, 1983b), and an appreciable amount of oxidative stress experienced during luteolysis is possibly produced by macrophages within the regressing corpus luteum (reviewed by Niswender *et al.*, 2000). Consistent with the concept of decreased cellular protection against oxidative stress in the regressing corpus luteum, levels of mRNA encoding protective enzymes such as superoxide dismutase and catalase are decreased in bovine corpora lutea during luteolysis (Rueda *et al.*, 1995).

Structural luteolysis

Morphological changes associated with structural luteal regression are visible in the late luteal phase. The corpus luteum begins to show signs of degeneration that include shrinkage of lutein cells and vacuolation of the cytoplasm. As regression continues cell shrinkage becomes more pronounced, and nuclear chromatin condensation and pyknosis are apparent (reviewed by Zeleznik and Benyo, 1994). This morphology is typical of cell death by apoptosis. Apoptosis is an active, energy-dependent process by which non-essential populations of cells delete themselves from a tissue (Kerr *et al.*, 1972). Granulosa cells deprived of FSH undergo apoptosis during follicular atresia (Hurwitz and Adashi, 1992; Tilly, 1997), and $PGF_{2\alpha}$ promotes apoptosis in cells comprising the ovine corpus luteum (Sawyer *et al.*, 1990). Apoptosis has been implicated as part of human corpus luteum degeneration (Shikone *et al.*, 1996; Yuan and Giudice, 1997), however, ultrastructural studies in the marmoset suggest cell death during luteolysis is predominately via a process other than apoptosis (Fraser *et al.*, 1999b).

Luteolysis is also associated with regression of luteal vasculature as demonstrated in many species (Niswender *et al.*, 1976; Lei *et al.*, 1991; Zheng *et al.*, 1993; Modlich *et al.*, 1996; Gaytan *et al.*, 1998). There is evidence from some species that luteal blood vessel degeneration is via endothelial cell apoptosis and that endothelial cell injury is an early marker of regression (O'Shea *et al.*, 1977; Azmi and O'Shea, 1984; Behrman *et al.*, 1991). Vascular apoptotic cells have been found in the sheep (Sawyer *et*

al., 1990) and human (Gaytan *et al.*, 1998) corpora lutea during luteolysis. However, if demonstration of this phenomenon is restricted to *in situ* visualisation of DNA fragmentation, this can be limited because endothelial cells have been shown to detach from the vessel wall into the lumen before becoming positive for nucleosomal fragmentation products, and are thus cleared from the corpus luteum in the circulation (Modlich *et al.*, 1996). Depletion of endothelial cells could be a consequence of previous regressive changes in the corpus luteum. Conversely, regression of blood vessels may also trigger degenerative changes leading to functional and/or structural luteolysis. The latter appeals as progesterone synthesis is dependent on uptake of LDL-cholesterol which in turn is dependent on an extensive vascular network supplying every steroidogenic cell with cholesterol precursor, nutrients and O_2 for active steroidogenesis.

1.4.4 Maternal recognition of pregnancy in the primate

The lifespan of the corpus luteum during the normal reproductive cycle is not adequate to provide progesterone for maintenance of pregnancy until the shift to placental progesterone can occur. Maternal recognition of pregnancy involves biochemical communication between the conceptus and its mother to provide uninterrupted synthesis and release of progesterone. There are many species differences concerning the mechanism of maternal recognition of pregnancy. The mechanisms in the primate are unique and involve production of a signal from the conceptus. Trophoblastic cells of the implanting blastocyst secrete chorionic gonadotropin (CG) 8-12 days after fetilisation and the plasma CG level increases exponentially over the first trimester of pregnancy. This rescues the corpus luteum from regression by providing a luteotropic signal. CG is structurally and biologically similar to LH and both interact with the same cell surface receptor (Cameron and Stouffer, 1982; Lapthorn *et al.*, 1994) and directly stimulate the primate corpus luteum to secrete progesterone. The question therefore arises how CG, unlike LH, is able to prevent the corpus luteum from involuting. The half-life of CG in blood is considerably longer than that of LH because of an increased sialic acid content of the β subunit of CG, which results in enhanced biological activity (reviewed by Niswender *et al.*, 2000). Therefore CG provides a more intense and sustained

gonadotropic stimulus to the ageing corpus luteum, overriding its diminished responsiveness to the intermittent LH pulses secreted by the pituitary gland.

1.5 Ovarian vascularisation

Neovascularisation of the ovary is fundamental to its function. The developing follicle appears to be dependent on an extensively vascularised theca layer, and Clark (1900) concluded that "the vital impulse to growth of the theca interna depends not on a maintenance of its primitive blood supply but upon a decided increase of that supply." Today it is known that the establishment and maintenance of preovulatory follicular dominance is dependent on an increased supply of androgen precursors and nutrients and O_2 for active steroidogenesis culminating in the synthesis of oestrogens, and on preferential delivery of gonadotropins to the dominant follicle, which are obtained from the increased blood supply of the follicle. Conversely, reduced thecal vascularisation appears to be a primary component of follicular atresia. Similarly, the vascular remodelling which occurs upon formation of the corpus luteum appears to be critical for normal luteal functioning, although this has not been demonstrated experimentally. To support the phenomenal rate of tissue growth in the corpus luteum, microvascular growth and development also have to be extremely rapid. For example, most luteal cell proliferation occurs in the microvascular compartment (reviewed by Reynolds *et al.*, 2000). As a result, in the mature corpus luteum microvascular endothelial cells and pericytes comprise 50-70% of the total cell population (Farin *et al.*, 1986; Lei *et al.*, 1991). The corpus luteum becomes so vascular that the majority of the steroidogenic cells are in contact with one or more capillaries (Dharmarajan *et al.*, 1985; Reynolds *et al.*, 1992; Redmer and Reynolds, 1996; Reynolds and Redmer, 1998). In addition the mature corpus luteum receives most of the ovarian blood supply, and ovarian blood flow is highly correlated with the rate of progesterone production (Reynolds, 1986; Niswender and Nett, 1994; Reynolds *et al.*, 1994).

It was demonstrated by Gospodarowicz and Thakral (1978) that the newly ovulated follicle produces diffusible angiogenic substances that direct capillary proliferation into the luteinising tissue. More recently, an array of potential angiogenic

growth factors and their receptors have been shown to be present in corpus luteum (Reynolds *et al.*, 1994; Redmer and Reynolds, 1996; Maisonpierre *et al.*, 1997; Goede *et al.*, 1998; Hazzard *et al.*, 1999a). The next section of this review considers the actual process of angiogenesis and reviews the current understanding of the primary factors which are involved in the control of luteal angiogenesis.

1.6 Angiogenesis

The term angiogenesis was first used in anatomical studies of the developing blood vessels of the placenta (Hertig, 1935). Angiogenesis is the process of new blood vessel growth that depends on the sprouting of capillaries from pre-existing vessels, and is essential for normal tissue growth and development (Folkman and Klagsbrun, 1987; Klagsbrun and D'Amore, 1991). It differs from vasculogenesis in which new microvessels arise *in situ* and endothelial cells are born from progenitor cell types, usually during embryonic development (Poole and Coffin, 1989; Risau, 1991). In the adult, angiogenesis is the predominant mechanism of microvascular growth. In most adult tissues, capillary growth occurs only rarely and the vascular endothelium represents a stable population of cells with a low mitotic rate (Denekamp, 1984).

Physiological angiogenesis

Physiological angiogenesis is tightly regulated. It is switched on and off over a brief time scale measured in days. The angiogenesis that occurs in repair of wounds, fractures, peptic ulcers and myocardial infarctions is of slightly longer duration than physiological angiogenesis and its termination is not tightly regulated (Folkman, 1992). Physiological angiogenesis is almost unique to the female reproductive organs: the ovary, uterus and placenta. Intense local angiogenesis is associated with follicular growth, corpus luteum formation, endometrial development, implantation of the fertilised ovum, and development of the placenta. The angiogenesis associated with follicular development and corpus luteum formation has been addressed. Here endometrial and placental angiogenesis is briefly discussed.

In the uterus, the innermost endometrial layer exhibits cyclical growth and vascularisation. In primates, growth of the endometrial vasculature begins during the proliferative (follicular) phase and continues at a lower level throughout the secretory (luteal) phase of the cycle (Meschia, 1983). Associated with endometrial capillary proliferation is increased DNA (deoxyribonucleic acid) synthesis of vascular endothelial cells (Ferenczy *et al.*, 1979). In the cow, endometrial vascularity is greatest in the early secretory phase (Ferenczy *et al.*, 1979). The rate of blood flow to uterine tissues also varies regularly throughout the non-pregnant cycle, being greatest at or just before ovulation when systemic levels of oestrogens are maximal, and least during the luteal phase of the cycle when systemic levels of progesterone are high (Meschia, 1983; Reynolds, 1986).

Placental vascular growth begins early in pregnancy and continues throughout gestation in association with a continued and dramatic increase in rates of uterine and umbilical blood flows (reviewed by Reynolds *et al.*, 1992). The importance of placental vascular development in supporting foetal growth and development has long been recognised (Ferrell, 1989; Meschia, 1983; Teasdale, 1976). In addition, inadequate vascular development may be a major contributor to embryonic loss and reduced birth weights (Ferrell, 1989; Meegdes *et al.*, 1988).

Pathological angiogenesis

In contrast to physiological angiogenesis, pathological angiogenesis is prolonged and often unabated (Folkman, 1992). Rampant and persistent capillary growth is associated with numerous pathological conditions, including tumour growth, retinopathies, haemangiomas, fibroses, and rheumatoid arthritis. Folkman and co-workers were the first to demonstrate that recruitment of a blood supply is required for sustained growth of tumours (reviewed by Folkman and Klagsbrun, 1987; Klagsbrun and D'Amore, 1991). Neovascularisation permits rapid tumour growth mainly because it solves the problem of exchange of nutrients, oxygen and waste catabolites by a crowded three-dimensional cell population. Simple diffusion of these molecules across the outer surface of a tumour spheroid would be inadequate (Folkman, 1992). Similarly, to support the growth of physiological structures such as the ovarian follicle and corpus

luteum angiogenesis must occur. In addition, vascular endothelial cells of growing tumours exhibit an extremely high mitotic rate compared with endothelial cells of most normal tissues (Denekamp, 1984). It has also been demonstrated that the extent of vascularisation of a tumour may have a correlation with survival rate. In patients with advanced ovarian carcinoma, Hollingsworth *et al.,* (1995) demonstrated a trend between higher average vessel counts in the tumour and worse overall patient survival. Similarly, in patients with the same disease, tumour endothelial cell area was compared between patients who survived for more than 6 years and those who died of the disease. The mean endothelial cell area of the survivors was significantly less than that of non-survivors (Schoell *et al.*, 1997).

Conversely, insufficient capillary growth occurs in several disease states, including delayed wound healing, non-healing fractures, chronic varicose ulcers, limb and myocardial ischaemia (Redmer and Reynolds, 1996). There is also a suggestion that inadequate luteal function is associated with decreased vascularisation (Redmer and Reynolds, 1996).

1.6.1 The angiogenic process

The field of angiogenesis research began as an enquiry into the mechanisms of tumour angiogenesis, and much of what is currently known about the angiogenic process at the morphological, biochemical and molecular levels has been gained from the study of how tumours induce angiogenesis (Folkman and Shing, 1992). Before the process of angiogenesis can be explained it is relevant to briefly outline the characteristics and cellular content of the blood vessels which constitute the vascular makeup of organs.

Arteries and arterioles

The arterial vessels are thick walled with variable quantities of elastic fibres. There are three layers within their walls: the inner endothelial lining, which is surrounded by layers of smooth muscle and an outer layer of connective tissue. Medium sized arteries have distinct strips of elastic material between the endothelial cells and smooth muscle layer, and between the smooth muscle layer and the connective tissue. These arteries have between 10 and 40 layers of smooth muscle arranged spirally and the connective

tissue layer is relatively thick. Arterioles have only 1 or 2 layers of smooth muscle cells, elastic fibres may be absent and the connective tissue is thin. The smaller arterioles are surrounded by discontinuous smooth muscle cells and together with larger arterioles contribute significantly to vascular resistance according to the state of relaxation or contraction of their smooth muscle. Endothelial cells contribute to vessel dilation and constriction. In response to changes in blood flow, exposure to histamine or acetylcholine for example, endothelial cells may release nitric oxide which results in vessel dilation, and can release endothelin which causes vasocontriction. Endothelial cells also produce anticoagulant and coagulant factors; the former predominate under normal physiological conditions. In addition, endothelial cells contain glycoproteins such as fibronectin and von Willebrand factor which are prothrombotic, acting to induce platelet plugs if the vessel is injured. The terminal arterioles with a diameter of approximately 30μm, reduce in size to give rise to capillaries, which usually have a diameter of 4-8μm.

Capillaries

Capillaries are endothelial tubes encircled by a basement membrane. Because of the slow blood flow, large surface area and very thin walls, capillaries are well adapted for the exchange of diffusible substances between blood and the surrounding environment. Capillaries are often associated with pericytes, which are contractile type cells located at intervals along the outer circumference of the capillary wall. Pericytes are found adjacent to capillaries in a variety of tissues in many species, continuous with vascular smooth muscle cells of arteries and veins, and distinctively shaped with many cytoplasmic processes that encircle capillaries (reviewed by Hirschi and D'Amore, 1996). Each pericyte possesses a cell body with a prominent nucleus and a small amount of surrounding cytoplasm (reviewed by Hirschi and D'Amore, 1996). Protruding from the cell body are long projections which parallel the long axis of the capillary and taper to smaller processes which encircle the capillary wall. Pericytes are embedded within the basement membrane which surrounds the capillary tubes. *In vitro* evidence suggests that both endothelial cells and pericytes contribute to the formation of the basement

membrane (Mandarino *et al.*, 1993). Their processes penetrate the basement membrane to directly contact the underlying endothelium (Tilton *et al.*, 1979).

Pericytes have a variety of proposed functions including regulation of capillary blood flow and regulation of new capillary growth (Hirschi and D'Amore, 1996). Pericytes exhibit a number of characteristics consistent with muscle cell activity and their location in capillaries would enable then to regulate the contraction of the underlying endothelium. The presence of actin in pericytes has been demonstrated in the cytoplasmic processes adjacent to the vessel lumen (Le Beux and Willemot, 1978; Wallow and Burnside, 1980). There is a suggestion of pericyte heterogeneity based on their expression of α-smooth muscle actin (α-SMA). Nehls and Drenckhahn (1991) found that only the pericytes of pre- and post-capillary microvessels of bovine retina expressed α-SMA, whereas mid-capillaries had no detectable levels. However, Hirschi and D'Amore (1996) suggest that lower levels of α-SMA may be present in pericytes of mid-capillaries that were not detectable by the methods used, and report of many findings of α-SMA in pericytes both *in vivo* and *in vitro*. Alpha-smooth muscle actin was not detectable in endothelial cells in culture or *in vivo* (Boado and Pardridge, 1994; Hirschi and D'Amore, 1996).

A study of mesenteric capillary growth in rats (Rhodin and Fujita, 1989) suggests that fibroblasts transform into capillary pericytes, which in turn, become vascular smooth muscle cells. This has been confirmed more recently (reviewed in Folkman and D'Amore, 1996). Hence, as capillaries are remodelled into larger vessels to meet an increased functional demand, pericytes are further differentiated to become true smooth muscle cells, as needed.

Venules and veins

Once blood leaves a capillary network it enters the first and smallest sized vessels of the venous vascular system, the post-capillary venules, which are 10-30μm in diameter. They also contain pericytes but have no smooth muscle layer as such. Larger venules of more than 50μm, begin to show some smooth muscle fibres and enlarge to form veins. Generally veins have a larger diameter than any accompanying artery, with a thinner

wall that has more connective tissue and less muscle fibres. Most medium sized veins have valves which prevent backflow of blood which is travelling at low pressure.

New capillary growth

New capillaries originate from pre-existing microvasculature, mainly from capillaries and venules, rather than large vessels with layers of smooth muscle. The development of a new capillary network is a complex process involving tissue disruption and reorganisation, cellular growth and changes in the composition of the fluid environment and the extracellular matrix (Folkman, 1985; Schor and Schor, 1983). The angiogenic process begins with capillary proliferation and culminates in the formation of a new microcirculatory bed composed of arterioles, capillaries and venules. The initial component of angiogenesis, capillary proliferation, consists of at least three processes: 1) Fragmentation of the basement membrane of the existing vessel and degradation of the extracellular matrix, on the side closest to the angiogenic stimulus. This is thought to result from the activity of collagenase and other matrix metalloproteinases (MMPs) and plasminogen activator secreted by the endothelial cells in response to the angiogenic stimulus. 2) Migration of elongated endothelial cells as cords of cells from the existing vessel towards the angiogenic stimulus. 3) Proliferation of endothelial cells occurring behind the tip of the growing capillary. The cells at the tip do not usually divide (Findlay, 1986; Folkman and Klagsbrun, 1987; Klagsbrun and D'Amore, 1991). Neovascularisation is completed by formation of capillary lumina, by cessation of endothelial cell proliferation, curvature of the endothelial cell and adherence to each other to form the capillary lumen. Canalisation follows as individual sprouts join or anastomose with each other. The newly formed vessels differentiate into arterioles and venules, as pericytes emerge along the length of the sprout. Blood flow begins slowly as the new vessels are highly permeable until the basement membrane is laid down and pericyte stabilisation is complete (Findlay, 1986).

Capillary proliferation

The major component of capillary growth is endothelial cell proliferation. Endothelial cells of normal, resting vasculature are quiescent due to their confluent nature,

unresponsiveness to growth factors, and the association of pericytes. Signals such as angiopoietin-2 (Section 1.6.3) cause dissociation of pericytes and endothelial cells allowing access of growth factors and activation of proteases *etc.* for basement membrane degradation, and endothelial cells begin to migrate toward the angiogenic stimulus. The change in shape of endothelial cells to a more elongated configuration confers responsiveness to mitogens (Ingber and Folkman, 1989). Under mitogenic stimulation, endothelial cells leave the G_0 resting phase of growth and re-enter the cell cycle. Proliferation of endothelial cells can be measured by quantifying the expression of specific proteins associated with the cell cycle, or by the incorporation of nucleotide analogues during the DNA synthesis phase of growth. Studies using these approaches have quantified luteal endothelial cell proliferation in the human (Rodger *et al.*, 1997; Gaytan *et al.*, 1998) rhesus macaque (Christenson and Stouffer, 1996b), ovine (Jablonka-Shariff *et al.*, 1993) and bovine (Zheng *et al.*, 1994) and all demonstrate peak endothelial cell proliferation in the early luteal phase in association with corpus luteum formation, whereas luteal regression was associated with a decreased proliferative rate. It has been suggested that endothelial cell proliferation is not a major factor contributing to the initial increase in vessel density in tumours (Gasparini *et al.*, 1996; Orre *et al.*, 1998). They suggest that incorporation of endothelial cells from surrounding vasculature, remodelling of the existing vasculature and decreased endothelial cell apoptosis contribute to increased vessel densities in certain kinds of tumour. Therefore when measuring capillary growth both endothelial cell proliferation and endothelial cell content in the population being studied should be considered.

Capillary stabilisation

Pericytes from pre-existing microvessels, or newly derived pericytes from fibroblast differentiation, come into contact with endothelial cells that are forming new vessels and exert an inhibitory effect on endothelial cell proliferation (Crocker *et al.*, 1970). The inhibitory effect is induced by cell-cell contact between pericytes and endothelial cells. Early in angiogenesis, during endothelial cell migration and proliferation, pericytes appear to play a different role in capillary sprouting. Nehls *et al.*, (1992) demonstrated that pericytes were regularly found lying at and in front of the advancing tips of

endothelial sprouts. At many sites pericytes were seen to bridge the gap between the edges of opposing endothelial sprouts, which were apparently preparing to merge, suggesting that pericytic processes may serve as guiding structures aiding outgrowth of endothelial cells. However, pericyte association (contact) with growing vessels marks the cessation of vessel growth and the deposition of a basement membrane (Crocker *et al.*, 1970).

In co-culture of pericytes and endothelial cells, cell-cell contact leads to the activation of latent transforming growth factor-β (TGF-β) that is produced by both cell types (Antonelli-Orlidge *et al.*, 1989). Transforming growth factor-β inhibits endothelial cell proliferation. Endothelial cells can also influence pericyte growth, depending on their morphology and stage of growth. Endothelial cells *in vitro* are refractory to growth factors when they are confluent, that is foreshortened (Ingber and Folkman, 1989), and media conditioned by post-confluent endothelial cells are strongly inhibitory for pericyte growth (Dodge *et al.*, 1993). Endothelial cell spreading increases sensitivity to specific growth factors (Ingber, 1990) and media collected from such endothelial cells are mildly stimulatory for pericyte growth (Dodge *et al.*, 1993).

Endothelial cells themselves are thought to be responsible for the recruitment and differentiation of mural cells, such as pericytes and smooth muscle cells, by the secretion of diffusible factors (Hirschi and D'Amore, 1996). Among the diffusible soluble factors synthesised and secreted by endothelial cells, are a variety of polypeptide growth factors, including platelet derived growth factor (PDGF) (Westermark *et al.*, 1990) and basic fibroblastic growth factor (bFGF) (Montesano *et al.*, 1986), which appear to function in a paracrine fashion to promote mural cell proliferation and or migration. Microcapillary endothelial cells express PDGF-B, and PDGF-B-receptor mRNA is readily detectable in fibroblast-like cells and smooth muscle cells (Holmgren *et al.*, 1991). Hirschi *et al.*, (1998) using an *in vitro* co-culture system of endothelial cells and smooth muscle cell precursors, demonstrated that endothelial cells induced migration of smooth muscle cell precursors, via PDGF-B, and these mural precursors differentiated into smooth muscle cells in the presence of endothelial cells but not when cultured alone, which was shown to be driven by TGF-β. In addition, PDGF-B ligand null mice die perinatally from haemorrhage and are reported to lack pericytes throughout the entire

microvascular bed (reviewed by Folkman and D'Amore, 1996). Basic FGF is angiogenic as well as mitogenic (D'Amore and Smith, 1993) and chemotactic (Sato *et al.*, 1991) for smooth muscle cells. Gap junctional formation and cellular adhesion molecules are also thought to mediate endothelial cell-pericyte interactions (Hirschi and D'Amore, 1996).

Neovascular regression

Two types of vascular regression have been demonstrated. Firstly, when an angiogenic stimulus is removed, microthrombosis of the capillary tips occurs before the subsequent disappearance of new blood vessels (Ausprunk *et al.*, 1978). Platelet thrombi accumulate at the tips of new capillaries, followed by stasis of the circulation in the more proximal capillary network. Macrophages infiltrate the new capillary bed, enter the lumen, and begin to phagocytose injured or dying endothelial cells. After a few days the tubular remnant of blood vessel contains mainly basement membrane without endothelial cells. The tubular structure gradually retracts and disappears (Folkman, 1992). A second type of involution is illustrated by endothelial cell rounding and detachment. Instead of microthrombosis, there is a gradual foreshortening and rounding of capillary endothelial cells over a period of about 24-48 hours which occurs after dissociation of pericytes from the vessel. These cells begin to detach, presumably dying by apoptosis, float in the lumen and are cleared by the circulation *in vivo*. The new capillary then retracts back into the parent venule from which it arose (Folkman, 1992).

1.6.2 Angiogenesis assays

Angiogenesis in normal tissues must remain in a constant state of readiness yet be held in check for long periods of time (Folkman and Klagsbrun, 1987). Angiogenesis is therefore thought to be regulated by both angiogenic and anti-angiogenic factors (Folkman and Klagsbrun, 1987; Klagsbrun and D'Amore, 1991) which remain to be identified in order for the process to be understood. The development of *in vivo* and *in vitro* assays over the last two decades has made possible the isolation and characterisation of some of these angiogenic and anti-angiogenic factors from numerous tissues (Folkman and Klagsbrun, 1987; Klagsbrun and D'Amore, 1991).

In vivo *assays*

In vivo methods have been used to evaluate the ability of a factor to influence neovascularisation, that is to influence the entire process of angiogenesis (Folkman and Klagsbrun, 1987; Klagsbrun and D'Amore, 1991). The most commonly used techniques are the corneal pocket assay, which permits linear measurement of capillary growth induced by a substance implanted into the cornea of a rabbit, mouse or rat, and the chorio-allantoic membrane (CAM) assay, which evaluates the ability of a substance to stimulate or inhibit neovascularisation when placed into the CAM of a chicken embryo (Folkman and Klagsbrun, 1987; Klagsbrun and D'Amore, 1991). A significant observation was that tissues from tumours, corpora lutea, uteri and placentae induce a neovascular response in the CAM assay, whereas most other foetal or adult tissues do not (Redmer *et al.*, 1988; Klagsbrun and D'Amore, 1991; Reynolds *et al.*, 1992).

In vitro *assays*

In contrast to *in vivo* techniques, *in vitro* assays evaluate the ability of a factor to influence one of the individual components of the angiogenic process. The assay tests the ability of a substance to influence 1) production of proteases by endothelial cells; 2) migration of endothelial cells, by the separation of endothelial cells and a test solution by a porous membrane, so that migration across the barrier is indicative of a chemoattractant present in the test solution; or 3) proliferation of endothelial cells, which measures either increased cell number or the incorporation of radiolabelled or modified nucleotides to detect cells in the S phase of the cell cycle (Folkman and Klagsbrun, 1987). Factors identified by these *in vitro* assays are likely to have similar effects *in vivo*, since close agreement has been shown among *in vitro* and *in vivo* assays for angiogenic factors (Folkman and Klagsbrun, 1987; Redmer *et al.*, 1988; Reynolds *et al.*, 1992). Nevertheless the angiogenic factors identified by using the *in vitro* assays need to be confirmed with one of the *in vivo* bioassays described above (Klagsbrun and D'Amore, 1991; Reynolds *et al.*, 1992). Bovine corpus luteum obtained from three stages of the oestrous cycle (early, developing corpus luteum; mid-cycle, mature corpus luteum; late cycle, regressing corpus luteum) produced angiogenic activity, as confirmed

by *in vivo* (CAM) and *in vitro* (endothelial cell migration and proliferation) assays (Redmer *et al.*, 1988).

1.6.3 Angiogenic growth factors

Much of the work on angiogenesis and its regulation has focused on pathological processes. However, during the last 10-15 years, many growth factors and cytokines have been found in luteal extracts, luteal cells, or luteinised granulosa cells in culture (reviewed by Reynolds *et al.*, 1994). A major finding from these studies was that the angiogenic activity present in media conditioned by bovine follicles and bovine and ovine corpus luteum binds relatively strongly to heparin affinity columns (Reynolds *et al.*, 1992; Grazul-Bilska *et al.*, 1992; Grazul-Bilska *et al.*, 1993; Reynolds *et al.*, 1994; Grazul-Bilska *et al.*, 1995). This observation led Reynolds *et al.*, (1992; 1994) to hypothesise that these ovarian angiogenic factors belong to one of the families of heparin-binding angiogenic factors, namely the fibroblastic growth factors (FGF) or the vascular endothelial growth factors (VEGF).

More recently a third family, the angiopoietins, quite distinct from the heparin-binding growth factors have been localised in the rat ovary (Maisonpierre *et al.*, 1997). Histological techniques have proved essential to the elucidation of the potential roles of some of these factors. Immunocytochemical staining for various growth factors and their receptors demonstrates the location of expression, *i.e.* the cell type, and receptor localisation indicates a site of action. By quantifying such expression throughout the reproductive cycle and using previous knowledge concerning the angiogenic activity of the tissue, perhaps from cell proliferation studies, potential roles of such growth factors in the process of angiogenesis can be established.

Fibroblastic growth factors

Using the aforementioned assays the first inducer of angiogenesis discovered, in 1982, was basic fibroblastic growth factor (bFGF), followed shortly by its relative acidic FGF (aFGF) (reviewed by Hanahan and Folkman, 1996). Each protein is unusual in its lack of a traditional sequence for secretion. Both however, can be released from cells under certain circumstances (reviewed by Hanahan and Folkman, 1996). A correlation

between expression of FGFs and angiogenic activity of a tissue has not been demonstrated. Similar amounts of bFGF protein and mRNA were present across all stages of the ovine and bovine oestrous cycles (reviewed by Reynolds *et al.*, 2000), and receptors for FGFs increased during the late luteal phase, the least angiogenic stage, therefore, it is not clear what function these factors play as angiogenesis occurs primarily early in the luteal phase (reviewed by Reynolds *et al.*, 2000). It is known that FGFs and other angiogenic factors can be sequestered in the ECM (extracellular matrix) of many cell types, including endothelial cells, presumably to be released by proteolytic degradation of the matrix (Baird and Ling, 1987; Folkman *et al.*, 1988), so it may be the activation of sequestered growth factors which confers their angiogenic nature.

Vascular endothelial growth factors

In 1983, a secreted protein was identified by its ability to elicit vascular permeability (Senger *et al.*, 1983); subsequently this factor, VEGF was shown to be a potent inducer of angiogenesis (reviewed by Brown *et al.*, 1996; Ferrara and Davis-Smyth, 1997). VEGF is a dimeric glycoprotein which elicits a strong angiogenic response in *in vivo* models including the CAM (Leung *et al.*, 1989; Plouet *et al.*, 1989), and the rabbit cornea (Phillips *et al.*, 1994). VEGF, which has three tyrosine kinase receptors that are located on endothelial cells (Flt-1, KDR/Flk-1 and Flt-4), is a potent mitogen, morphogen and chemoattractant for endothelial cells and is stimulated by hypoxia, cytokines and various hormones (reviewed by Klagsbrun and D'Amore, 1996). Development of blood vessels in the embryo is dependent on VEGF as the formation of vessels in mouse embryos lacking a single VEGF allele, was aberrant and resulted in embryonic lethality (Ferrara *et al.*, 1996). VEGF also increases expression of plasminogen activators (Pepper *et al.*, 1991) and collagenase (Unemori *et al.*, 1992), consistent with the predegradative environment that facilitates migration and sprouting of endothelial cells. VEGF can induce nitric oxide and so may mediate the vasodilation and increased blood flow that precedes angiogenesis (Ku *et al.*, 1993).

A number of isoforms of VEGF, resulting from mRNA splice variations of the transcribed VEGF gene, have been discovered. The 121 and 165-amino acid variants predominate. $VEGF_{121}$ is freely soluble and does not bind to heparin. $VEGF_{165}$ binds to

heparin and can be secreted or may bind to the cell surface and ECM. The larger isoforms, $VEGF_{189}$ and $VEGF_{206}$ are sequestered in the ECM and can be cleaved to release a diffusible proteolytic fragment, $VEGF_{110}$ (reviewed by Ferrara and Davis-Smyth, 1997).

VEGF binds with high affinity to two tyrosine kinase receptors, Flt-1 (*fms*-like tyrosine kinase-1) and KDR (Vaisman *et al.*, 1990). Binding of VEGF causes receptor dimerisation followed by autophosphorylation and signal transduction. There are significant differences in VEGF function depending on the receptor utilised. Disruption of the gene encoding Flt-1 does not prevent the early differentiation of endothelial cells but impairs development of functional vessels. Activation of Flt-1 results in autophosphorylation of receptor but does not activate the MAP kinase cascade and does not mediate mitogenic action of VEGF, it mainly promotes cell migration (Fong *et al.*, 1995). Disruption of the KDR gene prevents the differentiation of haemangioblasts into endothelial cells and prevents endothelial cell proliferation. VEGF stimulation of the receptor results in receptor autophosphorylation and activation of the MAP (mitogen activated protein) kinase cascade, resulting in increased expression of early response genes and stimulation of endothelial cell proliferation (Fong *et al.*, 1995). The distribution and role of Flt-4 seems to be restricted to venous and lymphatic vessels (Joukov *et al.*, 1996).

VEGF expression in the ovary has been documented in rats (Phillips *et al.*, 1990), the cynomolgus monkey (Ravindranath *et al.*, 1992a) and humans (Gordon *et al.*, 1996; Otani *et al.*, 1999). Yan *et al.*, (1993; 1998) have demonstrated VEGF expression in luteinising granulosa cells aspirated during IVF oocyte retrieval, and suggest that this factor serves as a paracrine signal in corpus luteum formation. In the corpus luteum granulosa lutein cells are strongly positive for VEGF in the early luteal phase, suggesting that luteinising granulosa cells are influenced by the LH surge and ovulation and are associated with an increased level of VEGF expression (Ravindranath *et al.*, 1992a; Kamat *et al.*, 1995; Neulen *et al.*, 1998). VEGF mRNA and protein expression is stimulated by increased LH or hCG levels, in cultured bovine and human granulosa cells (Gospodarowicz *et al.*, 1985; Neulen *et al.*, 1995; Christenson and Stouffer, 1997; Neulen *et al.*, 1998). In patients with polycystic ovarian syndrome characterised by

hypersecretion of LH, intense staining for VEGF occurs in both granulosa and theca cells, suggesting that VEGF expression is regulated by gonadotropins, especially LH and hCG (Kamat *et al.*, 1995), and functions in the corpus luteum.

VEGF is required to inhibit apoptosis of endothelial cells not associated to pericytes. These immature cells are susceptible to falling levels of VEGF causing disassembly of young vessels, leaving intact those mature vessels with associated pericytes. This has been shown in some prostate cancers where androgen ablation, caused VEGF withdrawal which in turn led to the selective demise of immature vessels not coated with pericytes (Benjamin *et al.*, 1999). Also in the late luteal phase, studies have shown a correlation with a decrease in VEGF and relative increase in the proportion of mature, pericyte coated vessels, which are said to function independently of VEGF (Goede *et al.*, 1998).

The family of VEGF-related molecules has recently grown and contains five mammalian family members: VEGF (referred to as either VEGF or VEGF-A), placental growth factor (PlGF), VEGF-B, VEGF-C and VEGF-D. PlGF expression is not restricted to the placenta, 3 forms have been described, which bind with high affinity to Flt-1 only (Park *et al.*, 1994). PlGF can potentiate the activity of suboptimal concentration of VEGF-A (Park *et al.*, 1994). However, because it can form heterodimers with VEGF-A, which are less potent than VEGF-A homodimers, PlGF may reduce the bioavailability of active VEGF-A molecules (Cao *et al.*, 1996). PlGF can stimulate angiogenesis in the rabbit cornea assay, and the mitogenic effect of PlGF is dependent on endothelial cell type, therefore it has been suggested that the preferential target of PlGF is the endothelium of postcapillary venules (Ziche *et al.*, 1997).

VEGF-B is particularly abundant in heart and skeletal muscle. Two isoforms have been detected: VEGF-B_{167}, which remains associated with the cell or extracellular matrix, and VEGF-B_{186}, homodimers of which are readily secreted (Olofsson *et al.*, 1996). In a similar way to PlGF, VEGF-B can heterodimerise with VEGF-A and influence the bioavailability of this molecule (Olofsson *et al.*, 1996). Mice lacking VEGF-B are healthy and fertile although hearts are reduced in size which signifies a role for VEGF-B in the development or function of coronary vasculature (Bellomo *et al.*, 2000).

VEGF-C binds to KDR and with greater affinity to the Flt-4 receptor. It increases vascular permeability and stimulates migration and proliferation of endothelial cells. VEGF-C is expressed during embryonic development in regions where lymphatics sprout from venous vessels (Kukk *et al.*, 1996). It is expressed in adult tissues and is postulated to play a role in the maintenance of lymphatic endothelial differentiation (Kukk *et al.*, 1996). VEGF-D is the newest member of the VEGF family, and is 48% identical to VEGF-C. It is strongly expressed in the foetal lung during development, and in the adult, it is primarily found in skeletal muscle, heart, lung and intestine (Yamada *et al.*, 1997).

The functions of these other VEGF family members in angiogenesis in the adult are unclear. PlGF and VEGF-B may play a role in the modulation of VEGF-A actions. Expression of these factors has not been clearly demonstrated in the primate ovary and so a role in ovarian angiogenesis remains to be elucidated. There is compelling evidence to suggest that VEGF-A plays a major role in physiological angiogenesis, it is expressed in the ovary and has multiple functions promoting the angiogenic process.

Angiopoietins

Over the last 3-4 years another family of angiogenic growth factors, the angiopoietins, have been discovered. Angiopoietin-1 (Ang-1) and Angiopoietin-2 (Ang-2) are specific for the endothelial cell receptor tyrosine kinase, Tie-2 (Tyrosine dinase with immunoglobulin and epidermal growth factor homology domains, also known as TEK). Ang-1 is an agonist for the receptor inducing autophosphorylation, whereas, Ang-2 is a naturally occurring antagonist, which has the same affinity for the receptor but does not induce phosphorylation. There is another related receptor, Tie-1, the ligand(s) for which have not been identified. The general functions of the Tie-2 receptor have been deduced from studies in mice where the gene has been removed or over expressed. (Puri *et al.*, 1995; Sato *et al.*, 1995; Suri *et al.*, 1996; Vikkula *et al.*, 1996; Maisonpierre *et al.*, 1997). The absence of Tie-2 or its agonist Ang-1 prevents normal angiogenesis (Sato *et al.*, 1995; Suri *et al.*, 1996), demonstrated by the severe retardation of remodelling and stabilisation of primitive vasculature, it also has a direct action on endothelial cell survival (Papapetropoulos *et al.*, 1999). *In vitro*, Ang-1 has no control over endothelial

cell proliferation but stimulates vessel sprouting (Koblizek *et al.*, 1998), Ang-2 inhibits this effect (Maisonpierre *et al.*, 1997). Similarly, mouse embryos with over expressed Ang-2 have defects similar to those lacking Tie-2 or Ang-1 (Maisonpierre *et al.*, 1997). In the adult, Ang-1 appears to be constitutively expressed serving to maintain the integrity of the already established vasculature (Maisonpierre *et al.*, 1997; Witzenbilcher *et al.*, 1998). The effect of Ang-1, has been attributed to a role in pericyte-endothelial cell interactions and stabilisation of the neovasculature.

In the presence of Ang-2 the role of Ang-1 is decreased by competitive inhibition at the receptor level. Ang-2 when implanted with VEGF to the cornea promoted angiogenic activity culminating in the formation of long, wide and immature vessels (Asahara *et al.*, 1998). Detailed localisation of Ang-2 mRNA in the rat ovary revealed that Ang-2 was either expressed at regions of active angiogenesis together with VEGF at sites of vessel sprouting and ingrowth, in the early corpus luteum, or at sites of vascular regression in the absence of VEGF, in atretic follicles (Maisonpierre *et al.*, 1997). This led to the hypothesis that Ang-2 causes destabilisation of the vessels by preventing Ang-1-induced pericyte-endothelial cell associations, facilitating vessel sprouting in response to VEGF; and that in the absence of VEGF Ang-2 destabilisation results in regression of the vasculature. Temporal changes in the expression of angiopoietins and VEGF in the rat ovary have been described and support this hypothesis of angiopoietin/VEGF regulation of angiogenesis (Maisonpierre *et al.*, 1997). Control of luteal function differs markedly between species and it is not known whether similar relationships between positive and negative mechanisms exist in the primate corpus luteum.

1.6.4 Anti-angiogenic factors

Endogenous

It appears that most endogenous angiogenesis inhibitors are stored as cryptic parts of larger molecules that are not themselves inhibitors of angiogenesis, with the exception of non-specific inhibitors such as platelet factor-4 and certain interferons. This prototype came from the discovery that a 29kDa (kilodalton) fragment of fibronectin inhibited endothelial cell proliferation *in vitro* (Homandberg *et al.*, 1985). Subsequently, a fragment of prolactin, the 16kDa fragment, was shown to be an inhibitor of endothelial

cell proliferation, whereas the intact fragment was not (Ferrara *et al.*, 1991; Clapp *et al.*, 1993). Also a potent inhibitor of angiogenesis, angiostatin, has been identified as a fragment of plasminogen (O'Reilly *et al.*, 1994). In tumour cases, circulating angiostatin is able to maintain the dormancy of metastases and primary tumours by blocking blood vessel growth, resulting in small nests of tumour cells that cycle through proliferation and apoptosis, restrained by their inability to induce angiogenesis to support their growth (O'Reilly *et al.*, 1994; Holmgren *et al.*, 1995). More recently, endostatin, a proteolytic cleavage product of collagen XVIII, itself a normal component of the basement membranes that envelope the vascular tubes formed by endothelial cells, inhibited subcutaneous growth of four tumour types reducing tumour volume by more than 90% (O'Reilly *et al.*, 1997).

The capability to release inhibitor fragments from storage as cryptic segments of abundant proteins may contribute to maintaining the normal quiescence of the vasculature and to turning off transitory angiogenic processes such as wound healing. Hanahan and Folkman (Hanahan and Folkman, 1996) suggest for tumour angiogenesis at least, that the switch to the angiogenic phenotype depends on the balance between expression of active angiogenic factors and inhibitors. They suggest that when the levels of inhibitors are sufficiently high, the signals of the positive activator(s) are overruled, keeping (or turning) the angiogenic switch off. And when the expression of angiogenic growth factors increases, most likely in the face of declining inhibition, the balance shifts and angiogenesis ensues. Activation of intense angiogenesis during the formation of the corpus luteum could be triggered from such a shift in balance. Angiogenesis inhibitors are blood or blood vessel borne and could be present in the extensive follicular vasculature, maintaining the low level of angiogenic activity necessary for the maintenance of follicular dominance. The balance may then shift, under stimulation from the LH surge, to increased production of angiogenic inducers, such as VEGF, which initiate a prolific angiogenic response.

Exogenous

In addition to endogenous inhibitors, synthetic compounds with anti-angiogenic activity have been identified using cell culture assays. In 1990, Ingber *et al.*, (1990) discovered a

fungal contamination that induced a local gradient of endothelial cell rounding, but was not toxic. Further work led to the isolation and identification of the fungus *Aspergillus fumigatus*. The active fraction was identified as a naturally secreted antibiotic fumagillin. TNP-470 (also known as AGM-1470) is a synthetic analogue that retains the potent anti-angiogenic activity of fumagillin without its toxic side effects. *In vitro*, both fumagillin and TNP-470 inhibit endothelial cell proliferation, migration and capillary tube-like formation with a minimal effect on growth of non endothelial cells. Systemic administration of TNP-470 inhibits bFGF-induced neovascularisation in subcutaneous sponge implants (Kusaka *et al.*, 1991) and has marked anti-tumour activity (Brem and Folkman, 1993). Klauber *et al.*, (1997) demonstrated that when non-pregnant cycling female mice were treated with TNP-470 an inhibition of both corpus luteum and endometrial maturation occurred. Exposure of pregnant mice resulted in complete failure of embryonic growth as a result of interference with decidualisation reflecting impaired endothelial maturation.

Other exogenous inhibitors of angiogenesis have been found. Suramin is a polyunsulphonated naphthylurea that blocks angiogenesis at several points. Initially it binds to heparin-binding growth factors, suppressing cell proliferation and interferes with the expression of cell adhesion molecules and produces significant cell shape changes, thus reducing the capacity of endothelial cells to respond to growth factors (Fan *et al.*, 1995). Platelet factor-4 has anti-coagulent activity which could create problems in its use as an angiogenic inhibitor. A recombinant synthesised version (rPF-4-241) has been developed in which the heparin binding site has been mutated and so the molecule has no anti-coagulent activity (Maione *et al.*, 1991). Suppressers of protease activity such as tissue inhibitors of matrix metalloproteinases (TIMPs) occur naturally and keep MMP activity in check in normal non-angiogenic tissues. A synthetic non-peptide MMP inhibitor, batimastat, has been shown to strongly inhibit tumour growth in murine models (Davies *et al.*, 1993).

With the increased knowledge of the factors which control angiogenesis monoclonal antibodies and soluble receptors have been developed to specifically inhibit growth factor biological activity, and have potential therapeutic use. Because VEGF is specific for endothelial cell receptors, VEGF is a promising target for the development

of specific anti-angiogenic drugs. Soluble VEGF receptor has been shown to inhibit angiogenesis *in vitro* (Kendall and Thomas, 1993), and antibodies to VEGF have been demonstrated to block tumour growth in three mouse models (Kim *et al.*, 1993). In addition, research has been carried out on the development of treatments to selectively inhibit protein tyrosine kinases and specifically kill endothelial cells. The selective tyrosine kinase inhibitors, lavendustin A and genistein, were shown to suppress the angiogenic action of VEGF in rats (Hu and Fan, 1995), and inhibit the growth of cultures of proliferating endothelial cells (Fotsis *et al.*, 1993), respectively. The selective toxicity of endothelial cells has been reported by the administration of a chemically linked recombinant VEGF conjugated to a truncated from of diphtheria toxin to mice with established subcutaneous tumours. The VEGF-toxin was shown to be selectively toxic to endothelial cell lines, inhibited experimental neovascularisation of the CAM (chorio-allantoic membrane), and the conjugate-treated animals displayed a significant inhibition of tumour growth with the absence of injury to highly vascularised normal tissues (Olson *et al.*, 1997).

1.7 Clinical relevance of luteal angiogenesis research

The physiological angiogenesis that occurs in the corpus luteum and other female reproductive organs occurs in a cyclical manner and therefore must be tightly regulated. Growth and development of the ovarian preovulatory follicle and subsequent formation of the corpus luteum is believed to be dependent on associated intense angiogenic activity for the supply of oxygen, nutrients, steroid precursors and gonadotropic stimulus for normal functioning. The corpus luteum is critical for successful maintenance of pregnancy in mammals because it is the primary source of the progestational hormone progesterone. In the corpus luteum in the absence of conception, this intense angiogenesis is followed by programmed cell death culminating in luteal vascular regression and luteolysis so that the next cycle can commence. This tight physiological control contrasts to that of tumours in which prolonged and often unabated angiogenesis takes places. This raises the possibility that endogenous inhibitors of angiogenesis play

an integral role in the reproductive tract. Therefore these tissues represent an outstanding, readily available system in which to study physiological angiogenesis.

The clinical relevance of such studies becomes apparent. The inhibition of luteal angiogenesis could lead to defects in progesterone production and provide a novel approach to post-ovulatory fertility control. Administration of the angiogenic inhibitor TNP-470, to cyclical mice resulted in inhibition of corpus luteum formation and endometrial maturation (Klauber *et al.*, 1997). Such luteal angiogenesis is believed to be necessary for progesterone production, which in turn is essential for the establishment of pregnancy. Therefore, inhibition of luteal angiogenesis could lead to decreased luteal function and failure to establish pregnancy. Conversely, promotion of ovarian angiogenesis, particularly in the follicle, could help treat some infertile conditions such as luteal phase deficiency, which is characterised by low plasma progesterone concentrations, and is primarily caused by an under developed follicle.

The association of angiogenesis and tumour growth and metastasis has been well documented. The growth of any tissue mass, demonstrated by Folkman in tumours, is dependent on an ever increasing vascular supply for provision of oxygen, nutrients and growth factors (Folkman *et al.*, 1985). Increased microvessel densities are characteristic of advanced tumours and are demonstrated to have a bearing on potential metastasis and patient survival. The corpus luteum offers a unique opportunity to study the factors involved in regulation of angiogenesis *in vivo* and may have direct clinical relevance on research into tumour biology.

1.8 Aims of the thesis

At the beginning of this project little was known about the effect of inhibition of the highly active physiological angiogenesis that occurs in the reproductive tissues, especially in the primate corpus luteum. The aims of this thesis were to increase our understanding of the control of primate luteal angiogenesis, and assess its role in luteal function, by specifically inhibiting this process in the marmoset monkey, and at the same time to develop a working primate model to test putative angiogenic inhibitors.

Before the effects of such putative angiogenesis inhibitors could be examined in the marmoset, increased knowledge of the control of angiogenesis in the corpus luteum of this species was needed. Firstly, the primary objectives of the thesis were to examine the angiogenic activity associated with the luteal phase, using semi-quantitative immunocytochemical methods to measure parameters of angiogenesis, such as endothelial cell proliferation, luteal endothelial cell content, and expression of the angiogenic growth factor, VEGF. Secondly, the periods of most prolific angiogenesis were targeted for inhibition by *in vivo* administration of potential luteal angiogenesis inhibitors. To assess the endocrine control of luteal angiogenesis, a GnRH antagonist was used. Subsequent studies targeted the angiogenic process directly with the use of TNP-470 and VEGF immunoneutralisation. The efficacy of such treatments were addressed by examining parameters of the angiogenic process, and their effects on luteal function determined by measurement of plasma progesterone concentrations. Lastly, the availability of hCG rescued human corpus luteum provided an opportunity to assess the contribution of angiogenic activity to the mechanisms of luteal rescue in early pregnancy; and to investigate the endogenous molecular control of luteal angiogenesis by analysing the relationship in expression of the angiopoietins, their Tie-2 receptor, and VEGF-A and its Flt-1 and KDR receptors.

Chapter 2

Subjects, Tissue Collection and General Materials and Methods

2.1 Sources of reagents, enzymes and antibodies

All reagents and Rnase (ribonuclease)-free H_2O were obtained from Sigma Chemical (Poole, Dorset, UK), all enzymes were from Promega (Promega UK, Southampton, UK), and all antibodies were from Dako Ltd., (High Wycombe, Bucks, UK), unless otherwise stated.

2.2 Experimental models

The marmoset monkey (*Callithrix jacchus*) was the animal model used for this *in vivo* exploration of luteal angiogenesis. Rodents were not suitable because the mechanisms which regulate luteal function in rodents and primates are markedly different, and in the non-fertile cycle of the rodent, the corpus luteum is active for less than a day, while that of many primates is functional for at least 2 weeks prior to its regression (Behrman *et al.*, 1993). The common marmoset is becoming more popular for biomedical science research. Some salient features of this versatile animal are: ease of handling, fecundity, absence of post-partum acyclicity related to lactation, and quick sexual maturation (Torii *et al.*, 1996).

2.2.1 The marmoset ovulatory cycle

The marmoset ovulatory cycle lasts approximately 28 days and there are usually two or three ovulations (Harding *et al.*, 1982; Hearn, 1983). The follicular phase lasts about 8 or 9 days (Harding *et al.*, 1982). In most cycles the 2 or 3 follicles grow at similar rates and ovulation occurs at approximately 12 hour intervals (Torii *et al.*, 1996). Follicular growth in primates was believed to be suppressed until the end of the luteal phase (Baird *et al.*, 1975; diZerega and Hodgen, 1981). However, Summers *et al.*, (1985) have demonstrated that an average interval of 10.7 days is required for growth of follicles to the ovulatory stage after the sudden termination of the corpus luteum with $PGF_{2\alpha}$ analogue, indicating that follicular growth begins during the last two days of the natural luteal phase, concomitant with a gradual decline in circulating progesterone and estradiol as luteal function is ending.

The luteal phase lasts approximately 20 days (Harding *et al.*, 1982). The primate corpus luteum is dependent on trophic support of LH from the pituitary gland. LH binds specifically to the LH receptor, a seven transmembrane G-protein-coupled receptor (Segaloff and Ascoli, 1993) on the surface of luteal cells, to stimulate steroidogenic enzymes to produce progesterone via an increase in intracellular cAMP. Luteal function in the marmoset is dependent on continuing LH secretion (Fraser *et al.*, 1986).

Luteal regression is characterised by decreasing steroid hormone production and a reduction in luteal mass; however, the exact mechanisms controlling structural and functional regression in primates are poorly understood. The decrease in steroid production associated with physiological luteal regression is not associated with any apparent changes on either serum LH concentrations or pulse frequency (Hutchison *et al.*, 1986). Neither is a uterine luteolytic signal responsible, as in ruminants and rodents. It is therefore likely that an intraovarian mechanism is important in controlling luteal regression in primates. In marmosets, luteal regression can be induced by treatment with either $PGF_{2\alpha}$ or a GnRH antagonist.

2.2.1.1 $PGF_{2\alpha}$-induced luteolysis

In the marmoset, induction of luteolysis by administration of $PGF_{2\alpha}$ is a commonly used tool in the investigation of marmoset luteal regression (Summers *et al.*, 1985; Webley *et al.*, 1989; Michael and Webley, 1993; Fraser *et al.*, 1995; Young *et al.*, 1997; Duncan *et al.*, 1998b; Fraser *et al.*, 1999b). It is known that a single intramuscular injection of $PGF_{2\alpha}$ analogue, such as cloprostenol, causes luteolysis when given after day 8 of the luteal phase (Summers *et al.*, 1985), and that only the mature corpus luteum is susceptible (Summers *et al.*, 1985), perhaps because of an age-related increase in PG receptors. However, the mechanism of action of $PGF_{2\alpha}$ in the marmoset corpus luteum is not fully understood. Webley *et al.*, (Webley *et al.*, 1991) demonstrated that within one hour of administration, clostoprenol induced a significant fall in peripheral progesterone concentrations and administration was not associated with any drop in circulating LH concentrations. Human CG failed to sustain progesterone when given with clostoprenol, thus providing indirect evidence that cloprostenol acts directly at the corpus luteum to prevent the luteotropic actions of LH.

Duncan *et al.*, (Duncan *et al.*, 1998b) demonstrate that $PGF_{2\alpha}$-induced luteolysis results in a rapid loss of LH receptor mRNA and protein inhibiting the luteotropic action of LH. *In vitro*, $PGF_{2\alpha}$ inhibited LH-stimulated progesterone production, which was thought to be a post-cAMP mediated effect (Abayasekara *et al.*, 1993; Auletta and Flint, 1988; Michael *et al.*, 1994). $PGF_{2\alpha}$ is known to activate protein kinase C (Niswender *et al.*, 1994), which has several effects on the steroidogenic pathway, one being the inhibition of cholesterol transport to the cytochrome $P450_{scc}$ enzyme (Wiltbank *et al.*, 1993). Duncan *et al.*, (1998b) have demonstrated that 3β-HSD mRNA and protein expression are also inhibited during $PGF_{2\alpha}$-induced luteolysis in the marmoset. These data and Michael and Webley (Michael and Webley, 1993) confirm that $PGF_{2\alpha}$-induced luteolysis involves the inhibition of LH action at sites both prior and subsequent to cAMP accumulation.

2.2.1.2 Comparison with GnRH antagonist-induced luteolysis

It is agreed that the GnRH antagonist acts at the pituitary to prevent the release of LH (Fraser *et al.*, 1986; Hodges *et al.*, 1988; Webley *et al.*, 1991). Webley *et al.*, (Webley *et al.*, 1991) demonstrated that progesterone concentrations declined after an initial decrease in LH, and that the corpus luteum could be rescued from luteolysis by administration of hCG, suggesting that the action of the GnRH antagonist in reducing progesterone was the result of LH suppression.

Ultrastructural studies of $PGF_{2\alpha}$- and GnRH antagonist-induced luteal regression demonstrate marked morphological changes (Fraser *et al.*, 1999b). Degenerative changes in the smooth ER were more advanced than any observed in the mitochondria, suggesting that the early failure to secrete progesterone was a result of the acute sensitivity of the smooth ER. After $PGF_{2\alpha}$ administration the smooth ER became markedly swollen and formed a number of vesicles, such that in the advanced state these vesicle coalesced into large vacuoles. After GnRH antagonist treatment, the membranes of the smooth ER and possibly segments of the redundant plasma membrane, became condensed into islands of concentric membranes that resulted in the formation of myelin bodies. This phenomenon was rarely observed following $PGF_{2\alpha}$ administration. While

the suppressive effects of GnRH antagonist treatment can be overcome by concomitant administration of hCG (Fraser *et al.*, 1987; Webley *et al.*, 1991), the marmoset corpus luteum cannot be rescued when PG analogue and hCG are given together (Webley *et al.*, 1991). Since both treatments result in failure of LH stimulation of steroidogenesis, the ultrastructural differences indicate an additional effect of PG on the lutein cell as a result of its direct action.

2.2.2 The primate luteal phase

There are three distinct phases during the normal structural and functional lifespan of the primate corpus luteum. The early luteal phase when the corpus luteum is forming and increasing its production of progesterone, the mid-luteal phase when the corpus luteum is fully formed and its progesterone production is maximal, and the late luteal phase when progesterone production falls and the gland begins to regress. Marmoset luteal tissue from these three stages of development was used to investigate the control of luteal angiogenesis in this species. In the human, the fall in progesterone production during the late luteal phase was prevented by exposure to logarithmically increasing concentrations of exogenous chorionic gonadotropin, simulating early pregnancy. This 'rescued' corpus luteum can be considered a fourth stage of the luteal lifespan. Human tissue from these four stages was available to investigate the control of angiogenesis throughout the normal lifespan of the human corpus luteum and during luteal rescue. In addition, subsequent studies involved the manipulation of marmoset luteal angiogenesis and function by specific targeting of factors involved in the angiogenic process.

Home Office regulations restrict the use of other mono-ovulatory species of primate with a luteal phase length more analogous to that of a human, for such experimentation. However, where appropriate it was possible to compliment this work with previously collected human luteal tissue. Together, using the marmoset and human corpora lutea, these models were powerful tools for the exploration of luteal angiogenesis throughout the normal functioning luteal phase and after manipulation with specific anti-angiogenic agents.

2.3 Marmoset tissue

2.3.1 Marmoset husbandry

All marmosets were housed in a 'state of the art' primate centre located on the outskirts of Edinburgh. Primate centre staff were responsible for upkeep and maintenance of the animals and unit. Common marmoset monkeys were housed in cages in rooms maintained at temperatures between 20°C and 25°C and artificially lit between 0.700 h and 19.00 h. The animals were fed daily with a selection of fruit, SDS Mazuri (E) primate diet pellets, and high protein porridge with multivitamin supplements three times per week and water was continuously available. Adult females having a body weight of approximately 350g, with regular ovulatory cycles, were housed together with a younger sister or prepubertal female in cages measuring 1.15m in height, 1.1m in depth and 0.6m wide. Each contained larch branches and a nest box with the floor of the cage filled with wood chippings to allow foraging. Blood samples were collected three times per week by femoral venepuncture without anaesthesia while the animals were held in a restraining device (Hearn *et al.*, 1978). Syringes were sealed and centrifuged for 20 minutes at 1000 x g, plasma was subsequently removed and stored at -20°C until assayed for progesterone to determine the date of ovulation and luteal stage.

2.3.2 Treatment regimes

Administration of treatments was undertaken by staff at the primate centre. All experiments were carried out in accordance with the Animals (Scientific Procedures) Act, 1986. To synchronise the timing of ovulation and administration of treatments, all control and experimental animals received 1μg $PGF_{2\alpha}$ analogue (chloprostenol, Planate, Coopers Animal Health Ltd., Crewe, UK) intramuscularly (i.m.) during the mid- to late luteal phase of the pre-treatment cycle to induce luteolysis. Ovulation normally followed 10 days later (Summers *et al.*, 1985). Specific details of the dose, timing and duration of treatment can be found in the relevant experimental chapters. The basic principle used was to either prevent the onset of angiogenesis by administration for 3 days in the early luteal phase (treatment regime 1) or continued treatment for 10 days from the early to the mid-luteal phase (treatment regime 2), or to intervene in the process by administration for 3 days specifically in the mid-luteal phase (treatment regime 3). A

diagrammatic representation of the regimes used is shown in Figure 2.1. Blood was taken daily for progesterone assay during experimentation.

Cell proliferation in luteal sections was measured as one parameter of angiogenesis. In order to visualise proliferation, bromodeoxyuridine (BrdU; Boehringer Mannheim, Sussex, UK) was administered. BrdU is a thymidine derivative which is incorporated into the DNA of proliferating cells during the S-phase (DNA synthesis phase) of the cell cycle. Twenty milligrams, dissolved in 500µl physiological saline, was administered intravenously (i.v.) to all animals 1h prior to tissue collection.

2.3.3 Collection of tissue

For most experiments tissue was collected throughout the luteal phase of the cycle or the day after final treatment. Additionally, follicular phase tissue was used where necessary to examine regressed corpora lutea, this had been obtained for previous experiments which took place in our laboratory. Animals were sedated using 100µl ketamine hydrochloride (Parke-Davis Veterinary, Pontypool, UK), i.m., and killed with an i.v. injection of 400ml Euthetal (sodium pentobarbitone, Rhone Merieux, Harlow, Essex, UK). Ovaries and uteri were removed immediately, weighed, fixed in 4% paraformaldehyde (PFA) in 0.01M phosphate-buffered saline (PBS; pH 7.4, containing 2.7mM KCl, 0.137M NaCl) for paraffin wax-embedding. For selected marmosets, a small piece of corpus luteum was fixed in 3% glutaraldehyde in 0.1M cacodylate buffer, pH 7.3, for araldite resin-embedding.

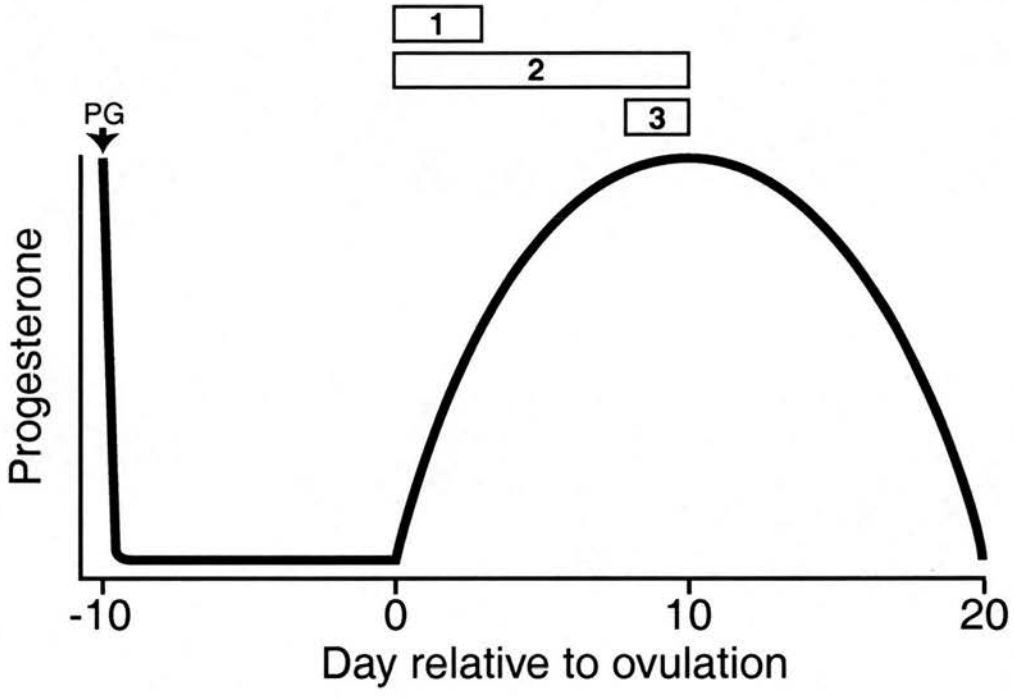

Figure 2.1 Schematic of treatment regimes

Prostaglandin is given in the mid-late luteal phase of the pretreatment cycle to induce luteolysis (progesterone levels decrease) and synchronise the timing of ovulation, which occurs 10 days later as seen by the rise in progesterone concentration. Treatment regime 1 is for 3 days starting from the day of ovulation, treatment regime 2 is for 10 days starting at the time of ovulation, and treatment regime 3 is for 3 days specifically in the mid-luteal phase, starting on luteal day 7.

2.3.4 Progesterone radioimmunoassay (RIA)

Marmoset ovulatory cycles were monitored by three times weekly measurements of plasma progesterone concentration for a number of cycles prior to use of the animal. After treatment had commenced progesterone concentrations were monitored daily. Progesterone RIA was carried out by the in-house assay according to Smith *et al.*, (1990). Marmoset plasma samples were thawed, vortexed and 2.5µl of the plasma added to 147.5µl of progesterone assay buffer (1M phosphate citrate and 1% gelatin, pH 6). A standard curve was prepared, from a progesterone standard, which was diluted in a volume of 100µl to 2.5, 5, 10, 25, 50, 100, 250, 500 and 1000ng/ml. In addition, human post-menopausal serum (PMS), which does not contain progesterone, was diluted in 47.5µl of assay buffer and added to each of the standard curve samples so that the volume in each was 147.5µl. All samples and the standard curve were prepared in duplicate. To each of the samples and standard curve, 100µl of primary antibody, sheep anti-progesterone, diluted 1:1000 in assay buffer, was added. To assess non-specific binding, a sample was prepared which contained 100µl of progesterone assay buffer, primary antibody was omitted. Iodinated tracer, thymidine progesterone (^{125}I-PGT, Amersham, Bucks, UK) was diluted 1:5000 in tracer buffer (1M phosphate citrate, pH6) and counts per minute (cpm) in 100µl determined. Thereafter, the tracer concentration was adjusted to 15000cpm per 100µl, 0.1% (w/v) ANSA (8-anilino-1-naptha-lenesulfonic-acid) was added and 100µl was aliquotted to each sample. In addition, 2 x 100µl samples of the diluted tracer containing 0.1% (w/v) ANSA was used in the assay to assess ^{125}I-PGT total counts. Assay samples were vortexed and incubated at room temperature for 3 hours. Subsequently, the secondary antibody, donkey anti-goat diluted 1:64 in assay buffer, was added to all samples except those measuring the ^{125}I-PGT total counts. Normal sheep serum (SAPU, Carluke, Lanarkshire, UK) was diluted 1:32000 in assay buffer and 100µl was added to all samples. Samples were vortexed and incubated overnight at 4°C. One millilitre of 0.9% saline/tritonX/polyethylene glycol was added to each sample and samples centrifuged at 4°C for 30 min. The supernatant was subsequently removed, the pellets air dried and the amount of the radioactivity incorporated into each pellet measured using a gamma counter. The sensitivity of the

assay was 0.07pmol per tube (0.022 ng/ml) and the inter- and intra-assay coefficients of variation were 15% and 4% at the centre of the standard curve, respectively. The inter- and intra-assay coefficients of variation were more varied at the extremes.

2.3.5 Classification of the stage of the ovulatory cycle

Classification of the stage of the marmoset ovulatory cycle was determined by progesterone plasma concentrations based on sampling three times per week (Monday, Wednesday and Friday). The follicular phase was defined as the period when plasma progesterone concentration was ≤ 12nmol/L. The luteal phase was determined as the stage when plasma progesterone concentration rose above 30nmol/L and was followed by a sustained increase. The specific day of the luteal phase was classified according to the following guidelines: 1) If the first measurement of plasma progesterone concentration above 30nmol/L was between 30 and 50nmol/L this was classified as day 0 (the day of ovulation). 2) If the first plasma progesterone measurement above 30 mnol/L was between 50 and 100nmol/L this was classed as day 1 (assuming ovulation on the previous day). 3) On the rare occasions when the first measurement above 30nmol/L was >100nmol/L (e.g. on a Monday) this was classed as day 2 (assuming ovulation had occurred on the Saturday). Animals were classified as early luteal, days 2-4 after a sustained rise in progesterone concentration above 30nmol/L; mid-luteal, days 8-10; and late luteal, days 14-20.

2.4 Human tissue

Patients were recruited and human tissue was collected by Dr Colin Duncan and Dr Faye Rodger for previous studies. Paraffin wax blocks and frozen tissue from the early, mid-, late and rescued stages of the luteal phase were available for use in subsequent studies. In brief, the following methods were used for patient recruitment and tissue collection.

2.4.1 Recruitment of patients

Healthy women, with regular menstrual cycles, who had not received any form of hormonal therapy in the last three months, who did not have a history of infertility, and who were having open abdominal hysterectomy for benign conditions, were identified from the case records of all women on the waiting list for hysterectomy at the Royal Infirmary of Edinburgh. A detailed menstrual history from women interested in participating in the study was taken, and the women categorised as to whether their operation would fall in the luteal phase of the cycle, would be suitable for luteal rescue *i.e.* the operation falling 2 days before or after expected menses, or unsuitable for the study. All women whose operation would fall in the luteal phase of the cycle collected an early morning urine specimen for LH assay 7 days after their last menstrual period (LMP) until hospital admission. Plasma was collected on the day of surgery and assayed for progesterone concentration. Those women who agreed to take part in the luteal rescue study took urine samples from day 7 of their menstrual cycle for LH assay. The date of ovulation was defined as 24 hours after the start of any clear single day of urinary LH peak (LH+1). Daily i.m. injections of hCG (Profasi; Serono, Welwyn Garden City, Herts, UK) were given from LH+7 until operation. Dosage commenced at 125 IU and doubled daily for 5-8 days. This regime has previously been shown to mimic the hormonal changes of early pregnancy (Illingworth *et al.*, 1990).

2.4.2 Collection and dating of tissue

Whole corpora lutea were enucleated from the ovary at the time of hysterectomy. The tissue was immediately divided into 4 radial segments to ensure that the whole thickness of the gland was represented by any one piece. Two blocks were snap frozen in liquid nitrogen and stored at –70°C for RNA extraction. One piece was frozen in embedding medium (Tissue-Tek OCT compound; Miles Inc., Elkhart, IN, USA) and stored at –70°C for sectioning. The final piece was fixed in 4% PFA for paraffin wax-embedding, as described previously for marmoset tissue, for subsequent immunocytochemical examination. In addition, an endometrial biopsy was obtained, fixed in 4% PFA and embedded in paraffin wax.

LH concentrations were measured in each of the serial urine samples. Corpora lutea were classified as early luteal if collected 1-5 days after the urinary LH peak. They were classified as mid-luteal 6-10 days after the LH peak, and late luteal from 11-14 days after. Those corpora lutea collected after hCG administration were classified as 'rescued'. In all cases, morphological examination of the luteal phase endometrium (Li *et al.*, 1988) was used to confirm the luteal phase classification. Only patients whose urinary LH dating, LMP and endometrial dating were in agreement were used in subsequent definitive studies.

2.5 Tissue fixation, processing and sectioning for paraffin blocks

Tissue fixation was needed to prevent autolysis and bacterial attack, and also to ensure that the tissue remained as close to its *in vivo* state as possible without loss or rearrangement. The fixative used in these studies was 4% paraformaldehyde (PFA). Aldehyde fixatives form cross-links between protein and aldehydes developing a stable, static structure. Morphology is retained to a satisfactory level and in their native states DNA and RNA do not react to any extent with formaldehyde so for the purposes of immunocytochemistry and *in situ* hybridisation this fixative was chosen. Ovaries and uteri obtained were fixed in 4% PFA for 24 hours and transferred to 70% EtOH until processed into paraffin wax. Ovaries were bisected through the maximal part of the largest corpus luteum to ensure that cross sections through the widest part of the gland could be obtained. Uteri were bisected longitudinally through the luminal cavity so that sections would contain endometrium. Processing and paraffin wax-embedding was carried out by the MRC HRSU Histology department. Tissue was dehydrated through a series of graded alcohols before being saturated by paraffin wax. This process was performed using a 17.5h automated cycle on a Leica TP-1050 processor (Leica UK Limited, Milton Keynes, UK). The tissue was then embedded with the cut surfaces facing up so that the maximal part of the corpus luteum and uterus containing endometrium could be sectioned. Glass microscope slides to be used for immunocytochemistry were dipped twice in a 4% (v/v) solution of 3-aminopropyl triethoxysilane (TESPA) in acetone (BDH, Merck Ltd., Poole, Dorset, UK), washed in

acetone, rinsed in double distilled water and dried overnight. The TESPA coating increased the adherence of the tissue to the slide. Slides used for *in situ* hybridisation were RNase free and electrostatically charged for improved binding (BDH). Paraffin wax sections were cut (5μm) using a hand-operated microtome (Jung RM2035; Leica) with disposable blades. Sections were floated onto a heated water bath (containing distilled water for immunocytochemistry sections or RNase free water for sections to be used for *in situ* hybridisation) at approximately 50°C. Sections were transferred onto slides and dried overnight before use.

2.6 Haematoxytin and eosin staining

These stains were routinely prepared in the Histology department. Harris's haematoxylin was prepared by dissolving 2.5g of haematoxylin (BDH) in absolute alcohol which was added to alum which had previously been dissolved in 500ml warm dH_2O (Stevens and Wilson, 1996). This mixture was boiled and either mercuric oxide (1.25g) or sodium iodate (0.5g) was carefully added. The stain was then rapidly cooled by plunging the flask into a sink containing cold water and crushed ice. Once cold 20ml of glacial acetic acid was added. Eosin Y is prepared by preparing a 1% solution with distilled water and 0.5ml of acetic acid added to 1L (Stevens and Wilson, 1996). The exact haematoxylin and eosin (H and E) staining protocol is detailed in Chapter 3.

2.7 Immunocytochemistry

Immunocytochemistry is a method used to localise a specific antigen (usually protein) within a cell using a specific antibody raised to an epitope of the protein in question. This is a useful technique as it allows an antigen to be localised to a specific cell type, often a specific cellular location. Quantification of immunocytochemical staining is possible and is generally based on parameters, such as the number of positive cells in a population, the area and intensity of staining, or any combination of the three. Advances in image analysis systems have increased the efficiency and accuracy of quantification of such immunostaining. The immunocytochemical procedure involves building up a

sandwich of antibodies to increase the available binding sites for the tracer and detection systems used, in this case either the alkaline phosphatase anti-alkaline phosphatase (APAAP) or avidin/biotin complex - horse-radish peroxidase (ABC-HRP) based tracer systems, as depicted in Figure 2.2.

2.7.1 Antigen retrieval

Fixation and paraffin wax-embedding can mask some antigenic epitopes. It was necessary in most cases to expose these using either proteolytic digestion (Huang *et al.*, 1976) or heat treatment (Shi *et al.*, 1991). These methods of antigen retrieval have to be optimised because over digestion or heating can result in tissue damage and substantial loss of morphology. Where proteolytic digestion was required, slides were incubated in 0.1% (w/v) trypsin with 0.1% (w/v) calcium chloride, buffered to pH 7.6 with 0.1M sodium hydroxide, for 20 min at 37°C. Proteolytic digestion was stopped by submerging slides in cold tap water. Where heat treatment was required slides were subjected to microwaving or pressure cooking. Slides were microwaved for 4 rounds of 5 min on full power (750W) in 0.01M citrate buffer, pH 6, after each round the volume of buffer was topped up with warm dH_2O. Slides were left to stand in hot buffer for a further 20 min before transferring to TBS. This was superseded by less time consuming pressure cooking which was more consistent for antigen retrieval than the microwave which contains 'hot' and 'cold spots'. Two litres of 0.01M citrate buffer or 3M glycine, 0.1% EDTA (ethylenediaminetetra acetic acid) buffer, pH 3, were heated to boiling point in the pressure cooker and the slides in a metal rack lowered in. The lid was sealed and pressure applied, timing (5 min) began well full pressure was reached. After release of pressure slides remained in hot buffer for a further 20 min before cooling in TBS.

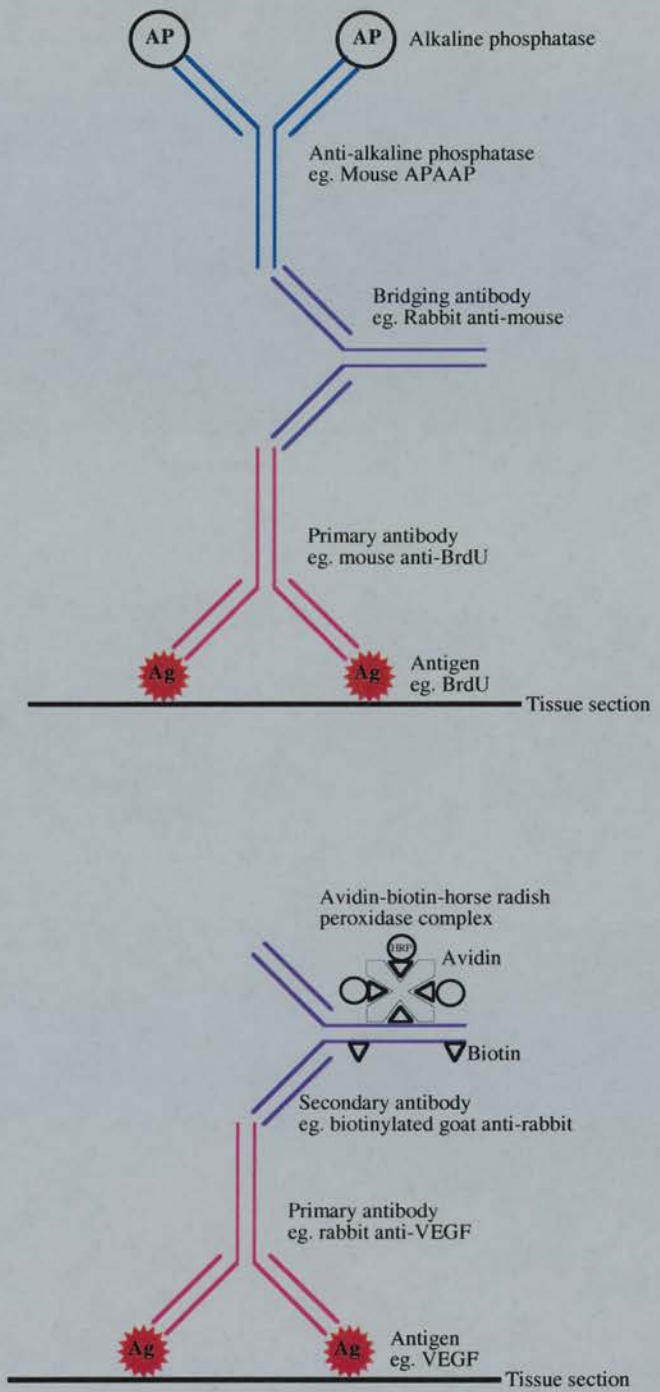

Figure 2.2 APAAP and ABC-HRP methods of immunocytochemistry

(a) The APAAP (alkaline phosphatase anti-alkaline phosphatase) method of immunocytochemistry. Primary antibody binds to its specific antigen. A bridging or secondary antibody permits binding of the APAAP label. A coloured substrate is then used for visualisation. (b) The ABC-HRP (avidin-biotin- horse radish peroxidase complex) method of immunocytochemistry. The secondary antibody is biotinylated which permits binding of the preconjugated AB-HRP complex. A coloured substrate is used for visualisation.

2.7.2 Blocking non-specific binding

The main cause of non-specific background was assumed to arise from non-immunological binding of specific immune sera by hydrophobic and electrostatic forces (Kraehenbuhl and Jamieson, 1974). As it was generally the first immune serum that gave rise to highest levels of non-specific background, these sites were blocked prior to the application of the primary antibody with immunoglobulins which would not react or interfere with primary specific antiserum. In both the APAAP and HRP methods sections were incubated in normal whole serum from species in which the bridging (secondary) antibody was raised.

The APAAP method was favoured for marmoset ovary due to the high endogenous peroxidase activity and biotin present in this tissue which gave false positive staining when the ABC-HRP was used. When it was necessary to use ABC-HRP detection in marmoset ovary, for example when haematoxylin counterstain for visualising tissue morphology and a brown reaction product to contrast was desired, endogenous peroxidase and biotin were blocked. Endogenous peroxidase activity was blocked by incubation of sections in 0.9% (v/v) methanol/0.1% (v/v) hydrogen peroxide (both BDH) for 30 min at room temperature.

Endogenous biotin was blocked by addition of exogenous avidin and biotin. Biotin has one binding site for avidin, and avidin has 4 for biotin. In this blocking regime exogenous avidin bound endogenous biotin, and all biotin binding sites on the avidin molecule were saturated with addition of excess biotin. Avidin (Vector Laboratories Inc., Burglingame, CA, USA) was added at a concentration of 8 drops per ml of normal blocking serum and allowed to bind endogenous biotin for 30 min at room temperature. Any unbound avidin was washed off with TBS (Tris-buffered saline). Sections were incubated in Biotin (Vector; 8 drops per ml of TBS) for 20 min at room temperature, and unbound biotin washed off with TBS.

When using APAAP detection endogenous alkaline phosphatase activity was blocked by the addition of levamisole to the substrate solution. The alkaline phosphatase tracer was of intestinal origin (calf) and so was resistant to blocking with levamisole.

2.7.3 Immunocytochemical procedure

Immunocytochemical procedures were performed using an automated incubation method, the Sequenza system (Shandon Scientific, Runcorn, Cheshire, UK), which works by capillary action and is believed to increase the ratio of specific to non-specific staining. Unbound antibody was washed from the section before incubation with the next layer using TBS. This prevents antibody-antigen complexes from precipitating into sections and giving rise to problems with interpretation and background staining.

Sections were dewaxed in Histoclear (National Diagnostics, Hull, UK) and rehydrated in descending concentrations of industrial methylated spirits and finally tap water. If necessary antigen retrieval was performed and the slides transferred to TBS. If the ABC-HRP system was to be used endogenous peroxidase activity was blocked and the sections washed in running tap water then TBS. Slides were set up in the Sequenza system ensuring that no air bubbles were present. Endogenous biotin was blocked (in normal serum block) if the ABC method was to be used in marmoset ovarian tissue. If a biotin block had not been performed sections were incubated in normal whole serum (SAPU) from the species in which the bridging antibody was raised, with the addition of bovine serum albumin (BSA, Sigma). Primary antibody was applied at the working concentration diluted in TBS and sections incubated overnight. For NBT (nitro blue tetrazolium) detection, slides were incubated in non-biotinylated secondary antibodies followed by a tertiary APAAP antibody. For ABC-HRP detection, the EnVision kit (Dako Ltd.) was used, which supplied the secondary antibody pre-conjugated to ABC-HRP.

2.7.4 Detection and mounting

The APAAP method can be used with a number of substrates to yield a variety of colours. The two most commonly used were nitroblue tetrazolium (NBT; Sigma) (McGadey, 1970) which forms a deep blue/black immunostain, and Fast red TR (Sigma) used with naphthol AS-MX phosphate sodium (Sigma) which gives a bright red reaction end product. The favoured substrate for HRP was 3,3` diaminobenzadine tetrahydrochloride (DAB) provided in the EnVision kit (Dako Ltd.), which yields a crisp, insoluble, stable, dark brown reaction product (Graham and Karnovsky, 1966). If

desired sections were counterstained with haematoxylin as described for H and E staining. Sections were then dehydrated in increasing concentrations of alcohol, cleared in xylene before being mounted using Pertex mounting medium (Cell Path, Hemel Hempstead, UK) and coverslipped, unless the alcohol soluble Fast red substrate was used. These sections were mounted from tap water using Permaflour aqueous mounting medium (Beckman Coulter, Luton, Beds, UK).

2.7.5 Negative controls

For immunocytochemical detection using a specific antibody for the first time on a particular tissue, negative controls were used. The primary antibody was either replaced with immunoglobulin G from the same species and at the same concentration as the primary antibody, or where possible, with the primary antibody preabsorbed with the peptide it was raised against.

2.8 Image analysis

2.8.1 Digital photomicroscopy

Tissue sections were examined using an Olympus Provis microscope (Olympus Optical, London, UK) and images were captured using a digital camera, either the Kodak DCS420 or Kodak DCS330 (Eastman Kodak, Rochester, NY, USA). Captured images were stored on a G4 Macintosh (Apple Macintosh, Apple Computer, Cupertino, CA) and montages were compiled using Photoshop 5.0 (Adobe Systems Inc., Mountain View, CA) and the Extensis Intellihance Pro 4.0 programme before being printed using the Epson Stylus Photo 750 printer.

2.8.2 Quantification of immunostaining

Quantification of BrdU incorporation into cells of the corpus luteum was done manually by counting the number of positive cells and total cells in 6 graticule fields, arranged in a cross formation, per corpus luteum, at a magnification of x400. A proliferation index for each animal was obtained from meaning the percentage of proliferating cells per corpus luteum.

Where it was not possible to count cell numbers as a result of the poor visibility of cell margins, for example when quantifying endothelial cell staining, area of immunostaining was measured using Image Pro Plus 3.0 software (Media Cybernetics, Silver Spring, Maryland, USA). An image was captured, converted to grey scale and the area of dark objects on a white background was counted using a pre-recorded macro. The threshold for recognition of staining intensity was set so that the captured image portrayed the live image as closely as possible. As many fields of view as possible were quantified, the number being dictated by the lens magnification and size of the corpus luteum in question.

2.9 *In situ* detection of apoptotic cell death

Apoptosis is a complex regulatory process that controls cell death by intrinsic programmed mechanisms (Erickson, 1997). Apoptotic and necrotic forms of cell death are quite distinct in their histology (Wyllie *et al.*, 1980; Walker *et al.*, 1988). A characteristic feature of necrosis is that cell death occurs in groups. In this form of death, increases in cell permeability lead to cell swelling and cell and organelle rupture, resulting in the release of cytoplasmic and nuclear contents into the interstitial space (Wyllie *et al.*, 1980; Walker *et al.*, 1988; Schwartzman and Cidlowski, 1993). Degradation of nuclear material and random DNA fragmentation occur at the later stages of necrotic death (Shikone *et al.*, 1996). Apoptosis occurs in single cells rather than groups, and it involves cell shrinkage with no swelling (Erickson, 1997). Morphological features are cell shrinkage, nuclear condensation, DNA fragmentation and formation of intensely stained regions of fragmented nuclear material, known as apoptotic bodies. DNA degradation during apoptosis is not random, endonucleases cleave DNA at 185bp (base pair) intervals or at multiples of 185bp (Wyllie *et al.*, 1980), and if extracted DNA is run on a gel, the DNA is visualised as a ladder, the bands being multiples of 185bp. The *in situ* 3' end labelling exploits the extensive DNA degradation process of apoptotic cell death. This technique enables visualisation of fragmented DNA in tissue sections by employing an enzyme, terminal transferase, to attach a digoxygenin label onto the 3' ends of fragments. This label is detected by immunocytochemical

methods. The *in situ* technique relies on the fact that a high number of DNA fragments are generated during apoptotic cell death (Negoescu *et al.*, 1998), but ideally this method should be used in conjunction with DNA separation by gel electrophoresis, as necrotic cell death also involves DNA fragmentation. However, for these studies DNA extraction was not possible. Therefore, the *in situ* 3' end labelling technique was used in conjunction with morphological analysis, which determines whether cell death is occurring in cellular groups or singly, permits the identification of apoptotic bodies and allows the type of cell to be confirmed. This method is used in more than one study and so will be described in full in this section, and referred to in the relevant experimental chapters.

Sections were dewaxed and rehydrated as normal for immunocytochemistry. Proteinase K digestion was needed for terminal transferase and digoxygenin access to the intracellular 3` end DNA fragments. Proteinase K was employed at a concentration of 20μg/ml in 0.1M Tris, 0.1M EDTA buffer, pH8, for 6 min at room temperature. This step was crucial and was optimised carefully depending on the fixative and tissue used. Slides were washed in TBS and endogenous peroxidase activity and endogenous biotin blocked as previously described for immunocytochemistry. 3`-OH ends of DNA fragments were labelled with 0.5nM digoxygenin-11-UTP (Uridine 5`triphosphate, Boehringer Mannheim) by 25U/ml terminal deoxynucleotidyl transferase (TdT, Boehringer Mannheim) in buffer containing 30mM Tris/HCl pH7.2, 140mM sodium cacodylate (Agar Scientific Ltd., Essex, UK) and 1.5mM $CoCl_2$ (Boehringer Mannheim) for 30 min at 37°C. Slides were washed in TBS and non-specific immunostaining blocked with normal rabbit serum (NRS, SAPU) diluted 1:5 in TBS + 0.25g bovine serum albumin (Sigma) for 30 min at room temperature. Sheep anti-digoxygenin antibody (Boehringer Mannheim) diluted 1:100 in blocking serum, was applied for 90 min at room temperature. Slides were washed in TBS and incubated in biotinylated rabbit anti-sheep IgG (immunoglobulin G, Vector Laboratories), diluted 1:500 in blocking serum, for 30 min at room temperature. Again slides were washed in TBS and incubated in pre-made ABC-HRP (Dako Ltd.; 1 drop each of avidin and biotin per ml of 0.05M Tris pH8) for 30 min at room temperature. Visualisation was with DAB (Dako Ltd.; 1 drop of chromagen substrate per ml of 0.05M Tris pH8).

Negative control sections were treated with reaction mixture not containing TdT enzyme. Staining was not only assessed in the corpora lutea but in atretic follicles which were positively stained in those sections treated with TdT enzyme and negative in those not treated with the enzyme, and healthy follicles which were negative in those sections treated with TdT enzyme.

2.10 *In situ* hybridisation

In situ hybridisation was used for the detection of specific mRNA in tissue sections via hybridisation with a complementary radioactive riboprobe and detection using photographic emulsion. Quantification of mRNA has also benefited from the recent advances in images analysis technology. All preparation of plasmids, riboprobes and *in situ* hybridisation was carried out by Helen Wilson and Dr. Christine Wulff, resident experts in the field (Wulff *et al.*, 2000). Quantification was performed by myself. The preparation of plasmids, synthesis of riboprobes and *in situ* hybridisation procedure were performed for localisation of VEGF-A mRNA. These methods are used in a number of studies and so will be described in detail in this section.

2.10.1 Preparation of plasmids

Riboprobes were synthesised from plasmids containing the cDNA sequence of interest and RNA polymerase initiation sites. These plasmids were not generated in-house but obtained already transfected into *Epicurian coli* (XL-1 Blue; Stratagene, La Jolla, CA, USA) as glycerol stocks from Dr Charnock-Jones (University of Cambridge, Department of Obstetrics and Gynaecology). Plasmids were amplified by growth of 10µl glycerol stock of the Ampicillin resistant bacterium in 10ml LB Broth (Anachem, Luton Beds, UK; 25 capsules per litre dH_2O) containing 0.5mg Ampicillin (Gibco BRL, Life Technologies Ltd., Paisley, UK), overnight at 37°C on a shaking platform. Plasmids were only extracted if the negative control solution, containing broth and ampicillin, was clear.

Plasmids were purified from their host bacterium using the QIAprep Spin Miniprep kit (QIAGEN Ltd., Crawley, West Sussex, UK), according to the

manufacturers instructions, which used alkaline lysis of bacterial cells followed by adsorption of DNA into silica in the presence of high salt. The concentration and purity of plasmids was determined by spectrophotometry using GeneQuant Pro (Amersham Pharmacia Biotech, Cambridge Science Park, Cambridge, UK). In addition, the quality was checked using agarose gel electrophoresis. A 0.5% agarose gel was prepared by heating 0.25g agarose per 50ml 1 x TBE buffer (containing 1M Tris, 1M boric acid and 0.02M EDTA in dH_2O). Ethidium bromide was added to the dissolved agarose at 2µl per 50ml of gel, for visualisation of the DNA under ultra violet (UV) light. The gel was cast and wells formed using a comb. One microlitre of the purified plasmid was loaded with 2µl DNA/RNA loading buffer (containing 5% v/v SDS, 0.25M EDTA, 250% w/v Ficoll, 1.5% w/v bromophenol blue) and 7µl H_2O. The gel was run at 100V for 1 hour, viewed under UV light and photographed.

Plasmids were linearised by restriction enzyme digestion using Xho1 and Not1 restriction enzymes for antisense and sense VEGF-A riboprobe synthesis, respectively. Briefly, 500ng-1µg plasmid was linearised with 50U restriction enzyme, 1 x corresponding buffer, and 0.1mg/ml bovine serum albumin in a 100µl reaction, at 37°C overnight. Agarose gel/ethidium bromide electrophoresis was performed on both cut and uncut plasmids to check linearisation.

Linearised plasmid was purified through a filter using the High Pure PCR (polymerase chain reaction) Product Purification kit (Boehringer Mannheim), according to the manufacturers instructions.

2.10.2 Synthesis of riboprobe

Antisense and sense riboprobes for VEGF-A were generated using T7 and T3 RNA polymerases, respectively. Riboprobes incorporating ^{35}S UTP (9.25mbq; Nen Life Science Products, Zaventem, Belgium) were synthesised using a MAXIscript *in vitro* transcription kit (Ambion Inc., Austin, Texas, USA). A reaction mixture of 1 x buffer, 0.5 mM each rNTP (ribonucleotide triphosphate; rATP, riboadenosine triphposphate;; rCTP, ribocytosine triphosphate; rGTP, riboguanine triphosphate), 2.3MBq ^{35}S UTP, 10U RNA polymerase and RNase-free H_2O to 20µl was added to 1µg linearised

plasmid. The riboprobe was synthesised at 37°C for 2 x 30-45 min and another 10U RNA polymerase was added between incubations. Plasmid DNA was degraded by addition of 1U Dnase (deoxyribonulease), and incubation at 37°C for 15 min.

Incorporation of ^{35}S UTP was measured by counting the total radioactivity (counts per minute, cpm) in 1µl of the final reaction mix after riboprobe synthesis, spinning through a ChromaSpin column (Clonetech Laboratories Inc., Palo Alto, CA, USA), according to manufacturers instructions, which retained any free radioactivity, and 1µl of the eluate counted again. The incorporated count was expressed as a percentage of total counts per minute. Thirty to fifty percent incorporation was acceptable.

2.10.3 *In situ* hybridisation procedure

In situ hybridisation was performed on 4% PFA-fixed 5µm sections. All solutions used in the *in situ* hybridisation procedure were made up using diethyl pyrocarbonate (DEPC)-treated and autoclaved H_2O. Washes were performed at room temperature unless otherwise stated. Sections were dewaxed for 10 min in xylene and rehydrated in 100%, 90% and 70% ethanol, 2 min in each. Sections were washed or incubated in the following: 0.1M HCl for 20 min, H_2O for 2 x 5 min, Proteinase K (5µg/ml; in buffer containing 1M Tris, 0.5 M EDTA, pH8) for 30 min at 37°C (optimised for VEGF-A probe), 0.2% glycine for 10 min at 4°C, 0.1M TEA buffer (triethanolamine, pH8 with NaOH) for 5 min, TEA buffer/0.25% (v/v) acetic anhydride for 10 min, and 4 x SSC (salt sodium chloride, containing 0.6M NaCl, 0.06M Na citrate) for 5 min. Sections were dried round, laid in humid boxes and incubated for 2 h at 50°C in 100µl each of prehybridisation buffer (containing 50% (v/v) deionised formamide, 4 x SSC, 1 x Denhardt's solution, 125µg/ml salmon testis DNA, 125µg/ml yeast tRNA, and 10mM DTT, dithiothreitol). Prehybridisation buffer was drained off and hybridisation buffer (containing the same as prehybridisation buffer plus 10% (v/v) dextran sulphate and 0.5 x 10^6 cpm of probe optimised for VEGF-A probe) added, sections were coverslipped (Gel Bond) and incubated overnight at 50°C (optimised for VEGF-A probe). From this point conditions did not need to be RNase-free. Coverslips were peeled off and sections

washed in the following: 4 x SSC for 10 min, RNase A (20μg/ml in buffer containing 0.2M Tris, 0.1M EDTA and 2.5M $NaCl_2$) for 30 min at 37°C, 2 x SSC for 30 min, 1 x SSC for 10 min at 60°C (optimised for VEGF-A probe), 0.1 x SSC for 30 min, 50% (v/v) ethanol / 0.3M ammonium acetate, 85% (v/v) ethanol / 0.3M ammonium acetate, and 94% (v/v) ethanol / 0.3M ammonium acetate, for 2 min each. Sections were air-dried for 3-4 h, and dipped in emulsion in a dark room. G5 Emulsion (Illford, H+A West, Edinburgh, UK) was diluted 1:1 with dH_2O, and heated until liquified at 45°C. The slides were dipped in emulsion and dried in a light proof humid box overnight at 4°C. Desiccant was added and the emulsion exposed at 4°C for 2 weeks (optimised for VEGF-A probe). Slides were developed in filtered Kodak D19 Developer (Edinburgh Cameras, Edinburgh, UK) for 4 min at 14°C, rinsed in dH_2O, fixed in Kodak GBS Fixer (Sigma) diluted 1:5 in dH_2O, for 10 min at room temperature, and rinsed in dH_2O. Sections were counterstained with haematoxylin and mounted in Pertex as previously described for immunocytochemistry.

2.11 Quantification of specific mRNA from total RNA

2.11.1 Total RNA extraction and quantification

Total RNA was extracted from tissues using Tri-Reagent, a guanidine thiocyanate based reagent (Chomczynski and Sacchi, 1987), according to the manufacturers instructions. This reagent allows simultaneous extraction of total RNA, DNA and protein. RNA extraction is a routinely used technique in molecular biology and therefore the methodology is assigned to this section. Extracted RNA can be used for Northern analysis, RNase protection assay or reverse transcription-polymerase chain reaction (RT-PCR). Extraction of DNA and protein was not carried out in these studies, so the methodology for RNA extraction only will be described here. Briefly, tissue stored at -70°C was placed in Tri-Reagent (10ml per gram of tissue) and homogenised using a Polytron PT1200 homogeniser (Philip Harris Scientific, Coatbridge, Lanarkshire, UK) followed by centrifugation at 4°C for 10 min at 12000 x g. The supernatant obtained was

transferred to a fresh tube and 0.2 volume of chloroform added. The mixture was shaken for 15 sec, allowed to stand at room temperature for 12 min and centrifuged at 4°C for 20 min at 12000 x g. The RNA, present in the upper aqueous layer, was transferred to a new tube and precipitated by the addition of 0.5 volume of isopropanol and incubation for 5 min at room temperature. The RNA was pelleted by centrifugation at 4°C for 20 min at 12000 x g. Thereafter, the supernatant was removed, the RNA pellet washed with 1 volume of 75% ethanol and centrifuged at 4°C for 20 min at 12000 x g. Following centrifugation, the supernatant was removed and the RNA pellet dissolved in RNase free H_2O (Sigma). RNA was stored at -70°C until required.

The concentration and purity of the RNA was determined by spectrophotometry using GeneQuant Pro (Amersham Pharmacia Biotech). This machine automatically calculates the concentration (A_{260}) and quality ($A_{260/280}$) of RNA. In addition, the quality of the RNA was assessed by 1.5% agarose gel/ethidium bromide electrophoresis. Two micrograms of RNA were loaded with 2µl DNA/RNA loading buffer. The gel was run at 100V for 1 hour, viewed under UV light and photographed.

2.11.2 Real time quantitative reverse transcription polymerase chain reaction

Reverse transcription-PCR is a two-stage process. Complementary DNA (cDNA) is initially produced from RNA; the cDNA is subsequently amplified in a cyclic process of DNA denaturation, specific primer annealing and primer extension to exponentially increase the primer specified cDNA fragment. Perkin Elmer have developed a new technique which allows quantification of specific mRNA species in total RNA. Before this method can be performed primers and probe, specific for the mRNA of interest must be designed (Section 2.11.2.1). Real time quantification of this process allows visualisation of the cDNA synthesised after each PCR cycle, through cleavage of a fluorescent probe from its quencher during strand synthesis. Quantification is based on calculations which consider an 18S control and the relationship between sample cDNA content and a nominated standard. The principles used in this technique are further clarified in Figure 2.3.

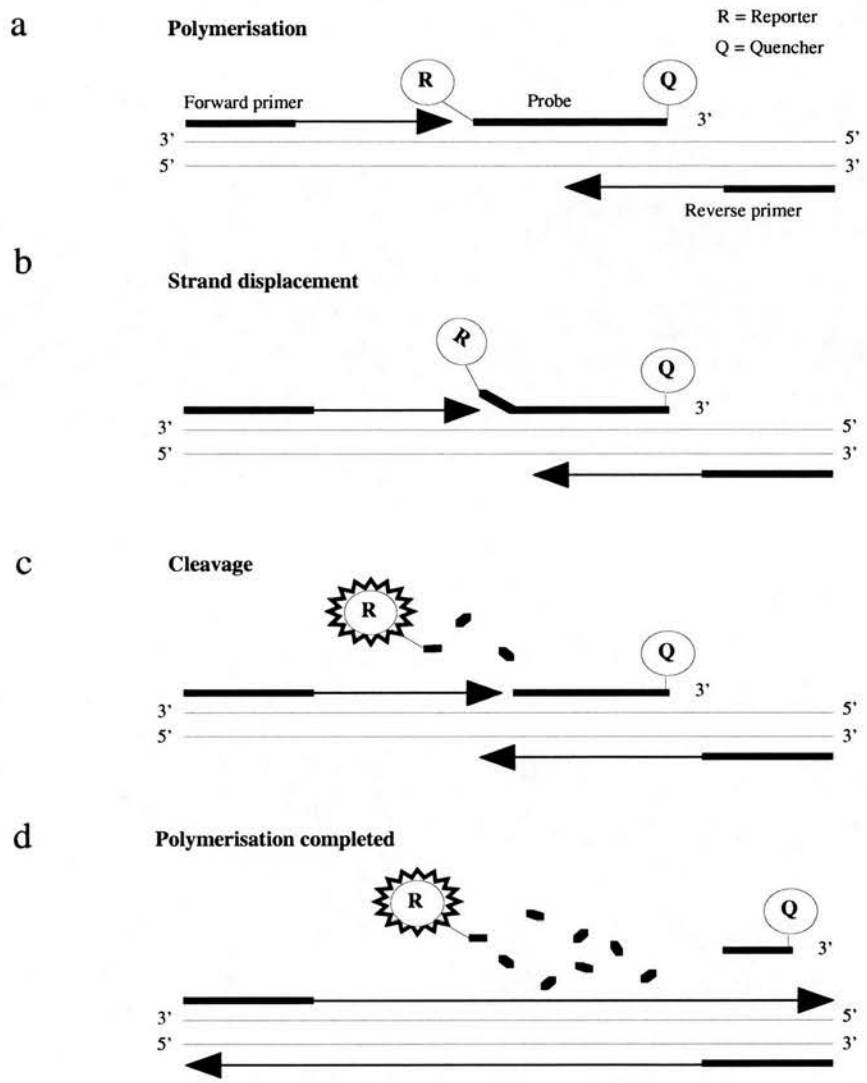

Figure 2.3 Basics of the TaqMan Real Time PCR method

(a) The PCR reaction exploits the 5' nuclease activity of AmpliTaq Gold DNA polymerase to cleave the TaqMan probe during PCR. The TaqMan probe contains a reporter dye at the 5' end of the probe and a quencher dye at the 3' end of the probe. When the probe is intact, the proximity of the reporter dye to the quencher dye results in suppression of the reporter fluorescence primarily by Forster-type energy transfer (Lakowicz, 1983). During PCR, if the target of interest is present, the probe specifically anneals between the forward and reverse primer sites.
(b) and (c) During the reaction, cleavage of the probe separates the reporter dye and the quencher dye, which results in increased fluorescence of the reporter. Accumulation of PCR products is detected directly by monitoring the increase in fluorescence of the reporter dye. The 5'-3' nucleolytic activity of the AmpliTaq Gold DNA Polymerase cleaves the probe between the reporter and the quencher dye only if the probe hybridises to the target.
(d) The probe fragments are then displaced from the target and polymerisation of the strand continues. The 3' end of the probe is blocked to prevent extension of the probe during PCR. This process occurs in every cycle and does not interfere with the exponential accumulation of the product. The increase of fluorescence signal is detected only if the target sequence is complementary to the probe and is amplified during PCR. Because of these requirements, any non-specific amplification is not detected.

2.11.2.1 Design of probe and primers

Complementary DNA sequences for target genes were acquired from the National Library of Medicine PubMed nucleotide enquiries, on the internet. Probe and primers were designed against segments of the sequence which displayed low homology with other genes of the same family and where possible to span two introns so that genomic, exon containing, sequences would not be amplified. Both probe and primers were designed using the Primer Express software which generated candidate probes and primers against a specific sequence, a choice of probe and primers was made from the list following certain guidelines. The probe was chosen first, the GC content was kept in the 30-80% range, runs of identical nucleotides were avoided especially four or more Gs, Gs were not put on the 5` end, the strand selected gave the probe more Cs than Gs and the T_m was 68-70°C. Primers were designed either side of the probe, as close as possible without overlapping the probe, to amplify short segments of DNA within the target sequence, between 50 and 150bp was recommended for consistent results. The same guidelines for designing the probe were used for primer design except that the T_m of the primers was optimally 58-60°C, and that the five nucleotides at the 3` end should have no more than two G and/or C bases.

The probe and primers for 18S were designed by Perkin Elmer Applied Biosystems (Foster City, CA, USA) the sequences of which were not made public. They were purchased in kit form from Perkin Elmer.

2.11.2.2 DNase treatment of RNA

RNA was extracted using Tri-Reagent which allows simultaneous extraction of DNA and protein and so it was possible that extracted RNA could be contaminated with genomic DNA, although steps to minimise this were taken. Before RT-PCR, RNA was subjected to DNase I (Gibco BRL) treatment to degrade any contaminating DNA. The methodologies for DNase treatment of RNA, reverse transcription and Real Time quantitative PCR can be found in Chapter 7.

2.12 Statistical analysis of data

Results of quantifications in three stages of the marmoset luteal phase, and four stages of the human luteal phase, where more than two variables were present, were analysed using an analysis of variance (ANOVA) with Fisher's protected least significant difference (PLSD) post-hoc test. For assessing the significance of results using potential inhibitors of angiogenesis, comparing treated against control measurements, two-tailed, unpaired t-tests were used. The level of significance for both tests was $P<0.05$. All tests were performed using StatView Version 4.0 for the Macintosh.

Chapter 3

Quantification of Luteal Angiogenesis

3.1 Introduction

Angiogenesis refers to the formation of new blood vessels from pre-existing ones, and is essential for normal growth and development (Folkman and Klagsbrun, 1987; Klagsbrun and D'Amore, 1991). The angiogenic process consists of capillary proliferation and stabilisation of newly formed vessels leading to the formation of a new vasculature tree. Capillary proliferation consists of at least three processes: (1) fragmentation of the basement membrane of the existing vessel, (2) migration of endothelial cells from the existing vessel toward the angiogenic stimulus and (3) proliferation of endothelial cells (Folkman and Klagsbrun, 1987; Klagsbrun and D'Amore, 1991). Neovascularisation is completed by formation of capillary lumina and differentiation of newly formed capillaries into arterioles and venules.

The female reproductive system (ovary, uterus and placenta) is unique in the fact that spontaneous angiogenesis occurs in a cyclic manner. In no other normal tissue in the adult does this happen. In a normal adult vessel, only one in every ten thousand endothelial cells is in the cell division cycle at any given time (Engerman *et al.*, 1967; Hobson and Denekamp, 1984). Growth and regression of the female reproductive organs however, is extremely rapid and is accompanied by equally rapid changes in their vasculature (Reynolds and Redmer, 1995). For example the rate of cellular proliferation in the early corpus luteum is comparable with or greater than that of rapidly growing tumours or regenerating tissues (Reynolds *et al.*, 1994; Zheng *et al.*, 1994; Nicosia *et al.*, 1995; Christenson and Stouffer, 1996b). In contrast to the angiogenesis observed during pathological tissue growth, vascular development of the female reproductive system is limited and, thus, must be tightly regulated (reviewed by Redmer and Reynolds, 1996).

Due to the fact that luteal angiogenesis is a naturally regulated process, occurring in a spontaneous cycle of active proliferation, vessel stabilisation and regression, for quantification of such a dynamic process *in vivo*, it is necessary to examine particular time points in the lifespan of the corpus luteum. Characteristically the non-pregnant luteal cycle is divided into three stages: the early, developing corpus luteum in which production of progesterone in increasing; the mid-luteal stage, when maturity of the gland is reached and progesterone production is maximal; the late luteal phase, which is associated with functional and structural regression. A fourth luteal stage is available for analysis in the human corpus luteum

which, by exposure to increasing concentrations of hCG, simulates the luteal rescue associated with early pregnancy (Illingworth *et al.*, 1990). It is therefore reasonable to investigate the angiogenesis associated with these luteal stages as changes in gland structure and function are directly related to the angiogenic activity of the system. In quantifying luteal angiogenesis *in vivo* it is imperative that the dynamic vascular changes are examined in context, *in situ*, so relationships with other luteal cells and the associated changes in luteal morphology can also be analysed. It is for this reason that quantification of luteal angiogenesis was performed on fixed luteal sections by immunocytochemical methods.

Quantification of endothelial cell proliferation in the corpus luteum and the resultant changes in luteal endothelial cell content are two effective methods of measuring *in vivo* angiogenesis in luteal sections. Analysis of proliferation depends on the assessment of the number of cells which are undergoing mitosis in any given population, however the mitotic process is completed in approximately 5 min, so the likelihood of observing mitotic figures in histological sections is very low (O'Shea *et al.*, 1986), therefore antigens expressed during other parts of the dividing cell cycle are exploited as proliferation markers for detection by immunocytochemical methods. The cell cycle has a period of intense DNA synthesis, the S phase, which can take 7 to 12 hours to complete. This is followed by a post synthesis gap (G_2) which lasts 1 to 6 hours when the cell undergoes growth and prepares for mitosis. After mitosis cells grow to an optimal size, known as the G_1 phase of growth. This stage can be of variable length and it is also at this stage when cells can enter G_0, during which they are not actively proliferating. Specific proliferative stimuli can cause some cells to re-enter the cell cycle, whereas some cells lose their proliferative competency and never re-enter the cell cycle, these are permanently in the G_0 phase and are often terminally differentiated (Boulton and Hodgson, 1995).

Cell proliferation antigens expressed during the cell cycle include: the nuclear non-histone protein, Ki67, and proliferating cell nuclear antigen, PCNA. Other markers, incorporated into DNA *in vivo,* include tritiated thymidine or a halogenated thymidine derivative, 5-bromo-2'-deoxyuridine (BrdU). Ki67 is expressed during all phases of the cell cycle except the early part of G_1 and G_0 (Gerdes *et al.*, 1984). PCNA is an auxiliary protein for DNA polymerase δ, it has a long half life of up to 20 hours (Diebold *et al.*, 1994) and is expressed over G_1, S phase and G_2 stages of

the cell cycle. It is immunolocalised to the nuclei of proliferating cells although non-specific cytoplasmic staining is also common (Wolf and Dittrich, 1992; Sabattini *et al.*, 1993). BrdU and tritiated thymidine label proliferating cells *in vivo* by incorporation into DNA during the S phase of the cell cycle. The labelling rate depends on the amount of time the substance is available for incorporation which, in turn, is dependent on its initial concentration and clearance rate. Best results are obtained when the labelling period is shorter than the duration of the S phase for the cell population concerned, so that only cells in the synthesis stage of the cycle are labelled (Boulton and Hodgson, 1995). Detection of tritiated thymidine involves autoradiography whereas monoclonal antibodies to BrdU are available to specifically detect proliferating cells by immunocytochemistry. Proliferation studies in the marmoset corpus luteum were performed using BrdU incorporation administered 1 hour before tissue collection to selectively label cells in the S phase of the cell cycle, and incorporation detected by immunocytochemistry. Proliferation studies in the human corpus luteum were performed using immunocytochemistry for Ki67.

Approximately 50% of the cells in the corpus luteum are endothelial cells (Lei *et al.*, 1991; Christenson and Stouffer, 1996b;), and an extensive capillary network penetrates the corpus luteum, so much so that every steroidogenic cell is in contact with at least one capillary (Redmer and Reynolds, 1996). The primary function of the corpus luteum is the production of steroid hormones, and steroidogenesis is entirely dependent on the delivery of cholesterol substrates and regulatory gonadotropins through the luteal vasculature. Maximal plasma progesterone concentrations do not occur until the luteal vasculature is fully developed. Development of the vasculature can be assessed by the quantification of luteal endothelial cells throughout the lifespan of the corpus luteum. Antibodies to specific endothelial cell antigens are commercially available and quantification of immunostaining using these antibodies is simplified with the advent of computer based image analysis systems.

There exists extensive endothelial cell heterogeneity (Bicknell, 1996), and expression of particular endothelial cell antigens for immunocytochemical detection may vary according to the species and tissue in question, or age of the endothelial cells. It is for this reason that immunocytochemistry was performed with antibodies raised against three specific endothelial cell antigens: von Willebrand factor (or

factor VIII-related antigen); CD31, (or PECAM-1, platelet endothelial cell adhesion molecule-1); and CD34. von Willebrand factor is a multimeric plasma glycoprotein, stored in endothelial cell cytoplasmic Weibel-Palade bodies. It mediates platelet adhesion to injured vessel walls and serves as a carrier and stabiliser for coagulation factor VIII (Zimmerman, 1987). It is often used to visualise the pattern of vascular elements within a tissue. CD31 or platelet endothelial cell adhesion molecule-1, is a single chain, endothelial cell membrane glycoprotein. It has an extracellular domain which mediates endothelial cell-cell adhesion, plays a role in endothelial cell contact and may serve to stabilise the endothelial cell monolayer, suggesting an involvement in interactive events during angiogenesis. Staining of vessels with antibody to CD31 has shown to be suitable in the judgement of angiogenesis in several types of tumour (Horak *et al.*, 1992; Charpin *et al.*, 1995; Giatromanolaki *et al.*, 1996; Takebayashi *et al.*, 1996; Fox *et al.*, 1997). CD34 is another single chain, endothelial cell transmembrane glycoprotein (Simmons *et al.*, 1992). Monoclonal anti-human CD31 and CD34, and rabbit polyclonal anti-von Willebrand factor antibodies were used for endothelial cell immunostaining.

Endothelial cell immunostaining was either located to the cell cytoplasm or plasma membrane making visualisation of individual cells difficult. It was therefore not possible to measure absolute endothelial cell numbers in the corpus luteum, so quantification based on area of immunostaining per unit area of the corpus luteum proved optimal. When changes in a particular cell content are quantified per unit area of luteal tissue, factors such as the change in luteal volume (translated to area in tissue sections) over the lifespan of the corpus luteum have to be addressed, or results will reflect the effects of expanding or contracting tissue as opposed to increases or decreases in content of the particular cell in question. Many factors affect the volume of the corpus luteum throughout the luteal phase. These include the proliferation and demise of endothelial cells themselves, or periendothelial support cells, the infiltration of immune cells, or proliferation of fibroblasts in the regressing corpus luteum. However, the contribution of changes in numbers of these small cells is believed to be negligible to overall luteal volume when compared to the effects of hypertrophy of the larger steroidogenic cells in the developing corpus luteum and atrophy in the regressing corpus luteum. The change in lutein cell cytoplasmic

volume thus had to be quantified and the area used to measure endothelial cell content adjusted accordingly.

In vivo angiogenesis can also be quantified by measuring the expression of known angiogenic factors. One such factor is VEGF (also referred to as VEGF-A). VEGF is a secreted angiogenic mitogen (Leung *et al.*, 1989), specific for endothelial cell receptors (Plouet and Maukadiri, 1990; Vaisman *et al.*, 1990). VEGF protein has been located to a subpopulation of granulosa cells in human follicles which sequester such growth factors in a novel mechanism, and may be released in a new mode of directed secretion which could serve to support rapid bursts of cellular growth during folliculogenesis and corpus luteum formation (Antczak *et al.*, 1997). Both VEGF mRNA and its transcribed protein have been localised to granulosa and theca derived lutein cells in the human corpus luteum (Kamat *et al.*, 1995; Otani *et al.*, 1999). It has a paracrine action: expression and secretion from steroidogenic cells and action at endothelial cells, thus the steroidogenic cells of the corpus luteum drive angiogenesis to increase vasculature for their own supply of O_2, nutrients and steroid precursors needed for survival and progesterone synthesis.

Termination of active angiogenesis is associated with the stabilisation of the newly formed vasculature by periendothelial support cells such as pericytes. Fully differentiated pericytes are contractile cells containing cytoplasmic actin and myosin filaments, they have large cytoplasmic processes which surround endothelial cells, converting capillaries to venules and arterioles. Their association with vessels renders the vessel mature and gives them the ability to survive without the aid of VEGF (Benjamin *et al.*, 1999). Recruitment of pericytes has been documented soon after induction of bovine luteal angiogenesis and the percentage of vessels with associated pericytes increases as the luteal phase progresses (Goede *et al.*, 1998). Coverage of blood vessels with differentiated pericytes can be regarded as a relative parameter of the maturity of a developing neovasculature, which can be detected by immunocytochemistry for the contractile protein, α-smooth muscle actin (Skalli *et al.*, 1989; Diaz-Flores *et al.*, 1991).

The aim of this chapter was to quantify angiogenesis in the primate corpus luteum, using the parameters outlined above, taking into consideration not only components of vessel proliferation, but also their maturation; and how this quantification was best performed in such dynamic tissue. Since the formation of a

corpus luteum is associated with prolific angiogenesis, and regression with a decreased angiogenic rate in the human (Rodger *et al.*, 1997; Gaytan *et al.*, 1998), rhesus monkey (Christenson and Stouffer, 1996b), bovine (Zheng *et al.*, 1994) and ovine (Jablonka-Shariff *et al.*, 1993), similar results are expected in the marmoset. A previous study has demonstrated that the rescue of the human corpus luteum by hCG in simulated early pregnancy is not associated with increased endothelial cell proliferation (Rodger *et al.*, 1997). This study aims to test this hypothesis using a more advanced quantitative method which assesses endothelial cell proliferation as a percentage of total luteal cells, by obtaining a proliferation index.

3.2 Materials and Methods

3.2.1 Animals, BrdU administration and tissue analysis

Marmoset monkeys were housed as previously described (Chapter 2), and procedures were carried out in accordance with the Animals (Scientific Procedures) Act, 1986. Blood samples were collected by femoral venepuncture, three times per week, without anaesthesia. Ovulatory cycles were monitored by RIA of plasma progesterone, as previously described (Chapter 2). The stage of the ovulatory cycle was determined according to plasma progesterone concentration following the guidelines described in Chapter 2. Ovaries were collected from animals in the early (luteal days 2-4), mid-(days 8-10), and late (days 16-20) luteal phase of the ovulatory cycle (n=5 animals per group), and in the follicular phase to examine regressed corpora lutea (n=4). Twenty milligrams of BrdU (Roche Molecular Biochemicals, Sussex, UK), dissolved in 500μl physiological saline, was administered i.v., 1h before tissue collection, to label proliferating cells in the S phase of the cell cycle, via incorporation into DNA. This allowed changes in endothelial cell proliferation throughout the luteal phase of the ovulatory cycle to be determined. Ovaries from these animals were also examined for expression of the specific endothelial cell antigens, von Willebrand factor VIII-related antigen (von Willebrand factor) and CD31; the pericyte marker, α-SMA; and the potent endothelial cell mitogen, VEGF. These studies were supplemented with examination of expression of the proliferation marker, Ki67; the endothelial cell antigen, CD34; and the pericyte marker, α-SMA, in archived human luteal sections throughout the early, mid- and late luteal phases

and in hCG rescued tissue (n=4-6 per luteal stage), to examine if luteal rescue is associated with increased angiogenic activity in the form of endothelial cell proliferation or with stabilisation of the existing vasculature. Different endothelial cell markers were immunolocalised in marmoset and human sections because of interspecies variance in immunoreactivity.

3.2.2 Immunocytochemistry

Immunocytochemistry for BrdU was performed to visualise proliferating cells in marmoset luteal sections. Sections were dewaxed in histoclear for 5-10 min and rehydrated by washing in decreasing concentrations (100%, 95% and 70% in H_2O) of industrial methylated spirits (20 sec in each), and finally in H_2O. Antigen retrieval by heat treatment, either microwaving or pressure cooking, in 0.01M citrate buffer (pH 6) was necessary to unmask the BrdU antigen covered by tissue fixation and processing. Methods of antigen retrieval by heat treatment are described in Chapter 2. Slides were cooled in TBS (0.05M Tris/HCl, pH8, + 0.85% w/v $NaCl_2$). The Sequenza system was set up and non specific background was blocked by incubation in normal rabbit serum (NRS, SAPU, diluted 1:5 in TBS + 5% w/v bovine serum albumin; BSA) for 30 min at room temperature. Slides were not washed and primary antibody, monoclonal mouse anti-BrdU (Boehringer Mannheim), was applied at a concentration of 3.3μg/ml in TBS (1:30 dilution) and incubated at 4°C overnight. For negative control sections primary antibody was replaced with mouse IgG at the same concentration. TBS was flushed through the Sequenza system 3 times to wash unbound antibody from sections. Secondary/bridging antibody, rabbit anti-mouse, was applied at a concentration of 26.6μg/ml in NRS (1:60 dilution) for 30 min at room temperature. Unbound antibody was washed from sections, and mouse APAAP in NRS (1μg/ml, 1:100 dilution) applied for 30 min at room temperature. Slides were placed in TBS for a thorough wash before NBT detection was performed. Slides were placed in NBT buffer (0.1M Tris, 0.1M $NaCl_2$, 0.05M $MgCl_2$, pH 9.7) for 5 min. Excess buffer was wiped from each slide and NBT solution (45μl 75mg/ml NBT in 70% dimethylformamide; 35μl X-phosphate/5 Bromo-4 chloro-3 inodyl-phosphate in 100% dimethylformamide; and 1mM levamisole; all in 10ml NBT buffer) applied in a dark humid box for 15-30 min at room temperature. Staining was evaluated under light microscopy and slides re-incubated in NBT solution if

necessary. When the desired colour had developed the reaction was stopped in tap water and sections were counterstained in haematoxylin for 1-5 min, and the colour developed in Scott's tap water (0.002% w/v potassium hydrogen carbonate, 0.02% w/v magnesium sulphate in tap H_2O) for 20-60 sec. Sections were dehydrated in absolute alcohol for 30 sec and rapidly cleared in xylene before being mounted using Pertex mounting medium and glass coverslips.

Dual staining for BrdU (Boehringer Mannheim) and either endothelial cell marker, von Willebrand factor or CD31, was carried out to determine the proportion of proliferating endothelial cells in the marmoset corpus luteum. Colocalisation of BrdU with von Willebrand factor was detected using TRITC (tetra rhodamine TRITC (tetra rhodamine isothyocyanate)/FITC (fluorescein isothyocyanate) conjugated secondary antibodies. Antigen retrieval was performed by microwaving as described in Chapter 2. Sections were washed in PBS (0.01M phosphate-buffered saline, pH 7.4, containing 2.7mM KCl, 0.137M NaCl). and treated for 30 min at room temperature with normal goat serum, (NGS, diluted 1:5 in PBS + 5% w/v BSA) followed by dual incubation in rabbit polyclonal anti-von Willebrand factor (22.8μg/ml in NGS), and mouse monoclonal anti-BrdU (6.6μg/ml in NGS) at 4°C, overnight. Immunolocalisation was undertaken using anti-rabbit FITC conjugate (diluted 1:50 in NGS, Sigma F-6005) and anti-mouse TRITC conjugate (diluted 1:50 in NGS, Sigma T-5393) dual incubation for 45 min at room temperature. Slides were mounted from PBS using Permafluor aqueous mounting medium. The U-MWIBA and U-MWG filters on the Olympus AX70 Provis fluorescent microscope were used to visualise FITC-stained von Willebrand factor positive cells, and TRITC-stained BrdU positive cells, respectively.

The occurrence of erythrocyte auto-fluorescence masked BrdU staining in most sections and this prevented quantification of endothelial cell proliferation in the majority of corpora lutea. To circumvent this problem a colorimetric approach for BrdU and CD31 antigens was also used for analysis. Sections were dewaxed and rehydrated as normal. Both antigens were retrieved by pressure cooking in 0.01M citrate buffer, pH6. Sections were incubated with anti-CD31 (20.5μg/ml, diluted 1:20 in TBS) alone at 4°C, overnight, and secondary and tertiary antibodies applied as described for single BrdU immunostaining. Detection was performed using Fast Red substrate (Sigma). Sections were incubated in Fast Red solution (1mg of Fast Red

BB salt, per 1ml buffer, containing 20mg naphthol AS-MX Phosphate, 2ml dimethyl formamide, and 98ml 0.1M Tris pH 8.2, all Sigma), for 15-30 min until a bright red reaction end product had formed. The reaction was terminated with cold tap water. For BrdU colocalisation, non-specific binding was blocked using NRS. Sections were incubated in mouse monoclonal anti-BrdU (3.3µg/ml, in TBS) at 4°C, overnight, or for 2h at room temperature. BrdU detection was performed as described for single BrdU immunostaining using NBT. Sections were faintly counterstained and aqueous mounted in Permaflour mounting medium.

Proliferating cells in human luteal sections were analysed by immunocytochemistry for Ki67. This was performed by Dr. Christine Wulff. Sections were dewaxed and rehydrated as previously described. Ki67 antigen was retrieved by microwaving. Sections were cooled in TBS, and an NRS block was applied for 30 min at room temperature. Monoclonal anti-human Ki67 antibody (Novacastra, Peterborough, Cambs, UK) was applied at a dilution of 1:50 in TBS, for 2 h at 37°C. Detection was carried out using biotinylated rabbit anti-mouse (Dako Ltd: E0464, diluted 1:500 in blocking serum) for 30 min at room temperature, followed by preconjugated ABC-AP in 0.05M Tris, pH 8, for 30 min at room temperature. NBT was used for visualisation, and sections were counterstained in haematoxylin.

Immunocytochemistry for the endothelial cell marker von Willebrand factor, was performed after dewaxing and rehydrating tissue sections. Proteolytic digestion was used for antigen retrieval as described in Chapter 2. The sequenza system was set up and non-specific binding blocked with at 30 min incubation at room temperature in normal swine serum (NSS, SAPU, diluted 1:5 in TBS + 5% w/v BSA). Rabbit polyclonal von Willebrand factor antibody was applied at a concentration of 22.8µg/ml (1:250 dilution in TBS) which bound overnight at 4°C. Negative controls were incubated in NSS in place of primary antibody. Sections were washed 3 times with TBS and incubated in swine anti-rabbit at a protein concentration of 1mg/ml (diluted 1:60 in NSS) for 30 min at room temperature. After washing with TBS, rabbit APAAP (Serotec, 2AB08A; diluted 1:100 in NSS) was applied for 30 min at room temperature. Sections were washed and NBT used for detection as described for BrdU immunostaining. Sections were not counterstained so that image analysis could be performed for quantification purposes.

Separate immunostainings for CD31 and α-SMA were performed following the same protocol as for BrdU. Primary antibody, mouse monoclonal CD31, was used at a working concentration of 20.5μg/ml, (diluted 1:20 in TBS), α-SMA was applied at 4.3μg/ml (diluted 1:20 in TBS). Negative controls were incubated in equivalent concentrations of mouse IgG in TBS. NBT detection was used and sections either counterstained faintly, or not at all, for image analysis quantification.

Immunocytochemistry for the endothelial cell specific antigen, CD34, was performed on human luteal sections. Sections were dewaxed and rehydrated as normal and endogenous peroxidase activity was quenched with a 30 min incubation in 3% hydrogen peroxide in methanol, at room temperature. NGS block was used and sections were incubated overnight at 4°C in mouse monoclonal CD34 antibody (Serotec: MCAP547) applied at a 1:25 dilution in TBS. Immunolocalisation was undertaken using the mouse EnVision kit (Dako Ltd, Cambridge, UK). One hundred microlitres of conjugated goat anti-mouse/ABC-HRP was applied for 30 min at room temperature. Sections were washed in TBS and liquid DAB substrate (EnVision kit) was used for detection. Sections were not counterstained as image analysis was to be performed.

Sections for VEGF-A immunocytochemistry were dewaxed and rehydrated. VEGF antigen was retrieved by pressure cooking slides on full power in 3M glycine, 0.1% EDTA buffer, pH 3.5, for 5 min. The slides remained in hot buffer for a further 20 min and were washed in TBS. Endogenous peroxidase activity and endogenous biotin were blocked as described in Chapter 2. Rabbit polyclonal VEGF antibody, specific for VEGF-A (2μg/ml pre-diluted in NGS; VEGF A-20, Santa Cruz Biotechnology, Santa Cruz, CA, USA), was added and sections incubated at 4°C, overnight. Negative controls were incubated in primary antibody pre-absorbed with VEGF-A peptide in a ratio of 1:5, VEGF-A antibody : blocking peptide (Santa Cruz). Immunolocalisation was undertaken using the rabbit EnVision kit in the same way as the mouse was used for CD34 immunostaining. Sections were counterstained and mounted.

Human luteal sections were dual stained for von Willebrand factor and α-SMA to verify that each antibody bound different cell types. Antigens were retrieved by trypsinisation as described in Chapter 2. An NGS block was performed and both primary antibodies applied simultaneously at their working concentrations incubating

overnight at 4°C. Detection and analysis was performed with TRITC/FITC fluorescent conjugated antibodies as for von Willebrand factor and BrdU dual staining in marmoset sections.

3.2.3 Haematoxylin and Eosin staining

Sections were dewaxed and rehydrated as described previously. Slides were placed in haematoxylin for 1-5 min, rinsed in tap water and the nuclear blue colour developed in Scott's tap water. Staining was checked by light microscopy, if too intense, staining was cleared by dipping slides in 1% acid alcohol, or back into haematoxylin if staining was too light. For the cytoplasmic pink stain sections were dipped for 10 sec in eosin, and rinsed in tap water. Sections were dehydrated in ascending concentrations of alcohol (70%, 95% and 100% in H_2O), cleared in xylene before being mounted and coverslipped.

3.2.4 Quantification

All marmoset sections were examined for appropriately staged corpora lutea as defined by the morphology of lutein cells and the presence of an antrum as described in Chapter 1. Those sections which had not been counterstained were analysed alongside serial sections stained with H and E to locate suitable corpora lutea for quantification.

BrdU positive and total cells were counted manually at x400 magnification in 6 fields per corpus luteum. In the early corpus luteum, fields were selected which formed a cross configuration throughout the corpus luteum, as close as possible without counting in the antrum if one was present in the section. In the larger mid-corpus luteum a cross formation was obtainable, this meant a fair representation of the whole corpus luteum was quantified. A PI was obtained by expressing the number of BrdU positive cells as a percentage of total cells per 6 fields, and the PI's meaned to get a value per animal. Selected sections were quantified by a second person independently to assess the reproducibility of such quantification. Also, from selected paraffin wax blocks a second section, cut from a distance into the block, was quantified to assess how representative quantification of proliferation in one section was to the whole corpus luteum.

Manual counting procedures were used to calculate the percentage of proliferating endothelial cells for each corpus luteum. Quantification was performed on both fluorescent sections and those stained using the colorimetric approach. Both left and right ovaries from five animals from the early and mid-luteal phases and from one animal in the late luteal phase were examined for appropriately staged corpora lutea and the percentage of proliferating endothelial cells quantified. Six fields per corpus luteum, arranged in a cross formation, at x400 magnification, were analysed using a grid overlay. The number of proliferating endothelial cells was expressed as a percentage of proliferating cells, *i.e.* (number of dual stained cells/total number of BrdU positive cells) x100.

Quantification of Ki67 immunostaining in human sections was performed by Dr. Christine Wulff using the Media Pro-Plus 3.0 image analysis system. Sections were examined using the x20 lens and 6-10 fields of view, randomly chosen, analysed per corpus luteum. The image analysis system was set to measure the number of dark stained nuclei only (Ki67 positive), and the number of dark and light stained nuclei (total cells) per field of view. A PI was obtained by expressing the number of Ki67 positive nuclei as a percentage of total nuclei per field of view, and the mean of 6-10 fields taken as representative for that corpus luteum.

The area of each of 10 steroidogenic cells in marmoset corpora lutea and granulosa lutein cells in human corpora lutea were measured to assess the change in area over the luteal phase of the cycle. Images of H and E stained sections were examined under the x40 lens and captured using the Media Pro-Plus 3.0 image analysis system. Ten cells in ten fields of view, again arranged in a cross formation, were outlined using the mouse and Outline tool, and a macro was recorded to measure the area of each outlined shape, and mean the results per field of view. An average of 10 corpora lutea were analysed per stage in the marmoset, and 4 corpora lutea in the human.

Immunostaining for von Willebrand factor, CD31, CD34 and α-SMA, in both the marmoset and human, was quantified by measuring area of staining using the Media Pro-Plus 3.0 image analysis system. These antigens are all located to cell cytoplasm or plasma membrane thus it was not possible to visualise cell margins, and so absolute cell numbers could not be measured. Immunostaining in marmoset corpora lutea were quantified using the x20 lens, for the larger human corpora lutea

the x10 lens was used. A macro was recorded to measure the area of dark objects on a white background in a predetermined area of interest (field of view), and the threshold for quantification set so that the captured image represented the live image as closely as possible. At least two thirds of each corpus luteum was quantified by selecting the next area of interest as close as possible to the previous one. Due to differences in size of corpora lutea form different stages of the luteal phase varying numbers of areas of interest were quantified for each luteal stage. To address the problem of change in luteal volume at different stages of the cycle, as primarily determined by steroidogenic cell hypertrophy and atrophy, different sized areas of interest were measured for each corpus luteum at a particular stage of the cycle. The "area of interest" was a comprehensive coverage of the randomly chosen field of view. For early luteal phase marmoset corpora lutea the area of interest covered $9.2x10^4$ μm^2, $1.3x10^5$ μm^2 for the mid-luteal phase marmoset corpus luteum, and $1.1x10^5$ μm^2 for the late luteal phase marmoset corpus luteum. The size of these areas of interest were calculated by multiplying the largest area of interest by the specific conversion factor for each stage of the luteal phase (as calculated from the change in steroidogenic cell area throughout the cycle). If quantification was performed using the same sized area of interest for corpora lutea from each stage of the cycle, the mean per group could be multiplied by the specific conversion factor for that stage which gave results with an identical trend and statistical significance to those gained from using different sized areas of interest for each luteal phase. Measurements from human luteal immunostaining were converted in this way using data gained from the change in area of granulosa lutein cells throughout the human luteal phase.

VEGF-A immunostaining was quantified using Photoshop version 5.0 according to the methods used by Otani *et al.,* (1999) for VEGF quantification as demonstrated by Lehr *et al.,* (1999). Tissue sections were examined using the x20 lens on an Olympus Provis microscope and images were captured using a digital camera, either the Kodak DCS420 or Kodak DCS330. Captured images were opened in Photoshop version 5.0, the default size and resolution was used for each image. To ensure that only the VEGF-A immunostaining would be quantified and not the counterstain, the colour contrast of the image was enhanced adjusting the Hue/Saturation tools in the Image Adjust menu to constant levels. The Magic Wand tool was used to select one positively stained cell, and using the Similar tool in the

Select menu all immunopositive tissue was selected. The pixel count of the selected chromogen was quantified using the Histogram command in the Image menu. The Histogram also displays the optical density of all pixels within the selected area in the form of a graph, in which each vertical line represents the number of pixels which are associated with a brightness level, on the left side the darkest areas and on the right side the brightest areas. The mean value represents the staining intensity of selected areas. The lower the optical density, the darker the area, *i.e.* the more intense the staining, and hence the greater the expression. For each image the pixel count (area of staining) and the mean value (intensity of staining) were noted. As many fields of view were photographed and quantified as the size of the corpus luteum would allow.

For quantification of all immunostaining the mean of all fields (and all corpora lutea per marmoset) were taken as representative for each subject, and the mean of all subjects per group was taken as representative for each stage of the luteal phase.

3.2.5 Statistical analysis

Data from each method of quantification of immunostaining was statistically analysed. Separate one way analysis of variance tests were carried out for each set of data, and a factorial Fisher's protected least significant difference post hoc test performed. When comparing just 2 groups, *i.e.* for the comparison of 2 sections per corpus luteum, or 2 independent quantifications of the same section, two-tailed, unpaired t tests were used. $P<0.05$ was taken as the level of significance for each test. All tests were performed using StatView Version 4.0 for the Macintosh.

3.3 Results

3.3.1 PI and marmoset plasma progesterone throughout the luteal phase

BrdU staining indicating proliferating cells was readily observed in all marmoset corpora lutea. In the marmoset, differences between theca and granulosa derived lutein cells are not readily apparent (Webley *et al.*, 1990), both types of hormone producing cells having a large spherical or polyhedral nucleus and abundant cytoplasm. It was clear that none of the hormone-producing cells had incorporated

BrdU. Incorporation was restricted to some cells surrounding the luminal microvessels and in those whose appearance and was consistent with capillary endothelial cells (Fig 3.1a). Low power micrographs of sections throughout the ovulatory cycle demonstrated that BrdU incorporation in the early luteal phase (Fig. 3.1b) appeared to be greater than that in mid- (Fig. 3.1c) and late (Fig. 3.1d) corpora lutea. Positive nuclei were not present in negative control sections.

Quantification of the PI (Fig. 3.2a) throughout the luteal phase of the marmoset ovulatory cycle revealed peak cell proliferation in the early corpus luteum, which declined markedly ($P<0.001$, as compared to early levels) in the mid- and late corpus luteum. The 2.5 fold decrease in PI from the mid- to late corpus luteum was significant ($P<0.05$). Correspondingly, plasma progesterone concentrations (Fig. 3.2b) were maximal ($P<0.01$) in the mid-luteal phase after proliferation of the endothelium which signifies growth of the microvascular network. Plasma progesterone concentration subsequently decreased ($P<0.01$) in the late luteal phase, coinciding with a fall in endothelial cell proliferation.

To test the reproducibility of calculation of the PI, selected sections (n=15 sections) were independently quantified by Helen Wilson. The two independent quantifications correlated highly ($r=0.978$) signifying the method used for quantification was reproducible (Fig. 3.3).

To examine the representative nature of the quantification of one section to the whole corpus luteum, the PI of a subsequent second section from selected corpora lutea were obtained. Figure 3.4a demonstrates that the trend remains the same over the luteal phase although results from quantification of the first sections demonstrated a significant difference between mid- and late corpora lutea, whereas PI's from the second sections showed no significant change between these stages. However, there were no significant differences between first and second section PI's within one stage of the cycle. This signifies that quantification of one section represents the whole corpus luteum.

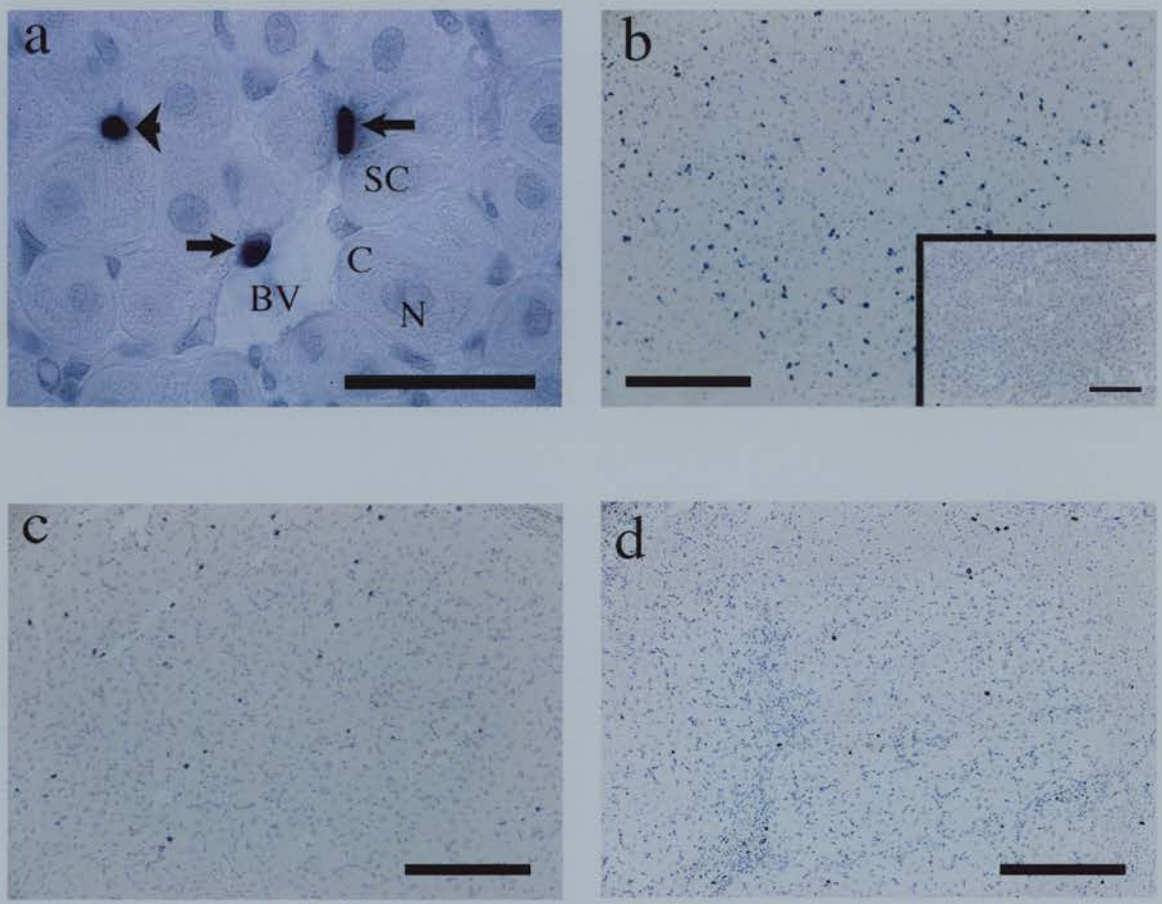

Figure 3.1 Incorporation of bromodeoxyuridine in marmoset corpora lutea
(a) High power photomicrograph showing the large steroidogenic cells (SC) with abundant cytoplasm (C), round nucleus (N) and absence of BrdU staining. Note the microvessel located centrally (BV) composed of endothelial cells with little cytoplasm and elongate nuclei. Note the presence of dark BrdU proliferating cells associated with the blood vessel as indicated by arrows, and in endothelial cells (arrow head) of capillaries distributed between the hormone producing cells. (b-d) low power photomicrographs of early, mid- and late corpora lutea, respectively. Dark staining indicates nuclear BrdU incorporation. The insert in (b) demonstrates the absence of staining in a negative control early corpus luteum. Scale bar on a = 50μm. Scale bars on b-d = 100μm.

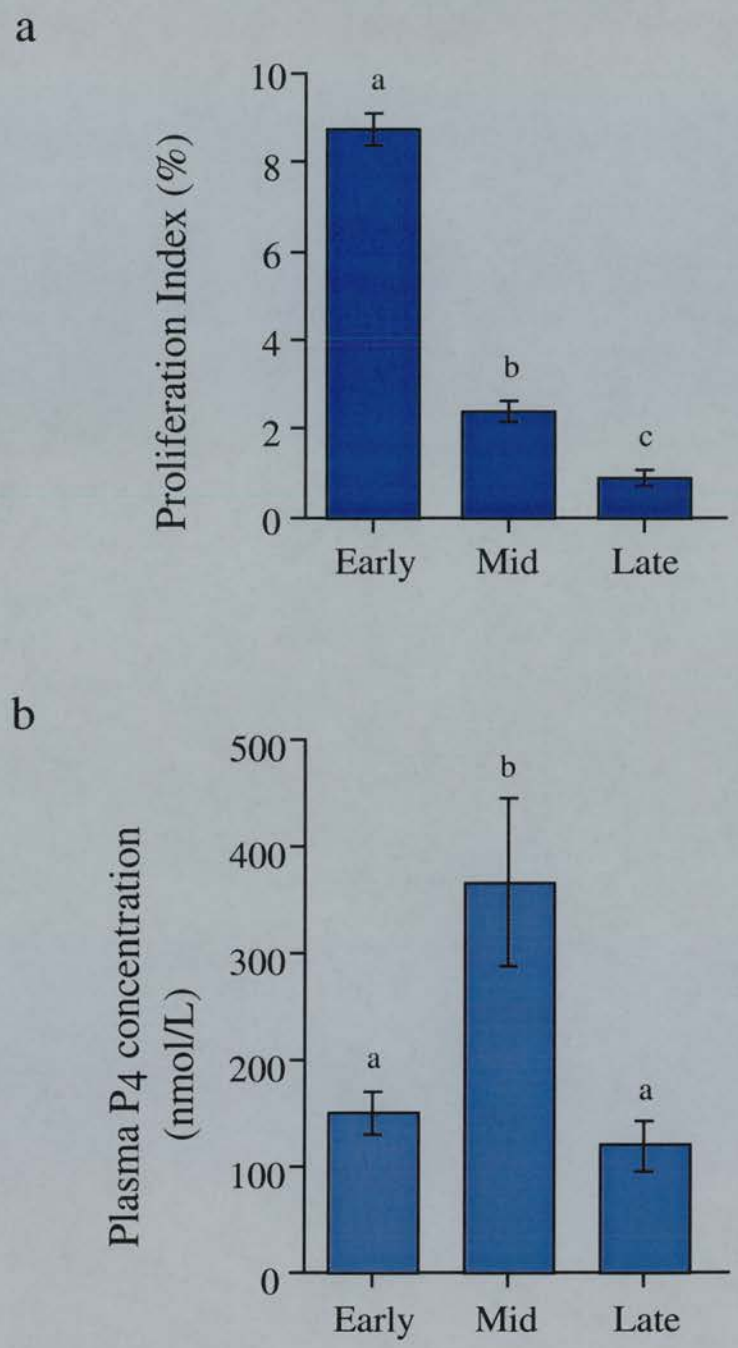

Figure 3.2 Proliferation index and plasma progesterone concentrations in marmoset corpora lutea

(a) Cell proliferation; and (b) plasma progesterone concentrations throughout the luteal phase of the marmoset ovulatory cycle. Values are means ± SEM. Different letters denote significant differences between groups, $P<0.05$. For each stage of the luteal phase n=5 animals.

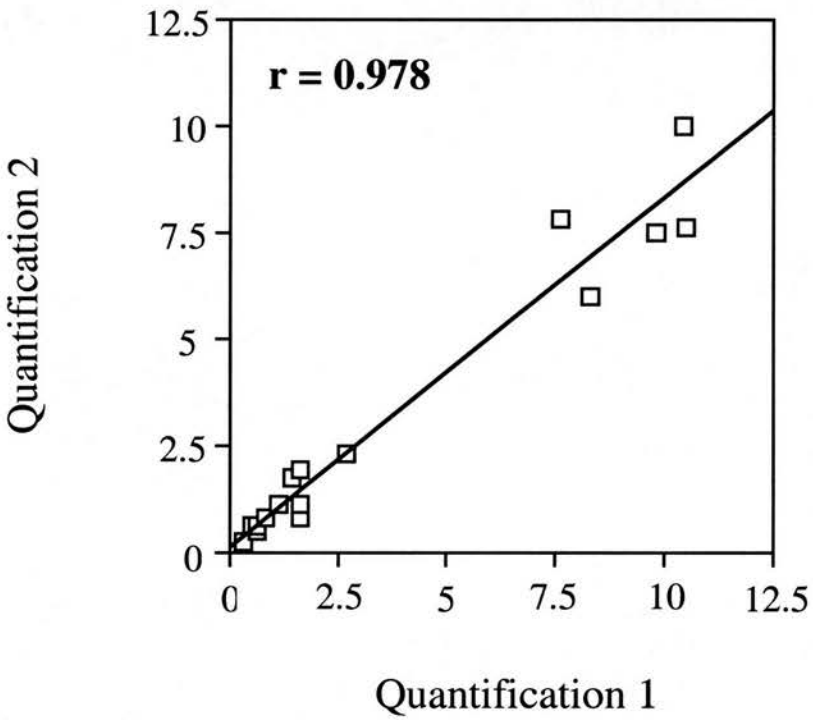

Figure 3.3 Correlation of two independent quantifications of the marmoset corpus luteum proliferation index

The correlation of two quantifications of marmoset luteal cell proliferation. The correlation coefficient r value from two independent PI quantifications is close to 1, signifying the method of quantification used is highly reproducible. 15 sections were quantified by a second individual.

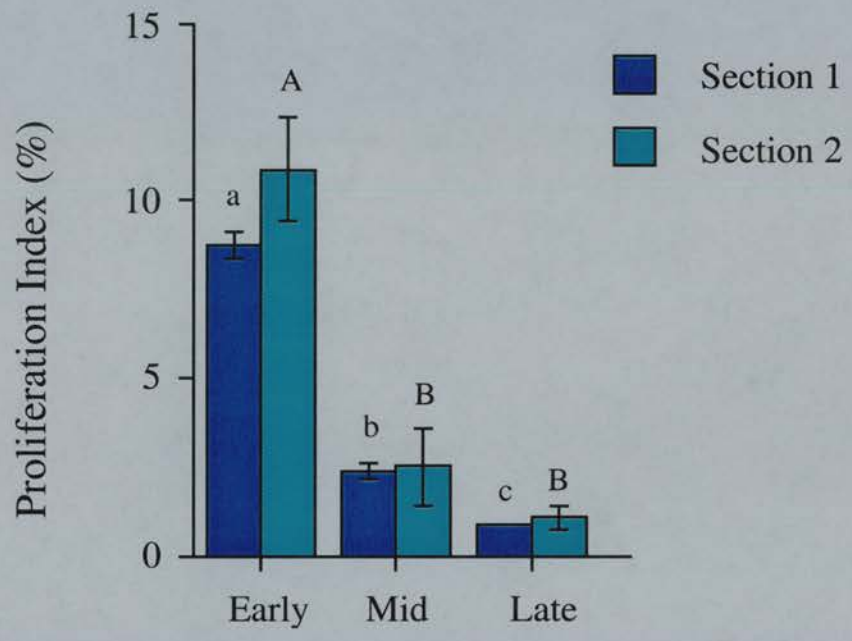

Figure 3.4 Correlation of proliferation indices from two sections of the same marmoset corpus luteum

Comparison of the trend in PI from marmoset luteal Section 1 (blue bars) and Section 2 (turquoise bars) during the luteal phase. There was no significant difference between sections of the same stage of the luteal phase. Values are means ± SEM. Different letters denote significant differences between groups, $P<0.05$. For each stage of the luteal phase n=5 animals.

To determine the number proliferating cells in the marmoset corpus luteum that were endothelial cells, sections (n=10 sections for early and mid-stage corpora lutea) from selected animals (n=5 for early and mid-stage corpora lutea) were dual stained with either BrdU and the endothelial cell marker von Willebrand factor, or BrdU and another endothelial cell marker, CD31 (Fig. 3.5). Colocalisation of the red, nuclear BrdU stain and the green, cytoplasmic von Willebrand factor stain (Fig.3.5c) demonstrated dual labelling of most proliferating cells in the early luteal phase. Similarly, colocalisation of the black, nuclear BrdU stain and red, cell membrane CD31 stain in the early, mid-, and late luteal phases shows dual staining of most proliferating cells, as demonstrated by the mid-luteal section under higher power (Fig. 3.5g). When the proportion of dual staining cells was quantified it was apparent that over 80% of proliferating cells in the marmoset corpus luteum were endothelial cells (Fig. 3.6).

Ki67 immunostaining indicating proliferating cells in human luteal sections was readily observable in all human corpora lutea. A high level of Ki67 positive cells was observed in sections from the early luteal phase (Fig. 3.7a) which was markedly reduced in mid- and late luteal sections (Fig. 3.7b-c). A similar pattern of staining as the early luteal phase was seen in sections after hCG rescue (Fig. 3.7d). When quantified, the PI for Ki67 staining in the human demonstrated a significant decrease in the percentage of Ki67 positive cells from early luteal phase levels in the mid- ($P<0.05$) and late ($P<0.05$) corpus luteum, and a marked increase in proliferation ($P<0.05$) similar to early luteal phase levels, after hCG rescue (Fig. 3.8).

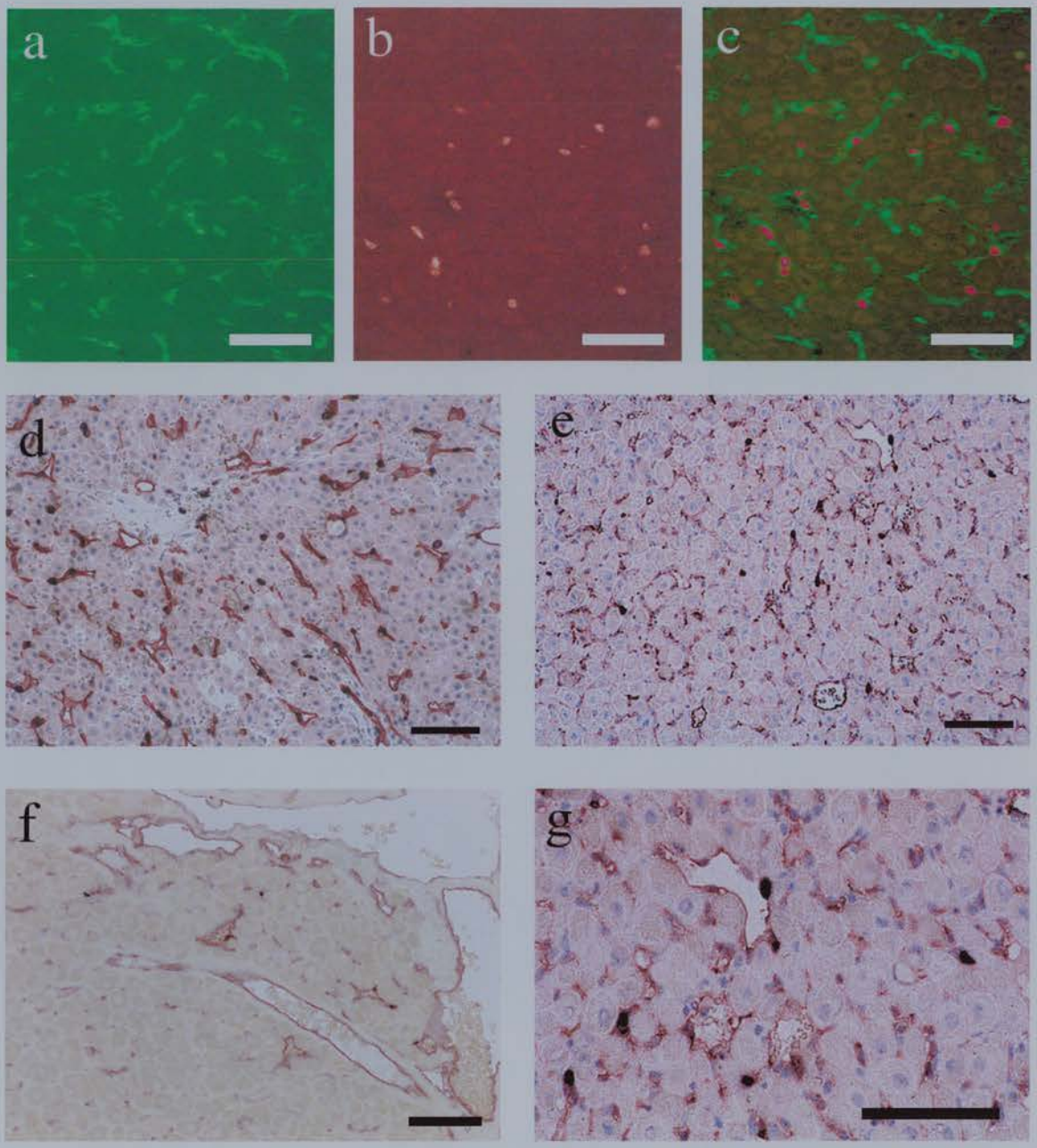

Figure 3.5 Colocalisation of BrdU with von Willebrand factor and CD31 in the marmoset corpus luteum

(a) Fluorescent immunocytochemical localisation of the endothelial cell marker, von Willebrand factor; (b) proliferation marker, BrdU; and (c) colocalisation of the two in an early corpus luteum. Note that most BrdU positive cells are also von Willebrand factor positive. (d-f) Colocalisation of BrdU (black nuclei) with CD31 (red staining) in an early marmoset corpus luteum; mid-luteal section; and late corpus luteum, respectively. (g) The mid-luteal section on higher power to demonstrate that fact that almost all BrdU positive cells are also CD31 positive. Scale bars on a-c = 50μm. Scale bars on d-g = 100μm.

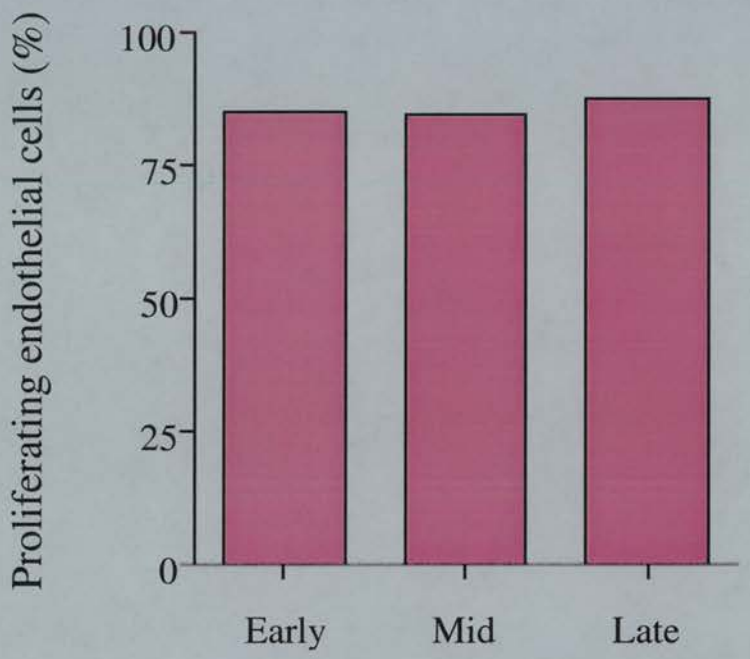

Figure 3.6 The proportion of proliferating endothelial cells in the marmoset corpus luteum

Quantification of proliferating endothelial cells (dual stained for BrdU and CD31) in the marmoset corpus luteum. At all stages of the luteal phase proliferating endothelial cells constituted over 80% of total proliferating cells. No significant differences between stages of the luteal phase were observed. Values for early and mid-luteal data are means, the SEM value was not great enough to be seen on this scale. In the early and mid-luteal stages n=5 animals, in the late luteal phase n=1 corpus luteum.

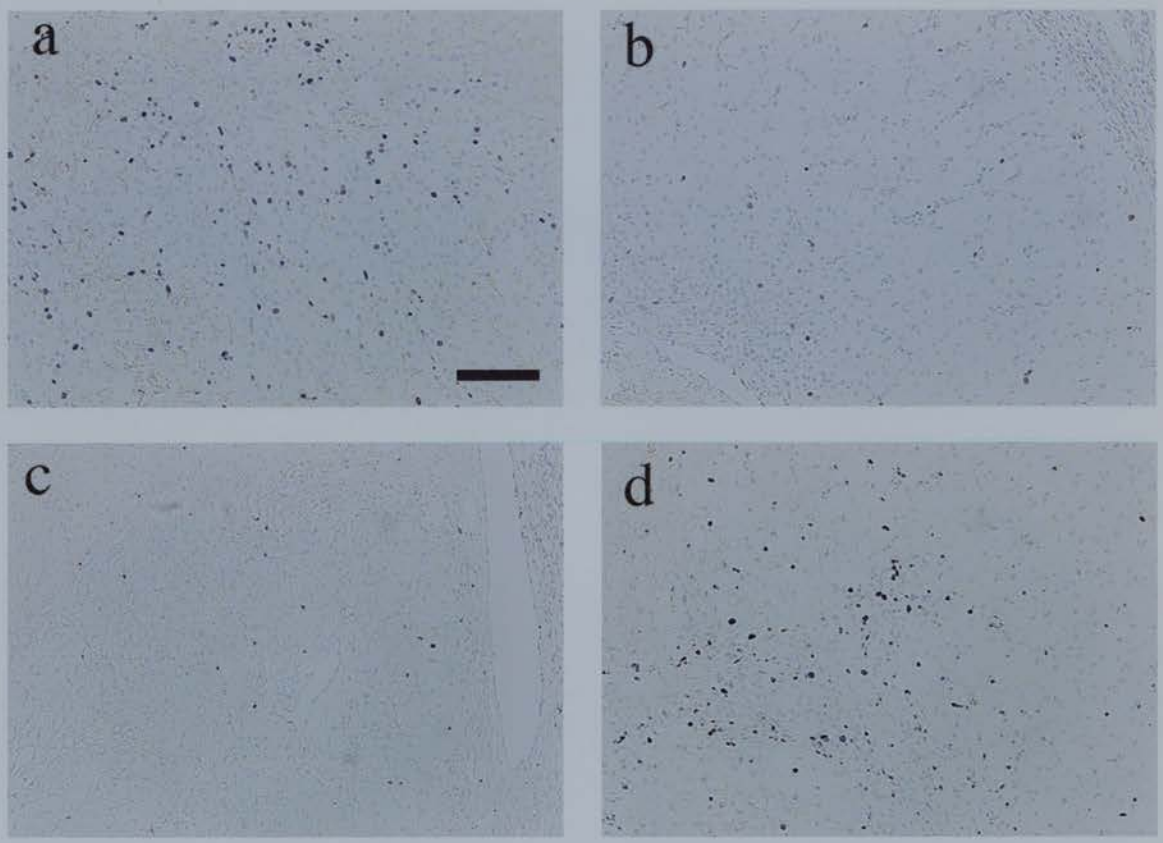

Figure 3.7 Ki67 immunostaining in the human corpus luteum
Low power photomicrographs of (a) Ki67 immunostaining (dark nuclei) in an early corpus luteum; (b) mid-corpus luteum; (c) late corpus luteum; and (d) after hCG rescue of the corpus luteum. Scale bar = 100μm.

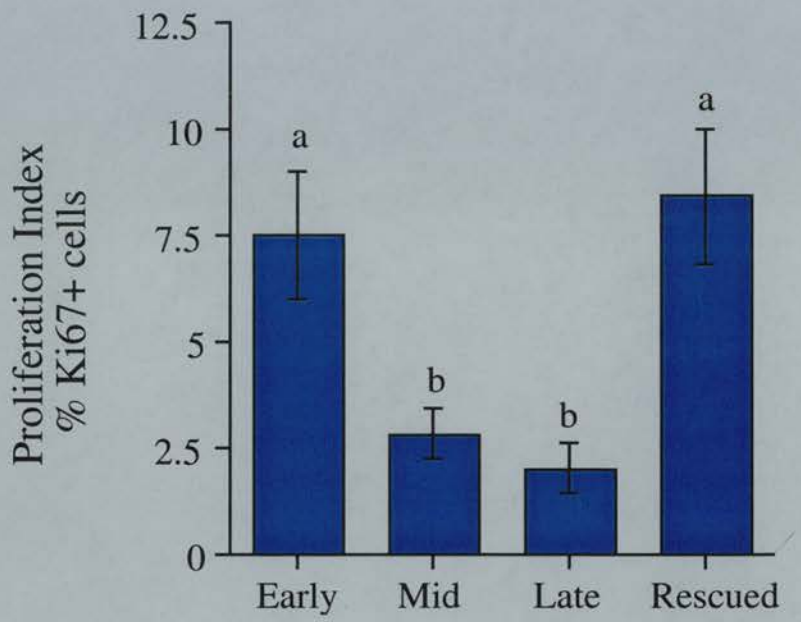

Figure 3.8 Proliferation Index in the human corpus luteum

The proliferation index, or percentage Ki67 positive cells throughout the lifespan of the human corpus luteum. Values are means ± SEM. Different letters denote significant differences between groups, $P<0.05$. For each luteal stage n=4-6 corpora lutea.

3.3.2 Change in steroidogenic cell area throughout the luteal phase

Haematoxylin and eosin stained sections from different stages of the luteal phase revealed marked changes in steroidogenic cell morphology and cell content of the corpus luteum (Fig. 3.9). Low power photomicrographs of early luteal phase sections demonstrate lutein cell streaming to fill the antrum of the developing corpus luteum giving the steroidogenic cells an elongated shape (Fig. 3.9a), which is clarified under higher power (Fig. 3.9b). By the mid-luteal phase the corpus luteum has fully developed both structurally and functionally (Fig. 3.9c and d). The increased cytoplasmic volume of steroidogenic cells, coinciding with maximal progesterone output, gives lutein cells a large round polyhedral morphology typical of this stage of the cycle. There is an increase in the incidence of luminal blood vessels and densely staining, probable endothelial cells, associated with each steroidogenic cell. In the late corpus luteum (Fig. 3.9e) degeneration is associated with lutein cell cytoplasmic vacuolation and disappearance of these cells which appear more sparsely distributed, and the infiltration of possible fibroblasts and immune cells, with densely stained nuclei and little cytoplasm. The intact lutein cells still present have abundant cytoplasm and obvious nuclei, and are not dissimilar from those in the mid-luteal phase (Fig. 3.9f).

Measurement of the change in steroidogenic cell area throughout the luteal phase demonstrated a significant increase ($P<0.001$) in lutein cell area from early to mid-luteal phase (Fig. 3.10). Mean steroidogenic cell areas in the late corpus luteum were greater than early luteal values and lower than mid-luteal results but were not significantly different from either. Mid-luteal phase steroidogenic cell area was greatest and so conversion factors for the measurement of immunostaining area in the early and late luteal phases were calculated from the ratio of change of means from early to mid- levels and from late to mid- values, respectively. The mean mid-luteal phase lutein cell area was divided into the early and late luteal phase values and the resulting figures multiplied by the size of the maximal area of interest available to measure immunostaining. This gave the size of areas of interest for early and late luteal sections, the mid-luteal sections were measured using the maximal of area of interest. These data are summarised in Table 3.1.

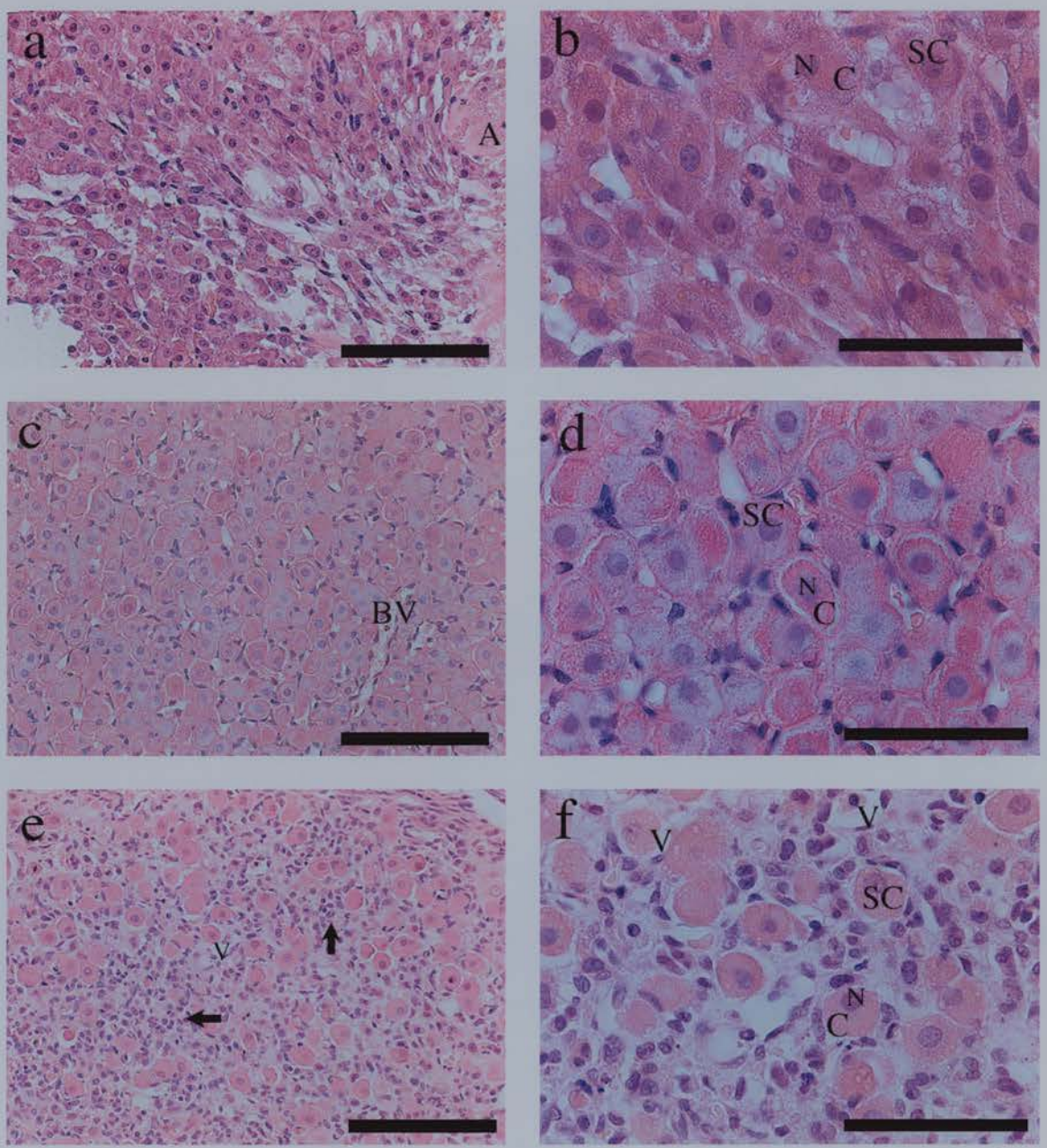

Figure 3.9 Morphology of the marmoset corpus luteum
(a) Low power photomicrograph of an early luteal phase marmoset corpus luteum stained with haematoxylin and eosin. Note the presence of the antrum (A) in the developing corpus luteum and the small elongated shape of lutein cells streaming in to fill the antrum. (b) The same section on higher power demonstrates the elongated lutein cells, some with very little cytoplasm. (c) Low power photomicrograph of a mid-luteal phase section. Steroidogenic cells are more evenly distributed and luminal blood vessels (BV) are apparent. (d) In higher power there is an increase in cytoplasmic volume and steroidogenic cells (SC) take on their characteristic appearance as large polyhedral cells with round nuclei (N) and abundant cytoplasm (C). (e) In the late corpus luteum low power photo-micrographs demonstrate lutein cell vacuolation (V), the decrease in steroidogenic cell numbers, and the presence of clusters (arrows) of densely stained cells with little cytoplasm typical of immune cells, which are characteristic of degenerative change. (f) Under higher power it is possible to see clearly the vacuolation (V) associated with lutein cell cytoplasm and the general disorganisation of the corpus luteum. The remaining healthy steroidogenic cells (SC) have obvious nuclei (N) and abundant cytoplasm (C) similar to mid-luteal cells. Scale bars on a, c and e = 100μm. Scale bars on b, d and f = 50μm.

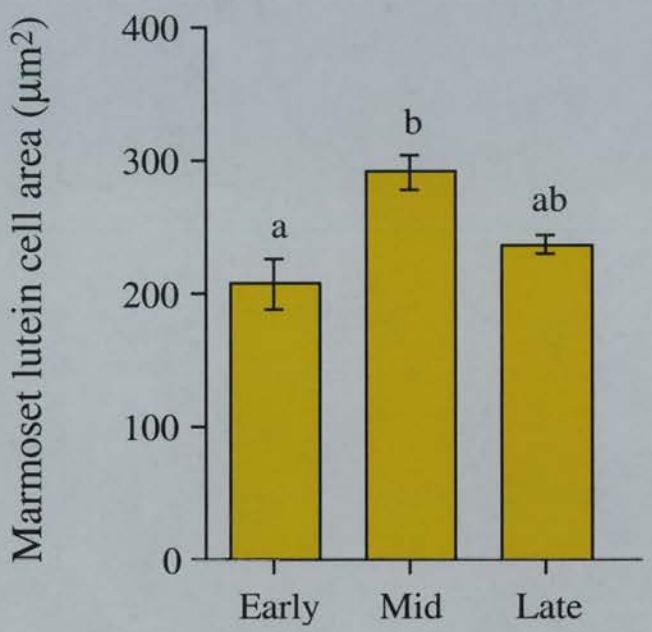

Figure 3.10 The change in steroidogenic cell area throughout the marmoset luteal phase

Quantification of marmoset lutein cell area in the early, mid- and late luteal phases. Values are means ± SEM. Different letters denote significant differences between groups, $P<0.05$. An average of 10 corpora lutea were analysed per luteal stage.

Stage of luteal phase	Lutein cell area (μm^2)	Conversion factor	Area used to measure immunostaining (μm^2)
Early	206	0.71	9.2×10^4
Mid-	290	1	1.3×10^5
Late	236	0.81	1.1×10^5

Table 3.1

Conversion of area used to measure immunostaining corresponding to change in lutein cell area throughout the luteal phase of the cycle

Changes in cell morphology were also evident in H and E stained sections of human corpora lutea (Fig. 3.11). In the human corpus luteum granulosa and theca derived lutein cells are distinguishable. Theca lutein cells are smaller with round nuclei and less cytoplasm and do not undergo noticeable hypertrophy during the luteal phase. Granulosa lutein cells are larger with central round nuclei and abundant cytoplasm which undergoes hypertrophy. The change in granulosa cells cytoplasmic volume over the luteal phase contributes largely to the overall change in luteal volume. It was the area of these cells which were measured in human luteal sections. Low power photomicrographs demonstrated the structure of the corpus luteum in which similar changes as described for the marmoset corpus luteum occurred. The change in cytoplasmic volume of the granulosa lutein cells was most evident in high power photomicrographs. After exposure to hCG (Fig. 3.11g-h) the degenerative changes witnessed in the late luteal phase did not take place and the steroidogenic cells increased in size, coinciding with an increase in progesterone output, as the corpus luteum was 'rescued' from luteolysis. When compared with mid-luteal granulosa lutein cell size it was apparent that luteal rescue caused granulosa lutein cell cytoplasmic volume to increase further.

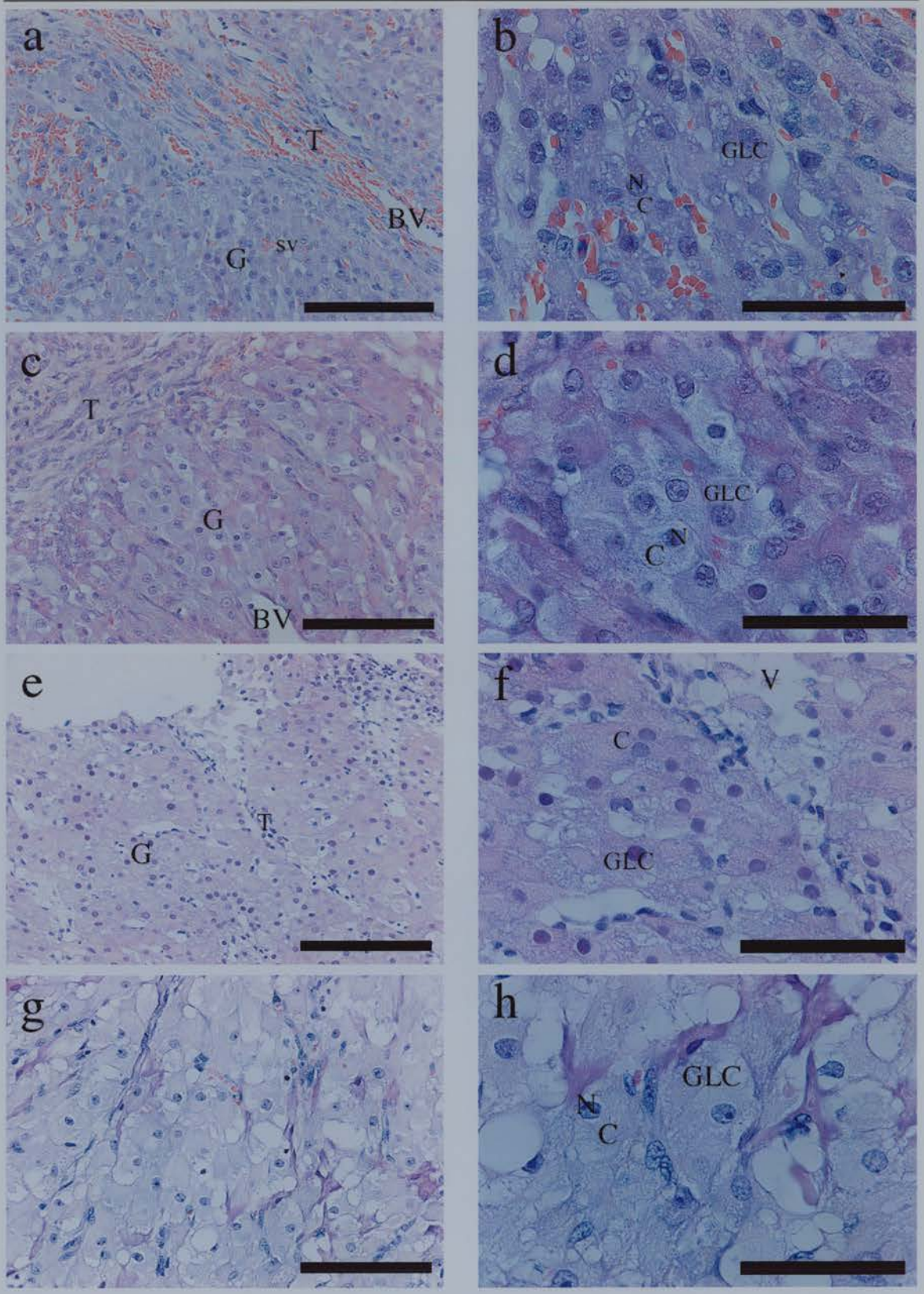

Figure 3.11 Morphology of the human corpus luteum

(a) Low power micrograph of an early luteal haematoxylin and eosin stained section. Note the presence of large blood vessels (BV) in the theca lutein cell compartment (T) and the smaller vessels (SV) in the granulosa lutein cell compartment (G). (b) The same section on higher power. Note the granulosa derived lutein cells (GLC) have a relatively small volume of cytoplasm (C) and large central nucleus (N). (c) Low power micrograph of a mid-corpus luteum. Note the presence of large blood vessels in the granulosa derived compartment (G); and (d) the same section on higher power revealing an increase in cytoplasmic volume (C) of the granulosa lutein cells (GLC) and the large central nucleus (N), typical of steroidogenic cells at this stage. (e) Low power micrograph of a late corpus luteum; and (f) a higher power micrograph of the same section. Note the presence of vacuoles in both the granulosa (G) and theca lutein compartments (T), and the decrease in cytoplasmic volume (C) of granulosa derived lutein cells (GLC). (g) Low power micrograph of a corpus luteum rescued from luteolysis with hCG; and (h) a higher power micrograph of the same section demonstrating the massive increase in cytoplasmic volume (C) of the rescued granulosa lutein cells (GLC). Scale bars on a, c, e and g = 100μm. Scale bars on b, d, f and h = 50μm.

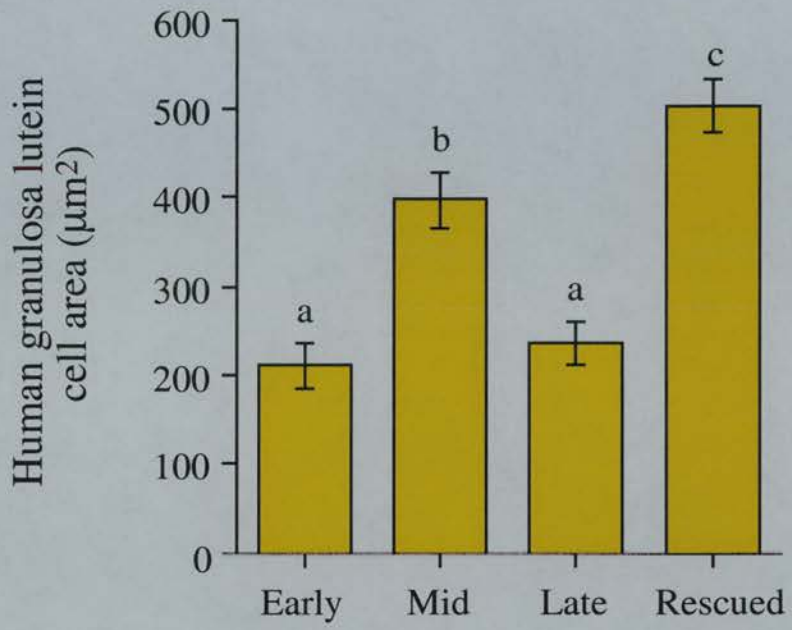

Figure 3.12 The change in granulosa lutein cell area in the human corpus luteum

Quantification of area of granulosa lutein cells throughout the luteal phase and after luteal rescue in the human. Values are means ± SEM. Different letters denote significant differences between groups, $P<0.05$. An average of 4 corpora lutea were analysed per luteal stage.

Measurement of granulosa lutein cell area (Fig. 3.12) demonstrated a marked increase in granulosa cell area from early to mid- ($P<0.001$), and decrease from mid- to late ($P<0.01$) luteal values. Following luteal rescue these cells were significantly ($P<0.03$) larger than at any other stage of the cycle. Again conversion factors were calculated in the same way as for marmoset cell measurements except that this time change was calculated against the rescued cell area. Conversion factors are shown in Table 3.2, and were used to convert immunostaining measurements after quantification which was performed using the same sized area of interest for all corpora lutea.

Stage of luteal phase	Lutein cell area (μm^2)	Conversion factor
Early	210	0.42
Mid-	397	0.8
Late	235	0.47
Rescued	503	1

Table 3.2

Conversion of immunostaining results corresponding to change in granulosa lutein cell area throughout the luteal phase of the cycle

3.3.3 Endothelial cell area

Immunostaining for von Willebrand factor was readily observed in all marmoset corpora lutea (Fig. 3.13). In the early luteal phase (Fig. 3.13a) staining demonstrated the initiation of development of the microvasculature, associated mainly with endothelial cells of non luminal smaller capillary vessels. By the mid-luteal phase (Fig. 3.13b) the microvascular tree was fully established with staining associated to larger luminal vessels and small capillaries. In the late luteal phase (Fig. 3.13c) von Willebrand factor positive cells associated to capillaries appeared to have decreased in number but endothelial cells of larger microvasculature remained present. Negative control sections were completely devoid of staining (Fig. 3.13d). Quantification of area of von Willebrand factor immunostaining (Fig. 3.14) showed a significant increase ($P<0.0001$) in endothelial cell area from the early to the mid-luteal phase, and a marked decrease ($P<0.001$) in area from the mid- to the late luteal phase.

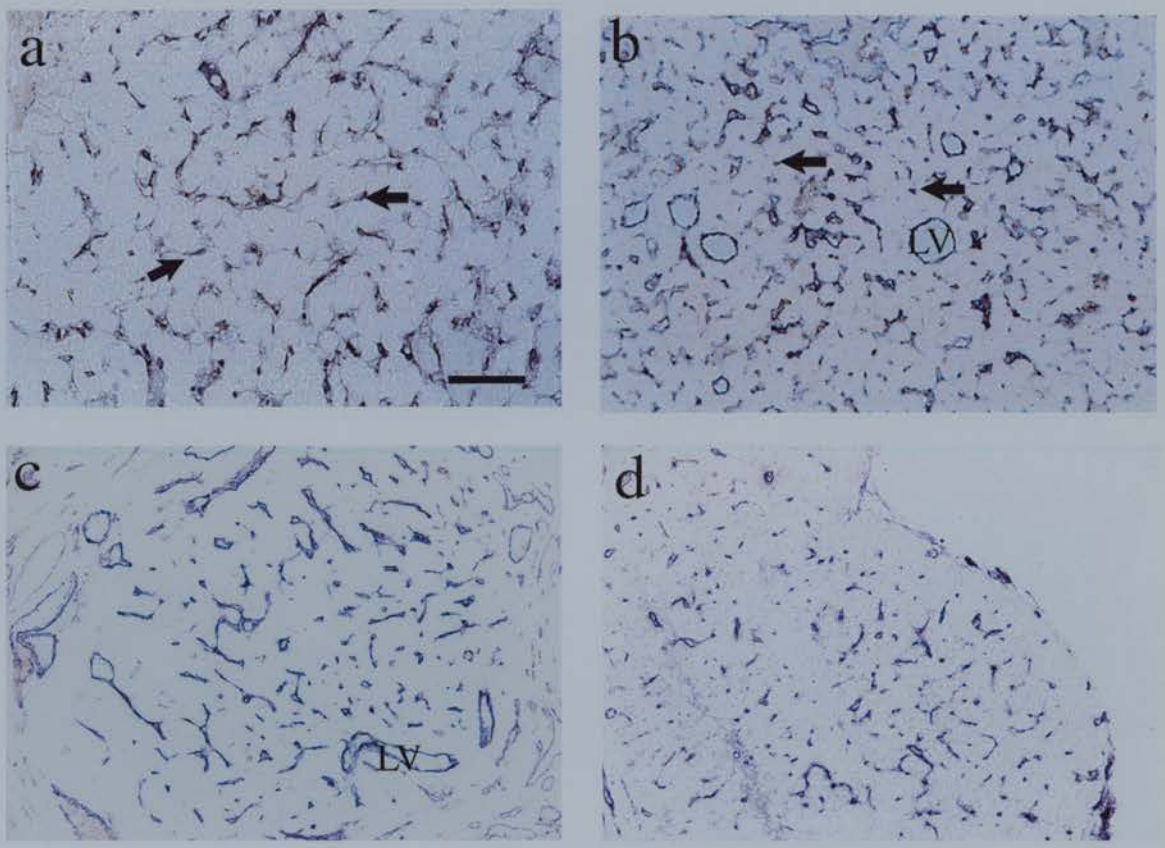

Figure 3.13 Immunostaining for von Willebrand factor in the marmoset corpus luteum

(a) Photomicrographs of immunostaining for the endothelial cell specific antigen, von Willebrand factor (dark staining) in the early marmoset corpus luteum, note the presence of endothelial cells which are associated to small non-luminal capillaries as indicated by the arrows. (b) A mid-luteal section demonstrating full development of the microvasculature in the form of luminal vessels (LV) and small capillaries (arrows). (c) A late corpus luteum showing the predominance of larger microvessels (LV), and the reduced appearance of small capillaries. (d) A regressing, follicular phase CL section demonstrating distinct vWF immunostaining. Scale bar = 100μm.

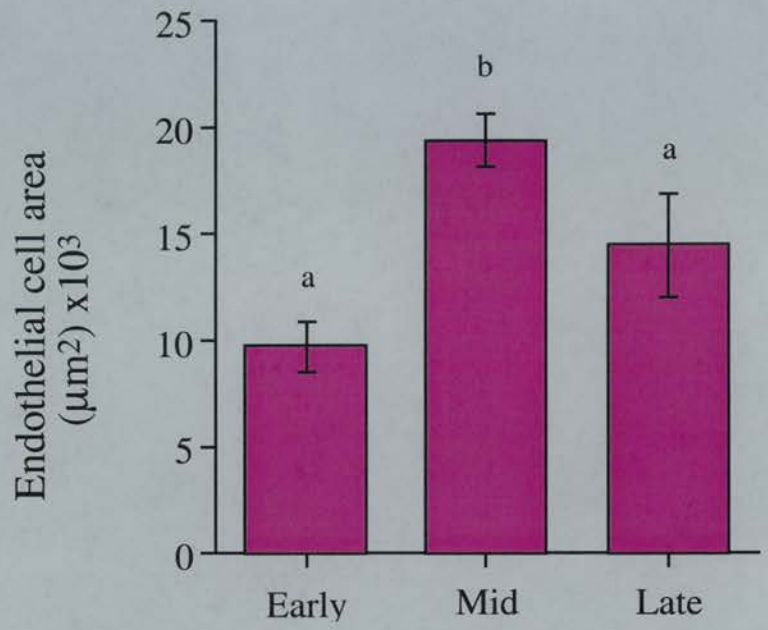

Figure 3.14 Measurement of endothelial cell area in the marmoset corpus luteum

Quantification of the area of endothelial cell staining, following immunocytochemistry for von Willebrand factor, throughout the marmoset luteal phase. Values are means ± SEM. Different letters denote significant differences between groups, $P<0.05$. For each luteal stage n=5 animals.

Immunostaining with the endothelial cell marker, CD31, in the same corpora lutea demonstrated a similar pattern of endothelial cell distribution in the early, mid-, and late luteal phases (Fig. 3.15a-c, respectively). It was also noticed that in the regressed follicular phase corpus luteum, CD31 staining was not as defined as in earlier luteal stages giving rise to areas of diffuse disorganised staining, which were not apparent in follicular thecal vasculature in the same section (Fig. 3.15d and insert). As this phenomenon had not been seen previously with von Willebrand factor immunostaining this suggested a specific breakdown of the CD31 antigen in luteal endothelium. Comparison of the quantification of CD31 immunostaining in the early, mid-, and late corpus luteum with von Willebrand factor staining revealed the same trend in endothelial cell area throughout the luteal phase (Fig. 3.16a). There did appear to be a significant difference between early and late luteal levels ($P<0.01$) which was not seen with von Willebrand factor quantification. There was however no significant differences between CD31 and von Willebrand factor results within one stage of the luteal phase, as suggested by the high correlation coefficient ($r=1.000$ when rounded to three decimal places) (Fig. 3.16b).

To examine whether measurement of endothelial cell area in one section was representative of the whole corpus luteum, CD31 immunostaining in second sections from a selection of corpora lutea (n=3 animals in each luteal stage) was quantified. The same trend in endothelial cell area was apparent during the luteal phase in both sections (Fig. 3.17a). There was no significant difference between mid- and late values from quantification of the second sections, as seen after quantification of the first sections. However there was no significant differences between endothelial cell area, in two distal sections, within one stage of the luteal phase, as suggested by the high correlation coefficient ($r=0.979$) (Fig. 3.17b).

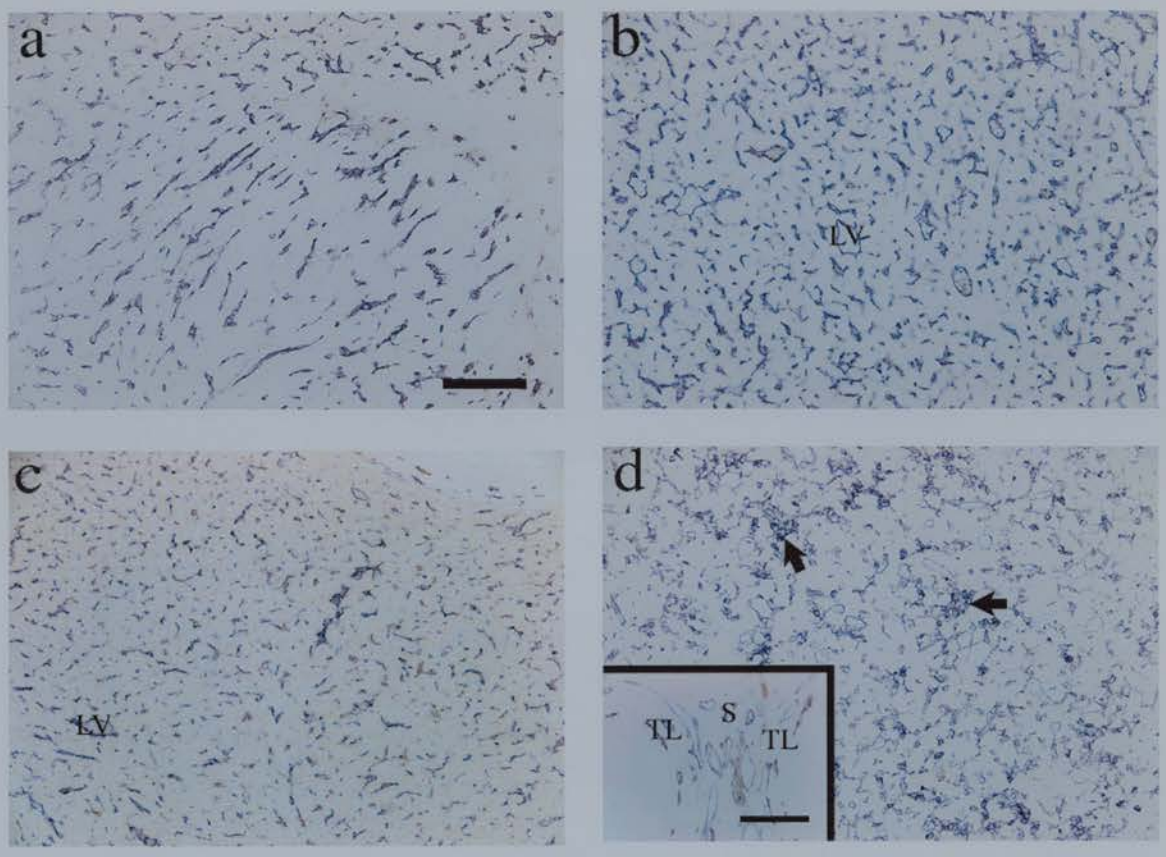

Figure 3.15 Immunostaining for CD31 in the marmoset corpus luteum
(a) Early luteal CD31 staining demonstrating the presence of small, non-luminal capillaries in the developing vasculature throughout the section; and (b) a mid-luteal phase section showing the incidence of larger luminal vessels (LV) and small capillaries indicating full development of the microvascular tree. (c) CD31 staining in the late luteal phase; and (d) in the regressing, follicular phase corpus luteum. Note the presence of diffuse luteal immunostaining for CD31 (arrows), less distinct than in earlier stages of development, and (insert in d) the intact staining visible in the ovarian stroma (S) and theca layer (TL) of two developing follicles in the same section. Scale bars = 100μm.

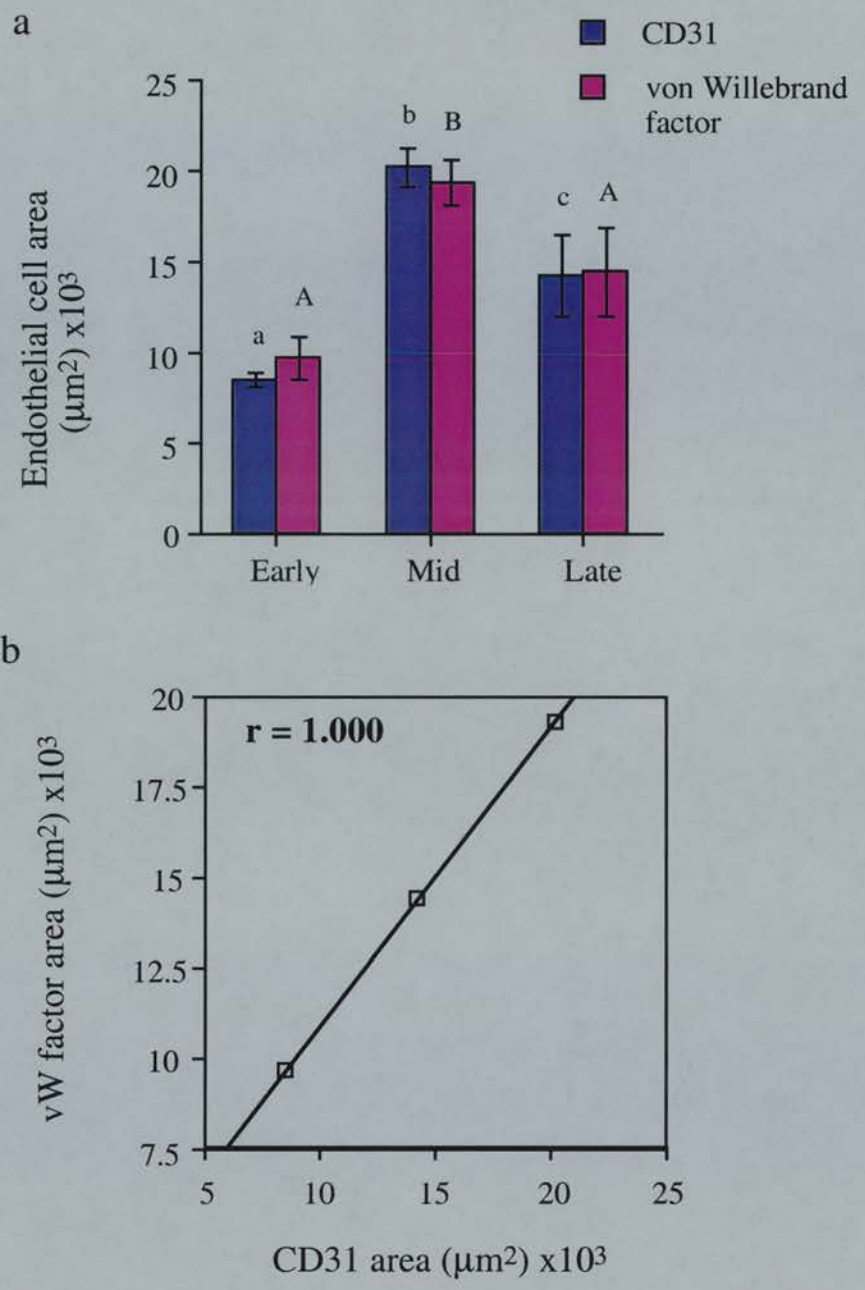

Figure 3.16 Comparison of quantifications of CD31 and von Willebrand factor immunostaining in the marmoset corpus luteum

(a) Bar graph comparing endothelial cell area measurements from CD31 (purple bars) and von Willebrand factor (pink bars) immunostaining throughout the lifespan of the marmoset corpus luteum. (b) The correlation of the trend in CD31 and von Willebrand factor immunostaining area throughout the luteal phase. Values are means ± SEM. Different letters denote significant differences between groups, $P<0.05$. There were no significant differences between quantification of CD31 and von Willebrand factor staining within a particular group as suggested by the high correlation co-efficient. For each luteal stage n=5 animals.

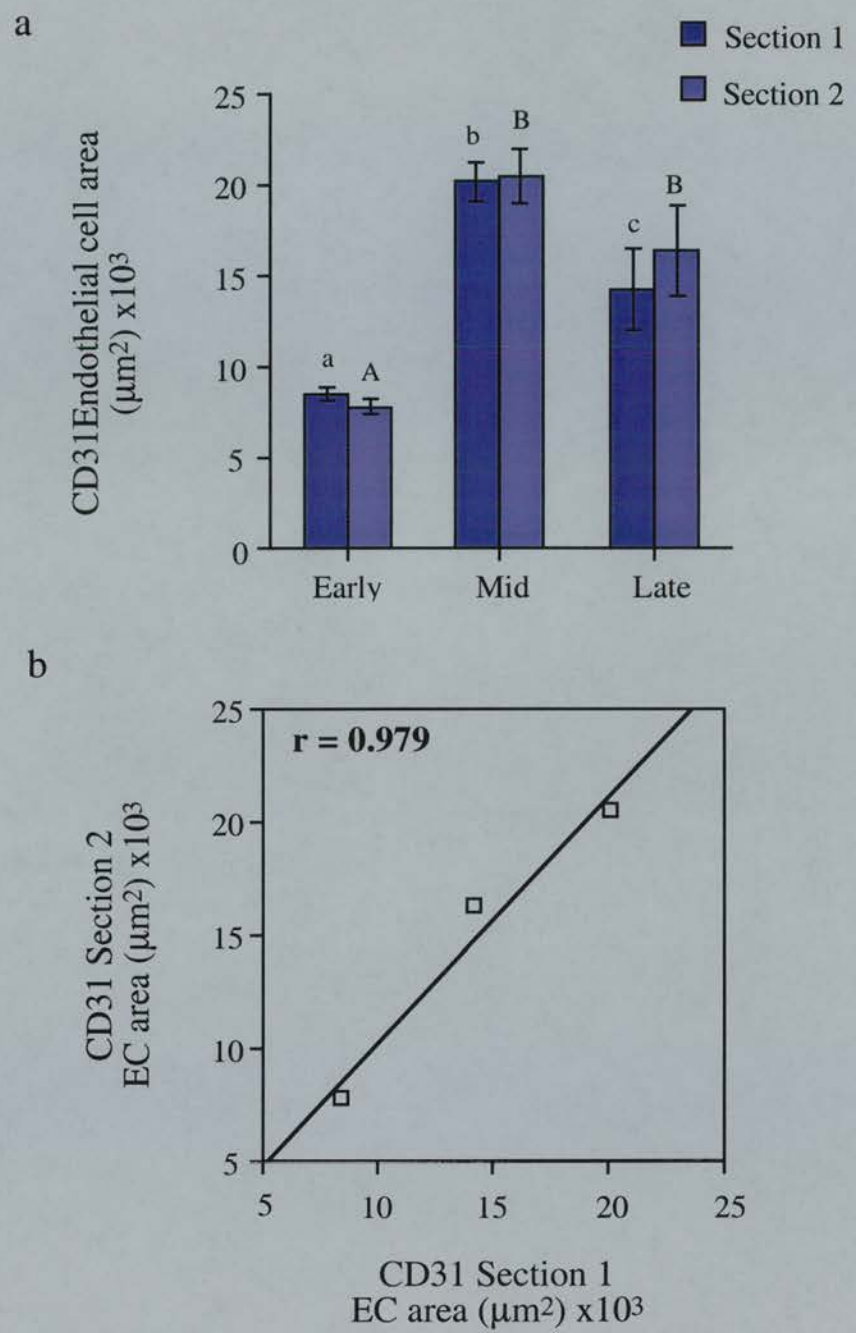

Figure 3.17 Correlation of CD31 immunostaining in two distal sections from the same marmoset corpus luteum

(a) Comparison of CD31 immunostaining from Section 1 (purple bars) and Section 2 (lilac bars) throughout the luteal phase in the marmoset corpus luteum. There was no significant difference between sections of the same stage of the luteal phase. (b) The correlation coefficient of quantification of the two sections. Values are means ± SEM. Different letters denote significant differences between groups, $P<0.05$. For each luteal stage n=5 animals.

In the human corpus luteum, measurement of CD34 immunostaining was used to quantify endothelial cell area (Fig. 3.18). In a similar pattern to the microvasculature in the marmoset corpus luteum endothelial cells associated to small non-luminal vessels were apparent in the developing corpus luteum (Fig. 3.18a), and by the mid-luteal phase (Fig. 3.18b) the microvascular tree was fully established with staining associated to larger luminal vessels and small capillaries (Fig. 3.18c). In the late luteal phase vessels appeared smaller and more sparsely distributed throughout the corpus luteum. After luteal rescue vessels remained small but were more tightly packed signifying an increase in luteal microvasculature (Fig. 3.18d). Quantification, without converting for the effects of tissue expansion and shrinkage (Fig. 3.19a), revealed there was no change in endothelail cell area at any stage of the luteal phase. However, when these values were converted for the effects of tissue expansion and shrinkage reflecting the true *in vivo* situation, quantification (Fig. 3.19b) confirmed the effect seen following immunocytochemistry. An increase ($P<0.05$) in endothelial cell area from the early to the mid-luteal phase, and a marked decrease in the late corpus luteum ($P<0.05$) was demonstrated. Following luteal rescue, endothelial cell area significantly increased ($P<0.05$) from all other luteal levels.

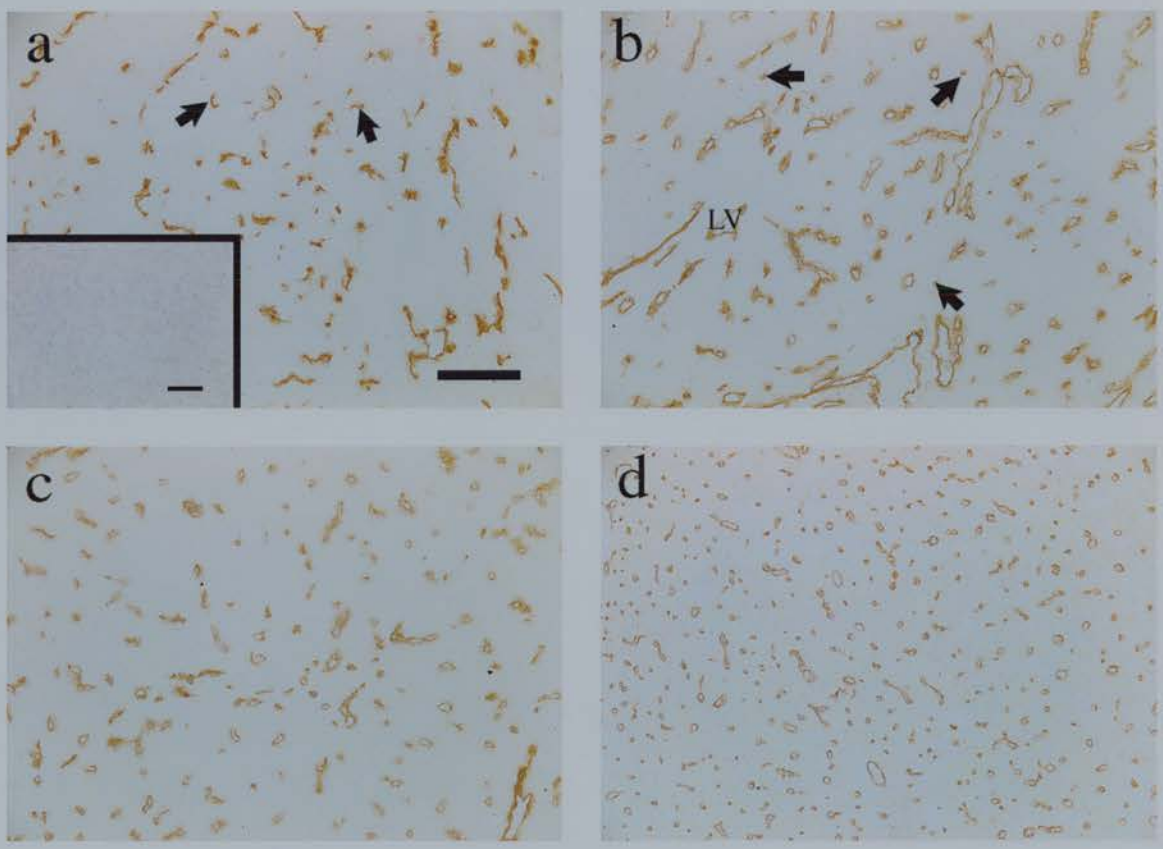

Figure 3.18 CD34 immunostaining in the human corpus luteum
Photomicrographs of CD34 immunostaining in (a) an early corpus luteum, note the presence of small capillaries in the developing vasculature, and the absence of staining in (inset in a) the negative control section. (b) A mid-corpus luteum, note the incidence of larger luminal vessels (LV) in addition to the small capillaries (arrows) in the established microvasculature. (c) The late luteal phase, note the presence of small and large luminal vessels; and (d) the hCG rescued corpus luteum at the same magnification, in which there is a dramatic increase incidence of small luminal vessels throughout the corpus luteum. Scale bars = 100μm.

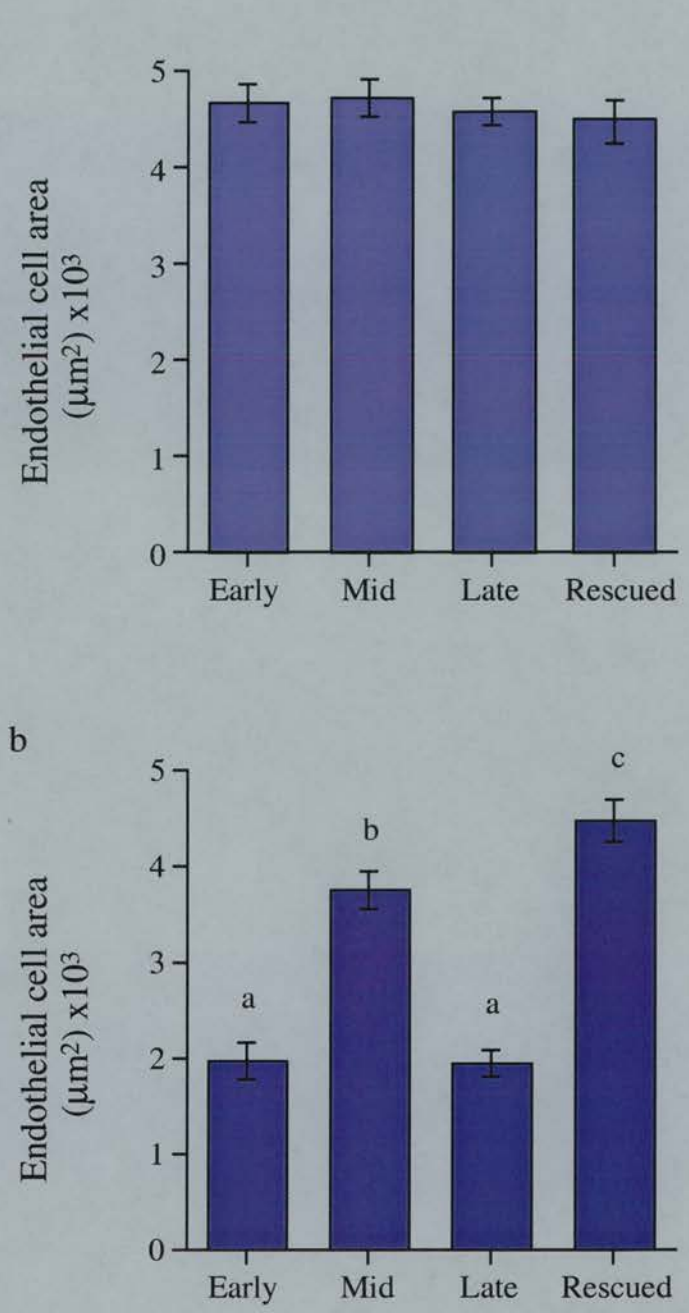

Figure 3.19 Quantification of endothelial cell area in the human corpus luteum

(a) Quantification of area of endothelial cell CD34 staining in all luteal phases in the human corpus luteum. Data not converted for effects of tissue expansion and shrinkage. (b) Quantification of area of endothelial cell CD34 staining in all luteal phases in the human corpus luteum. Data converted to consider the effects of tissue expansion and shrinkage. Values are means ± SEM. Different letters denote significant differences between groups, $P<0.05$. For each luteal stage n=4-6 corpora lutea.

3.3.4 Cyclic VEGF-A expression

In the marmoset antral follicle the avascular granulosa layer and the vascularised theca layer are separated by a basement membrane. VEGF-A expression was exclusively located to the vascularised thecal layer (Fig. 3.20a). However, in the preovulatory follicle, estimated hours before ovulation, degeneration of the separating basement membrane can be seen and expression of VEGF-A is located to the granulosa as well as the thecal layer of the follicle (Fig. 3.20b). Early luteal sections show intense, punctate VEGF-A staining in the cytoplasm of lutein cells (Fig. 3.20c) becoming more uniform and widespread in the mid-corpus luteum (Fig. 3.20d). Staining was absent from recognisable endothelial cells. In the late corpus luteum, VEGF-A staining was markedly reduced (Fig. 3.20e). Positive immunoreactivity was not seen in the negative control section (Fig. 3.20f). Quantification confirmed a high area of staining in the early and mid-luteal phase which declined markedly in the late corpus luteum, as compared to early and mid-luteal levels ($P=0.04$ and $P=0.02$, respectively) (Fig. 3.21a). VEGF-A immunostaining was significantly more intense ($P<0.0001$) in the early luteal phase as compared to mid- and late luteal levels (Fig. 3.21b, the optical desity of the early luteal phase group being significantly lower than other luteal phase values).

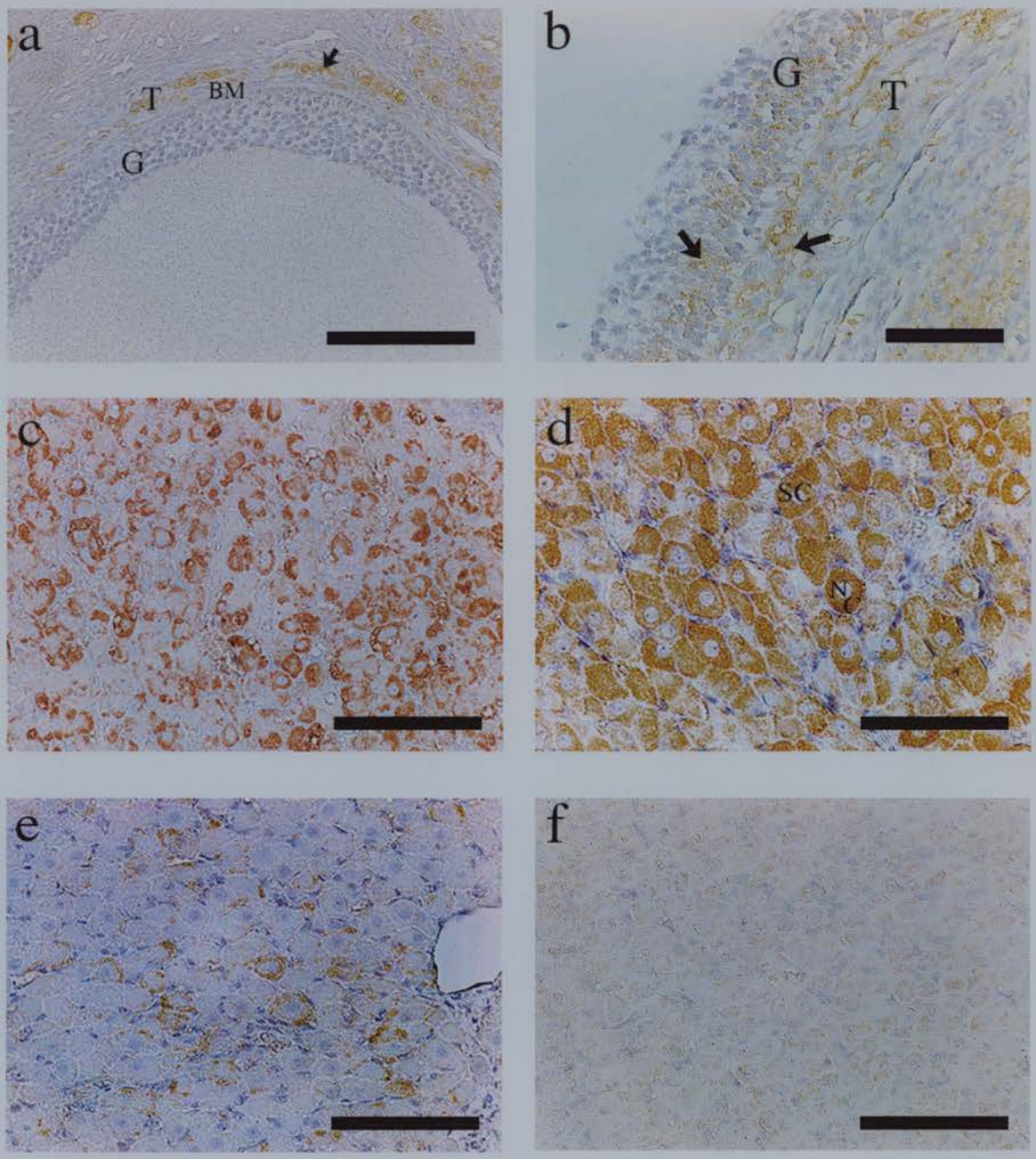

Figure 3.20 VEGF-A immunostaining in marmoset follicles and corpus luteum
(a) Immunostaining for VEGF (brown staining) in an antral follicle. Note that the basement membrane (BM) separating the theca (T) and granulosa (G) cell layers is intact and that staining is restricted to the theca layer of the follicle as indicated by the arrow. (b) In a marmoset follicle at the time of ovulation there is disintegration of the basement membrane and VEGF immunostaining is localised to both granulosa (G) and theca (T) cell layers as indicated by the arrows. (c) In the early corpus luteum VEGF staining is found throughout the corpus luteum; and (d) in the larger mid-corpus luteum it is noted that staining is more widespread and located to the cytoplasm (C) of most steroidogenic cells (SC). (e) In the late corpus luteum VEGF staining is considerably reduced showing a punctate pattern located to the edges of some steroidogenic cells. (f) Shows the negative control section in which primary antibody was preabsorbed with the epitope it was raised to. Scale bars on a, c-f = 100μm. Scale bar on b = 50μm.

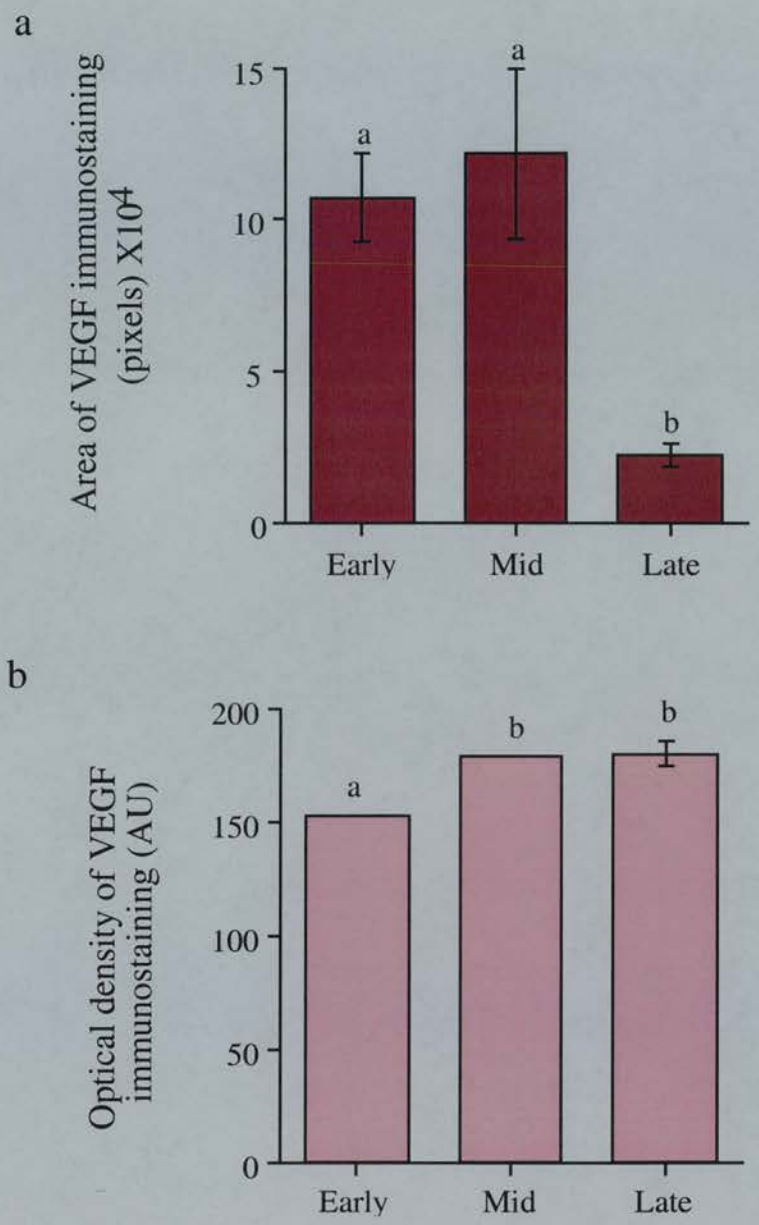

Figure 3.21 Quantification of VEGF-A immunostaining in the marmoset corpus luteum

Quantification of area of VEGF immunostaining throughout the luteal phase of the marmoset corpus luteum. (b) Quantification of intensity of VEGF immunostaining in the marmoset corpus luteum. There is an inverse relationship between staining intensity and the units of measurement. A low value indicates dark staining/high intensity. Values are means ± SEM unless the SEM value was too small for the scale of the graph. Different letters denote significant differences between groups, $P<0.05$. For each luteal stage n=5 animals.

Immunostaining for VEGF-A in the human corpus luteum was also measured. In the developing corpus luteum, low power photomicrographs demonstrate intense VEGF-A staining at the tips of the finger-like processes of granulosa derived lutein cells invading the antrum (Fig. 3.22a). There is also expression in other granulosa lutein cell areas and in the theca lutein cell compartment. High power microscopy reveals that VEGF-A immunostaining is located to the cytoplasm of these cells (Fig. 3.22b). By the mid-luteal phase, expression appears to have spread more evenly across the granulosa lutein cell compartment and decreased in theca lutein cells (Fig. 3.22c-d). As in the marmoset, VEGF-A immunostaining had markedly declined in the late human corpus luteum, with only small area of punctate expression remaining localised predominantly to granulosa lutein cells (Fig. 3.22e-f). After hCG rescue the decrease in VEGF-A immunostaining seen in the late luteal phase was prevented (Fig. 3.22g-h) and a tendency for VEGF-A protein content to increase as compared to the mid-luteal phase. Expression remained located to lutein cell cytoplasm and was uniformly distributed, similar to the pattern of expression in the mid-luteal phase. Quantification (Fig.3.23a) confirmed a high area of VEGF-A immunostaining in the early and mid-luteal phases, and a decreasing trend to late luteal phase levels, which was not significant. There was however, a significant increase ($P<0.05$) in the area of VEGF-A protein detected in the rescued corpus luteum from early and late luteal levels. The intensity of immunostaining remained unchanged over all luteal stages (Fig. 3.23b).

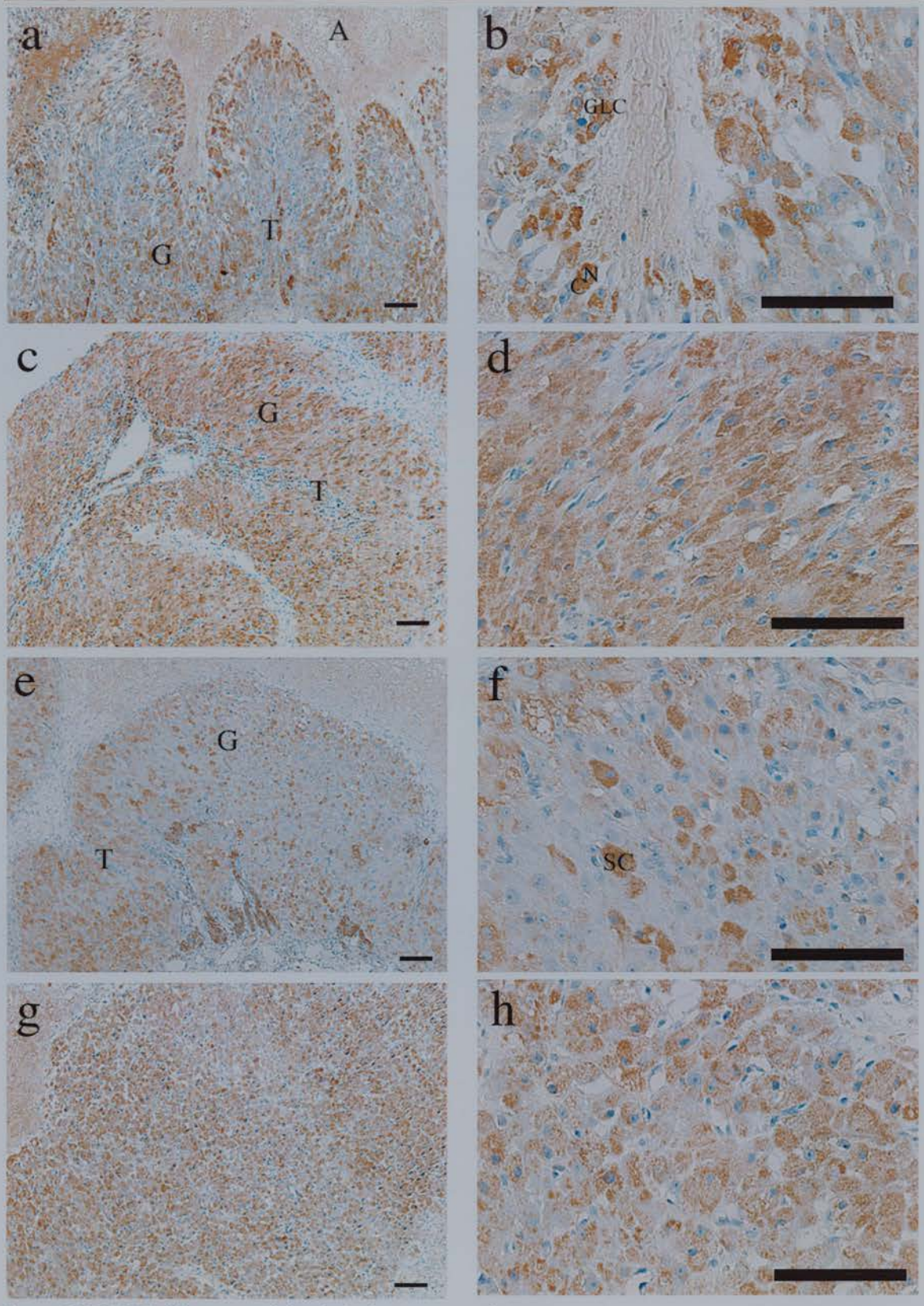

Figure 3.22 VEGF-A immunostaining in the human corpus luteum
(a) Low power photomicrograph of VEGF immunostaining (brown staining) in an early luteal human corpus luteum. Note the presence of VEGF immunostaining in both the theca (T) and granulosa (G) derived compartments, and the greater intensity in staining at the leading edge of the granulosa compartment (arrows) invading the antrum (A). (b) The same section on higher power, note that VEGF staining is located in the cytoplasm (C) of the steroidogenic cells. (c) Low power micrograph of a mid-corpus luteum, note the widespread appearance of staining throughout the granulosa (G) and theca (T) compartments. (d) The same section on higher power, notice that almost every steroidogenic cell (SC) is expressing VEGF, staining being located to the cytoplasm (C). (e) Low power micrograph of a late corpus luteum. Note the more punctate patter of VEGF staining in both the granulosa (G) and theca (T) compartments, which on higher power (f) can be seen located to the cytoplasm (C) of some steroidogenic cells (SC). (g) Low power micrograph of an hCG rescued corpus luteum, note the widespread distribution of VEGF staining throughout the corpus luteum. (h) The same section on higher power reveals that almost all steroidogenic cells demonstrate staining for VEGF.
Scale bars = 100um.

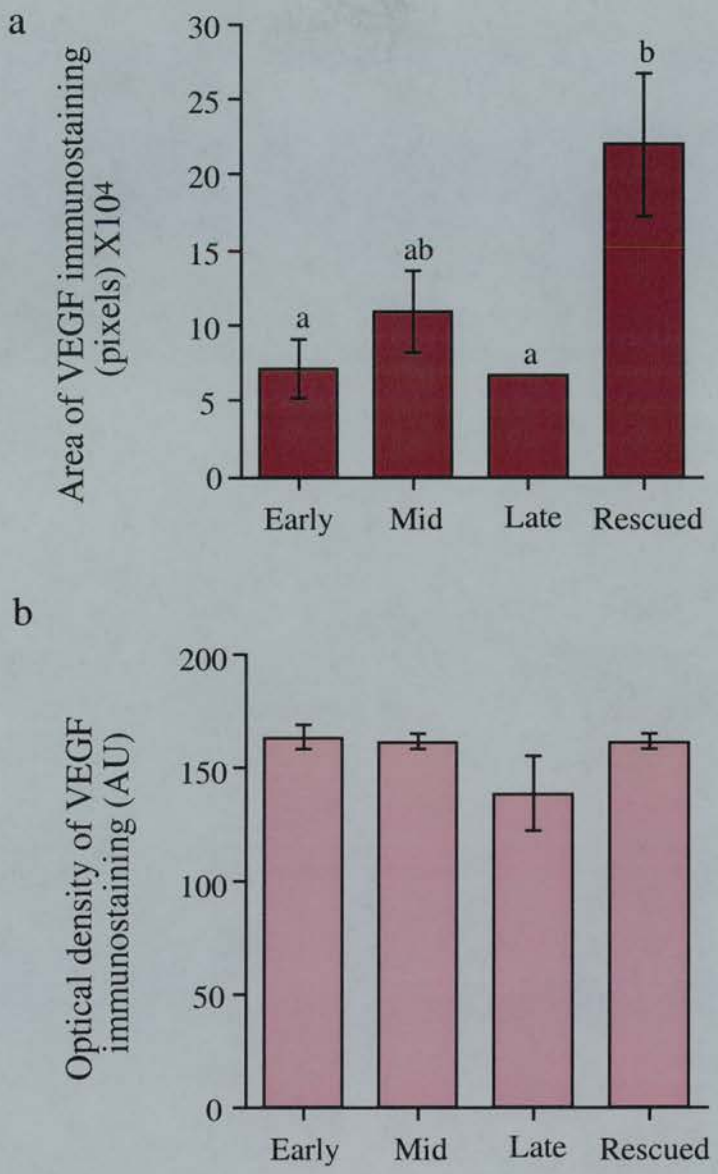

Figure 3.23 Quantification of VEGF-A immunostaining in the human corpus luteum

(a) Quantification of area of VEGF immunostaining throughout the luteal phase of the human corpus luteum. (b) Quantification of intensity of VEGF immunostaining in the human corpus luteum. There is an inverse relationship between staining intensity and the units of measurement. A low value indicates dark staining/high intensity. Values are means ± SEM unless the SEM value was too small for the scale of the graph. Different letters denote significant differences between groups, $P<0.05$. For each luteal stage n=4-6 corpora lutea.

3.3.5 Luteal pericyte area

Immunostaining for α-SMA was high in the developing marmoset corpus luteum associated to both non-luminal, capillary vessels and the occasional present luminal vessel (Fig. 3.24a). In the mid- and late corpus luteum staining was restricted to pericytes located in rings surrounding luminal vessels (Fig.3.24b-c). This pattern of staining was particularly evident in the late luteal phase where most luminal vessels had associated pericytes. Quantification of α-SMA immunostaining area showed a decreased trend from high levels in the early luteal phase to significantly lower ($P<0.02$) levels in the late corpus luteum (Fig. 3.25). A low area of α-SMA staining in the late corpus luteum corresponds with a decrease in total vasculature at that stage as seen by von Willebrand factor and CD31 staining.

Colocalisation of staining for α-SMA and von Willebrand factor in the human revealed the close association of pericytes to endothelial cells at all stages of the luteal phase, but that staining was in two distinct cell types (Fig. 3.26). Light field α-SMA staining using NBT detection (Fig. 3.27), demonstrated that pericytes associated to luminal vessels appeared to be restricted to the theca lutein vasculature, and the occasional single pericyte was present in the granulosa compartment of the early corpus luteum. Later in luteal development, pericytes were present associated only to large luminal vessels in both the theca and granulosa lutein compartments. Quantification of area of pericyte staining (Fig. 3.28a), not adjusting for changes in tissue volume during the luteal phase and after rescue, failed to show any significant differences in pericyte content in the corpus luteum, although there was a tendency for increased staining during the mid-luteal phase. This trend was amplified when quantification was converted for the effects of tissue expansion and shrinkage which represents the *in vivo* environment more closely (Fig. 3.28b). Quantification of pericyte area after conversion showed increased staining ($P<0.0001$) from early to the mid- corpus luteum, and a significant decrease ($P<0.0001$) in the late corpus luteum. Pericyte area increased to maximal levels ($P=0.02$ as compared to mid-luteal levels) following hCG rescue. In the late luteal phase almost all endothelial cells were associated to luminal vessels, as seen by CD34 immunostaining, which appeared to have associated pericytes, as demonstrated by positive α-SMA immunostaining, suggesting the selective demise of small capillary vasculature. The

endothelial cell content per unit area also decreased at this time which indicates a loss of endothelial cells, not their evolution to a mature form.

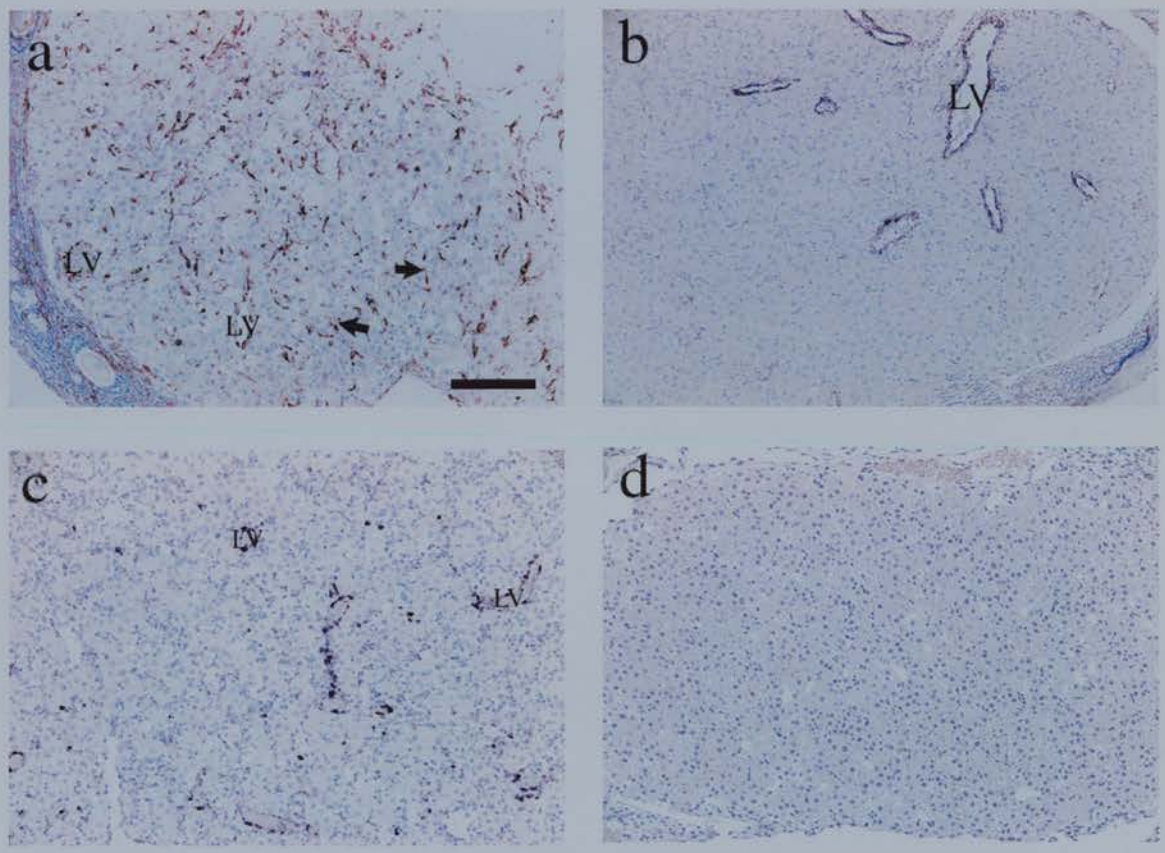

Figure 3.24 The incidence of pericytes in the marmoset corpus luteum
(a) Photomicrograph of α-SMA immunostaining (dark staining) in an early marmoset corpus luteum. Note the presence of single positive cells (arrows) which do not appear to be associated with mature luminal vessels (LV), and staining which is associated with luminal vessels (LV). (b) α-SMA immunostaining in a mid-corpus luteum, note the absence of single immunopositive cells and that all staining is associated to large luminal vessels (LV). (c) A late corpus luteum, again staining is associated to large luminal vessels only. (d) A negative control section demonstrating the absence of immunostaining. Scale bar = 100μm.

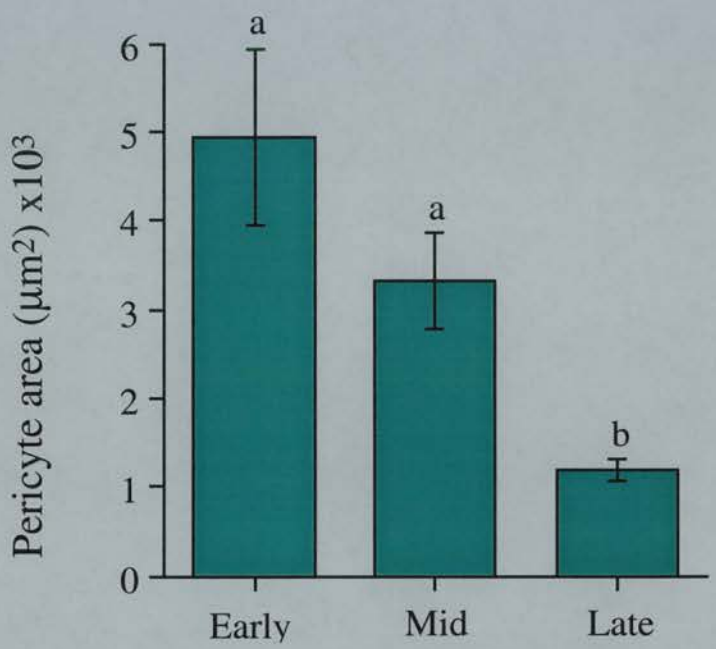

Figure 3.25 Quantification of pericyte content in the marmoset corpus luteum

Quantification of pericyte area throughout the lifespan of the marmoset corpus luteum. Values are means ± SEM. Different letters denote significant differences between groups, $P<0.05$. For each luteal stage n=5 animals.

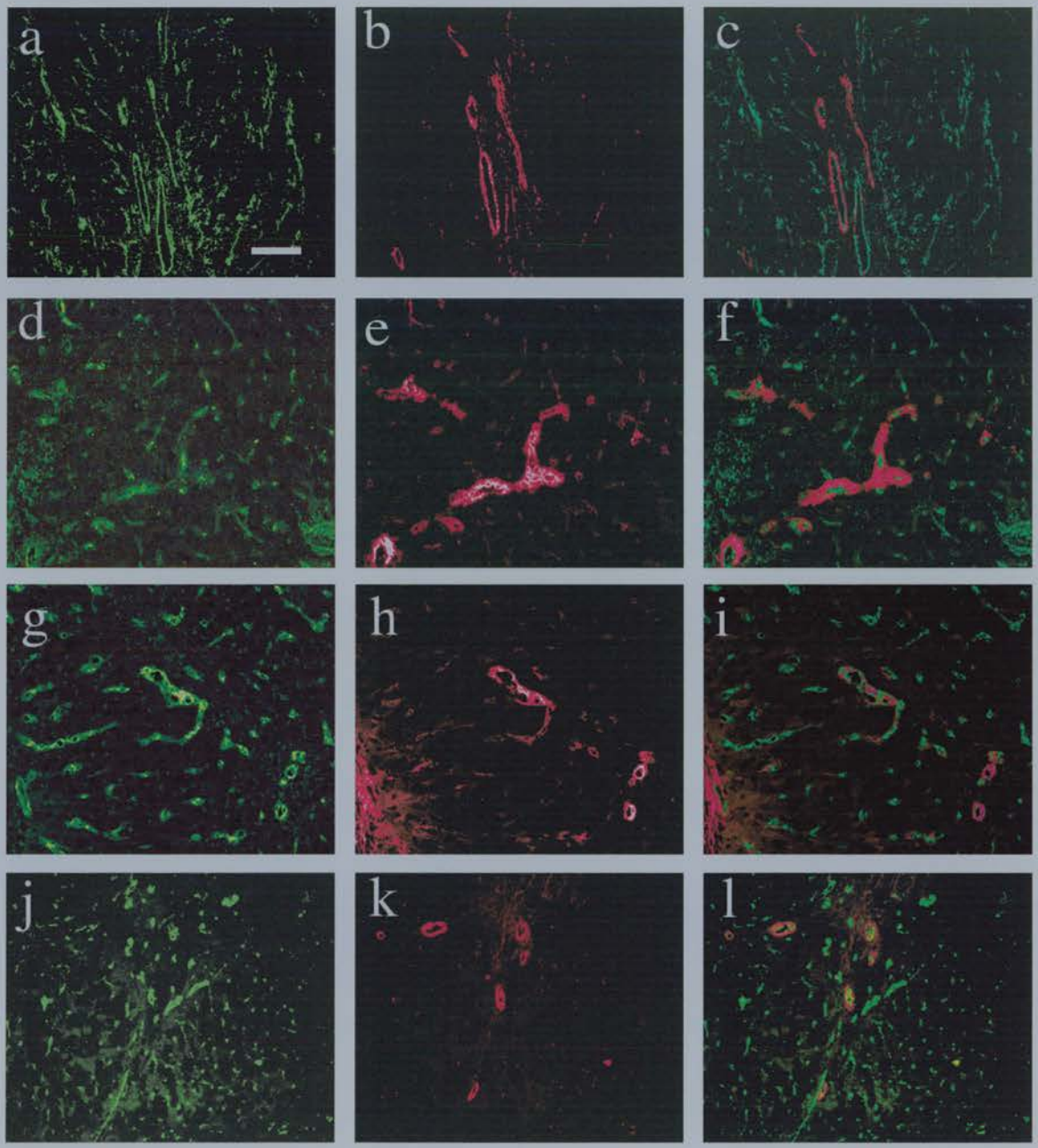

Figure 3.26 Colocalisation of pericytes and endothelial cells in the human corpus luteum

Dark field photomicrographs showing fluorescent immunostaining of the endothelial cell marker, von Willebrand factor (green staining) and the pericyte marker, α-SMA (red staining) and colocalisation of the two, in (a-c) an early luteal phase human corpus luteum; (d-f) a mid luteal phase human corpus luteum; (g-h) a late corpus luteum; and (j-l) after hCG rescue. Note in the colocalised panels that pericytes are closely associated to, almost intertwined with, endothelial cells of some luminal vessels, but that staining appears to be in two distinct cell types. Scale bar = 100μm.

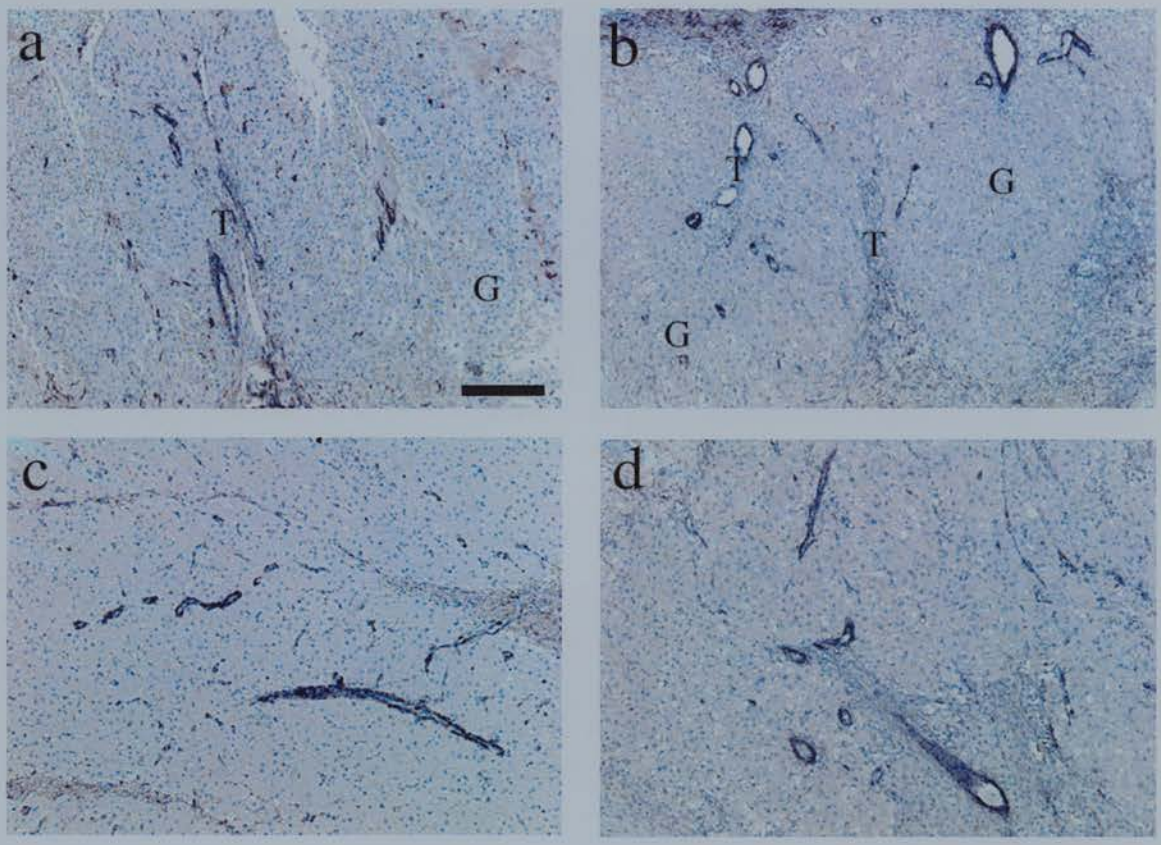

Figure 3.27 Pericyte distribution in the human corpus luteum
(a) Low power micrograph of α-SMA immunostaining in an early corpus luteum, note that staining is associated with luminal vessels (LV) in the theca (T) derived compartment and some small single cells are immunopositive in the granulosa compartment (G). (b) α-SMA immunostaining in a mid-corpus luteum, note that staining is associated to luminal vessels (LV) only, present in both the theca (T) and granulosa (G) compartments; similarly in (c) a late corpus luteum; and (d) after hCG rescue. Scale bar = 200μm.

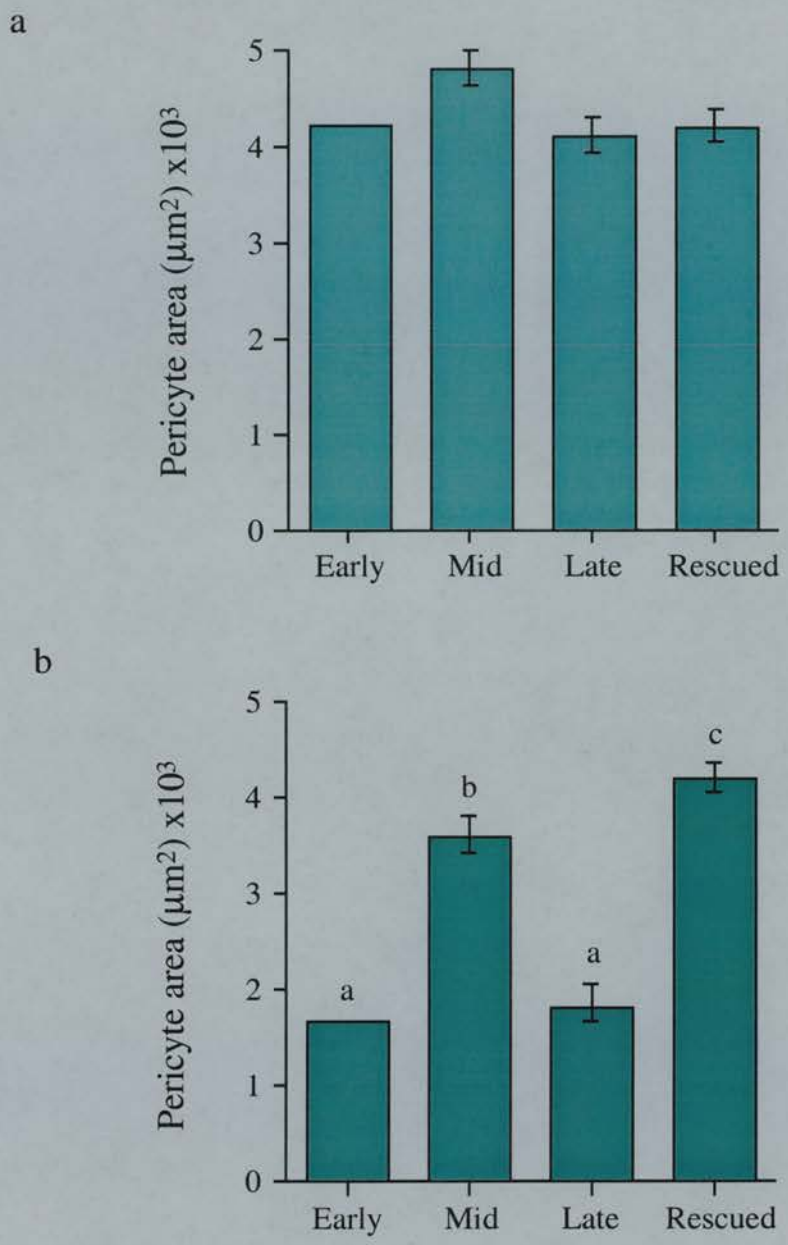

Figure 3.28 Quantification of pericyte area in the human corpus luteum

(a) Quantification of pericyte area throughout the lifespan of the human corpus luteum. Data not converted for the effects of tissue expansion and shrinkage. (b) Quantification of pericyte area throughout the lifespan of the human corpus luteum. Data converted for the effects of tissue expansion and shrinkage. Values are means ± SEM unless the SEM value was too small for the scale of the graph. Different letters denote significant differences between groups, $P<0.05$. For each luteal stage n=4-6 corpora lutea.

3.4 Discussion

This study has demonstrated that luteal angiogenesis can be measured by assessing parameters associated with the process in tissue sections collected at specific time points throughout the lifespan of the corpus luteum. Quantification of endothelial cell proliferation and resultant changes in luteal endothelial cell area; the expression of potent angiogenic agents, such as VEGF; and factors associated with vessel maturation, give detailed information about the rate of angiogenic activity in such tissue.

It was found that the early luteal phase is associated with intense angiogenesis, and high VEGF expression, as the initiation of development of luteal microvasculature and its stabilisation is underway. By the mid-luteal phase, endothelial cell proliferation continues at a lower rate, although VEGF expression remains high, and the formation of the microvascular tree is complete, with the presence of mature, luminal vessels and small capillaries. Late luteal phase regression is associated with a further decline in endothelial cell proliferation, a decrease in VEGF production, and the apparent selective degradation of non-luminal, immature vessels. It also appears that the process of luteal rescue, simulating early pregnancy, in the human is associated with an increased rate of angiogenesis and vessel stabilisation as seen by marked increases in cell proliferation, endothelial cell content, VEGF expression, and pericyte recruitment.

The use of incorporation of BrdU as a marker for cell proliferation for the first time in the primate demonstrated its specificity as compared with other markers such as Ki67 and PCNA. These proteins are expressed throughout most of the cell cycle and so may still be immunoreactive after division has taken place, which could give rise to false positive staining in some steroidogenic cells. The extent of this is decreased when using BrdU as a proliferation marker (Young, 1999). This technique has been used previously to quantify luteal proliferation in the sheep (Jablonka-Shariff *et al.*, 1993) and rat (Gaytan *et al.*, 1996) but, to our knowledge, this is the first description of its use with respect to the primate ovary. It was clear that few (if any) of the hormone-producing cells had incorporated BrdU; positive staining was restricted to some cells surrounding the luminal microvessels and others whose appearance was consistent with that of capillary endothelial cells. From colocalisation studies using BrdU with both endothelial cell markers, von Willebrand

factor and CD31, it was shown that over 80% of proliferating cells in the marmoset corpus luteum are endothelial cells. Observations in rhesus monkeys (Christenson and Stouffer, 1996b), rodents (Gaede *et al.*, 1985; Tamura and Greenwald, 1987), domestic animals (Meyer and McGeachie, 1988; Jablonka-Shariff *et al.*, 1993), and humans (McClure *et al.*, 1994; Rodger *et al.*, 1997) also suggest that that endothelial cell proliferation comprises the majority of the mitotic activity in the corpus luteum. Thus it is reasonable to consider cell proliferation in the marmoset corpus luteum, based on the PI from single BrdU immunostaining as being reflective of endothelial cell proliferation. There is evidence that there is little or no proliferation of fully differentiated primate lutein cells (Christenson and Stouffer, 1996b), which implies that the remaining BrdU positive cells in the corpus luteum are most likely fibroblasts, infiltrating macrophages or endothelial support cells, such as pericytes. This study has also demonstrated that the method of quantification of the PI as based on the percentage of cells which incorporated BrdU in 6 fields of view per corpus luteum is a robust, reproducible technique. Quantification of one 5μm section per corpus luteum is sufficient to represent the whole tissue, as based on correlation studies when two distal sections were analysed.

The demonstration that endothelial cell proliferation was maximal in the early primate corpus luteum, and significantly decreased in the mid- and late stages of luteal development is in agreement with previous studies evaluating cell proliferation in corpora lutea from other species. Proliferation studies in the human (Rodger *et al.*, 1997; Gaytan *et al.*, 1998), rhesus monkey (Christenson and Stouffer, 1996b), ovine (Jablonka-Shariff *et al.*, 1993) and bovine (Zheng *et al.*, 1994) show peak levels at the early stages of luteal development whereas luteal regression is associated with a decreased proliferative rate. Young *et al.*, (2000), measure cell proliferation in the marmoset corpus luteum using both Ki67 and BrdU immunocytochemistry, and demonstrate similar results to those obtained here. It is worth noting that although levels of proliferation in the mid-luteal phase are considerably lower than early luteal levels, the rate of angiogenesis remains higher than that of most other normal adult tissues in which turnover time to replace the endothelium is measured in years (Hanahan and Folkman, 1996).

Proliferation studies in the non-pregnant human corpus luteum, as seen by Ki67 immunostaining, show a similar pattern to that seen in the marmoset. Luteal

development is associated with an intense period of endothelial cell proliferation which declines in the mature and early regressing corpus luteum. Although co-localisation studies were not performed in this study, others have previously shown that the majority of proliferating cells in the human corpus luteum are endothelial cells (McClure *et al.*, 1994; Rodger *et al.*, 1997). However, it has not been demonstrated that luteal rescue by exogenous hCG, simulating early pregnancy, is associated with an increase in endothelial cell proliferation. Luteal rescue in a similar study in the human (Rodger *et al.*, 1997), in the ewe (Jablonka-Shariff *et al.*, 1993) and in the rhesus monkey (Christenson and Stouffer, 1996b) detected no increase in endothelial cell proliferation. Measurements in these studies were performed per unit area of luteal tissue and so do not address changes in the expansion of granulosa lutein cells during luteal rescue which would serve to spread proliferating endothelial cells further apart, and give a result not representative of the true rescued environment. Proliferating cells in this study were expressed as a percentage of total cells which portrays a more accurate picture. Because colocalisation with an endothelial cell marker was not performed it is possible that the proliferating cells we observed in rescued tissue may reflect another cell type, for example periendothelial support cells. It is unlikely that there is an influx of proliferating macrophages after hCG administration as the macrophage content of rescued corpora lutea is considerably lower than in those not subjected to hCG rescue at the same stage of the luteal phase (Duncan *et al.*, 1998a).

The observed differences in endothelial cell proliferative rate in the marmoset corpus luteum are in agreement with the changes witnessed in luteal endothelial cell content in this study. The intense proliferation in the early luteal phase when the area of endothelial cells is relatively low, leads to increased vascularisation during luteinisation and luteal establishment. By the mid-luteal stage in which there was peak endothelial cell area, it is thought that the majority of steroidogenic cells are in contact with at least one capillary (Reynolds *et al.*, 1992; Zheng *et al.*, 1994). Peak plasma progesterone concentration in the mid-luteal phase correlates with the presence of an extensive capillary network in the corpus luteum, for optimal delivery of progesterone precursors to, and progesterone from the cell. Decreased endothelial cell proliferation in the late corpus luteum coincides with the observed fall in

vascular area and decrease in plasma progesterone concentration and luteal regression.

The finding of maximal endothelial cell area from von Willebrand factor immunostaining in the marmoset mid-luteal phase however, is not in agreement with other similar studies in the marmoset (Young *et al.*, 2000) and bovine corpus luteum (Augustin *et al.*, 1995). These studies demonstrated maximal vascularisation in the early luteal phase. However, quantification of von Willebrand factor immunostaining was performed per area of luteal tissue, this area of measurement was standardised throughout the cycle and therefore did not consider the effects that tissue expansion and shrinkage, typical of the corpus luteum, would have on results. In our study we attempted to address this problem by assuming the major contribution to such change in gland volume would be from the differences in lutein cell cytoplasmic volume after lutein cell hypertrophy and atrophy which is known to occur throughout the lifespan of the corpus luteum (Adams and Hertig, 1969). It is possible that the effects of tissue fixation and processing may distort the steroidogenic cells, however this was standardised at each stage of the luteal phase and was not expected to contribute as greatly as the changes caused by cytoplasmic hypertrophy. In the late luteal phase, the relative population of other cells, such as fibroblasts and immune cells, may also play a role in changing luteal volume. Measurements of these cells was however, beyond the scope of the thesis. Therfore, the contribution of changes in steroidogenic cell volume only was quantified by measuring steroidogenic cell area in tissue sections at each of the stages of the luteal phase. Significant differences were found and so the area used to quantify von Willebrand factor immunostaining was altered accordingly and not standardised for each luteal stage.

In human luteal tissue, similar changes in luteal volume are seen. Granulosa derived lutein cells undergo hypertrophy and atrophy as quantified by measuring their area in luteal sections in all luteal stages and after hCG rescue. The importance of considering the effects of tissue expansion and shrinkage is reinforced when quantification of endothelial cell or pericyte areas in the human corpus luteum were compared before and after conversion for this phenomenon. Prior to conversion, there were no significant differences in endothelial cell or pericyte content throughout the luteal phase, as quantification was performed per standard unit area of tissue. However after conversion for the effect of tissue expansion and shrinkage,

significant differences were seen, which appeared to more closely reflect the changes observed *in vivo*. Gaytan *et al.,* (1998) recognised the problem when measuring macrophage content of the human corpus luteum, and performed quantification per number of granulosa derived lutein cells, the area occupied by which was not static throughout the luteal phase..

The pattern of vascularisation measured using a second endothelial cell marker, CD31, in the marmoset corpus luteum confirmed results gained with von Willebrand factor immunostaining, and there were no significant differences within groups between endothelial cell areas measured from immunostaining with the two markers. It appears that endothelial cells in the early, mid- and late stages of luteal development in the marmoset corpus luteum express both von Willebrand factor and CD31 antigens. Interestingly, it was noted that CD31 immunostaining in the late regressing, follicular phase corpus luteum was less distinct and more diffuse than in earlier stages of development. The regressed corpus luteum in the follicular phase is believed to be associated with a slump in angiogenic activity, although this was not measured in this study, and so a temporal correlation of decreased angiogenesis and disturbances in CD31 signifies the association of CD31 in the angiogenic process. This study does demonstrate that the quantification of one section per corpus luteum was sufficient to represent the endothelial cell content of the whole corpus luteum, as no significant differences in area of endothelial cell staining was observed when two distal sections were compared. In all further experimental work concerning the marmoset corpus luteum immunostaining for either von Willebrand factor or CD31, in one luteal section per corpus luteum, were used to measure endothelial cell content as a parameter of angiogenic activity.

A similar pattern in luteal vasculature to that seen in the marmoset corpus luteum was observed in the non-pregnant human corpus luteum by quantification of CD34 immunostaining. After conversion for the effects of tissue expansion and shrinkage, a significant increase in endothelial cell area was seen from the early to mid-luteal phase, and a marked reduction in the late luteal regressing corpus luteum. What was particularly interesting in the human was that hCG-induced luteal rescue, simulating early pregnancy, demonstrated a significant increase in endothelial cell content of the corpus luteum. This, taken with the fact that endothelial cell proliferation, as seen from Ki67 analysis, dramatically increased at this stage,

suggests that rescue of the human corpus luteum is associated with an increased angiogenic activity of the tissue. Rodger *et al.,* (Rodger *et al.*, 1997), following von Willebrand factor immunocytochemistry, demonstrated an increase in endothelial cell number per unit area of tissue, from the early to mid-luteal phase which remained high in the late corpus luteum and after luteal rescue. A concomitant elevation of cell proliferation after rescue was however, not demonstrated. It is proposed that this was due to the technique used to quantify proliferation which did not consider the tissue expansion associated with rescue of the corpus luteum.

The potent endothelial cell growth factor, VEGF, was expressed exclusively in the theca layer of marmoset antral follicles which correlated with the selective vascularisation of the theca. Interestingly, in the periovulatory follicle immunolocalisation of VEGF was detected in the granulosa layer, which correlates with disintegration of the basement membrane separating the granulosa and theca layers and the neovascularisation of the granulosa layer during this period for corpus luteum formation. In both the marmoset and human non-pregnant corpus luteum, the level of VEGF expression was high not only in the early luteal period of intense angiogenesis, but also in the less prolific mid-corpus luteum, and was only down regulated after initiation of luteolysis. These findings agree with VEGF measurements throughout the lifespan of the corpus luteum in the bovine (Goede *et al.*, 1998) and the human corpus luteum (Otani *et al.*, 1999). VEGF was localised to the cytoplasm of lutein cells in the marmoset and granulosa- and theca-derived lutein cells in the human. There was no visible staining in endothelial or periendothelial support cells. Similar cellular localisation was also demonstrated in the human ovary (Kamat *et al.*, 1995; Gordon *et al.*, 1996). Other studies have demonstrated the expression of VEGF in endothelial cells and pericytes in culture (Yonekura *et al.*, 1999) and in pericytes *in vivo* in the ovine (Reynolds *et al.*, 2000). Placental growth factor, VEGF-B and C were expressed in pericytes and endothelial cells in culture, however, the VEGF type was not mentioned in the *in vivo* study, and so it is possible that these mural cells express predominantly these other forms of VEGF, which explains why they were not detected with the antibody (specific for VEGF-A) used in this study.

In this study, intense VEGF expression was observed in lutein cells adjacent to the antrum of the developing corpus luteum, particularly in the human, giving

support for the endothelial cell mitogenicity of VEGF, in the antral invasion of blood vessels forming the mature, mid-corpus luteum. It is possible that a change in intensity of staining may not reflect an increase in protein concentration as it is likely that a linear association between staining intensity and amount of protein present does not exist. This is a particular concern when using immunocytochemistry to quantify protein content per cell. On the other hand, the area of immunostaining would consider the number of cells in which the protein is present, and quantitative immunocytochemistry based on this parameter is fair.

A high area of VEGF immunostaining was demonstrated in the mid-corpus luteum suggesting a role for VEGF in the ongoing angiogenic process, and in the survival and maintenance of the extensive mid-luteal phase vasculature. It could also reflect some of the non-angiogenic functions of VEGF, such as the regulation of vascular permeability or the mediation of endothelial cell survival as suggested by Goede *et al.*, (1998). Immunostaining for VEGF was significantly prevented from down regulation regulated in the rescued human corpus luteum, again signifying that rescue is associated with an increase in angiogenesis. Although the role of VEGF at this time may reflect some of the other functions of VEGF as suggested by high expression in the mid-luteal phase, the finding that endothelial cell proliferation and content increase dramatically with luteal rescue does suggest a role for VEGF in active angiogenesis at this time.

Previous studies in the human (Rodger *et al.*, 1997), rhesus monkey (Christenson and Stouffer, 1996b), and ovine (Jablonka-Shariff *et al.*, 1993) which do not demonstrate increased angiogenesis associated with luteal rescue suggest that early pregnancy may be associated with an increase in vessel stability. Vessel maturation is thought to signify the termination of angiogenic activity and maturation of the newly formed vasculature, and is a parameter which can be used in the quantification of angiogenic activity of a tissue. It was for this reason that luteal tissue from both marmosets and humans were used to study pericyte recruitment, following immunocytochemistry for α-SMA, throughout the luteal phase and in simulated early pregnancy in the human. A heterogeneity in the quantification of expression of α-SMA was found in the marmoset and human corpus luteum. In the marmoset corpus luteum, the area of α-SMA immunostaining was greatest in the early luteal phase, which had significantly declined by the late luteal phase

coinciding with a decrease in vasculature. However the proportion of vessels with associated pericytes in the regressing corpus luteum, appeared to increase. In the human corpus luteum, immunostaining for pericytes was associated mostly with luminal vessels, the area of which was maximal in the mid-luteal phase and hCG rescued corpus luteum. Similarly, in the late human corpus luteum absolute pericyte area decreased but the proportion of vessels with associated pericytes appeared to increase.

In the marmoset early luteal phase there was a high incidence of single pericytes not associated to the endothelial cells of luminal blood vessels, and to a lesser extent in the developing human corpus luteum. This was surprising considering that pericyte recruitment was believed to be a marker for vessel maturation and termination of angiogenesis, not consistent with the intense angiogenesis of the early corpus luteum. However, a role for pericytes in capillary sprouting has been demonstrated *in vitro* where pericytes were regularly found between leading edges of opposing sprouts, serving as guiding structures aiding the outgrowth of endothelial cells (Nehls *et al.*, 1992). Endothelial cells themselves are thought to be involved in the recruitment of pericytes *in vitro* where co-culture of non-contacting endothelial and periendothelial support cells caused migration and proliferation of pericytes, driven by PDGF-B (Hirschi *et al.*, 1999). Also, VEGF has been shown to cause pericyte proliferation and migration (Nomura *et al.*, 1995; Benjamin *et al.*, 1998; Yamagishi *et al.*, 1999) and may drive such recruitment in the corpus luteum. In culture, contact between endothelial cells and pericytes leads to pericyte differentiation of endothelial cells and inhibition of growth of both pericytes and endothelial cells, most likely via the activation of TGFβ (Hirschi *et al.*, 1999). This appears to be the situation in the mid-corpus luteum, when pericyte expression was specifically located in rings surrounding and contacting endothelial cells of luminal vessels, signifying the maturation and cessation of associated angiogenic activity of these vessels. In the late luteal phase the area of both endothelial cells and pericytes decreases, however the remaining vessels almost all appear to have pericyte contact. The removal of immature vessels, with no associated pericytes, coincides with a marked decrease in VEGF expression in the regressing corpus luteum. Benjamin *et al.*, (Benjamin *et al.*, 1999) demonstrate in primary human prostate tumours that VEGF withdrawal, as a consequence of androgen ablation therapy,

leads to the selective obliteration of immature vessels, suggesting that the smaller capillaries without pericyte association require VEGF for survival, whereas vessel maturation in the form of pericyte contact offers independence from VEGF loss. It seems likely that VEGF is required in a positive way to maintain endothelial cell-cell adhesion until periendothelial cells facilitate a more permanent mode of adhesion (Benjamin *et al.*, 1998).

Rescue of the human corpus luteum by hCG administration is associated with high pericyte coverage as seen by increased α-SMA immunostaining area, and a concomitant increase in angiogenic activity, demonstrated by prolific endothelial cell proliferation and the continued presence of small capillaries with no associated pericytes, along with high levels of VEGF expression. This indicates that during luteal rescue both vessel growth and stabilisation are occurring. The increase in VEGF could lead to: 1) a second angiogenic wave, this time restricted to small capillaries, the endothelial cells of which are not terminally differentiated by contact with pericytes recruited in the mid-luteal phase, but remain growth factor responsive; and 2) the recruitment of pericytes to stabilise the newly formed vasculature and the continued presence of pericytes from mid-luteal phase mature vessels.

These observations give rise to questions pertaining to the origin and stimuli for recruitment of luteal periendothelial support cells. The origin of pericytes remains unclear, suggestions include, *in-situ* differentiation from fibroblastic precursors at the time of endothelial sprouting (Nehls *et al.*, 1992), or the formation of pericytes from the migration and de-differentiation of arterial smooth muscle cells (Nicosia and Villaschi, 1995). One parameter of pericyte differentiation is α-SMA immunoreactivity, it seems unlikely therefore that primate luteal pericytes originated from the differentiation of fibroblastic precursor cells which are negative for α-SMA when considering the extended α-SMA immunostaining observed in the early corpus luteum of the marmoset and to some degree in the human, and that the migration and proliferation of smooth muscle cells along the existing vasculature of the theca would be a more plausible explanation. A stimulus for pericyte recruitment could be VEGF. VEGF receptors have been located to pericytes *in vitro*, and exogenous application of VEGF to cultured pericytes stimulated their migration in a dose dependent manner (Yamagishi *et al.*, 1999). In the early marmoset corpus luteum,

and rescued human corpus luteum there is a correlation with expression of VEGF and pericyte coverage signifying a role in VEGF in pericyte recruitment *in vivo*.

This study has demonstrated that *in vivo* angiogenesis can be effectively quantified using immunocytochemistry for factors associated with the angiogenic process. There is a high percentage of BrdU incorporation into proliferating endothelial cells in the marmoset corpus luteum and reproducible quantification by formulation of a Proliferation Index can be made. Quantification of endothelial cell content by area of immunostaining is highly reproducible as seen when more than one endothelial cell specific antigen was used, and also considers the expansion and contraction of luteal tissue. This indicates that these techniques are suitable for use in the analysis of angiogenic activity in the primate luteal phase. Using this approach, we have demonstrated that the formation of the primate corpus luteum is associated with intense angiogenesis, which continues as a lower rate in the fully formed gland. We have also shown that vascularisation of the human corpus luteum shows significant similarities to the marmoset. The early luteal phase exhibits intense angiogenesis which declines in the mid- and late corpus luteum. Of particular interest in the human is that the hCG rescue of the corpus luteum, simulating early pregnancy, is associated with increased angiogenic activity of the tissue, similar to the early luteal situation, and with an increase in stabilisation of the newly formed vasculature, in a dynamic situation of vascular growth and maturation, ultimately to maintain the high production of progesterone of the mid-luteal phase.

The quantification of *in vivo* primate luteal angiogenesis and vascularisation provides a powerful model in the elucidation of the control of such processes by testing the effects of putative angiogenesis inhibitors in the marmoset. The knowledge that the early luteal phase is associated with intense angiogenesis which is ongoing to a lesser degree in the mid-, leads to the development of treatment regimes which specifically target the early luteal phase to prevent this prolific angiogenesis, and the mid-luteal phase to intervene once the process has already been established. It was under this premise that the remaining experimental work was carried out in the marmoset.

Chapter 4

Inhibition of Luteal Angiogenesis by GnRH Antagonist Treatment in the Primate

4.1 Introduction

The corpus luteum is formed subsequent to follicular development and rupture of the preovulatory follicle at ovulation (Zeleznik and Benyo, 1994). It is well established that LH is the major luteotrophic factor regulating the function of the primate corpus luteum. GnRH antagonist treatment has proved a valuable tool in for the study of the regulation of the corpus luteum in a number of species. Withdrawal of LH by GnRH antagonist administration results in luteolysis of the corpus luteum in the Old World primate (Fraser *et al.*, 1986), New World primate (Webley *et al.*, 1991) and women (Dubourdieu *et al.*, 1991), as reflected by decreased plasma progesterone levels.

Chapter 3 has demonstrated that luteinisation is accompanied by prolific angiogenesis. Regulation of angiogenesis is controlled by endothelial growth factors which regulate cell-cell interactions. Most attention has focused on VEGF. In most tissues VEGF is stimulated by hypoxia (Shweiki *et al.*, 1992), but in the endocrine system the tropic hormones appear to play a role. A relationship between gonadotropin stimulation of cultured luteinised granulosa cells and VEGF production *in vitro* has been established (Christenson and Stouffer, 1997; Neulen *et al.*, 1998; Yan *et al.*, 1998; Hazzard *et al.*, 1999b). In turn, addition of VEGF to isolated macaque luteal endothelial cells stimulates proliferation (Christenson and Stouffer, 1996a). However, the *in vivo* connection between gonadotropic stimulation of lutein cells and angiogenesis has not been established. In this study, the intense early luteal phase angiogenesis and the mid-luteal continued angiogenesis were targeted for the effects of gonadotropin withdrawal by treatment with GnRH antagonist in 2 separate treatment regimes. Assessment of treatment effects was based on examination of luteal endothelial cell proliferation, establishment of the microvascular tree, morphology of the lutein cells and mode of cell death, expression of VEGF protein and mRNA, and plasma progesterone concentration.

4.2 Materials and Methods

4.2.1 Animals and treatments

Marmoset monkeys (*Calithrix jacchus*) were housed as described previously (Chapter 2) and procedures carried out in accordance with the Animals (Scientific Procedures) Act, 1986. Blood samples were collected by femoral venepuncture three times per week without anaesthesia. Ovulatory cycles were monitored by radioimmunoassay of plasma progesterone as described in Chapter 2. The stage of the luteal phase was determined according to plasma progesterone concentration following the guidelines described in Chapter 2.

Animals to receive GnRH antagonist treatment and early and mid-luteal control animals were given 1μg prostaglandin $F_{2\alpha}$ analogue i.m. in the mid-late luteal phase of the pretreatment cycle to induce luteolysis and synchronise subsequent ovulation (luteal day 0). Blood samples were collected daily from the day of presumed ovulation and the animals were subsequently treated with either 1mg/kg/s.c. GnRH antagonist, Antarelix™ (Deghenghi *et al.*, 1993) or vehicle on luteal days 1 and 2, or 8 and 9 (n=4 per group). Ovaries were collected on day 3 or day 10 as previously described (Chapter 2), 1h after administration of BrdU to animals in both control and treatment groups. The regime of treatment is depicted in Figure 4.1. Ovaries were fixed immediately in 4% paraformaldehyde for paraffin-embedding as described previously (Chapter 2). A small piece of corpus luteum was fixed in 3% glutaraldehyde in 0.1M cacodylate buffer, pH 7.3, for araldite resin-embedding, which was carried out in the Histology department. These specimens were fixed for 2h, rinsed in the same buffer, post-fixed in buffered 2% osmium tetroxide for 2h, and embedded in Araldite after dehydration in ethyl alcohol. Semi-thin (1μm) sections were stained with toluidine blue for light microscope analysis.

4.2.2 Immunocytochemistry and toluidine blue staining

Paraffin-embedded ovarian sections (5μm) were mounted onto TESPA coated glass slides and dried at 50°C overnight. The procedures for BrdU, von Willebrand factor and VEGF immunostaining are described in Chapter 3. The methodology used for 3' end labelling of fragmented DNA for *in situ* detection of apoptotic cell death is described fully in Chapter 2.

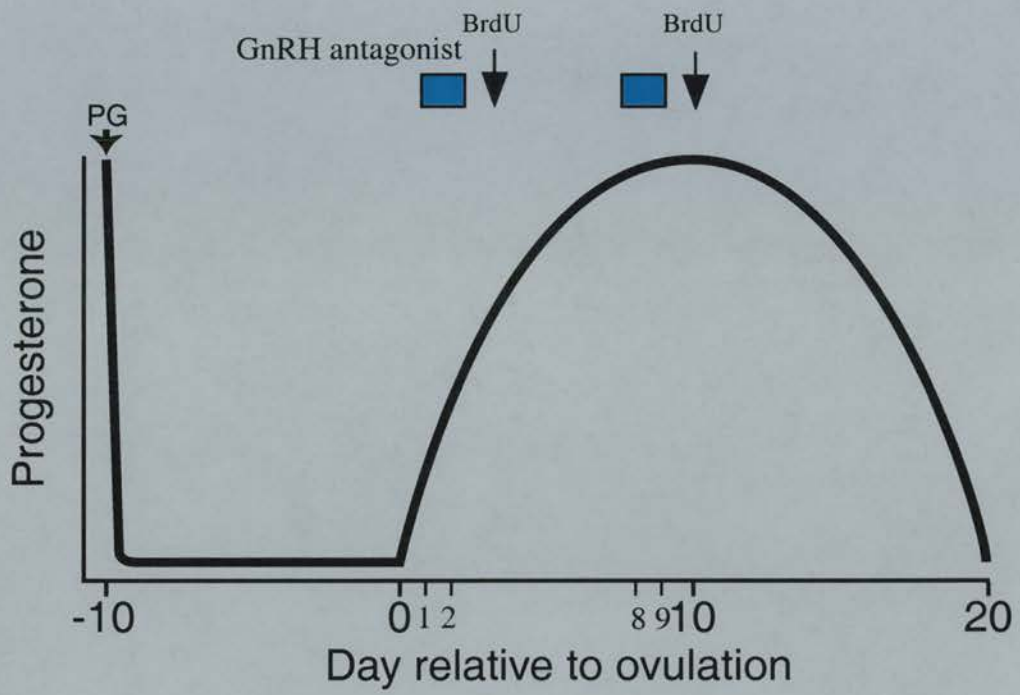

Figure 4.1 The regime of GnRH antagonist treatment in the marmoset

Prostaglandin analogue was given in the pretreatment cycle to synchronise the timing of ovulation and administration of treatment. GnRH antagonist was either administered on luteal days 1 and 2, or 8 and 9. To investigate the effect of gonadotropin withdrawal on endothelial cell proliferation, BrdU was administered 1 hour before tissue collection on day 3 or day 10.

To examine the effect of GnRH antagonist treatment on luteal morphology, treated and control sections were stained with toluidine blue (BDH) by the Histology department. Araldite resin-embedded, 1μm sections were incubated in toluidine blue at 70°C for 8 min, dried, and examined under the light microscope.

4.2.3 *In situ* hybridisation

In situ hybridisation for VEGF-A mRNA was performed using a riboprobe, synthesised from cDNA, specific for all isoforms of human VEGF-A, gifted from Dr Charnock-Jones (University of Cambridge). Sequence details are documented in Appendix A. The procedures involved in riboprobe synthesis and *in situ* hybridisation are described in Chapter 2. Due to the absence of cDNA sequences for marmoset-specific VEGF-A, this tissue was tested for hybridisation with the human specific probe on a 'trial and error' basis. The methodology for *in situ* hybridisation with a probe specific for human VEGF-A mRNA in marmoset ovary is detailed in Chapter 2. Sections were counterstained with haematoxylin and mounted in Pertex.

4.2.4 Quantification and statistical analysis

Early and mid-luteal phase, left and right ovaries for each animal were examined for appropriately staged corpora lutea. The PI was calculated by analysis of six randomly chosen fields per corpus luteum, at x400 magnification, using a grid overlay. The number of proliferating cells was expressed as a percentage of total number of cells per graticule field, *i.e.* (number of BrdU positive cells/total cells) x100.

Immunostaining for von Willebrand factor was quantified as described fully in Chapter 3. Images were captured using the x20 lens and an area of 9.2×10^4 μm^2 for the early corpus luteum, and the x10 lens and an area of 1.3×10^5 μm^2 for the larger mid-luteal sections, and measured for von Willebrand factor immunostaining. Between 4 and 8 fields of view were quantified, the number being dictated by the size of the luteal section and lens magnification used.

Quantification of VEGF protein and mRNA was performed by measuring the area and intensity of VEGF immunostaining (described fully in Chapter 3) and grain area and density after *in situ* hybridisation. VEGF mRNA grain area and density were measured using the Image Pro-Plus 3.0 image analysis programme. Images

were captured at x40 lens magnification, as white images on a black background, and the threshold set so the captured image resembled the live image as closely as possible. The total area of grain clusters signifying specific VEGF mRNA staining, not background, and the mean density of grains within clusters were measured using a pre-recorded macro. Ten fields of view, selected in a stratified random manner were quantified per corpus luteum.

The effects of GnRH antagonist treatment on PI, endothelial cell area, plasma progesterone levels, and VEGF expression as compared to controls were determined using separate two-tailed, unpaired t-tests, with a 95% confidence interval ($P<0.05$), using StatView version 4.0.

4.3 Results

4.3.1 Effect of GnRH antagonist treatment in the early luteal phase on PI

An elevation of plasma progesterone was observed prior to treatment in all animals and confirmed by the identification of recently formed corpora lutea in early luteal control and GnRH antagonist treated animals. Figure 4.2a-c shows a comparison of BrdU immunolocalisation and PI in an early luteal control corpus luteum and a GnRH antagonist treated corpus luteum. BrdU positive staining (dark nuclei) and haematoxylin stained (pale nuclei) are apparent. A significant decrease ($P<0.001$) in PI was seen in corpora lutea from the treated group of animals as compared to the early luteal controls. Clusters of densely stained nuclear fragments, characteristic of apoptotic cell death, were rarely apparent in the GnRH antagonist treated corpus luteum (Fig. 4.2b).

4.3.2 Effect of GnRH antagonist treatment in the early luteal phase on endothelial cell area

Immunostaining for von Willebrand factor in control and treated corpora lutea (Fig. 4.2d and e) demonstrated the beginning of development of the microvascular tree. Many endothelial cells associated with small capillary, non-luminal vessels were present in both control and treated sections. Quantification revealed that GnRH antagonist treatment did not have any apparent effect on formation of the capillary network (Fig. 4.2f).

4.3.3 Effect of GnRH antagonist treatment in the early luteal phase on luteal morphology and plasma progesterone concentration

Figure 4.2g and h shows toluidine blue stained sections of an early control corpus luteum and a GnRH antagonist treated corpus luteum. There is a marked effect on lutein cell morphology in the treated corpus luteum as compared to controls. The lutein cells of the early control corpus luteum appeared normal for this species, with distinct cell margins and well formed nuclei, containing a single nucleolus within an abundant cytoplasm, typical of a steroidogenic lutein cell. This contrasted with the appearance of corpora lutea following GnRH antagonist treatment. After treatment the corpus luteum showed severe disorganisation, and the lutein cells had much less clearly defined margins. In addition there was evidence of lipid accumulation and the occurrence of dense bodies. Typical apoptotic bodies were not observed. Recognisable lutein cells were smaller than in the control tissue, even those in which the nucleus remained intact. GnRH antagonist treatment was associated with a marked reduction ($P<0.001$) in plasma progesterone concentration to follicular phase levels (Fig. 4.2i).

4.3.4 3`end labelling after GnRH antagonist treatment in the early luteal phase

Control and treated sections were screened for signs of apoptotic cell death. *In situ* 3` end labelling revealed an absence of staining in the control tissue (Fig. 4.3a) and a marked presence of staining after GnRH antagonist treatment (Fig. 4.3b). It is debatable if this form of cell death was apoptotic because apoptotic bodies were rarely seen and positive cells were arranged in clusters, whereas apoptosis tends to occur in single cells. A positively stained atretic follicle is shown in Figure 4.3c, and as a negative control the same follicle not treated with TdT enzyme is depicted in Figure 4.3d. In addition, healthy follicles, treated with TdT enzyme displayed no positive staining (Fig. 4.3e)

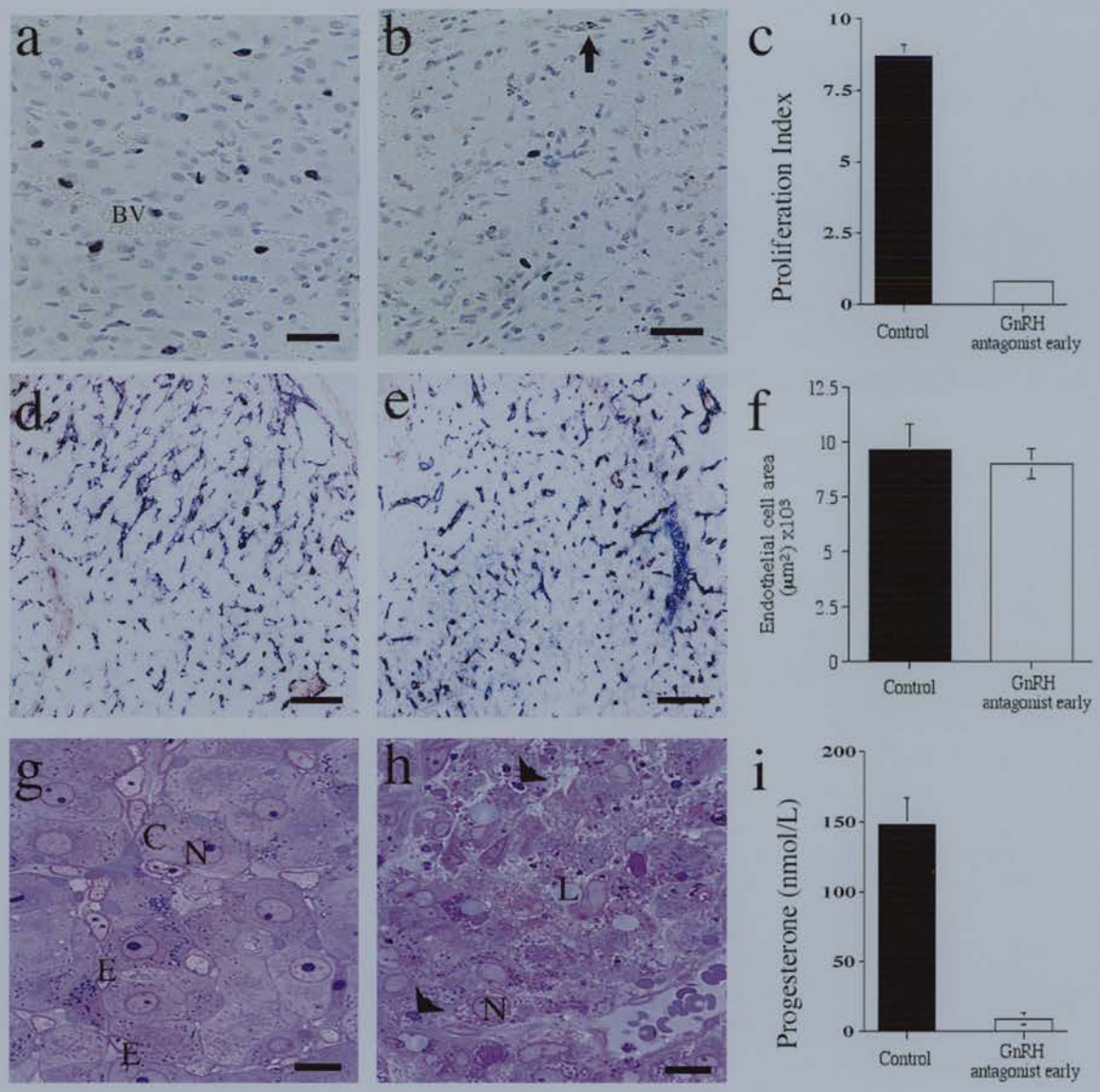

Figure 4.2 The effect of early luteal GnRH antagonist treatment on proliferation index (PI), establishment of the microvascular tree, cell morphology and progesterone output
Immunocytochemical localisation of BrdU in (a) an early control corpus luteum and (b) the corpus luteum of a GnRH antagonist treated animal at the same stage of the cycle. Note the marked reduction in BrdU incorporation and cellular disruption after treatment. Note also the presence of the blood vessel (BV), and possible apoptotic body indicated by the arrow. (c) The effect of GnRH antagonist treatment on PI (% BrdU incorporation). (d-f) von Willebrand factor immunostaining for endothelial cells in (d) control and (e) treated sections. Note that the preliminary establishment of the microvascular tree, typical of the early luteal phase, has not been disrupted after GnRH antagonist treatment. (f) Quantification of endothelial cell area confirms this. Values are means ± SEM. $P<0.001$. (g-h) Toluidine blue stained sections of (g) an early control corpus luteum and (h) after GnRH antagonist treatment. Note the healthy appearance of steroidogenic cells (SC) with abundant cytoplasm (C), clear nuclei with nucleoli (N) and probable endothelial cells (E) in the control corpus luteum. After treatment the cellular integrity is severely disrupted and dense bodies, indicated by the arrow heads, lipid droplets (L), and some intact nuclei (N) are present. (i) The effect of GnRH antagonist treatment on plasma progesterone concentration. Values are means ± SEM. $P<0.001$. Scale bars on a and b = 50μm. Scale bars on d and e = 100μm. Scale bars on g and h = 20μm.

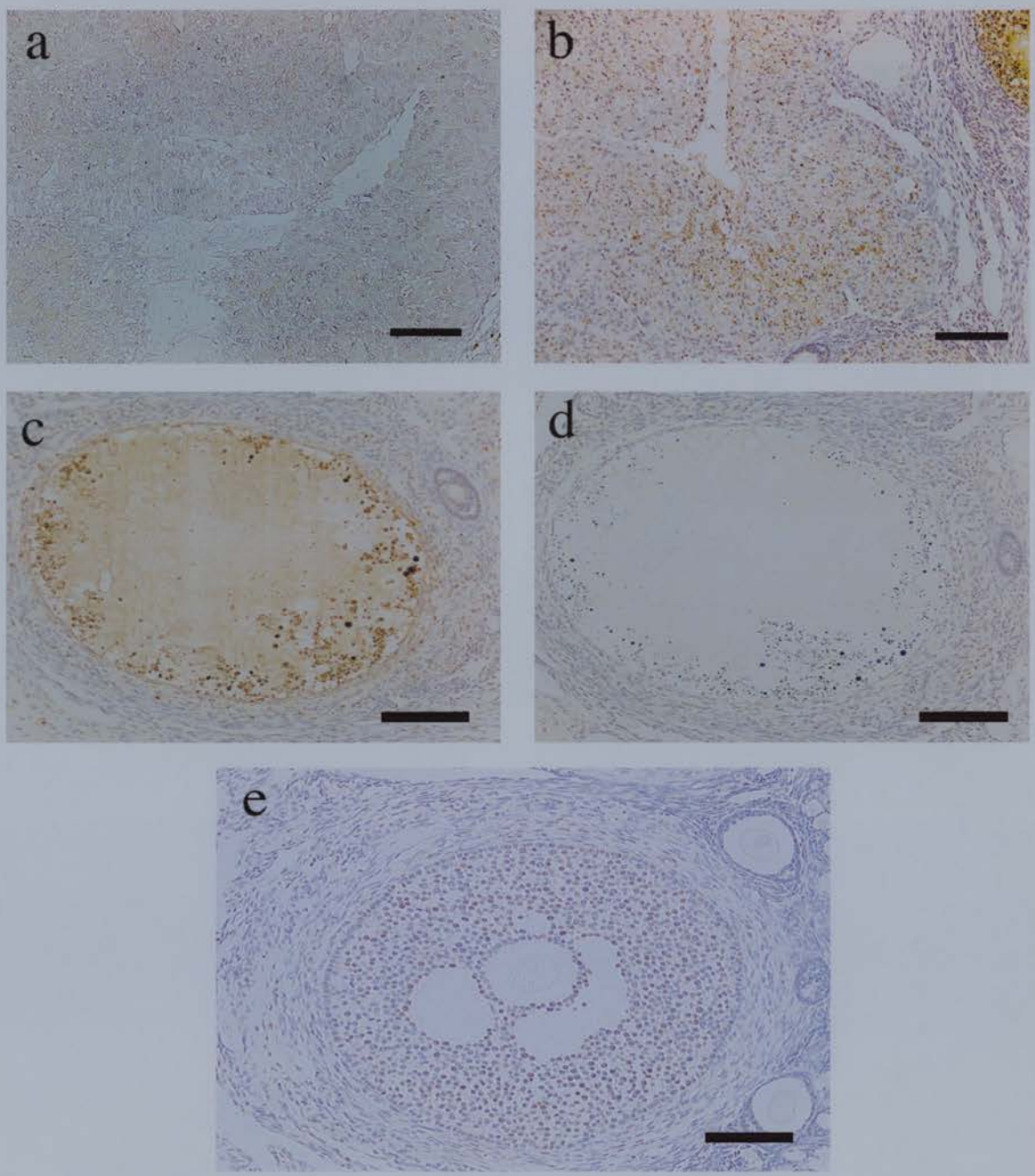

Figure 4.3 *In situ* 3' end labelling in early luteal control tissue and after GnRH antagonist treatment

(a) An early control corpus luteum with no staining signifying a lack of DNA fragmentation, and (b) a 3' end labelled (brown staining) section after GnRH antagonist treatment in the early luteal phase, note the extent of DNA damage throughout the corpus luteum as a whole. (c) A positively stained atretic follicle and (d) the same follicle in a serial section incubated without terminal transferase enzyme, as a negative control. (e) A negative healthy follicle, which was treated with terminal transferase enzyme.
Scale bars = 100μm.

4.3.5 Effect of GnRH antagonist treatment in the early luteal phase on VEGF-A protein and mRNA

Immunocytochemical localisation of VEGF-A protein demonstrated high levels of expression in both the early luteal control corpus luteum (Fig. 4.4a) and after GnRH antagonist treatment (Fig. 4.4b). Quantification of VEGF-A immunostaining revealed there was no decrease in area of VEGF-A protein or intensity of staining after GnRH antagonist treatment in the early luteal phase (Fig. 4.5a-b). However, a marked decrease in VEGF-A mRNA expression was seen after GnRH antagonist treatment as compared to early luteal controls (Fig. 4.4c-f). Figure 4.4g shows intense staining after *in situ* hybridisation with the antisense probe, and Figure 4.4h, demonstrates the absence of staining in a serial section after incubation with the negative sense probe. This indicates that any VEGF-A mRNA expression would have been detected after GnRH antagonist treatment when using the antisense probe.

4.3.6 Effect of GnRH antagonist treatment in the mid-luteal phase on PI, luteal morphology and plasma progesterone concentration

Administration of GnRH antagonist treatment in the mid-luteal phase failed to show a significant decrease in endothelial cell proliferation (Fig. 4.6a-c). However, similar effects as with treatment in the early luteal phase were seen on lutein cell morphology. Toluidine blue staining of the mid- control corpus luteum (Fig. 4.6d) revealed normal, healthy steroidogenic cells and the presence of many luminal vessels, typical at this stage of the cycle. After treatment there was a different picture. Mass accumulation of lipid, severe vacuolation, and the presence of many densely staining bodies, typical of an unhealthy corpus luteum, were apparent (Fig. 4.6e). Coincidentally a marked decrease in plasma progesterone concentration in mid-luteal treated animals as compared to controls was observed (Fig. 4.6f).

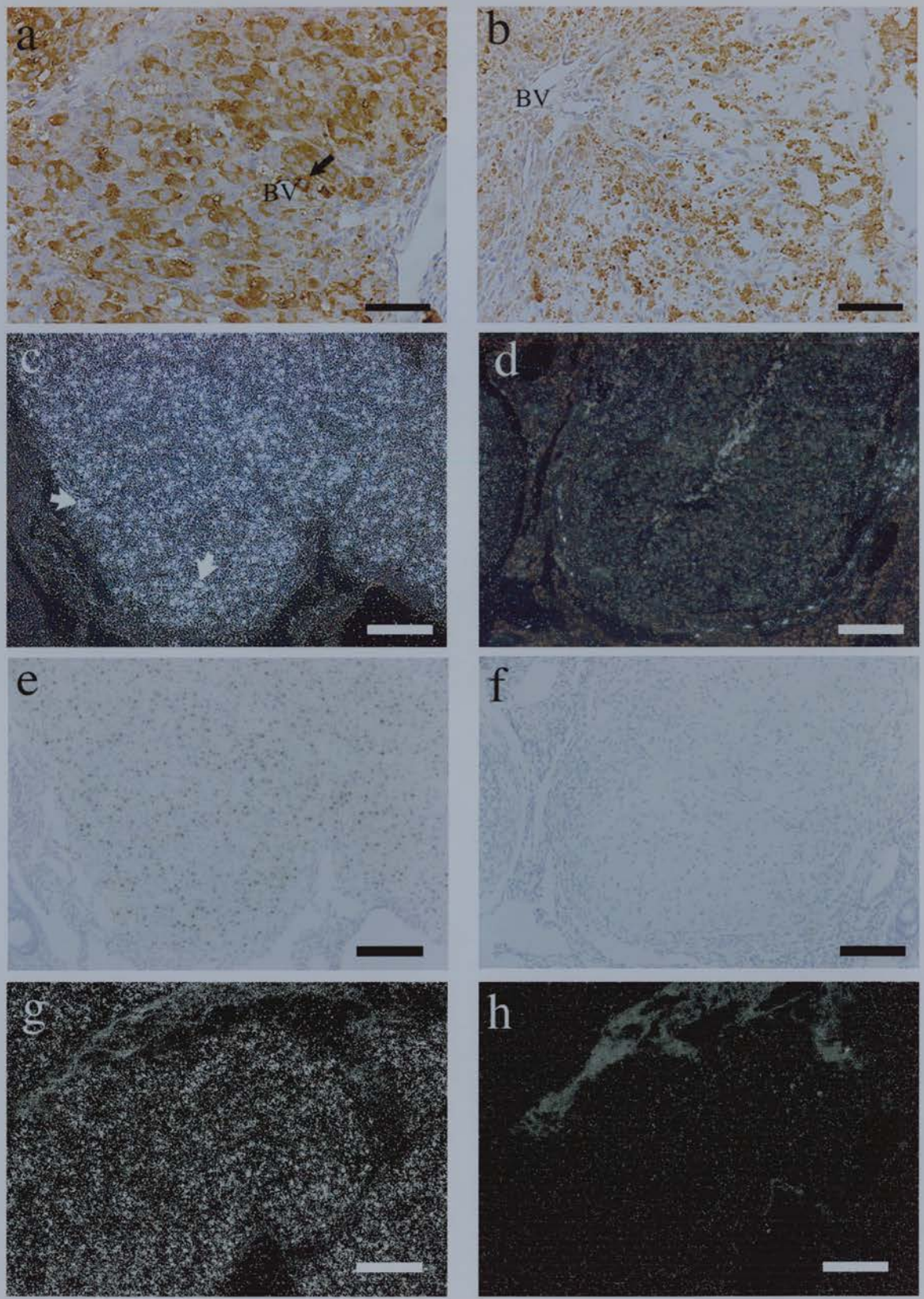

Figure 4.4 VEGF-A protein and mRNA in early luteal control tissue and after GnRH antagonist treatment
(a) Localisation of VEGF (brown staining) in an early luteal control section. Note that most lutein cells are positively stained also that intense staining can be seen in a lutein cell, indicated by the arrow, adjacent to a blood vessel (BV), which demonstrates the quantitative nature of this immunocytochemical staining. (b) VEGF immunostaining after GnRH antagonist treatment. Note the extent of disruption of the corpus luteum and that apparent VEGF staining is more granular and not restricted to intact lutein cells. Note also the presence of luminal blood vessels (BV). (c) Dark field micrograph of VEGF-A mRNA (white grains) in an early control section. Note that expression is located in clusters corresponding to the steroidogenic cells of the corpus luteum (white arrows). (d) Expression of VEGF-A mRNA in a GnRH antagonist treated section. Note the great reduction in VEGF-A expression. (e) Light field micrograph of the same early luteal control section. VEGF-A mRNA expression is located in the steroidogenic cells (black grains). (f) Light field micrograph of the same GnRH antagonist treated section, where a marked reduction in VEGF-A mRNA expression is seen. (g and h) In situ hybridisation with the anti-sense and sense VEGF-A probes in serial sections, respectively. Notice the very low level of staining after hybridisation with the sense probe indicating that the high level of staining in (g) reflects VEGF-A mRNA. Scale bars on a and b = 50μm. Scale bars on c-h = 100μm.

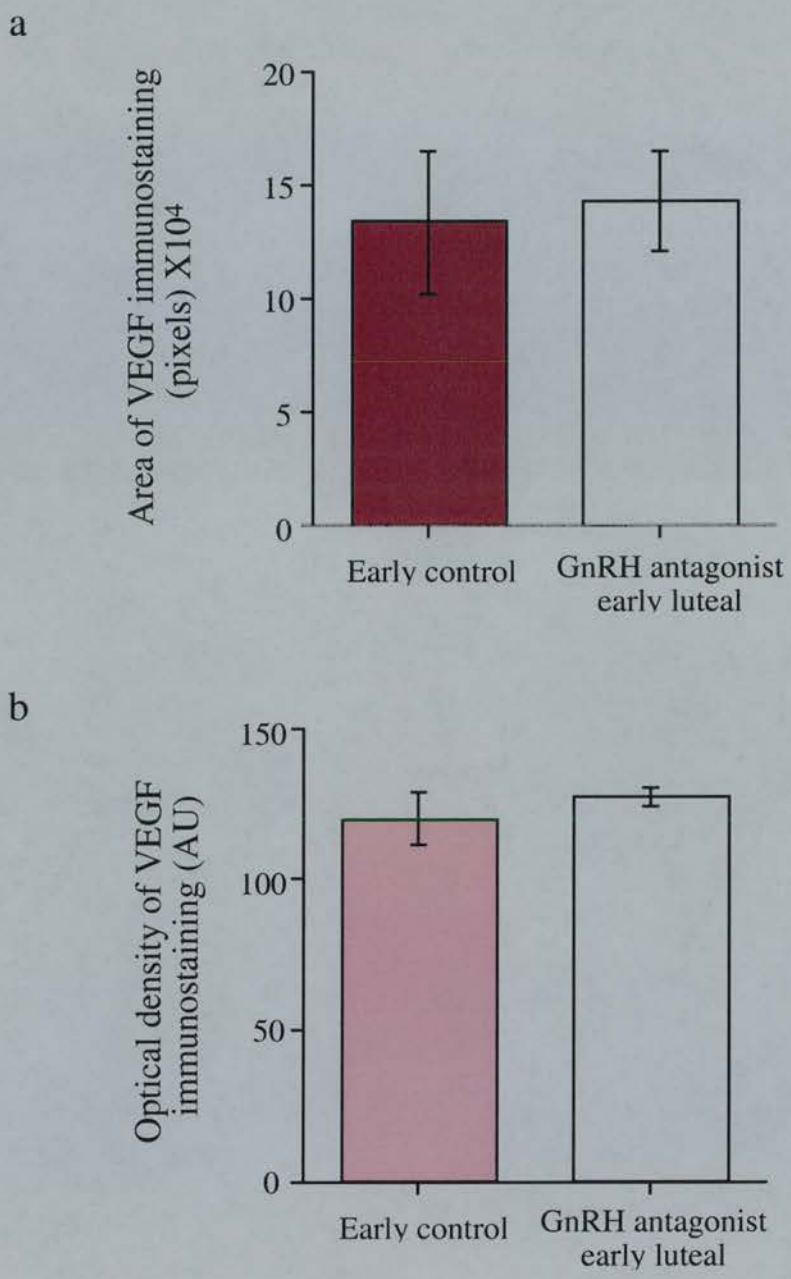

Figure 4.5 Quantification of area and intensity of VEGF-A immunostaining in control and after GnRH antagonist treatment in the early luteal phase.

(a) Area of VEGF immunostaining (in pixels) in early luteal control sections (closed bar) was not significantly different from the area measured after treatment (open bar). (b) The intensity of staining in control section (closed bar) and after treatment (open bar). Differences were not significant. Values are means ± SEM.

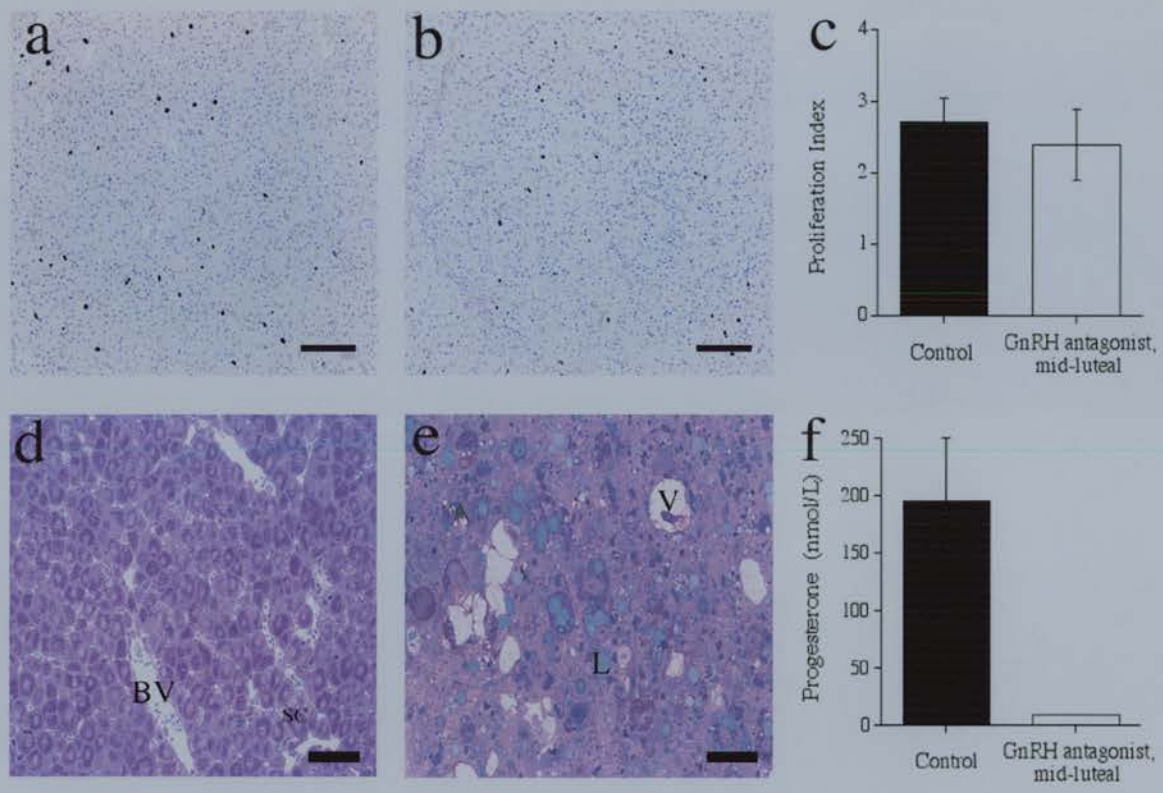

Figure 4.6 The effect of mid-luteal GnRH antagonist treatment on proliferation index (PI), cell morphology and progesterone output

(a-c) Immunocytochemical localisation of BrdU in (a) a mid- control corpus luteum and (b) a GnRH antagonist treated corpus luteum. Note the similar level of incorporation in control and treated corpora lutea. (c) The effect of GnRH antagonist treatment on PI (% BrdU incorporation). (d-f) Toluidine blue stained sections of (d) a mid- control corpus luteum and (e) after GnRH antagonist treatment. Note the healthy appearance of steroidogenic cells (SC) with abundant cytoplasm, and central round nuclei, and the presence of many luminal blood vessels (BV) typical of the mid-control corpus luteum. After treatment the cellular integrity is severely disrupted, many lipid droplets (L) and large vacuoles (V) are present. (f) The effect of GnRH antagonist treatment on plasma progesterone concentration. Values are means ± SEM. P=0.01. Scale bars = 100µm.

4.3.7 Effect of GnRH antagonist treatment in the mid-luteal phase on VEGF-A protein and mRNA

VEGF-A immunostaining appeared to be consistently lower after treatment than in mid-luteal controls (Fig. 4.7a-b). This was demonstrated after quantification of area of VEGF-A immunostaining (Fig. 4.8a) in control sections and after GnRH antagonist treatment in the mid-luteal phase. The intensity of staining however, increased as a result of treatment (Fig. 4.8b; a decrease in optical density indicates an increase in immunostaining intensity, as described in Chapter 3). However, GnRH antagonist treatment in the mid-luteal phase, when compared to mid-luteal controls (Fig. 4.7c) resulted in a marked decrease in VEGF-A mRNA expression (Fig.4.7c).

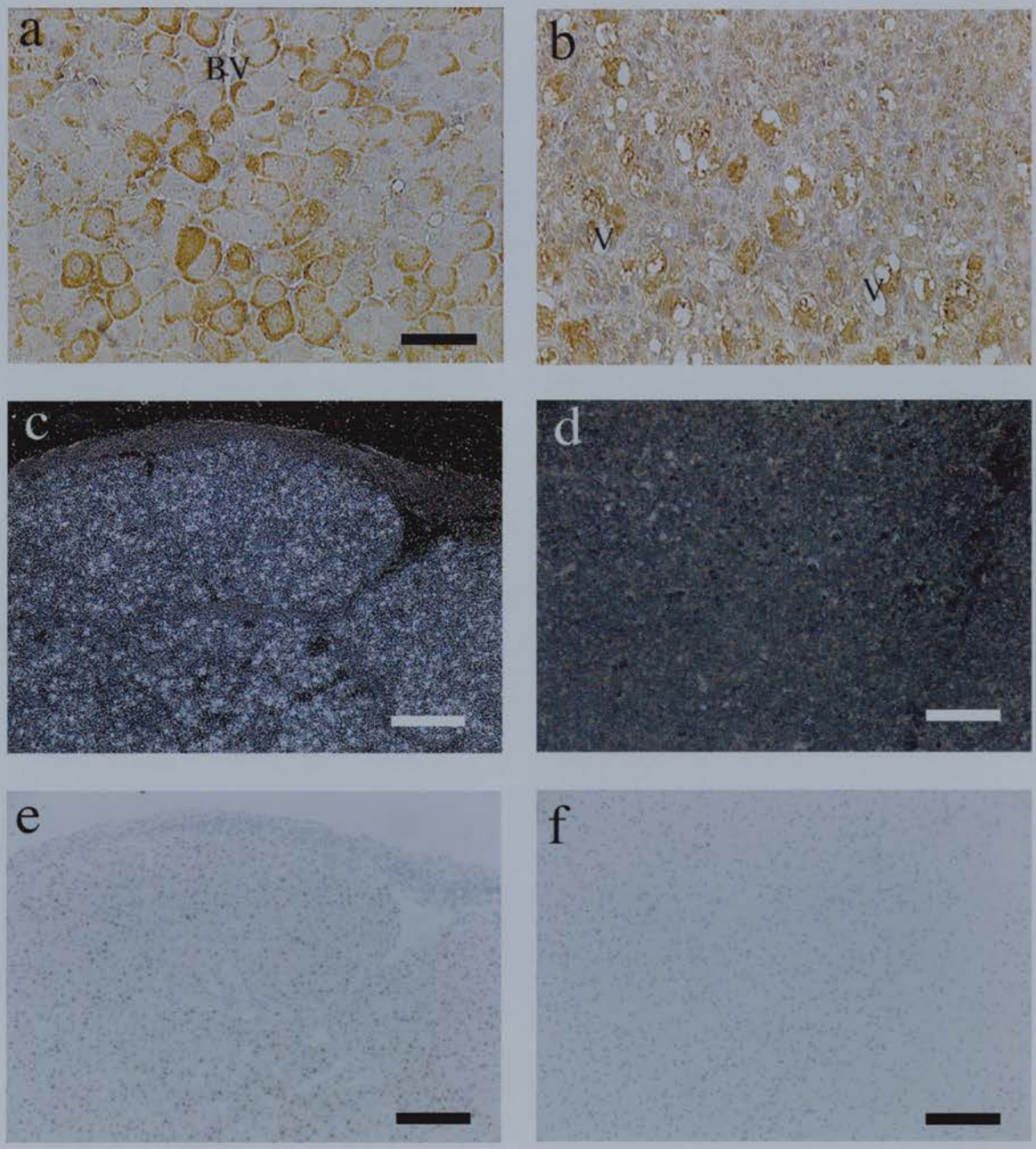

Figure 4.7 VEGF-A protein and mRNA in mid-luteal control tissue and after GnRH antagonist treatment

(a) Localisation of VEGF (brown staining) in mid-luteal control section. Note that many lutein cells are positively stained at this stage of the cycle and the presence of the blood vessel (BV). (b) VEGF immuno-staining after GnRH antagonist treatment. Note the extent of disruption of the corpus luteum and that apparent VEGF staining is more granular and associated to vacuolated cells (V). (c) Dark field micrograph of VEGF-A mRNA (white grains) in a mid- control section. Note that expression is located in clusters corresponding to the steroidogenic cells of the corpus luteum (white arrows). (d) Expression of VEGF-A mRNA in a GnRH antagonist treated section. Note the great reduction in VEGF-A expression. (e) Light field micrograph of the same mid-luteal control section. VEGF-A mRNA expression is located in the steroidogenic cells (black grains). (f) Light field micrograph of the same GnRH antagonist treated section, where a marked reduction in VEGF-A mRNA expression is seen. Scale bars on a and b = 50μm. Scale bars on c-f = 100μm.

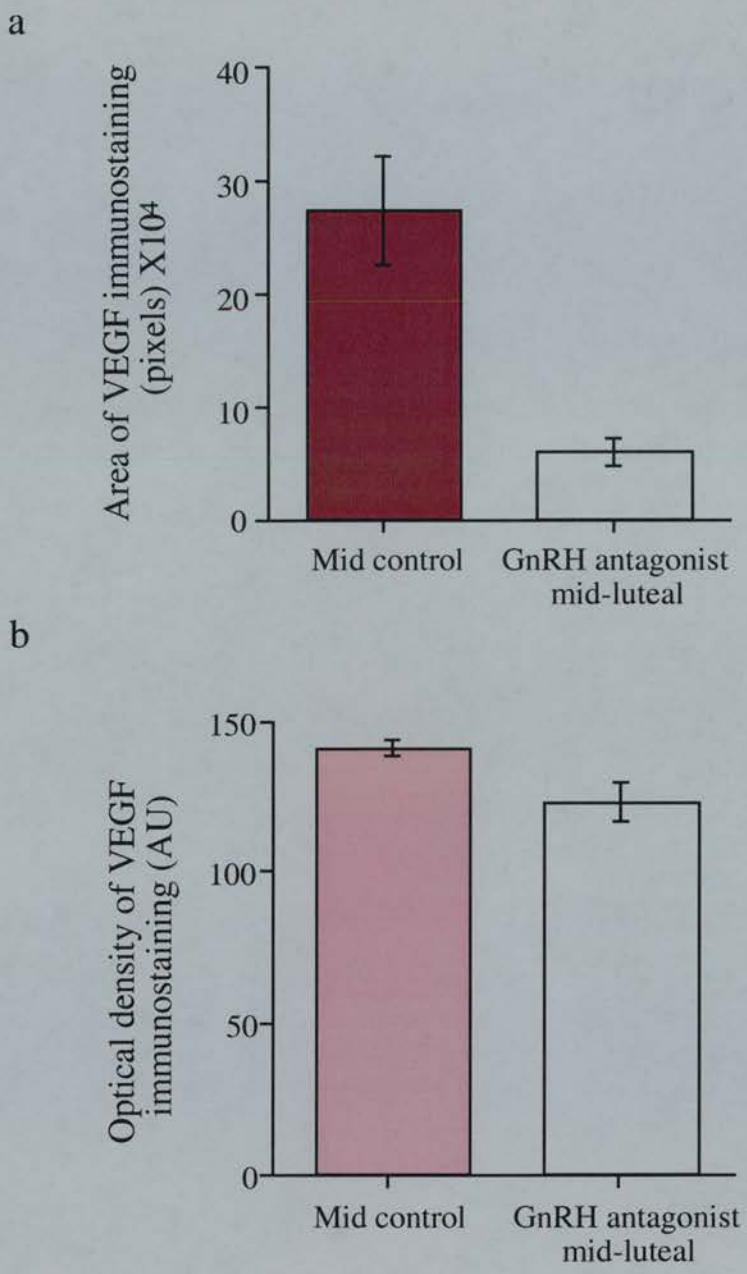

Figure 4.8 Quantification of area and intensity of VEGF-A immunostaining in control and after GnRH antagonist treatment in the mid-luteal phase

(a) The area of VEGF immunostaining (in pixels) in mid-luteal control sections (closed bar) and after treatment (open bar). P=0.002 (b) The intensity of staining in control (closed bar) to treated (open bar) levels. P=0.01. A low value indicates dark staining/high intensity. Values are means ± SEM. Different letters denote significant differences.

4.4 Discussion

This study has established for the first time *in vivo* that the intense angiogenesis in the primate corpus luteum associated with the early luteal phase is dependent on gonadotropin support. GnRH antagonist treatment was employed to examine the gonadotropin dependence of the intense angiogenesis associated with the early luteal phase, and the ongoing angiogenesis of the mid-luteal phase. The treatment is presumed to be a consequence of pituitary withdrawal of LH as described previously in the marmoset (Webley *et al.*, 1991), macaque (Fraser *et al.*, 1986) and human (Dubourdieu *et al.*, 1991) luteal phase.

In the early luteal phase study, deprivation of gonadotropin support to steroidogenic cells reduced endothelial cell proliferation by 90%, and plasma progesterone concentration by 95%, demonstrating the dependence of early luteal angiogenesis and function on gonadotropin support. Although administration of GnRH antagonist in the mid-luteal phase failed to effect luteal endothelial cell proliferation as seen by unchanged levels of BrdU incorporation after treatment, plasma progesterone concentration was decreased by 95%, signifying the gonadotropin-dependence of mid-luteal steroidogenic function.

Light microscopy of toluidine blue stained sections revealed a severe disruption of normal steroidogenic cell morphology in both groups of GnRH antagonist treated corpora lutea when compared to controls. Accumulation of lipid, appearance of densely staining bodies and the absence of distinct cell margins were obvious after treatment. Evidence of fragmented nuclei, characteristic of apoptosis, was apparent in haematoxylin stained corpora lutea and *in situ* 3' end labelling demonstrated positive results after treatment in the early luteal phase. However, analysis of semi-thin sections indicated widespread cell death by a process other than apoptosis, as also suggested previously (Fraser *et al.*, 1995; Young *et al.*, 1997), and ultrastructural studies of GnRH antagonist-induced luteolysis in the marmoset do not indicate widespread cell degeneration via apoptosis (Fraser *et al.*, 1999b). DNA fragmentation is characteristic of necrotic as well as apoptotic forms of cell death, therefore *in situ* 3' end labelling does not distinguish between necrotic and apoptotic DNA in tissue sections (Phelouzat *et al.*, 1996). It is only possible to characterise this form of tissue degradation as apoptotic cell death in the presence of typical DNA 'laddering' following electrophoresis of extracted DNA, and observations of

apoptotic bodies following ultrastructural analysis of treated corpora lutea. Since the former was not measured and the latter was not evident, it is difficult to ascertain the method of luteal cell death seen in this study. It is however, clear that the extent of luteal cell disruption was such that steroidogenic cell function was significantly impaired, preventing secretion of progesterone and most likely other factors involved in normal luteal function.

The proliferation of non-endothelial cells in the distressed corpus luteum after GnRH antagonist treatment in the mid-luteal phase may explain the unexpected failure to observe a decrease in proliferation index after treatment at this stage. During normal luteolysis the proportion of apparent fibroblasts in the corpus luteum increases. Thus, in a response similar to that seen during natural regression, proliferating luteal fibroblasts may incorporate BrdU. Similarly, proliferating immune cells, such as leukocytes or macrophages, which infiltrated the distressed corpus luteum after initiation of an immune response may also incorporate BrdU. Another explanation may be a result of the increased incidence of cell death in the mid-luteal phase treated corpus luteum. It has been reported that during cancer therapy DNA damage induced by a number of chemical and radiation treatments is known to activate DNA repair (reviewed by Berges *et al.*, 1993). To detect DNA repair in androgen-dependent normal prostatic glandular cells after castration in rats, high dose, long exposure to BrdU was used, maximising the detection of both scheduled DNA synthesis and unscheduled DNA repair. A 10 fold increase in BrdU incorporation was seen, which was considered part of a futile G_0 DNA repair process (Berges *et al.*, 1993). It is therefore possible that cells in the corpus luteum after GnRH antagonist treatment incorporated BrdU in a futile DNA repair mechanism during a process of cell death which involves DNA fragmentation.

Early luteal phase administration of GnRH antagonist to macaques (Fraser *et al.*, 1987) and women results in suppression of progesterone secretion and a marked reduction in response to exogenous hCG administrated in the mid-luteal phase (Fraser *et al.*, 1987; Dubourdieu *et al.*, 1991). Here we show that administration of GnRH antagonist in the early luteal phase causes a severe disruption of steroidogenic cell morphology and angiogenesis, thus providing an explanation, at the cellular level, for the effects of GnRH antagonist treatment seen previously.

It is tempting to suggest that the adverse effect of GnRH antagonist treatment on early luteal angiogenesis is predominantly a consequence of decreased VEGF production from the dysmorphic steroidogenic cells of the developing corpus luteum. VEGF is a secreted angiogenic mitogen (Leung *et al.*, 1989), specific for endothelial cell receptors (Plouet and Maukadiri, 1990; Vaisman *et al.*, 1990). Both VEGF mRNA and its transcribed protein have been localised to the granulosa and theca lutein cells of the human corpus luteum (Chapter 3; Kamat *et al.*, 1995; Otani *et al.*, 1999), and protein in marmoset lutein cells (Chapter 3). Cultured human (Neulen *et al.*, 1998; Yan *et al.*, 1998) and macaque (Christenson and Stouffer, 1997; Hazzard *et al.*, 1999b) luteinised granulosa cell-VEGF expression has been shown to be up regulated by gonadotropins *in vitro*. In the current investigations using immunocytochemistry to determine changes in VEGF in the corpus luteum after GnRH antagonist treatment in the early luteal phase we did not observe the expected decrease in immunostaining. However, it appears that production of VEGF-A message was severely compromised by GnRH antagonist treatment, as seen by the marked reduction in VEGF mRNA expression after treatment in the both the early and mid-luteal phases. Hypoxia-induced VEGF translation (Stein *et al.*, 1998), the presence of residual, non-active, or metabolised VEGF, or non-specific staining by lutein cell debris in the treated corpus luteum may explain the unexpected failure to demonstrate decreased expression of VEGF protein.

Angiogenesis is a multi-step process involving a number of angiogenic growth factors, degradation of the extra-cellular matrix by matrix metalloproteinases and cell-cell interactions. Neutralisation of VEGF in the marmoset over the same time period reduces endothelial cell proliferation by 80% as compared to control levels (Chapter 6; Fraser *et al.*, 2000), a significantly lower suppression than the reduction after GnRH antagonist treatment in this study. This suggests that the reduction in luteal angiogenesis seen here is most probably a consequence of a decrease in other angiogenic factors in addition to VEGF, and/or by a break-down in endothelial-steroidogenic cell interactions following disruption of lutein cell morphology as caused by treatment. The reduction in local progesterone concentration may also act to reduce angiogenesis. Progesterone is thought to have a local action in the peri-ovulatory follicle to regulate expression of factors such as

matrix metalloproteinase-1 and its tissue inhibitor (Chaffin and Stouffer, 1999), implying a role in angiogenesis in the early corpus luteum.

The current results establish that the intense angiogenesis associated with the formation of the corpus luteum is necessary for normal luteal function, and is almost exclusively dependent upon normal gonadotropin support. The failure of any apparent effect on endothelial cell area may be a result of the methods used to quantify endothelial cell staining which do not consider the shrinkage of tissue after treatment. The ongoing angiogenesis in the mid-luteal phase appears not to be dependent on gonadotropin support, although this may be explained by the increased proliferation of non-endothelial cells. However, this study demonstrates that luteal function in the mid-luteal phase is completely dependent on the luteotropic action of LH as plasma progesterone levels were reduced by 95%.

Chapter 5

The Effect of the Angiogenesis Inhibitor TNP-470 on Luteal Establishment and Function in the Primate

5.1 Introduction

The corpus luteum is essential for the establishment of pregnancy through the production of progesterone from the lutein cells. In the primate, intense angiogenesis occurs during early luteal development (Chapter 3; Christenson and Stouffer, 1996b; Rodger *et al.*, 1997; Gaytan *et al.*, 1998; Dickson and Fraser, 2000) and it is believed that this angiogenesis is critical for transport of hormonal precursors of progesterone to, and progesterone from, the lutein cells (Redmer and Reynolds, 1996). The angiogenesis inhibitor, TNP-470, is a synthetic analogue of fumagillin which has been shown to inhibit endothelial cell proliferation, migration and capillary-like tube formation with a minimal effect on the growth of non-endothelial cells (reviewed by Fan *et al.*, 1995). Studies have shown that TNP-470 acts directly on endothelial cells to inhibit growth-factor induced DNA synthesis, and inhibit activation of cyclin-dependent kinases and phosphorylation of retinoblastoma gene product (Abe *et al.*, 1994). It has been suggested that the corpus luteum could be a target for fertility regulation by virtue of its susceptibility to anti-angiogenic agents (Klauber *et al.*, 1997). The importance of angiogenesis in the establishment of the mouse corpus luteum has been shown by studies in which TNP-470 inhibited luteal development and prevented pregnancy by interfering with the process of decidualisation and placental and yolk sac formation (Klauber *et al.*, 1997). However, the mechanisms which regulate luteal function in rodents and primates are markedly different, and in the non-fertile cycle of the rodent, the corpus luteum is active for less than a day, while that of many primates is functional for 2 weeks prior to its regression (Behrman *et al.*, 1993). The aim of this study was to investigate the effects of TNP-470 on the primate corpus luteum. The information gleaned from this primate model should be useful to the projected clinical use of this compound.

The study was designed to investigate the effects of TNP-470 on angiogenesis at the time of transformation of the preovulatory follicle into the functional corpus luteum. We investigated the effects of TNP-470 in the marmoset monkey in which we have built up considerable information on the cellular and molecular control of luteal function, and established the temporal relationship between angiogenesis and establishment of the microvascular tree (e.g. Chapter 3; Young *et al.*, 1997; Duncan *et al.*, 1998b; Fraser *et al.*, 1998; Fraser *et al.*, 1999a; Fraser *et al.*, 1999b; Dickson and Fraser, 2000; Fraser *et al.*, 2000). The

establishment and function of the corpus luteum was determined by measuring circulating progesterone concentrations. Cellular responses were studied in the marmoset by determining the number of mitotic cells, following BrdU incorporation, and by examining the establishment of the microvascular network using von Willebrand factor staining to identify endothelial cells.

5.2 Materials and Methods

5.2.1 Animals and treatments

Marmoset monkeys (*Calithrix jacchus*) were housed as described previously (Chapter 2) and experiments carried out in accordance with the Animals (Scientific Procedures) Act, 1986. Blood samples were collected 3 times per week by femoral venepuncture without anaesthesia to confirm normal ovulatory cycles. Criteria for the occurrence of ovulation and normal luteal phase length (18-22 days) were based on determination of plasma progesterone concentrations as described previously (Chapter 2). To synchronise timing of ovulation during the treatment cycle, eight animals were treated with 1μg prostaglandin $F2_\alpha$ analogue i.m., during the mid- to late luteal phase of the pre-treatment cycle to induce luteolysis. Four marmosets were treated with TNP-470 (*O*-chloroacetylcarbamoyl fumagillol, also known as AGM-1470) starting 11 days post-prostaglandin, the day of anticipated ovulation, at a dose of 18 mg/kg/day (equivalent to 120mg/m^2), by slow i.v. injection. This treatment was repeated for a further 9 days. Four controls were treated with vehicle following the same schedule.

On day 10 after commencement of TNP-470, each marmoset received by slow i.v. infusion, 20mg BrdU in saline. One hour later, the animals were sedated and euthanased as described previously (Chapter 2). Ovaries were removed rapidly, weighed, fixed immediately in 4% paraformaldehyde for 24h and embedded in paraffin as described in Chapter 2. A small piece of corpus luteum was fixed in 3% glutaraldehyde in 0.1M cacodylate buffer, pH 7.3, for araldite-resin embedding and toluidine blue analysis as described previously (Chapter 4).

5.2.2 Immunocytochemistry and quantification

Proliferating endothelial cells were visualised in ovarian sections using a mouse monoclonal antibody to BrdU as previously described (Chapter 3). Cell proliferation was assessed by counting the number of BrdU positive cells in six randomly chosen fields per corpus luteum and expressed as a mean percentage of the total cells in these fields. Differences between groups were determined using a two tailed, unpaired t test, $p<0.05$ being taken as the level of significance.

Localisation of von Willebrand factor as a marker for endothelial cells was determined by immunocytochemistry as described in Chapter 2. These sections were not counterstained, so that quantitative image analysis could be performed. von Willebrand factor immunostaining was quantified using the Image Pro-Plus 3.0 image analysis programme. Sections were examined at 400x magnification. The image was converted to grey scale and the area of dark objects on a white background was counted. For each corpus luteum, six randomly chosen areas, each of 27860 μm^2 were analysed using the x40 lens, and their mean taken as being representative for that animal. Differences between groups were determined using a two tailed, unpaired t test, $p<0.05$ being taken as the level of significance. Plasma progesterone results were analysed using a repeated measures ANOVA with Fisher's PLSD post-hoc test at 5% significance.

5.3 Results

BrdU staining indicating proliferating cells was readily observed in all corpora lutea from control and treated marmosets (Fig. 5.1a-b). The Proliferation Index showed there was no significant difference between the groups (Fig. 5.1c). The development of the microvasculature of the corpus luteum was confirmed in the control marmosets by an extensive network of microvessel and capillary staining for von Willebrand factor and this was also evident in the TNP-470 treated animals (Fig. 5.1d-e). Quantification of von Willebrand factor immunostaining showed no significant difference associated with treatment (Fig. 5.1f).

Examination of toluidine blue stained sections revealed there was no apparent effect of TNP-470 treatment on lutein cell morphology. In both control (Fig. 5.1g) and treated (Fig. 5.1h) sections steroidogenic cells had large spherical or polyhedral nuclei and abundant cytoplasm; endothelial cells, with elongated nuclei, little cytoplasm and in some cases association with obvious blood vessels, were prevalent; suggesting these were normal healthy corpora lutea. There was no significant difference in plasma progesterone concentrations in control and TNP-470 treated animals (Fig 5.2).

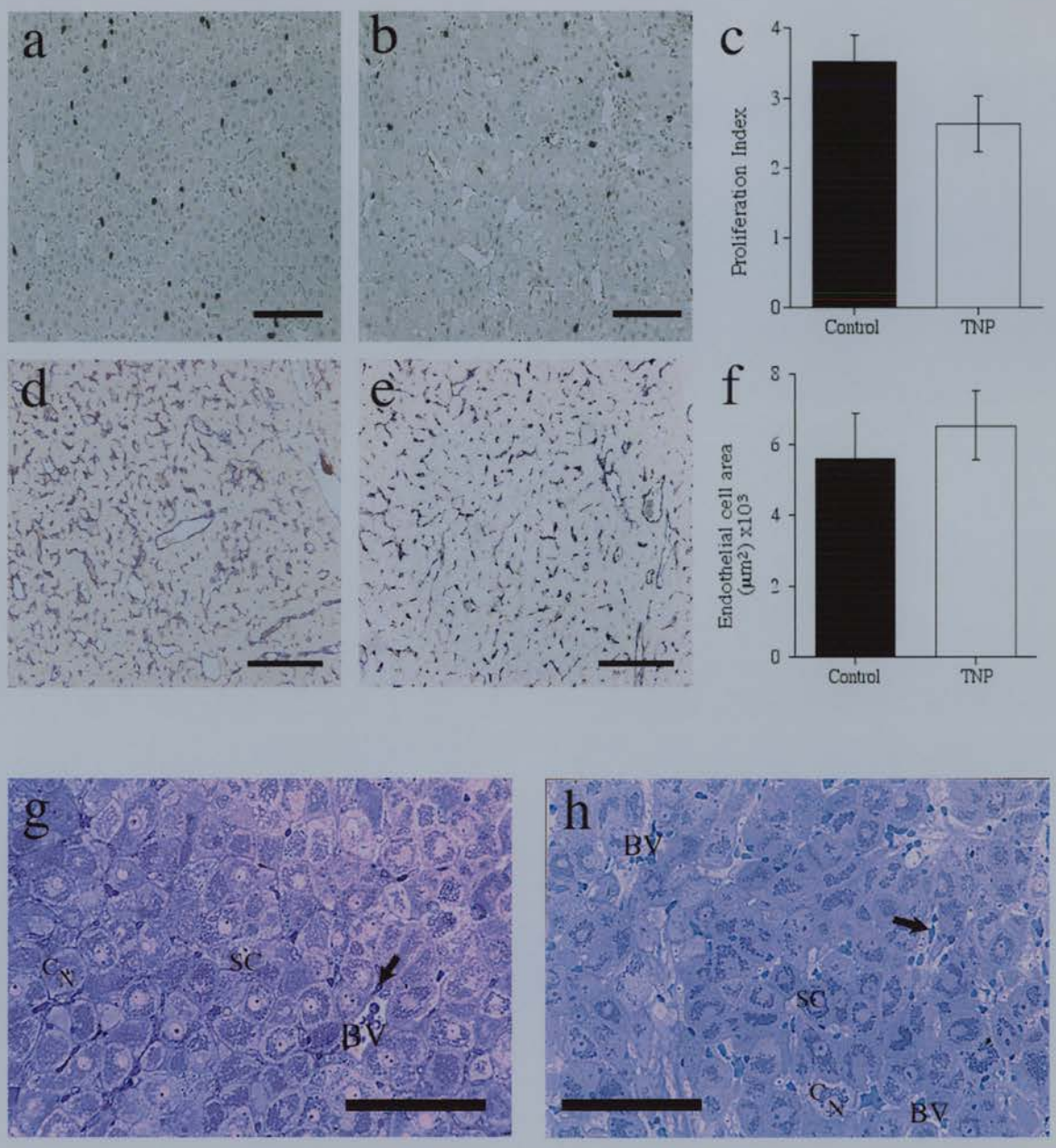

Figure 5.1 Effect of TNP-470 on endothelial cell proliferation, endothelial cell area and lutein cell morphology

BrdU incorporation, von Willebrand factor immunostaining and toluidine blue staining in corpora lutea from control and TNP-470 treated marmosets. (a-b) Low power micrographs showing the general distribution of BrdU staining (dark nuclei) in a control, and a TNP-470 treated corpus luteum, respectively. (c) The proliferation index in corpora lutea from control (closed bar) and TNP-470 treated (open bar) animals. (d-e) von Willebrand factor localisation in the corpus luteum of a control and a TNP-470 treated corpus luteum. (f) Quantification of von Willebrand factor immunostaining in control (closed bar) and TNP-470 treated (open bar) marmoset corpora lutea. (g-h) Toluidine blue stained sections from a control and a treated corpus luteum. Note the presence of large healthy steroidogenic cells (SC) with central round nuclei (N) and abundant cytoplasm (C), and endothelial cells (arrow heads) and luminal blood vessels (arrows) in both control sections and after treatment. Data are means ± SEM. Scale bars = 100µm.

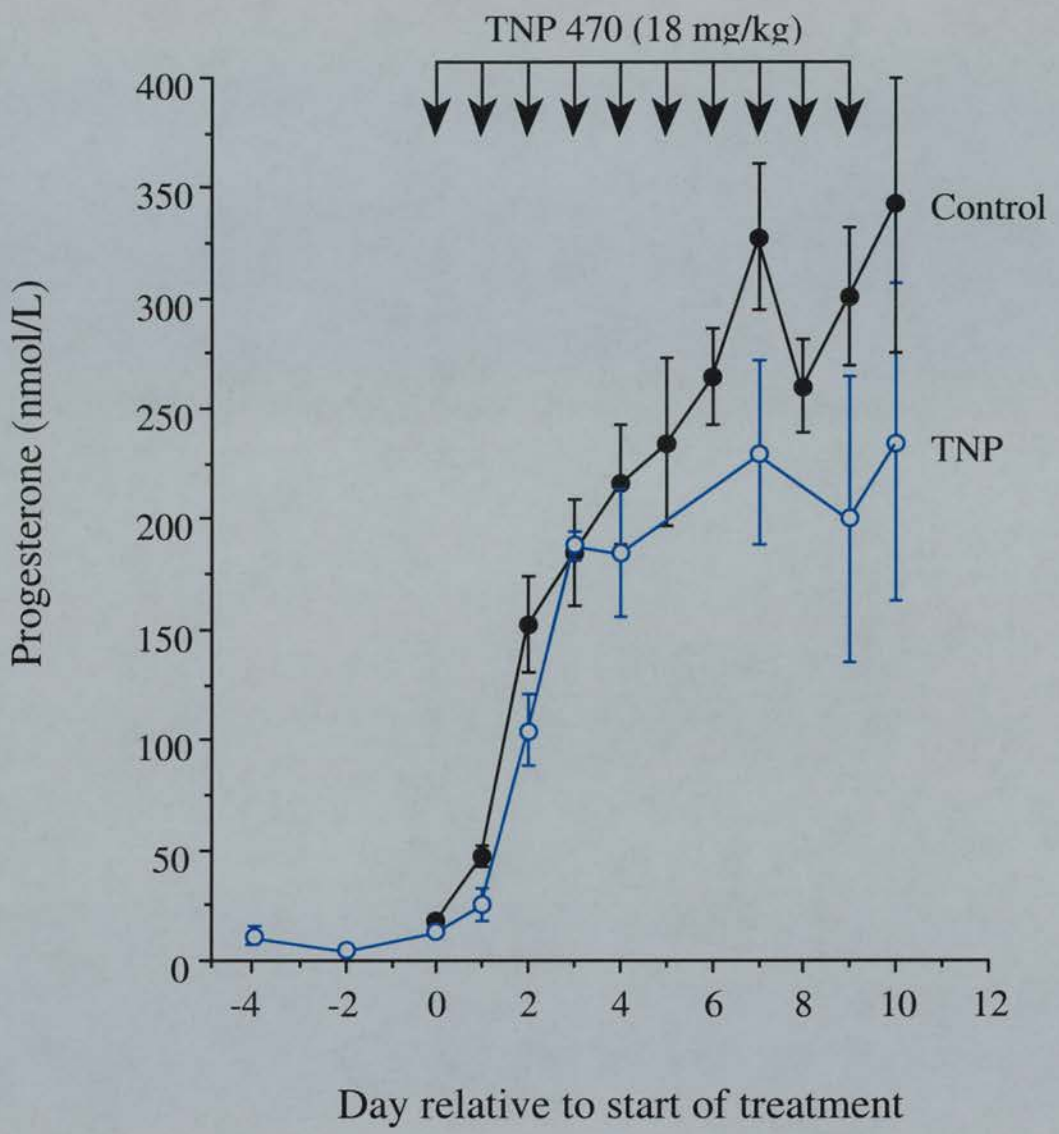

Figure 5.2 Plasma progesterone concentrations in control and TNP-470 treated animals

Plasma progesterone concentrations in control marmosets (closed plot symbols) and in those treated with TNP-470 (open plot symbols) starting on the day of expected ovulation (n=4 per group). Values are means ± SEM.

5.4 Discussion

The results show that treatment with TNP-470 had little or no detectable effect on the development and function of the marmoset corpus luteum. The experiment was designed to target the intense angiogenesis which occurs in the corpus luteum during the early stages of development (Chapter 3; Dickson and Fraser, 2000). Accordingly, treatment was started at the time of predicted ovulation and covered the period of the early luteal phase to the mid-luteal phase. These studies allowed the examination of its potential consequences on cell proliferation, the luteal vasculature and luteal function. As expected, BrdU incorporation demonstrated a moderate level of proliferation of endothelial cells during the mid-luteal phase and this was unaffected by treatment with TNP-470. Furthermore, staining for von Willebrand factor illustrated the establishment of the luteal vascular tree despite treatment with the putative angiogenesis inhibitor. The morphology of lutein cells remained normal after treatment and progesterone secretion by these cells was not impaired. Collectively, these results suggest that TNP-470 does not have negative effects on the structure and function of the normal corpus luteum of the marmoset, in contrast to the findings in the mouse (Klauber *et al.*, 1997). At this early stage of experiments to specifically inhibit angiogenesis in the primate corpus luteum, we were forced to conclude that the differences between the present results and those in the mouse may reflect inter-species variance, perhaps because of the presence of compensating mechanisms in primates and not rodents, and/or differential susceptibility to the anti-angiogenic effect of TNP-470.

The latter possibility could arise from the dose of TNP-470 employed in the present study being insufficient to prevent luteal angiogenesis, or the route of administration being suboptimal. The clinical dose of TNP-470 is 60mg/m^2 administered by 1h i.v. infusion three times per week (Dezube *et al.*, 1998). Studies in the mouse employed the s.c. route at a dose of 30mg/kg every second day. The marmosets in the present study were treated with 18mg/kg daily, so approaching the murine dose. It should be noted that TNP-470 is metabolised very rapidly and that its pharmacodynamic properties are incompletely understood (Cretton-Scott *et al.*, 1996). Thus, differences in the pattern of exposure to the drug may result from the different routes of administration. However, at present, a preparation of TNP-470

that can be administered by the s.c. route to larger animals and humans is not available.

This was the first report of an attempt to block angiogenesis in the primate corpus luteum with a specific angiogenic inhibitor. Although inhibitory effects were not observed, the approach used to study angiogenesis was of value to future experiments on the effects of angiogenesis inhibitors, such as anti-VEGF treatment (Chapter 6), on luteal function in the marmoset.

Chapter 6

Suppression of Luteal Angiogenesis in the Primate after Neutralisation of Vascular Endothelial Growth Factor

6.1 Introduction

In Chapter 5, it was demonstrated that TNP-470 failed to affect luteal function in the marmoset which emphasises the need for caution when extrapolating results from the rodent in which this angiogenesis inhibitor prevented pregnancy (Klauber *et al.*, 1997). Thus it is of major importance to investigate the regulation of angiogenesis specifically in the primate corpus luteum. Chapter 4 demonstrated that luteal function and angiogenesis was driven by pituitary gonadotropins. However, this treatment resulted in lutein cell death and prevented the action of all locally produced growth factors. To identify the factors involved in the regulation of luteal angiogenesis potential factors should be specifically targeted and the consequential effects on luteal angiogenesis investigated. The angiogenic process is regulated by a number of growth factors, degradation of the extracellular matrix and cell-cell interactions. VEGF is highly expressed in the early and mid-luteal phases of the primate corpus luteum (Chapter 3). It is evident therefore, that the role of VEGF in the primate corpus luteum should be addressed.

This study examined the potential role of VEGF in regulating luteal angiogenesis by specific neutralisation of this potent endothelial cell mitogen, using a monoclonal antibody in three separate treatment regimes (Figure 2.1). We investigated whether it was possible to prevent luteal angiogenesis by administration of anti-VEGF treatment on the day of ovulation for 3 days (regime 1), or after chronic treatment for 10 days after ovulation (regime 2). We also analysed if it was possible to intervene in the already established angiogenic process by administering anti-VEGF treatment for 3 days in the mid-luteal phase (regime 3). The effects of VEGF withdrawal on luteal angiogenesis were examined by quantifying endothelial cell proliferation and establishment of the microvascular tree. It was also of relevance to examine the effect of such VEGF inhibition on VEGF expression itself.

Previous studies on the effects of withdrawal of VEGF in other angiogenic dependent systems report the requirement on VEGF for the survival of immature endothelial cells. For example in human prostate cancer the acute loss of VEGF, as a result of androgen ablation therapy, leads to selective apoptosis of endothelial cells in vessels devoid of periendothelial support cells (Benjamin *et al.*, 1999). To investigate whether the recently formed endothelial cells of the primate corpus

luteum may be susceptible to withdrawal of VEGF we determined the incidence of apoptosis after acute anti-VEGF treatment in the mid-luteal phase (regime 3).

There is evidence to suggest that the recruitment of periendothelial support cells for vessel stabilisation is dependent on VEGF (Nomura *et al.*, 1995; Yamagishi *et al.*, 1999). To assess the relationship between pericyte coverage and VEGF bioactivity in the early and mid- corpus luteum, the area of pericyte coverage in control corpora lutea and after anti-VEGF treatment was quantified. Finally, to examine the effect of VEGF inhibition on endometrial angiogenesis, endothelial cell proliferation in the vascularised endometrial stroma was measured.

6.2 Materials and Methods

6.2.1 VEGF antibody

Mouse monoclonal anti-VEGF, VG76e, was obtained from Dr Roy Bicknell (ICRF, Cambridge). It was raised by immunisation with recombinant human VEGF-189. Using recombinant proteins on western blots, it was demonstrated that VG76e recognises the 121, 165 and 189 isoforms of VEGF-A. VG76e was shown to be a blocking antibody *in vitro* by its inhibition of the growth stimulatory activity of VEGF on human umbilical vein endothelial cells (HUVEC) (Fraser *et al.*, 2000).

6.2.2 Animals

Common marmoset monkeys *(Callithrix jacchus)* were housed in cages as described previously (Chapter 2). Adult females with a body weight of approximately 350g, with regular ovulatory cycles, were housed together with a younger sister or prepubertal female. Blood samples were collected three times per week by femoral venipuncture without anaesthesia and plasma was stored at -20°C until required for progesterone assay (Chapter 2) to confirm normal ovulatory cycles. Criteria for the occurrence of ovulation and normal luteal phase length (18-22 days) were based on determination of plasma progesterone concentrations as described previously (Chapter 2).

6.2.3 Treatment

The experiments were carried out in accordance with the Animals (Scientific Procedures) Act, 1986. The timing of ovulation was synchronised during the pre-treatment cycle as described previously (Chapter 2). Four marmosets were treated with VEGF antibody at a concentration of 2.7 mg/ml starting on the day of anticipated ovulation (luteal phase day 0), at a dose of 2 mg followed by 1 mg on days 1 and 2 (regime 1). Four controls were treated with the same dose of mouse gamma globulin (Sigma) following the same schedule. Treatment was extended to the mid-luteal phase in a further 6 marmosets; additional injections of 1mg anti-VEGF were administered on days 3, 5, 7 and 9, with six animals receiving mouse gamma globulin as controls (regime 2). Another four animals were treated with 2mg VEGF monoclonal antibody on luteal day 7 and 1mg on luteal days 8 and 9 (regime 3), and four control animals were given equivalent doses of mouse gamma globulin. All treatments were by slow i.v. injection. The regimes of administration of treatment are depicted in Figure 2.1.

Ovaries were obtained the day after final treatment, luteal day 3 or 10, after the animals had received 20mg BrdU in saline by slow i.v. injection. One hour later, the animals were sedated and ovaries and uteri were removed immediately and fixed in 4% paraformaldehyde as previously described (Chapter 2). It was presumed that an effect on lutein cell morphology would most likely be seen after treatment with anti-VEGF for 10 days (regime 2), so a small portion of a representative corpus luteum was placed in 3% glutaraldehyde in 0.1M cacodylate buffer, pH 7.3, for araldite-resin embedding and toluidine blue analysis as described in Chapter 4. When the mid-luteal group were examined, it was apparent that the density of the lutein cells had increased following treatment. In order to quantify this change, paraffin sections were stained with haematoxylin and eosin (Chapter 3) and lutein cell density in 12 corpora lutea per group, determined by Dr. Christine Wulff.

The establishment and function of the corpus luteum were determined by measuring plasma progesterone concentrations in daily blood plasma samples as described previously (Chapter 2). Only marmosets in which treatment was started at the time of presumptive ovulation (plasma progesterone having reached >30nmol/L and found retrospectively to be sustained at luteal phase values) were included in the study. Analysis of differences in plasma progesterone concentrations was performed

by repeated measures analysis of variance followed by a post-hoc Fisher's Protected Least Significant Difference test, $P<0.05$ taken as the level of significance.

6.2.4 Immunocytochemistry, *in situ* hybridisation, *in situ* 3' end labelling and quantification

Cellular responses were studied: 1) by determining the number of mitotic cells, following BrdU administration as a marker; 2) by examining the establishment of the microvascular network using von Willebrand factor and/or CD31 staining to identify endothelial cells; 3) by quantifying pericyte coverage using α-SMA as a marker; and 4) by analysing the expression of VEGF mRNA and protein in lutein cells by immunocytochemistry. Uterine sections were dual-stained for CD31 and BrdU to assess endometrial angiogenic activity.

Methods for all immunocytochemical procedures and analyses not outlined here were described in detail in Chapter 3. For von Willebrand factor, CD31 and α–SMA immunostaining, a minimum of four randomly chosen areas per corpus luteum were quantified using the Image Pro-Plus 3.0 image analysis programme, as described previously (Chapter 2). For early luteal treated and control sections areas of $1.3x10^5$ μm^2 (using x20 lens), and for the larger mid-luteal treated and control sections areas of $1.3x10^5$ μm^2 (using x10 lens) were studied; in total these areas covered approximately two thirds of each corpus luteum. Uterine sections stained with BrdU and CD31 were analysed at x400 magnification and a minimum of 10 fields of view quantified per section. Uterine endometrium was located under the light microscope, the vasculature of which was restricted to the stroma, and the number of cells co-localising BrdU and CD31 per field, manually counted. The mean of all fields of view for one section was taken as representative for that animal.

In situ hybridisation for VEGF-A was performed using a riboprobe synthesised from plasmid inserted VEGF-A cDNA from Dr Charnock Jones (sequence details are documented in Appendix A), and following the same methodology as described in Chapter 2. Quantification was carried out using the Image Pro-Plus 3.0 image analysis as described in Chapter 4. *In situ* 3' end labelling was performed using the protocol described in detail in Chapter 2. An index of cell death in the corpus luteum was obtained by manually counting the number of positively stained cells per luteal section, and the mean per animal calculated. A

statistical comparison of the size of each sectioned corpus luteum in treated and control groups was made using a standard two-tailed, unpaired t-test. The size of each corpus luteum from treated and control groups was not significantly different.

Following quantification of all parameters, differences between treated and control groups were determined using separate two-tailed unpaired t tests, $P<0.05$ being taken as the level of significance. Plasma progesterone results were analysed using a repeated measures ANOVA with Fisher's PLSD post-hoc test at 5% significance.

6.3 Results

6.3.1 Regime 1: Cell proliferation, endothelial cell area and periendothelial support cell coverage

Treatment with anti-VEGF during the early luteal phase did not prevent the formation of clearly identifiable corpora lutea, and ovarian sections revealed the presence of recently formed corpora lutea in all control and treated marmosets. Proliferation was high within corpora lutea from control marmosets (Fig. 6.1a) and was markedly reduced by anti-VEGF treatment (Fig. 6.1b), as confirmed by the decreased proliferation index (Fig. 6.1c). von Willebrand factor immunostaining demonstrated the initiation of development of the microvasculature in control corpora lutea (Fig. 6.1d) but although there was an indication of reduced capillary number associated with anti-VEGF treatment (Fig. 6.1e), quantification of von Willebrand factor immunostaining showed no significant difference at this time (Fig. 6.1f). Sections stained with a second endothelial cell marker, CD31, also revealed similar staining in control (Fig. 6.1g) and treated (Fig. 6.1h) corpora lutea. Quantification of CD31 staining also showed that there was no significant difference in endothelial cell area after treatment in the early luteal phase (Fig. 6.1i).

The incidence of periendothelial support cells was high in corpora lutea from early luteal control animals, associated with mainly small capillary endothelial cells, (Fig. 6.1j) and was markedly reduced by anti-VEGF treatment (Fig. 6.1k), as confirmed by a decrease in pericyte area (Fig. 6.1l).

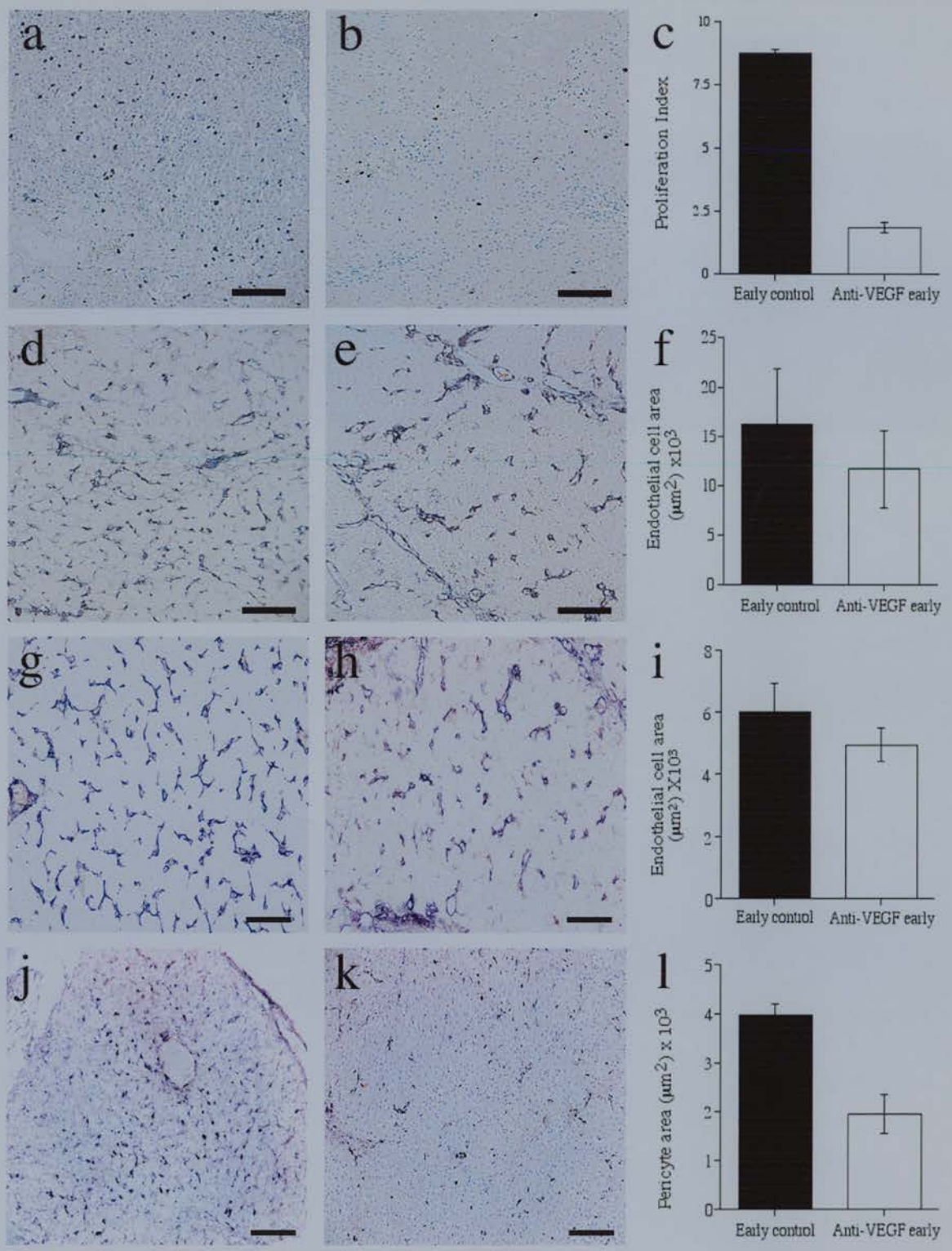

Figure 6.1 Effects of anti-VEGF treatment in the early luteal phase (regime 1) on BrdU incorporation, endothelial cell area, and pericyte recruitment

Low power photomicrographs of early luteal phase marmoset corpora lutea showing the general distribution of BrdU incorporation (dark-staining nuclei) into endothelial cells of microvessels and capillaries in (a) a control corpus luteum showing high incorporation and (b) reduced incorporation following anti-VEGF treatment. (c) The proliferation index in corpora lutea from early luteal phase control (closed bar) and anti-VEGF treated (open bar) marmoset corpora lutea. Values from treated animals were significantly lower ($P<0.01$) than in controls. (d) and (e) von Willebrand factor localisation (dark staining) in the endothelial cells of microvessels and capillaries of corpora lutea from control and anti-VEGF treated marmosets, respectively. (f) Quantification of von Willebrand factor immunostaining in control (closed bar) and anti-VEGF treated (open bar) marmoset corpora lutea. There was no significant difference between the groups. (g) and (h), CD31 (dark staining) in vascular endothelial cells in control and anti-VEGF treated corpora lutea, respectively, and (i) quantification of control (closed bar) and treated (open bar) CD31 immunostaining reveals no significant change in endothelial cell area between groups. (j) High α-SMA immunostaining (dark staining) is present throughout control corpora lutea and (k) is greatly reduced in treated sections. (l) Quantification of α-SMA area shows a significant decrease ($P=0.01$) in staining. Data are means ± SEM. Scale bars = 100μm.

6.3.2 Regime 1: VEGF-A expression

VEGF protein was localised to the cytoplasm of the majority of steroidogenic cells in the early control corpus luteum (Fig. 6.2a). Staining appeared most intense in leading lutein cells, adjacent to the antrum, streaming inwards to form the full corpus luteum, suggesting angiogenic activity in this direction. The pattern and intensity of VEGF immunostaining was similar in treated animals treatment (Fig. 6.2b) to that in controls.

In situ hybridisation with a probe to VEGF-A demonstrated, in dark field micrographs, that VEGF mRNA was arranged in clusters in control (Fig. 6.2c) and anti-VEGF treated (Fig. 6.2d) sections. From bright field microscopy, VEGF mRNA was localised to both nuclei and cytoplasm of lutein cells in control sections (Fig. 6.2e). After treatment, however, clusters appeared more densely located to the nuclei of lutein cells (Fig. 6.2f).

Quantification of VEGF protein expression demonstrated there was no effect of treatment on area of VEGF immunostaining (Fig. 6.3a) or intensity of immunostaining (Fig. 6.3b). Similarly, measurement of grain area (Fig. 6.4a) and density (Fig. 6.4b) after *in situ* hybridisation revealed there were no effects of anti-VEGF treatment in the early luteal phase on expression of VEGF mRNA, although some dark field micrographs suggested otherwise (Fig. 6.2d).

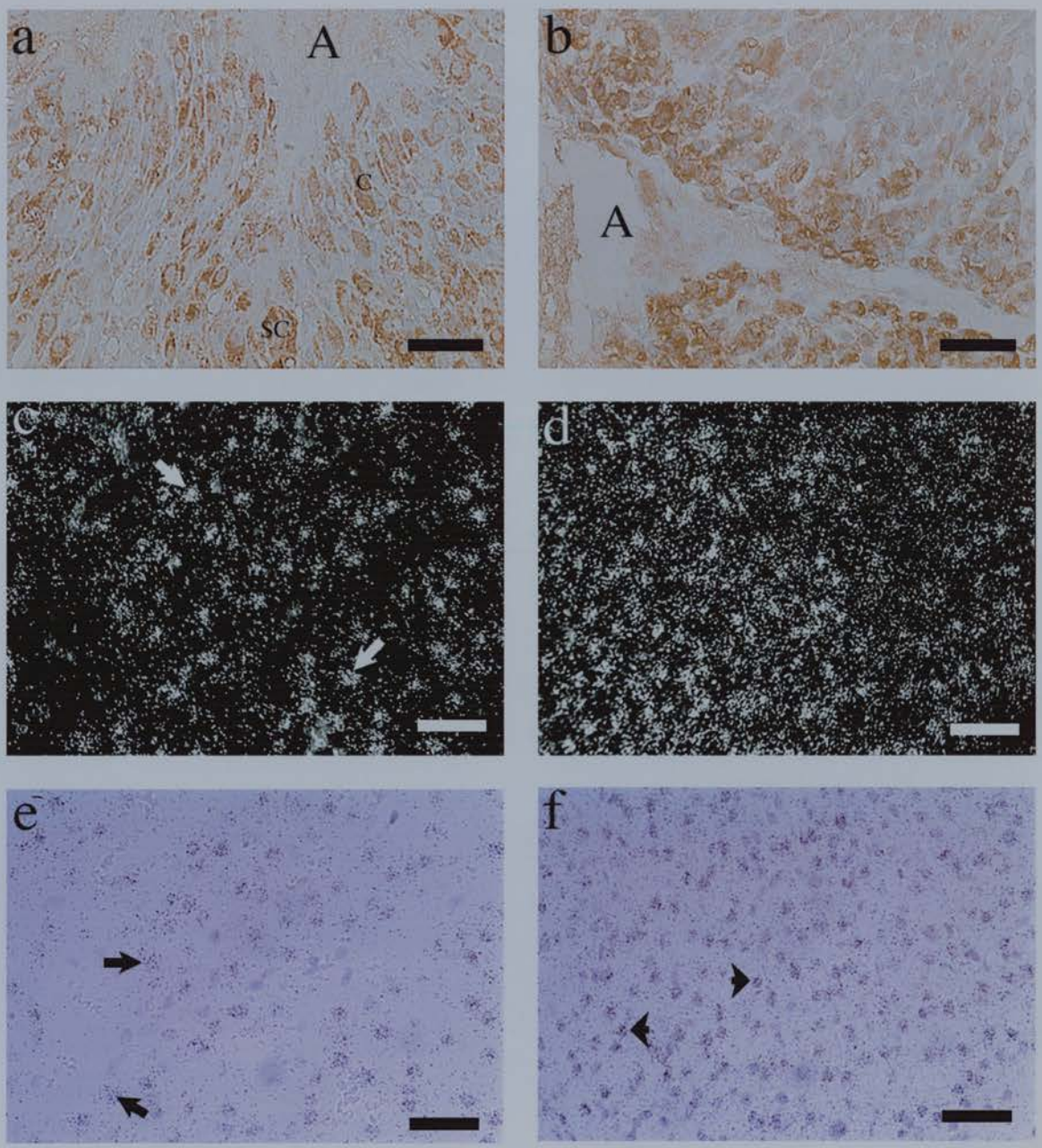

Figure 6.2 VEGF-A expression in control sections and after anti-VEGF treatment in the early luteal phase (regime 1)

Immunolocalisation of VEGF protein (brown staining) in (a) early luteal control sections and (b) after anti-VEGF treatment. VEGF is localised to the cytoplasm (C) of steroidogenic cells (SC), most intense staining is found in those lutein cells adjacent to the antrum (A) which is still visible in the early corpus luteum. (c) Dark field micrograph showing location of VEGF mRNA (white grains) in control sections and (d) in anti-VEGF treated sections. VEGF mRNA is located in clusters (white arrows). (e) Light field micrographs of the same control section reveal expression is associated with nuclei and cytoplasm of lutein cells as indicated by the black arrows. (f) After treatment VEGF mRNA appears to be more densely expressed, exclusively in the nuclei of lutein cells (black arrow heads). Scale bars = 50μm.

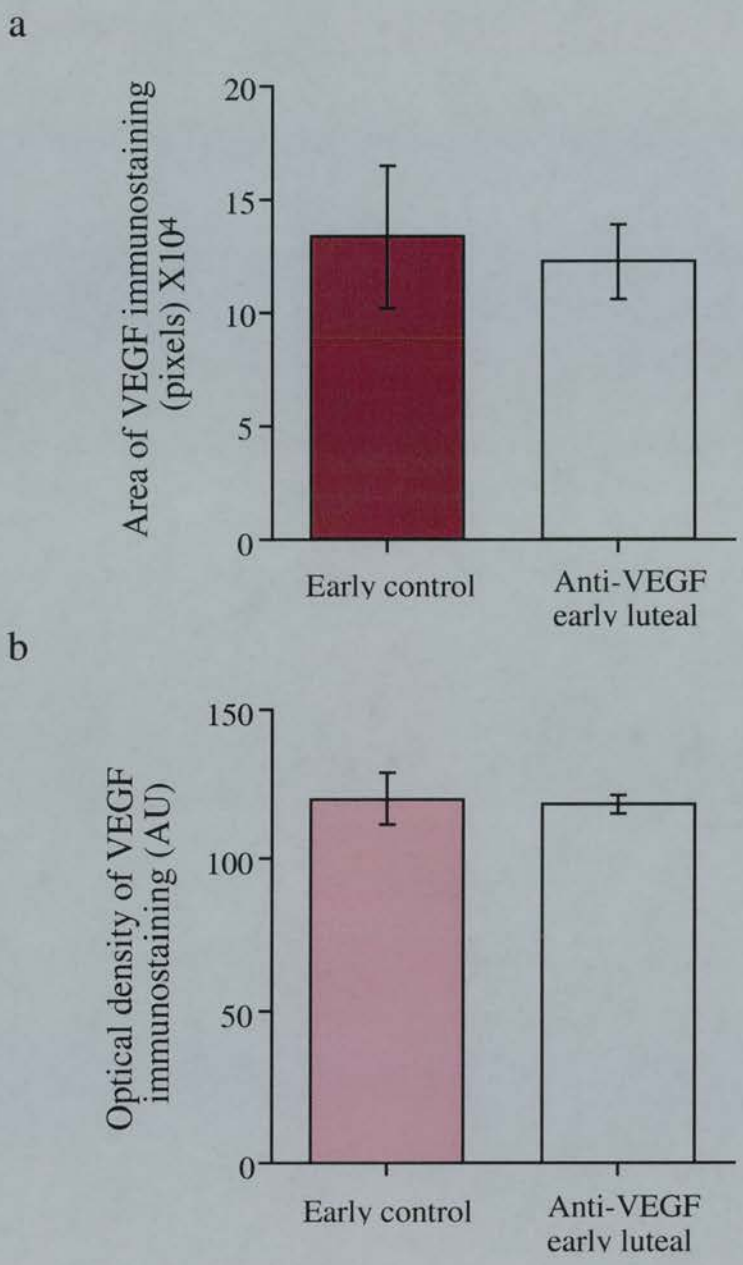

Figure 6.3 Quantification of VEGF-A immunostaining in controls and after anti-VEGF treatment in the early luteal phase (regime 1)

(a) The area of luteal VEGF immunostaining in controls and anti-VEGF treated animals. There was no significant difference after treatment. (b) Quantification of intensity of VEGF immunostaining, indicating no significant difference in the level of expression by any one cell in treated sections as compared to controls. Values are means ± SEM.

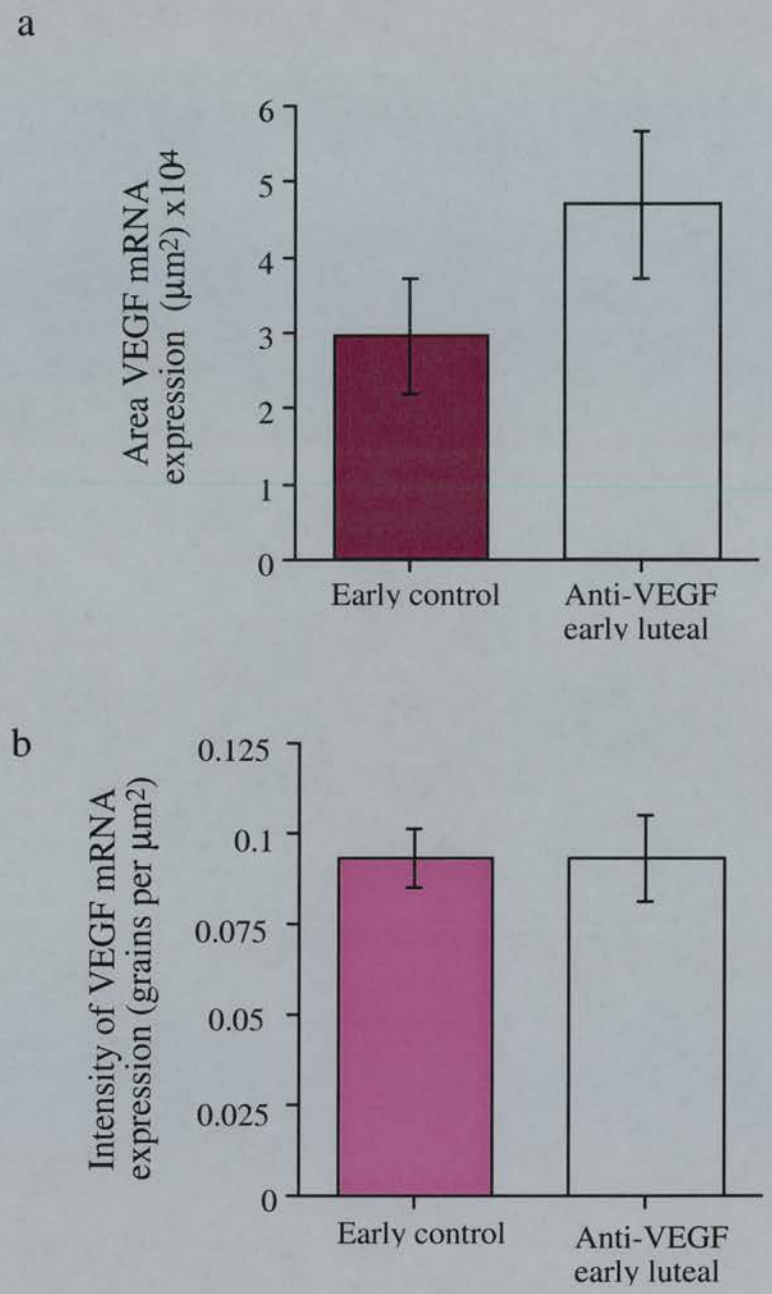

Figure 6.4 Quantification of mRNA for VEGF-A in controls and after anti-VEGF treatment in the early luteal phase

(a) The area of clusters of VEGF mRNA expression in control and treated sections. There was no significant increase in overall expression of VEGF mRNA after anti-VEGF treatment. (b) Quantification of grain density per unit area of luteal tissue in control and treated sections. There was no significant difference of VEGF mRNA expression by any one cell between groups. Values are means ± SEM.

6.3.3 Regime 2: Cell proliferation, endothelial cell area and periendothelial support cell coverage

In the mid-luteal phase group, treatment with anti-VEGF for 10 days from the day of ovulation did not prevent formation of fresh corpora lutea. In corpora lutea from control animals, the numbers of proliferating cells had declined, as expected by this stage of the luteal phase (Fig. 6.5a). Some moderate proliferation was also evident in all corpora lutea from the anti-VEGF treated marmosets (Fig. 6.5b), and the proliferation index showed no significant treatment differences (Fig. 6.5c). However, while in control corpora lutea staining for von Willebrand factor revealed that a fully developed microvasculature had been established (Fig. 6.5d), treatment with anti-VEGF resulted in corpora lutea with a much lower degree of vascularisation and absence of an extensive capillary bed, similar to that observed in the early luteal phase (Fig. 6.5e). Quantification of von Willebrand factor immunostaining showed a marked suppression ($P<0.001$) of endothelial cell area associated with treatment (Fig. 6.5f). Figure 6.5g and h depicts CD31 immunostaining with the second endothelial cell marker, CD31, in control and treated corpora lutea, respectively. Quantification revealed the same effect as seen with staining for von Willebrand factor, demonstrating a significant reduction ($P<0.01$) in endothelial cell area with treatment (Fig. 6.5i).

In control sections, pericytes were mostly found aggregated in rings surrounding luminal vessels (Fig. 6.5j), whereas after anti-VEGF treatment single immunopositive cells were also found distributed through the corpus luteum (Fig. 6.5k). This was confirmed by quantification of pericyte area (Fig. 6.5l) which had increased significantly ($P<0.01$).

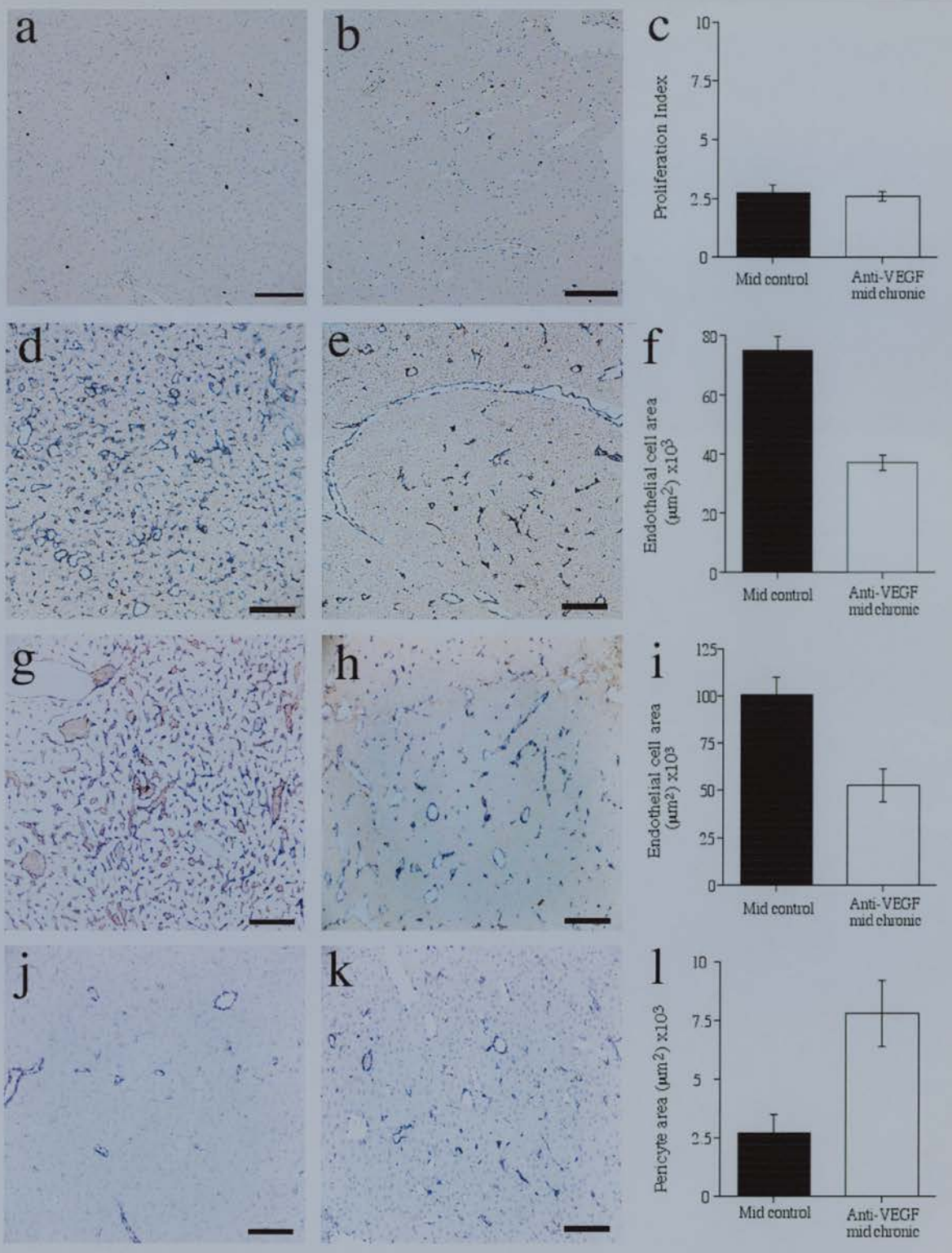

Figure 6.5 Effects of anti-VEGF treatment, for 10 days from the early to the mid-luteal phase (regime 2), on BrdU incorporation, endothelial cell area, and pericyte recruitment

Low power photomicrographs of mid-luteal phase marmoset corpora lutea showing the general distribution of BrdU incorporation (dark-staining nuclei) into endothelial cells of microvessels and capillaries in (a) control and (b) similar incorporation after anti-VEGF treatment. (c) The proliferation index in corpora lutea from mid-luteal phase control (closed bar) and anti-VEGF treated (open bar) marmoset corpora lutea. There was no significant difference between the groups. (d) von Willebrand factor localisation (dark staining) in the endothelial cells of microvessels and capillaries of corpora lutea in a control corpus luteum and (e) reduced staining, especially for incidence of capillary endothelial cells after anti-VEGF treatment. (f) Quantification of von Willebrand factor immunostaining in control (closed bar) and anti-VEGF treated (open bar) marmoset corpora lutea. Values from treated animals were significantly lower ($P<0.001$) than in controls. (g) and (h), CD31 (dark staining) in vascular endothelial cells in control and anti-VEGF treated corpora lutea, respectively, and (i) quantification of control (closed bar) and treated (open bar) CD31 immunostaining which reveals a significant decrease ($P<0.0001$) in endothelial cell area after treatment. (j) Low α-SMA immunostaining (dark staining) aggregated in rings surrounding luminal vessels, is present in control corpora lutea. (k) In treated sections staining is greatly increased, being associated with non-luminal smaller vessels. (l) Quantification of area shows a significant increase ($P=0.04$) in staining. Data are means ± SEM. Scale bars =100 μm.

6.3.4 Regime 2: VEGF-A expression

VEGF protein was localised to the cytoplasm of lutein cells in both mid-luteal control (Fig. 6.6a) and treated (Fig. 6.6b) corpora lutea. Coverage in both control and treated corpora lutea was quite uniform and appeared not to be altered by treatment.

VEGF mRNA was again arranged in clusters in both control (Fig. 6.6c) and treated (Fig. 6.6d) corpora lutea and localised to both the cytoplasm and nuclei of control corpora lutea (Fig. 6.6e) and after treatment (Fig. 6.6f).

Quantification of VEGF immunostaining area (Fig. 6.7a) and intensity (Fig. 6.7b), and mRNA grain area (Fig. 6.8a) and density (Fig. 6.8a) showed there was no effect of treatment on either VEGF protein or VEGF mRNA expression.

6.3.5 Regime 3: Cell proliferation and endothelial cell area

Moderate BrdU incorporation into endothelial cells was observed in control corpora lutea (Fig. 6.9a) but was significantly lowered by anti-VEGF treatment (Fig. 6.9b). This was confirmed by comparing the PI from control and treated groups ($P<0.01$) (Fig. 6.9c). In the control corpus luteum, CD31 immunostaining revealed the establishment of the microvascular tree demonstrated by numerous blood vessels and capillary endothelial cells which were observed in association with each lutein cell (Fig. 6.9d). In the treated animals, the number of capillaries appeared reduced (Fig. 6.9e) and quantitative analysis revealed a significant ($P=0.02$) decrease in endothelial cell area after treatment (Fig. 6.9f).

Again in mid-luteal control sections, pericytes were mostly found aggregated in rings surrounding luminal vessels (Fig. 6.9g), and after anti-VEGF treatment immunopositive cells were also found distributed through the corpus luteum (Fig. 6.9h), as confirmed by quantification of periendothelial support cell area (Fig. 6.9l) where a significant increase with treatment was seen ($P<0.01$).

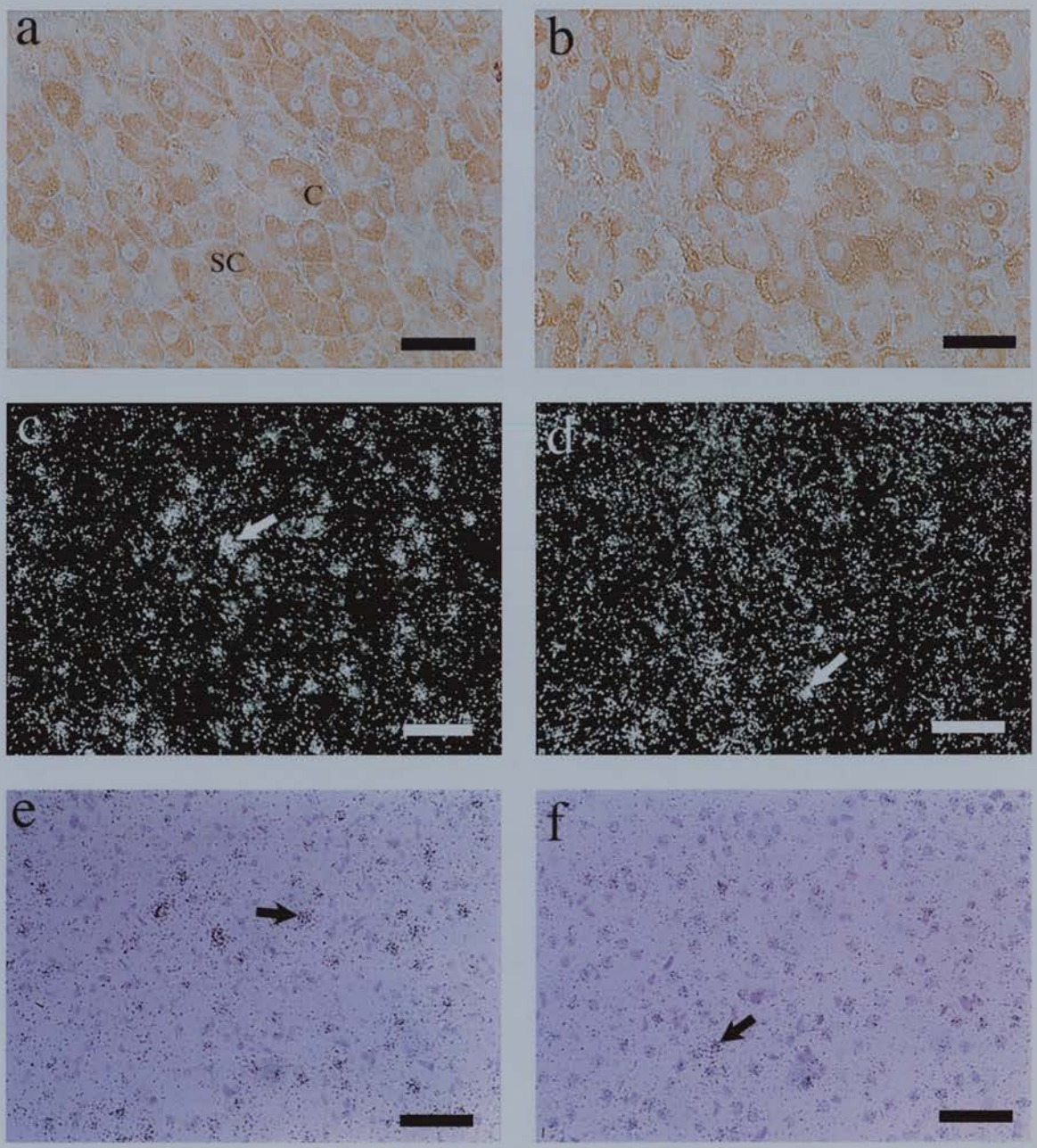

Figure 6.6 VEGF-A expression in control sections and after anti-VEGF treatment from the early luteal to the mid-luteal phase (regime 2)

(a) Immunolocalisation of VEGF protein (brown staining) in early luteal control sections and (b) after anti-VEGF treatment. VEGF is localised to the cytoplasm (C) of most steroidogenic cells (SC) of the mid-luteal phase. (c) Dark field micrograph showing location of VEGF mRNA (white grains) in control sections, and (d) in anti-VEGF treated sections. VEGF mRNA is located in clusters (white arrows). (e) Light field micrographs of the same control and (f) treated sections reveal expression is associated with nuclei and cytoplasm of lutein cells as indicated by the black arrows. Scale bars = 50µm.

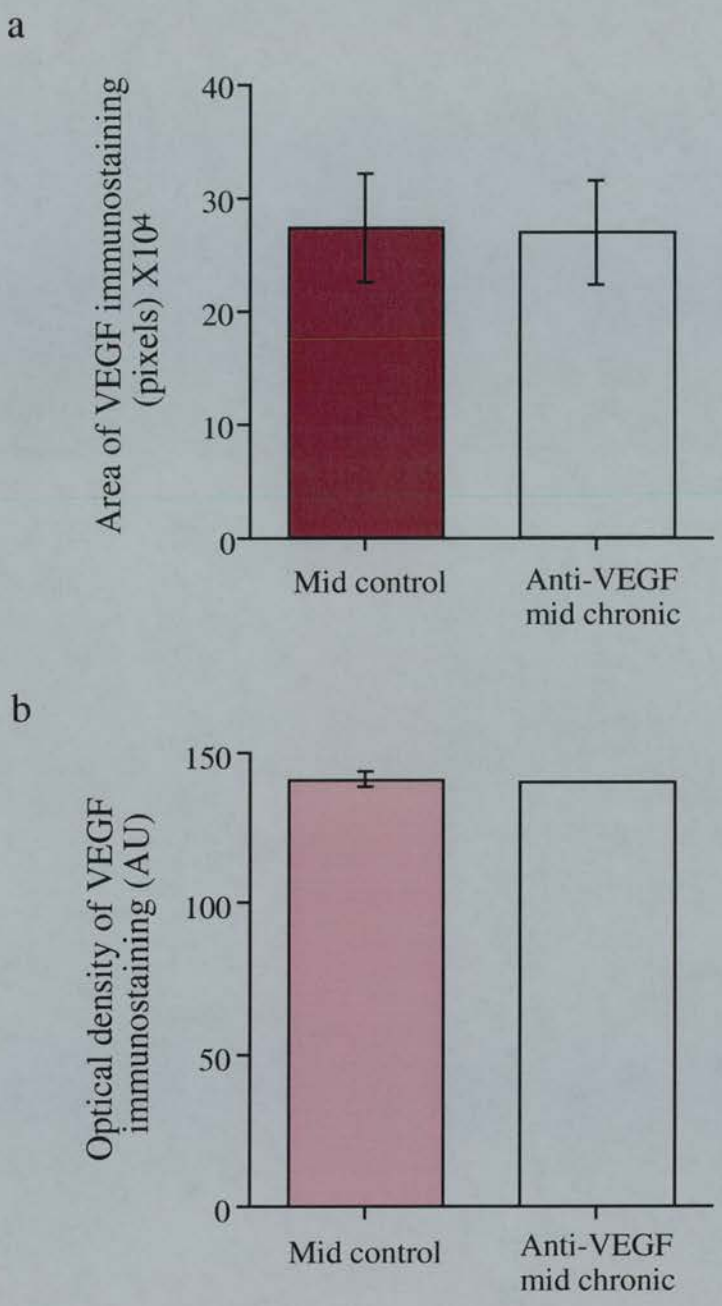

Figure 6.7 Quantification of VEGF-A immunostaining in controls and after anti-VEGF treatment from the early to the mid-luteal phase (regime 2)

(a) Shows the area of luteal VEGF immunostaining in controls and anti-VEGF treated animals. There was no significant difference after treatment. (b) Quantification of intensity of immunostaining, indicating no significant difference in the level of expression by any one cell in treated sections as compared to controls. Values are means ± SEM.

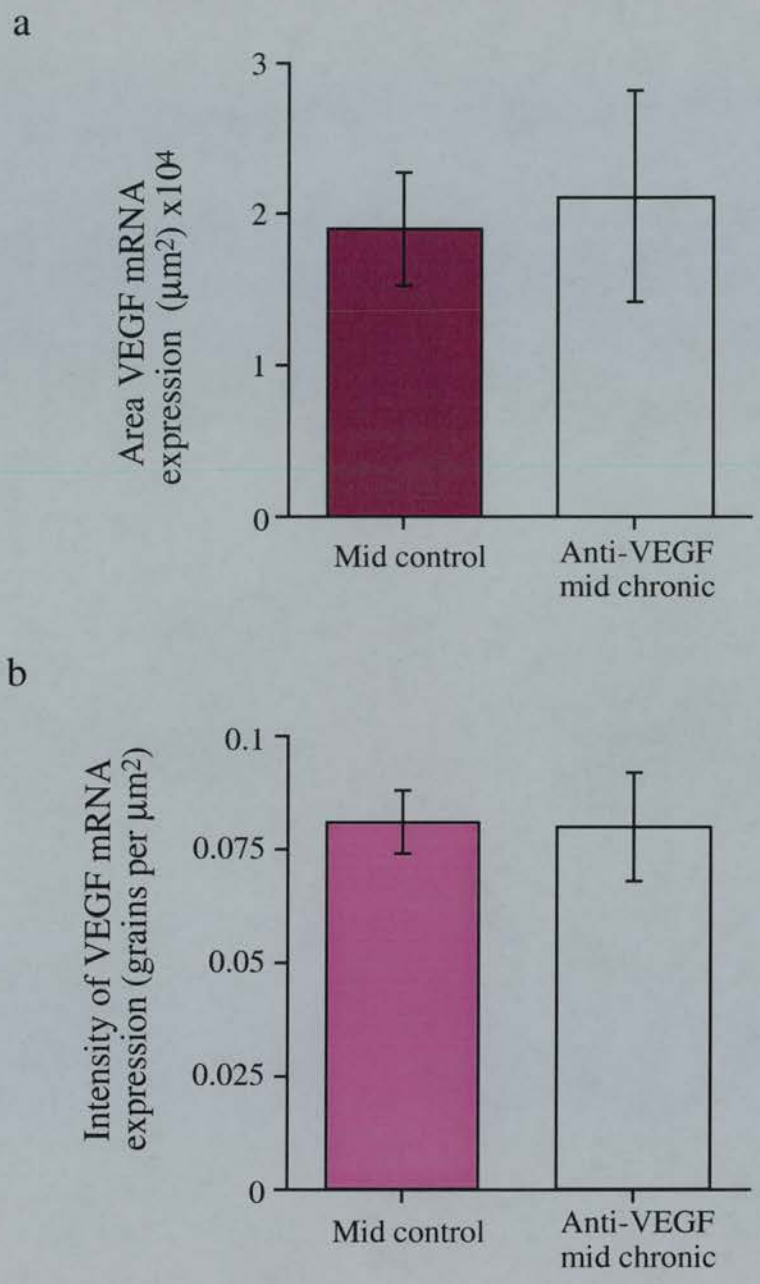

Figure 6.8 Quantification of mRNA for VEGF-A in controls and after anti-VEGF treatment from the early to the mid-luteal phase

(a) The area of clusters of VEGF mRNA expression in control and treated sections. There was no significant increase in overall expression of VEGF mRNA after anti-VEGF treatment. (b) Quantification of grain density per unit area of luteal tissue in control and treated sections. There was no significant difference of VEGF mRNA expression by any one cell between groups. Values are means ± SEM.

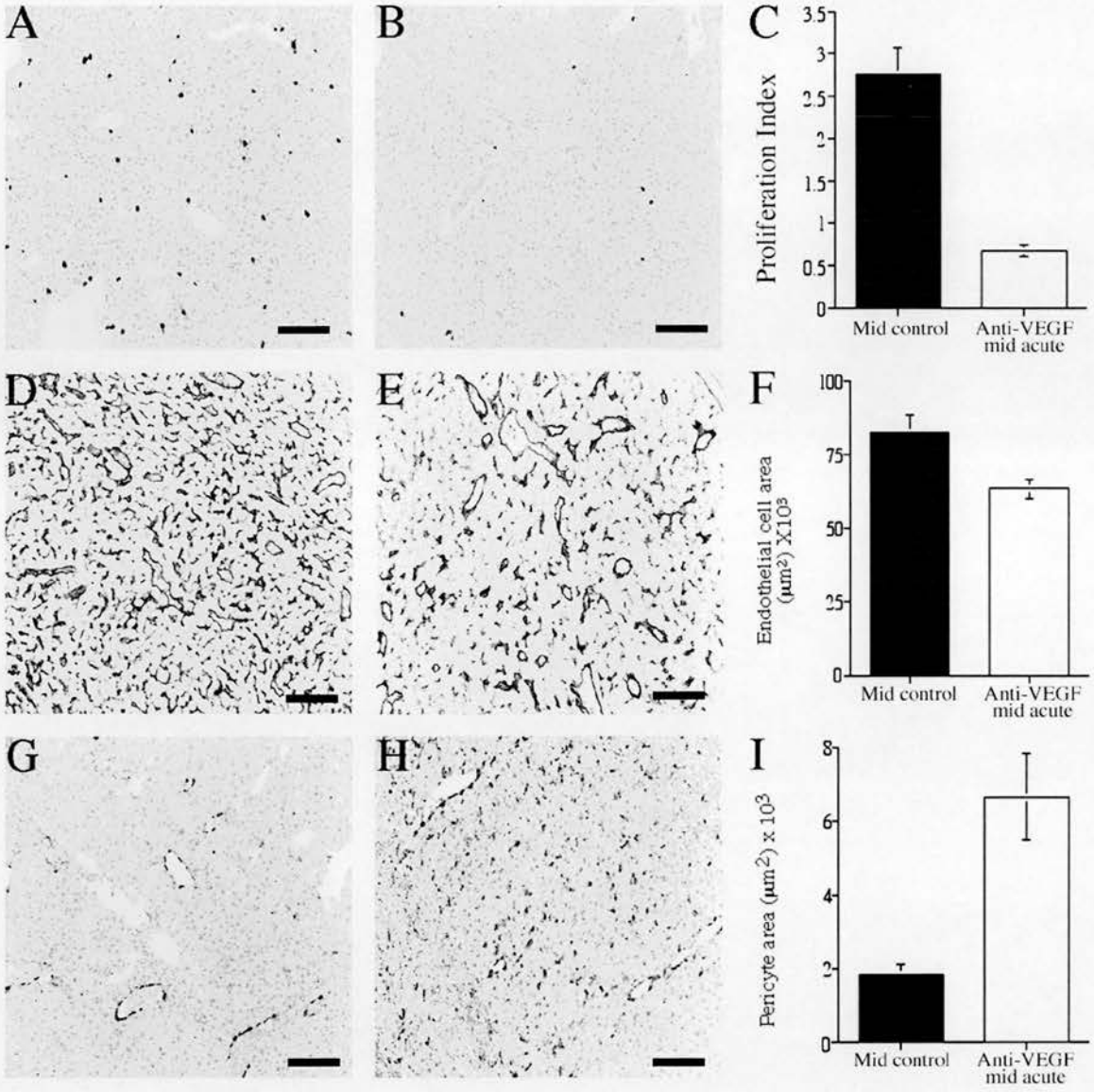

Figure 6.9 Effects of anti-VEGF treatment in the mid-luteal phase (regime 3) on BrdU incorporation, endothelial cell area, and pericyte recruitment

Low power photomicrographs of mid-luteal phase marmoset corpora lutea showing (a) the general distribution of BrdU incorporation (dark-staining nuclei) into endothelial cells of microvessels and capillaries in control and (b) decreased incorporation after anti-VEGF treatment. (c) The proliferation index in corpora lutea from mid-luteal phase control (closed bar) and anti-VEGF treated (open bar) marmoset corpora lutea. There was a significant reduction after treatment ($P<0.01$). (d) von Willebrand factor localisation (dark staining) in the endothelial cells of microvessels and capillaries of corpora lutea in a control corpus luteum and (e) reduced staining, especially for incidence of capillary endothelial cells after anti-VEGF treatment. (f) Quantification of CD31 immunostaining in control (closed bar) and anti-VEGF treated (open bar) marmoset corpora lutea. Values from treated animals were significantly lower ($P=0.02$) than in controls. (g) Low α-SMA immunostaining (dark staining) aggregated in rings surrounding luminal vessels, is present in control corpora lutea. (h) In treated sections staining is greatly increased, also being associated with non-luminal capillary vessels. (i) Quantification of area shows a significant increase ($P<0.001$) in staining. Data are means ± SEM. Scale bars = 100μm.

6.3.6 Regime 3: VEGF-A expression

After anti-VEGF treatment according to regime 3 no apparent difference in VEGF immunostaining was seen in either mid-luteal control (Fig. 6.10a) or anti-VEGF treated (Fig. 6.10b) corpora lutea.

VEGF mRNA expression appeared, from dark field microscopy, to be greater than control levels (Fig. 6.10c) after anti-VEGF treatment (Fig. 6.10d). The apparent location of expression appeared not to differ with treatment (Fig. 6.10e-f).

Measurement of VEGF immunostaining area (Fig. 6.11a) demonstrated a lack of effect of treatment on area of VEGF expression. However, quantification of the intensity of VEGF staining demonstrated a significant increase (P=0.001) in intensity of VEGF expression in any one cell after treatment (Fig. 6.11b, a decrease in optical density indicates an increased intensity of VEGF staining). Following quantification of VEGF mRNA grain area (Fig. 6.12a) and density (Fig. 6.12b) no effect of treatment on VEGF mRNA expression was demonstrated, although dark field microscopy suggested otherwise.

6.3.7 *In situ* 3`end labelling

Figure 6.13 demonstrates 3` end labelling in mid-luteal control sections and sections after acute withdrawal of VEGF in the mid-luteal phase. One positive apoptotic endothelial cell associated with a blood vessel can be seen in Figure 6.13a. Incidence of apoptotic nuclei increased with anti-VEGF treatment (Fig. 6.13b) which shows two positive nuclei probably of endothelial cell origin. Positive apoptotic nuclei remained sparsely distributed, even though anti-VEGF treatment significantly (P=0.03) increased the occurrence of apparent endothelial cell apoptosis (Fig. 6.13c). The incidence of apoptotic cells was measured per sectioned corpus luteum as the size of the control and treated corpora lutea did not significantly differ. Atretic follicles in sections treated with the terminal transferase enzyme and digoxygenin label were positively 3` end labelled (Fig. 6.13d). Atretic follicles in serial sections not treated with terminal transferase were negative (Fig. 6.13e). In addition, healthy follicles in sections treated with the enzyme were negative (Fig. 6.13f).

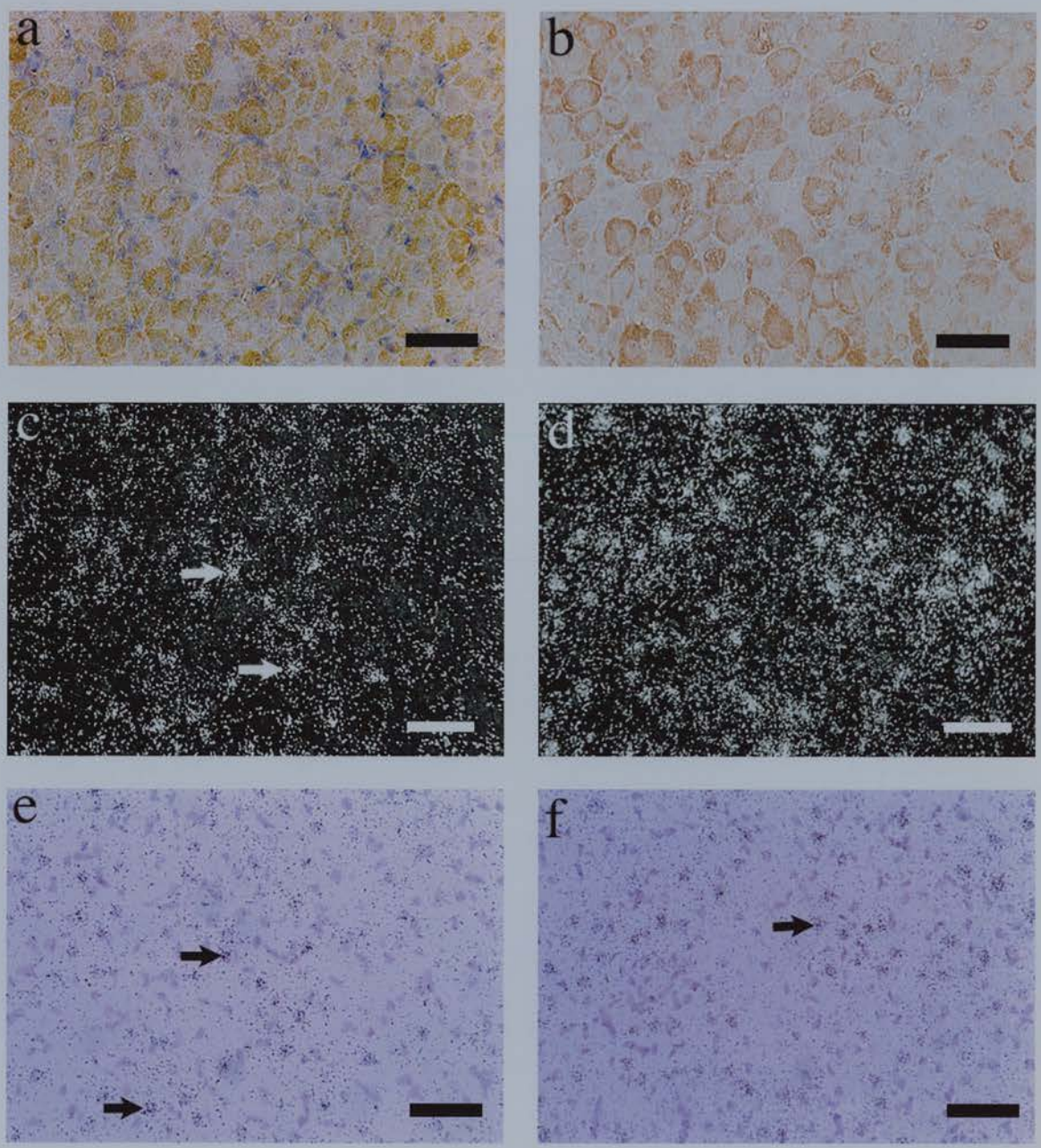

Figure 6.10 VEGF-A expression in control sections and after anti-VEGF treatment specifically in the mid-luteal phase (regime 3)

(a) Immunolocalisation of VEGF protein (brown staining) in mid-luteal control sections and (b) after anti-VEGF treatment. VEGF is localised to the cytoplasm (C) of most steroidogenic cells (SC) in the mid-luteal phase. (c) Dark field micrograph showing location of VEGF mRNA (white grains) in control sections, and (d) in anti-VEGF treated sections. VEGF mRNA is located in clusters (white arrows). Light field micrographs of (e) the same control and (f) treated sections reveal expression is associated with nuclei and cytoplasm of lutein cells as indicated by the black arrows. Scale bars = 50μm.

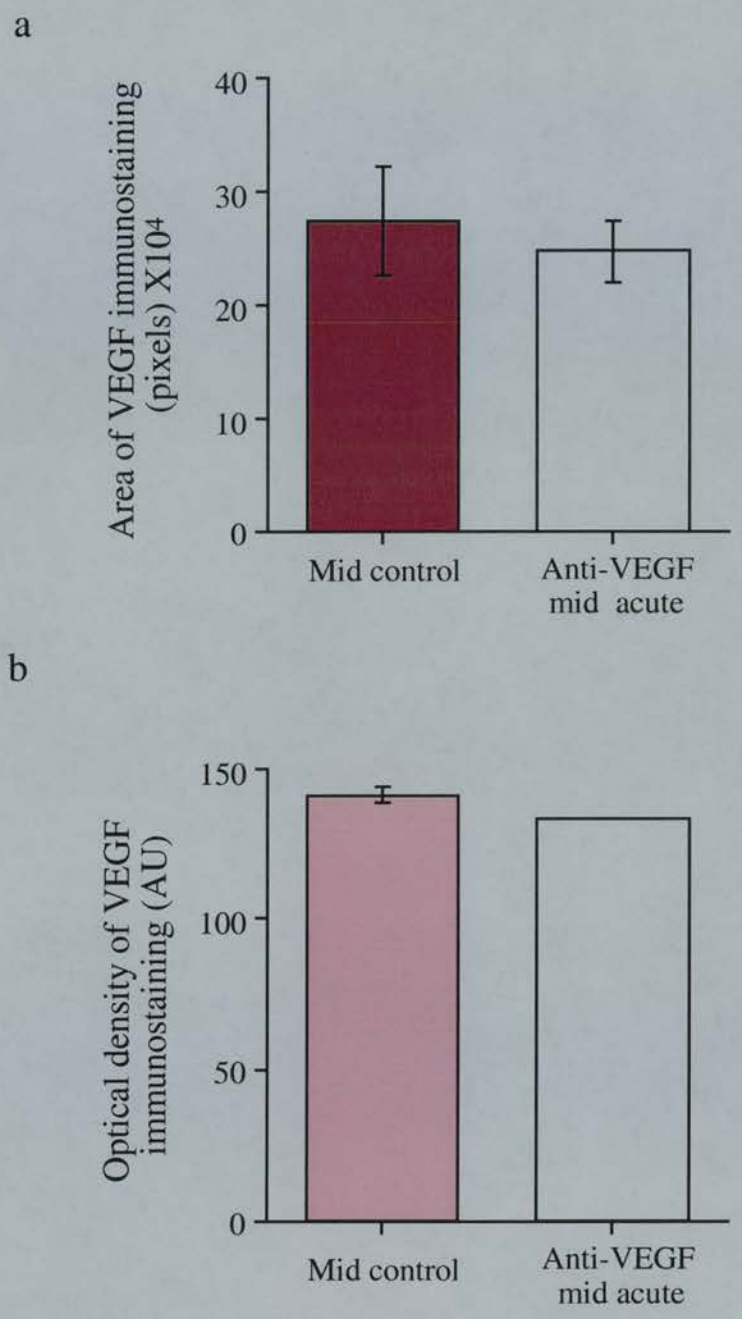

Figure 6.11 Quantification of VEGF-A immunostaining in controls and after anti-VEGF treatment specifically in the mid-luteal phase (regime 3)

(a) The area of luteal VEGF immunostaining in controls and anti-VEGF treated animals. There was no significant difference after treatment. (b) Quantification of intensity of immunostaining, indicating a significant increase (P=0.001) in the level of expression by any one cell in treated sections as compared to controls. Values are means ± SEM.

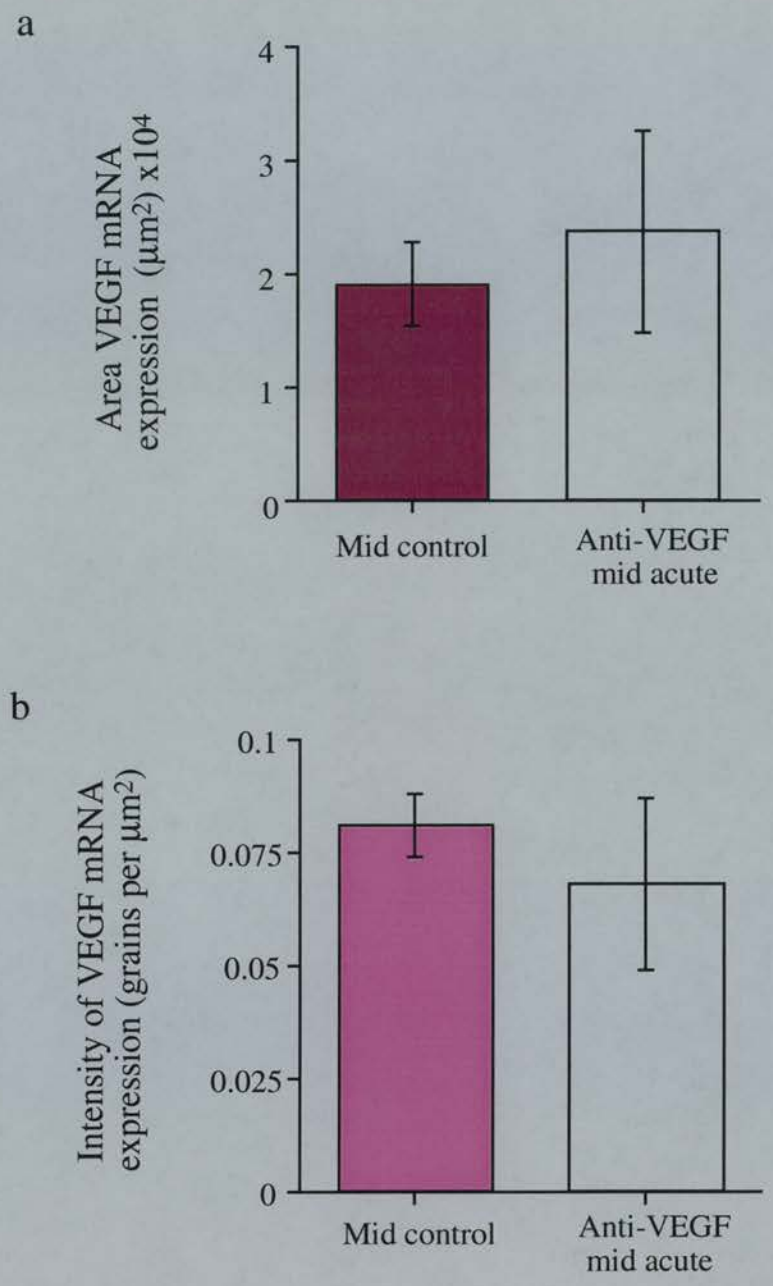

Figure 6.12 Quantification of mRNA for VEGF-A in controls and after anti-VEGF treatment specifically in the mid-luteal phase (regime 3)

(a) The area of clusters of VEGF mRNA expression in control and treated sections. There was no significant increase in overall expression of VEGF mRNA after anti-VEGF treatment. (b) Quantification of grain density per unit area of luteal tissue in control and treated sections. There was no significant difference of VEGF mRNA expression by any one cell between groups. Values are means ± SEM.

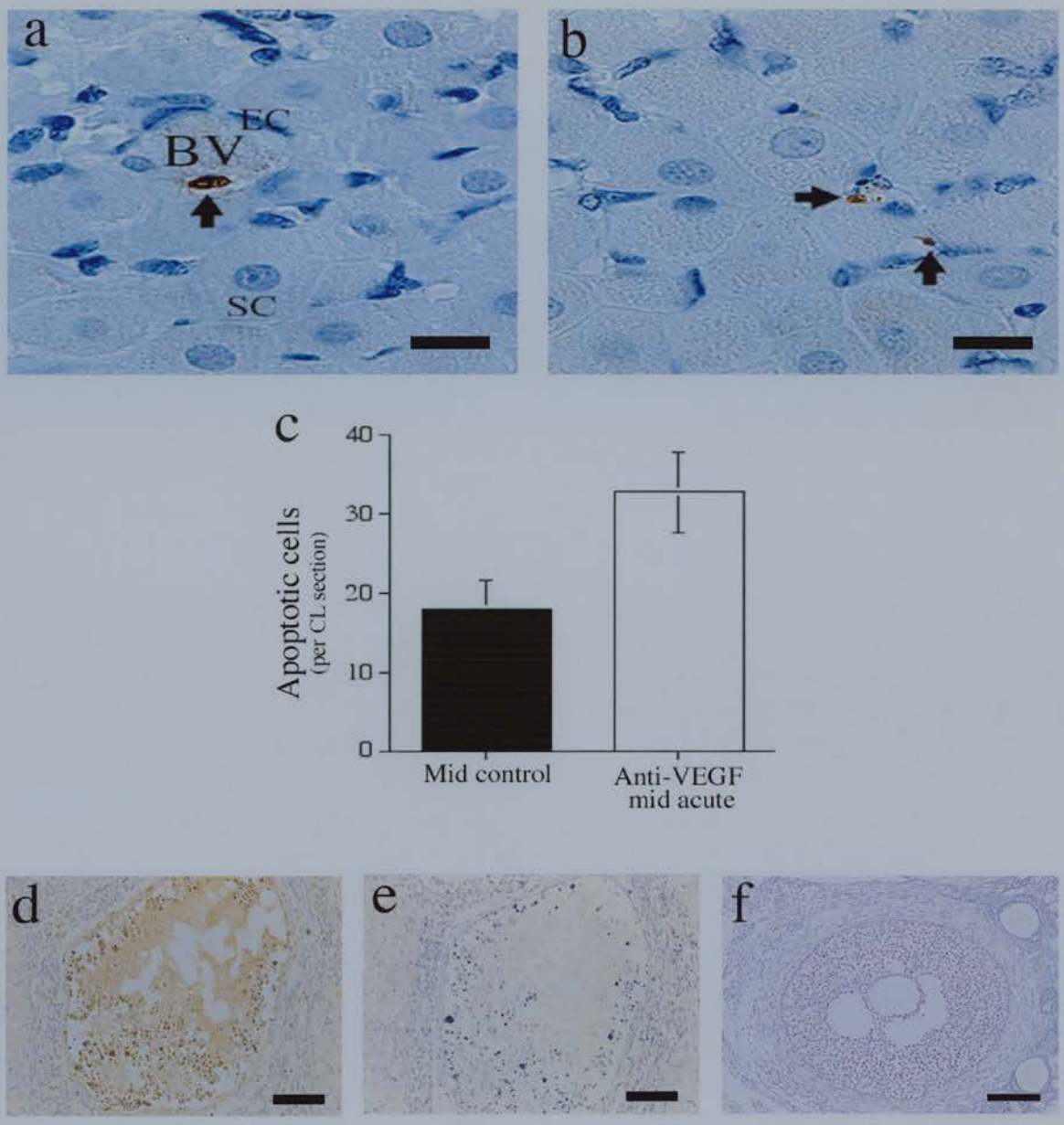

Figure 6.13 Effect of acute removal of VEGF in the mid-luteal phase (regime 3) on endothelial cell death

High power photomicrographs of 3` end labelled apoptotic cells (brown staining) in (a) a mid-control marmoset corpus luteum and (b) after anti-VEGF treatment. Note the presence of endothelial cells (EC) surrounding a blood vessel (BV) in the control section, and smaller dark haematoxylin-stained nuclei representing endothelial cells and periendothelial support cells in both control and treated corpora lutea. Arrows point to positive apoptotic nuclei assumed to be endothelial cells by their small, elongated form. (c) Quantification of positive cells in control (closed bar) and treated sections (open bar) shows increased presence of positive nuclei in anti-VEGF treated sections. Note that values are per corpus luteum section so the incidence of apoptosis even after treatment is very low. (d) An atretic follicle positively stained for DNA fragmentation, and (e) the same atretic follicle in serial section not treated with terminal transferase enzyme as a negative control for the in situ 3' end labelling method. (f) A negative healthy follicle, in a section which has been treated with terminal transferase. Data are mean ± SEM. Scale bars on a and b = 20µm. Scale bars on d and e = 100µm. Scale bar on f = 50µm.

6.3.8 Morphology

Semi-thin sections stained with toluidine blue showed that the most prominent features in the control corpora lutea collected during the mid-luteal phase were the large polyhedral lutein cells, characterised by circular nuclei in cross-section with a nucleolus and large cytoplasmic volume (Fig. 6.14). Within the cytoplasm were mitochondria and lysosomes together with occasional, less basophilic inclusions typical of lipid droplets. The lutein cells were supported by connective tissue including fibroblasts and there was an extensive blood supply characterised by the occurrence of endothelial cell nuclei and numerous lumina, often containing erythrocytes. In the corpora lutea from the mid-luteal anti-VEGF-treated marmosets, lutein cells appeared more densely packed (Fig. 6.14b), with a closer contact with neighbouring lutein cells. Quantification of lutein cell number showed that numbers of lutein cells per area were significantly greater ($p<0.001$) in the treated group (79.2±3 for controls, versus 103.8± 5.5 after anti-VEGF). In addition, numerous clusters of basophilic cells, presumably lutein, were present principally in the central area of the corpus luteum. Higher magnification revealed that although the majority of the lutein cells had retained their integrity, they exhibited an increased occurrence of lipid droplets in the peripheral zone of the cytoplasm identified by their grey coloration and homogeneous appearance (Fig. 6.14d).

6.3.9 Plasma progesterone concentrations

Plasma progesterone concentrations were reduced ($p<0.001$) by anti-VEGF treatment to at least 50% of the normal values in the early luteal (data not shown), mid-luteal chronic treatment (Fig. 6.15a) and mid-luteal acute treatment (Fig. 6.15b).

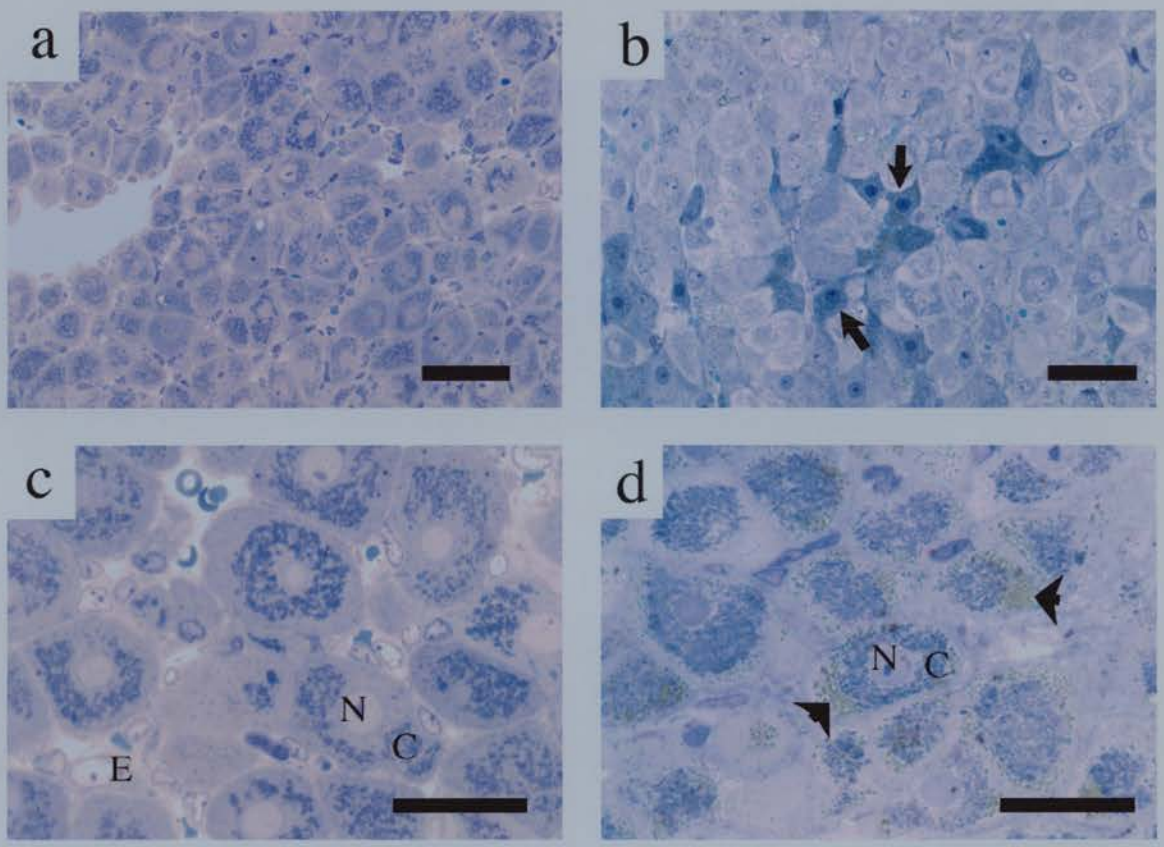

Figure 6.14 Examination of cell morphology after anti-VEGF treatment
Photomicrographs of toluidine blue-stained corpora lutea to show the appearance of hormone-producing lutein cells in the mid-luteal corpus luteum of (a) control, and (b) anti-VEGF treated marmosets. Note how the lutein cells of the treated animal are more closely packed and the cluster of densely stained cells (arrows), presumably of luteal origin. Higher magnification of a control corpus luteum shows (c) the appearance of the lutein cell nucleus (N) and cytoplasm (C), with each cell being in contact with an endothelial cell (E). (d) In the anti-VEGF corpus luteum, the lutein cells have maintained their integrity, but contain numerous lipid droplets (grey staining, arrowhead) in the peripheral zone. Scale bars on a and b = 50μm. Scale bars c and d = 20μm.

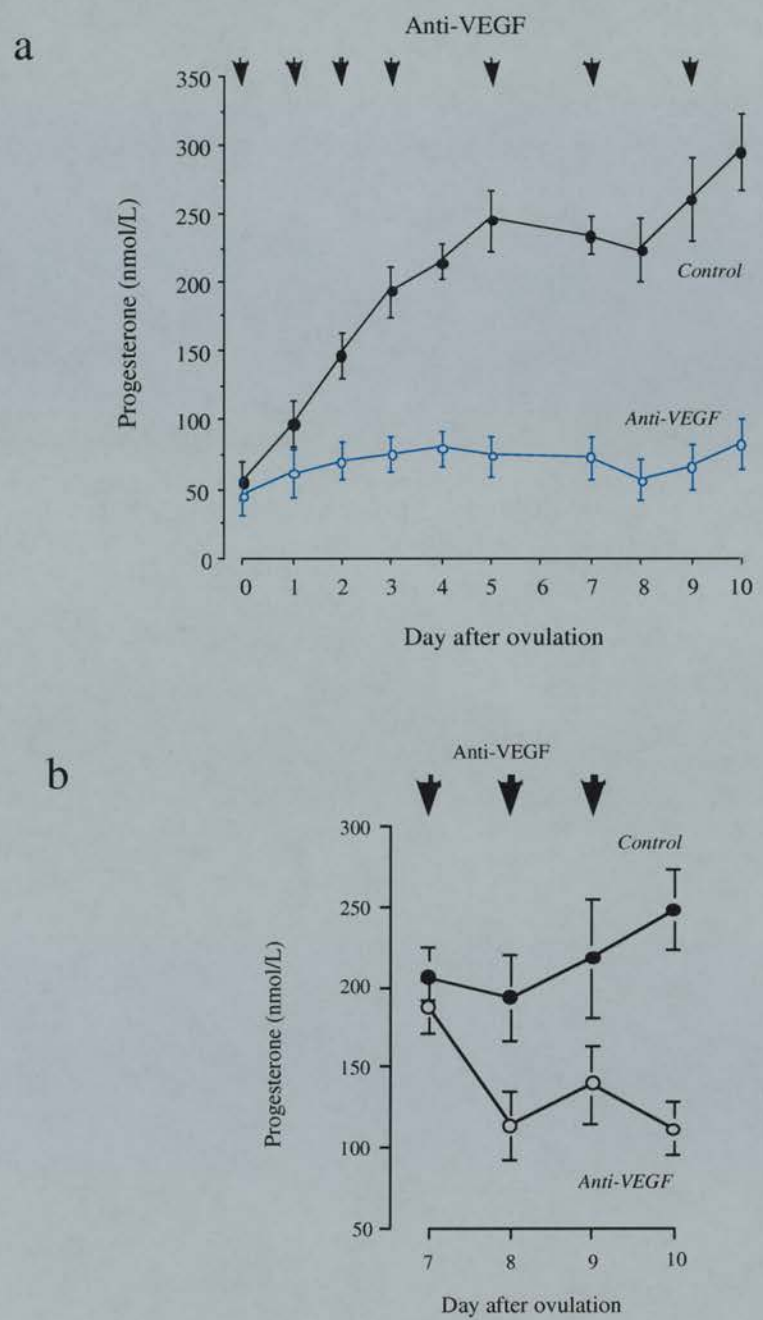

Figure 6.15 Plasma progesterone concentrations in control and anti-VEGF treated marmosets

(a) Marmoset plasma progesterone concentrations in controls (closed plot symbols) and after anti-VEGF treatment for 10 days from the early luteal phase to the mid-luteal phase (open plot symbols) (n=6 per group). Treatment started on the day of expected ovulation and is associated with a significant suppression ($P<0.001$). (b) Marmoset plasma progesterone concentrations in controls (closed plot symbols) and after anti-VEGF specifically in the mid-luteal phase (open plot symbols) (n=4 per group). A sustained elevation of plasma progesterone was observed prior to treatment in all animals. After administration of anti-VEGF treatment starting on luteal day 7 there was a marked reduction in plasma progesterone concentrations which had fallen by over 50% by day 10 ($P=0.01$). Values are means ± SEM.

6.3.10 Proliferation of endometrial endothelial cells

Endothelial cell proliferation in the stroma of uterine endometrium was measured to examine the effect of anti-VEGF treatment on angiogenesis *in utero*. Dual staining of uterine sections with CD31 and BrdU revealed a relatively low level of stromal endothelial cell proliferation overall (Fig. 6.16), which appeared not to be affected by anti-VEGF treatment at any stage of the cycle. Quantification of proliferating endothelial cells revealed there was no effect of treatment on stromal angiogenesis in the uterine endometrium (Fig. 6.17). It is worth noting that stromal endothelial cell proliferation had almost decreased by a factor of 10 from levels in early control endometrium to those in mid- controls.

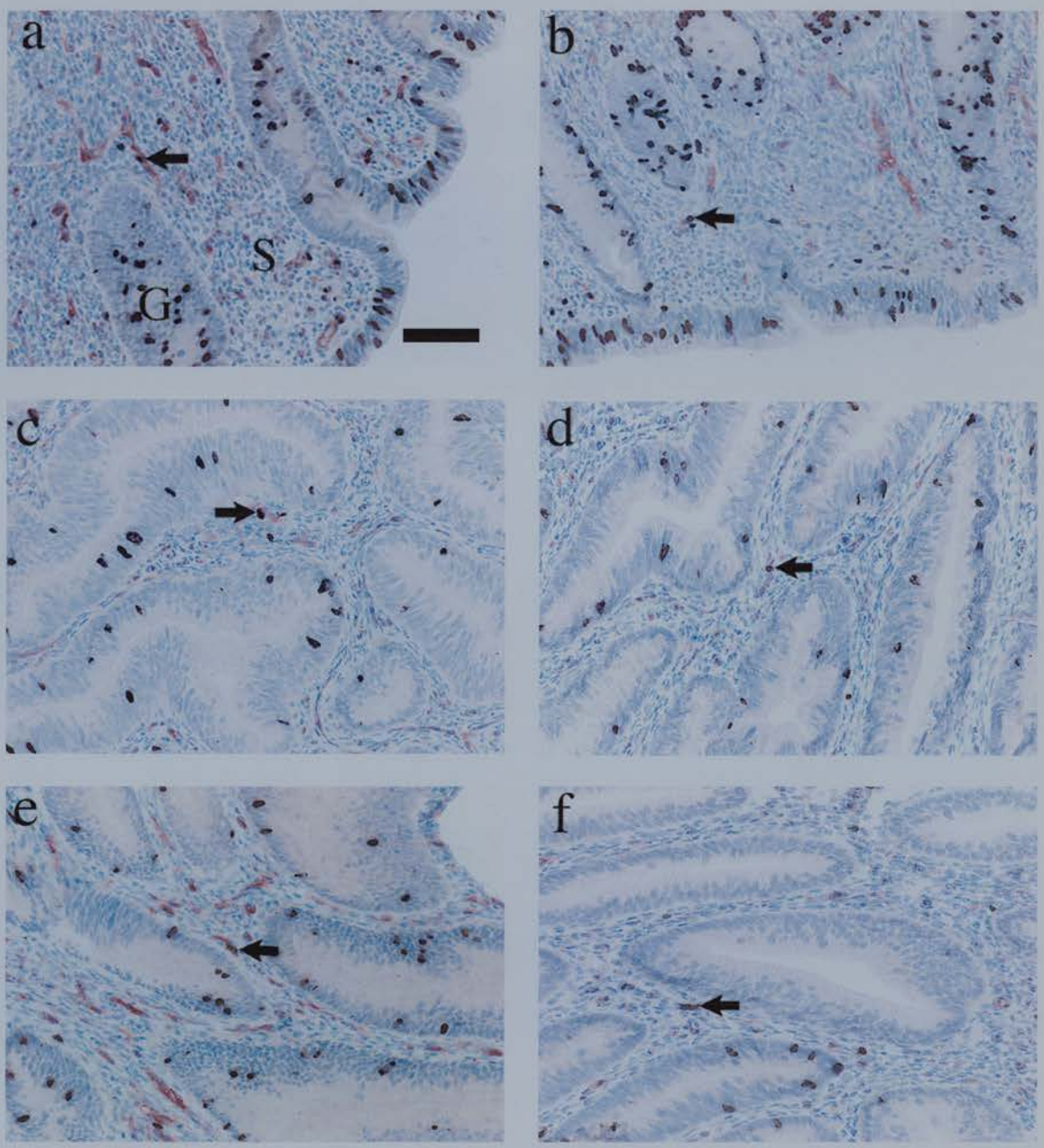

Figure 6.16 Effect of anti-VEGF treatment on endometrial angiogenesis
Dual immunocytochemistry for BrdU (black nuclear staining) and CD31 (red cytoplasmic staining) in (a) an early luteal control uterine section, and (b) after anti-VEGF treatment in the early luteal phase (regime 1). Note that only the stroma (S) not the epithelial glands (G), is vascularised. (c) and (d) Dual staining for BrdU and CD31 in mid-luteal control and after anti-VEGF treatment from the early luteal to the mid-luteal phase (regime 2), respectively. (e) Similar staining in mid-luteal control and (f) after anti-VEGF treatment specifically in the mid-luteal phase (regime 3). Note the decrease in endothelial cell proliferation (dual stained cells) from the early control endometrium (a) to the mid control sections (c) and (e). Arrows point to proliferating endothelial cells which stain for both BrdU and CD31. Scale bars = 50μm.

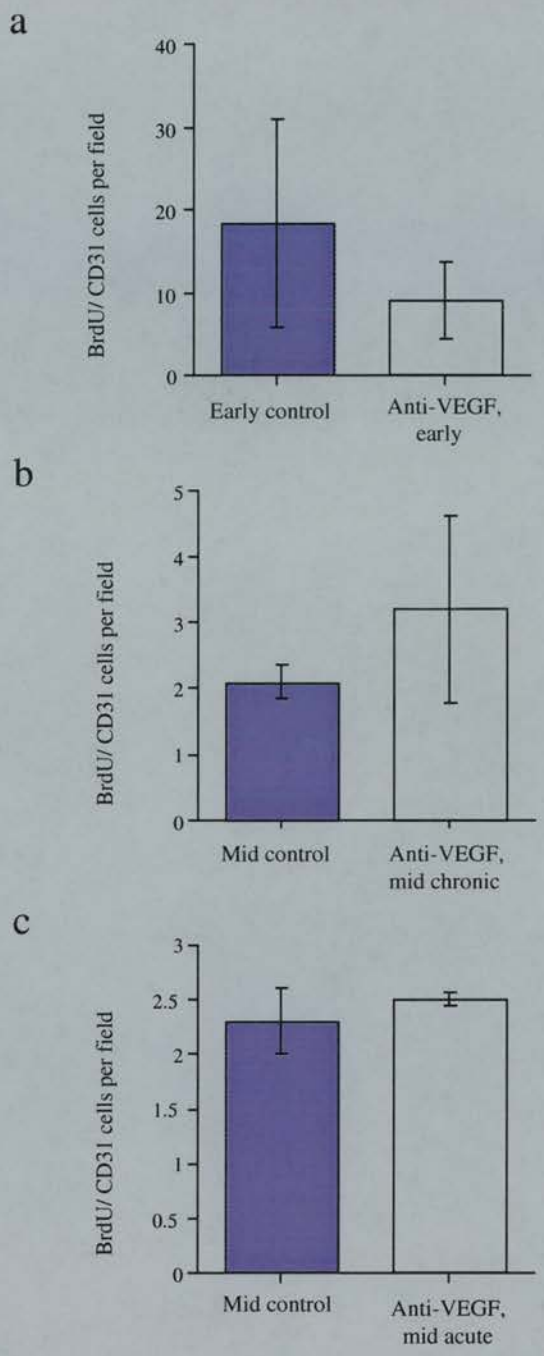

Figure 6.17 Quantification of endometrial angiogenesis after anti-VEGF treatment

The number of cells colocalising BrdU and CD31 immunostaining in endometrial stroma in (a) control sections and after early luteal phase treatment, (b) in mid-luteal controls and those treated with anti-VEGF from the early to the mid-luteal phase, and (c) in controls and after specific mid-luteal phase inhibition of VEGF. Note that endothelial cell proliferation in the early control has decreased by a factor of 10 in the mid-controls. There was no significant effect of any regime of treatment employed. Values are means ± SEM.

6.4 Discussion

This study has shown not only that the intense angiogenesis in the early luteal phase, but also the ongoing angiogenesis of the mid-luteal phase are susceptible to inhibition by VEGF neutralisation. Inhibition of the intense early luteal phase angiogenesis was demonstrated by the marked decrease in BrdU incorporation in the marmosets treated with antibody during the early luteal phase. An effect on endothelial cell area was not initially apparent after this short term treatment, but by the mid-luteal phase, this parameter was markedly inhibited in anti-VEGF-treated corpora lutea, as a consequence of the inhibition of endothelial cell proliferation during the intense period of angiogenesis. Although larger blood vessels were established by the mid-luteal phase in treated animals, there was a marked overall reduction in the number of endothelial cells, suggesting the establishment of early luteal vasculature (possibly from pre-existing vessels) and its survival through the mid-luteal phase, but indicating blockade of development of the normally extensive capillary bed. The absence of an effect on cell proliferation in the mid-luteal animals treated with anti-VEGF was surprising. However, by this stage, proliferation in controls was much reduced over that seen during the early luteal phase and this mid-luteal proliferation suggests that the rate is maintained either by low levels of VEGF that remain as a result of incomplete neutralisation, or has resulted from the action of other angiogenic factors in the corpus luteum.

Whilst it is recognised that VEGF has an angiogenic function during the prolific early luteal phase it has been suggested that the presence of VEGF in the less prolific mid-luteal phase signifies other functions of VEGF at this time. This study demonstrates that VEGF in the mid-luteal phase is essential for mid-luteal angiogenesis and function as shown by the suppression of endothelial cell proliferation and endothelial cell area, and the decline in plasma progesterone concentrations. By the mid-luteal phase, the vasculature is becoming highly developed and progesterone is being maximally secreted. If the effect of anti-VEGF was solely to suppress angiogenesis it might be anticipated that progesterone would be maintained at pretreatment levels, at least during the first 1-2 days of treatment. The rapid decline in plasma progesterone concentration seen on the first day of this acute mid-luteal phase anti-VEGF treatment, indicates that in addition to the regulation of ongoing mid-luteal angiogenesis, VEGF also modulates vascular

permeability in the corpus luteum. An effect on corpus luteum vascular permeability could deprive the lutein cells of both the necessary precursors for progesterone production and the efficient release of their products into the bloodstream, which would result in marked reductions in plasma progesterone values.

It was observed that acute removal of VEGF in the mid-luteal phase resulted in endothelial cell death as seen by positive *in situ* 3` end labelling. Benjamin *et al.*, (1999) demonstrated that in both xenografted tumour and primary human tumours VEGF withdrawal resulted in specific obliteration of immature vessels; and in human prostate cancer loss of VEGF led to selective apoptosis of endothelial cells devoid of periendothelial cells. Mature vessels with associated pericytes are believed to be VEGF independent (Benjamin *et al.*, 1998). Thus, in the current study, it appears that the increase in death of endothelial cells after anti-VEGF treatment is a consequence of lack of VEGF support to susceptible, immature vessels with no associated pericytes. It could follow therefore, that endothelial cells of more mature vessels with associated pericytes would be VEGF independent and not susceptible to anti-VEGF treatment. Our finding that mid-luteal VEGF withdrawal led to an increase in endothelial cell death in the presence of extended pericyte coverage suggests that it is the endothelial cells associated with the few remaining immature capillaries, which were susceptible to loss of VEGF support. This in turn indicates that the reduction in endothelial cell area after anti-VEGF treatment may not only be a consequence of a decreased angiogenic rate, but also of increased endothelial cell death.

VEGF inhibition in the early luteal phase and from the early through to the mid-luteal phase also had an effect on luteal pericyte recruitment. Pericytes are believed to be involved in the remodelling process which occurs during blood vessel maturation (reviewed by Darland and D'Amore, 1999) a process thought also to take place in the corpus luteum (Tsukada *et al.*, 1996; Goede *et al.*, 1998). High levels of periendothelial support cells in the early luteal phase is consistent with the infiltration of the preformed thecal vasculature from the mature follicle to the newly formed corpus luteum. VEGF is thought to have a role in recruitment of these periendothelial support cells. Yamagishi *et al.*, (1999) demonstrated the proliferation and migration of pericytes in a dose dependent manner upon addition of VEGF. This action of VEGF was blocked with polyclonal antibodies to VEGF. In addition, they

found pericytes express the gene for Flt-1 the predominant form of VEGF receptor. Thus the decline in pericytes after VEGF withdrawal in the early luteal phase in this study can be explained. However, it is surprising that VEGF inhibition from the early to the mid-luteal phase, and in the mid-luteal phase alone served to significantly increase luteal pericyte coverage.

It appears therefore that a stage specific regulation of pericyte recruitment is occurring in the marmoset corpus luteum. In the early luteal phase, pericyte differentiation and/or proliferation appears to be regulated by VEGF. However, in the mid-luteal phase the absence of VEGF results in increased pericyte recruitment, perhaps through activation of other factors. For example, a stage specific increase in other members of the VEGF family, not neutralised by the monoclonal antibody which is specific for VEGF-A, such as PlGF, VEGF-B or C, which are believed to stimulate pericyte proliferation *in vitro* (Nomura *et al.*, 1995; Yamagishi *et al.*, 1999), some of which are shown to be regulated by hypoxia (Yonekura *et al.*, 1999). Other factors involved in the recruitment of pericytes include platelet-derived growth factor-B (reviewed by Darland and D'Amore, 1999) and angiopoietin-1 (Davis *et al.*, 1996; Maisonpierre *et al.*, 1997; Koblizek *et al.*, 1998), while TGFβ is thought to regulate pericyte differentiation (Hirschi *et al.*, 1999). It thus remains to be determined whether factors such as angiopoietin-1 may be activated specifically in the mid-luteal phase after VEGF inhibition, to act as a survival mechanism to "rescue" existing vessels from the absence of the immature endothelial cell survival factor, VEGF.

VEGF inhibition specifically in the mid-luteal phase exhibited an increase in the intensity of VEGF immunostaining without an increase in area of staining or mRNA production, which suggests this was not an effect of treatment *per se*. The other treatment regimes employed had no effect on lutein cell VEGF expression as seen by unaltered VEGF immunostaining and *in situ* hybridisation signal for VEGF mRNA in treated as compared to control corpora lutea. Considering the probable hypoxic conditions enforced as a consequence of decreased vascularisation a more conclusive increase in VEGF production was expected after VEGF immunoneutralisation. It may be that oxygen tension did not reach critical levels, or that a local VEGF feedback mechanism did not detect the decline in VEGF, VEGF having a paracrine action on endothelial cells not an autocrine action on lutein cells.

One other possibility is that with the reduction in luteal vasculature, lutein cells were starved of nutrients essential for growth factor biosynthesis.

There was also no effect of VEGF inhibition on endometrial angiogenesis. Growth of the endometrial vasculature begins during the proliferative phase and continues at a lower level in the secretory phase (Meschia, 1983). although there is some discrepancy concerning this matter (Rogers *et al.*, 1998). Nevertheless, this chapter demonstrates a low level of stromal endothelial cell proliferation in the secretory phase, and that from the early to the mid-secretory phase such proliferation declines, suggesting maximal vascular proliferation in the proliferative endometrium. It is therefore possible that VEGF could be a major driving force of angiogenesis in the proliferative endometrium, and its expression/action in the secretory endometrium is probably decreased, thus its inhibition would not effect the low level of angiogenesis occurring at this stage. It is however likely that the decrease in plasma progesterone concentration following anti-VEGF treatment would have a detrimental effect on endometrial differentiation.

The absence of marked morphological change in the lutein cells after anti-VEGF treatment contrasts with observations on the characteristic effects of withdrawal of the tropic factor, LH, described in Chapter 4 and by Fraser et al., (1999b), and Dickson and Fraser, (2000). Such treatment also results in inhibition of early luteal angiogenesis, but this is secondary to the destruction of the lutein cells in which it is assumed most of the principal angiogenic factors are produced (Chapter 4; Dickson and Fraser, 2000). The observed changes in the structure of the corpus luteum after neutralisation of VEGF are likely to result from the specific inhibition of angiogenesis. The increased density of the lutein cells resulted primarily from the dearth of capillaries, whereas the occurrence of aggregates of subsets of lutein cells with more densely stained nuclei and cytoplasm, found principally in the central area of the corpus luteum, suggests a premature onset of cell death. This observation would be compatible with a failure of blood vessel development to deliver essential survival factors. The increased presence of lipid droplets is more difficult to explain, but suggests either a lack of tropic hormone stimulus for steroid hormone release or a failure of the normal secretory process. The accumulation of lipid is often associated with the onset of degenerative change in steroid-producing cells including the early stages of luteolysis in the marmoset (Fraser *et al.*, 1999b). Despite the absence of

major structural effects within lutein cells, secretion of the principal steroidal hormonal product of these cells is reduced by over 50%. The most likely explanation for these findings is that the reduction in development of the microvasculature deprives the lutein cells of both the low density lipoprotein precursors necessary for progesterone production and the transport system for efficient release of their products into the bloodstream.

This study demonstrates almost conclusively that VEGF-A is the primary factor driving luteal angiogenesis in the early and mid-luteal phases in the marmoset corpus luteum. The rapid reduction in plasma progesterone concentrations also suggest a role for VEGF in regulating vascular permeability in this tissue. We have provided compelling evidence that VEGF is required for luteal angiogenesis in the primate, and in turn, that luteal angiogenesis is essential for normal luteal function in the primate.

Chapter 7

Molecular Control of Human Luteal Angiogenesis: Changes in Angiopoietin, Tie-2, VEGF, Flt-1 and KDR mRNA.

7.1 Introduction

Angiogenesis is thought to depend on a balance between endogenous positive and negative regulatory molecules (Hanahan and Folkman, 1996). This is particularly prominent during the spontaneous cyclic angiogenesis which occurs in the corpus luteum, where vessel proliferation is followed by regression unless luteal rescue occurs as a result of conception. It follows that such a potentially divergent series of events must be tightly controlled. Perhaps the best characterised of the pro-angiogenic factors is VEGF. The VEGF family of growth factors totals at least 5 members and VEGF-A (or VEGF) provides the first example of a growth factor specific for the vascular endothelium. The specific actions of VEGF on the endothelium are a result of the restriction of its two VEGF receptors (Flt-1 and Flk-1/KDR) to these cells (Plouet and Maukadiri, 1990; Vaisman *et al.*, 1990). The effects of VEGF on vascular growth have largely been elucidated from studies examining embryonic vascular development in transgenic mice which lack VEGF or either receptor. VEGF is shown to be involved in the proliferation, migration and sprouting of endothelial cells, promoting the formation of tube-like vascular structures. This function of VEGF in early vasculogenesis is mediated largely through the Flk-1/KDR receptor (Shalaby *et al.*, 1995; Carmeliet *et al.*, 1996; Ferrara *et al.*, 1996). Murine Flt-1 knock-outs demonstrate a later role for Flt-1 in vasculogenesis. Vessels do form in mutant embryos but are organised abnormally, with seemingly excess levels of endothelial cells being generated and entering the lumens of the abnormal vascular channels (Fong *et al.*, 1995). Thus, Flt-1 may actually be involved in down regulating VEGF-A activity to ensure that the right number of endothelial cells are generated (Gale and Yancopoulos, 1999).

A second family of growth factors, termed the angiopoietins, specific for the vascular endothelium has been identified (Suri *et al.*, 1996; Davis *et al.*, 1996; Maisonpierre *et al.*, 1997). These growth factors are specific for the endothelial cell tyrosine kinase, Tie receptors, Tie-1 and Tie-2. All known angiopoietins bind to Tie-2, but it is still unclear whether they utilise Tie-1 (Holash *et al.*, 1999). The angiopoietins seem to act in a complementary and co-ordinated fashion with VEGF, playing a later role in vascular development (Holash *et al.*, 1999). Ang-1 appears to play a key role in mediating interactions between endothelial cells and surrounding support cells such as pericytes and smooth muscle cells (Folkman and D'Amore,

1996; Suri *et al.*, 1996). This was demonstrated by the severe retardation of remodelling and stabilisation of primitive vasculature in mice lacking Ang-1 or Tie-2. Ang-1 is also shown to have a direct action on endothelial cell survival (Papapetropoulos *et al.*, 1999). In the adult, Ang-1 appears to be constitutively expressed serving to maintain the integrity of the already established vasculature (Maisonpierre *et al.*, 1997; Witzenbilcher *et al.*, 1998).

Ang-2 is believed to act as a naturally occurring antagonist to Ang-1, binding the Tie-2 receptor but inhibiting its phosphorylation (Maisonpierre *et al.*, 1997). Transgenic over-expression of Ang-2 leads to a phenotype reminiscent of that seen in embryos lacking either Ang-1 or Tie-2 (Maisonpierre *et al.*, 1997). Whereas Ang-1 is widely expressed in normal adult tissues, correlating with increased vessel maturity, Ang-2 is typically expressed at sites of vascular remodelling, notably the female reproductive tract (Maisonpierre *et al.*, 1997). Detailed localisation of Ang-2 mRNA in the rat ovary revealed that Ang-2 was either expressed at regions of active angiogenesis together with VEGF at sites of vessel sprouting and ingrowth, in the early corpus luteum, or at sites of vascular regression in the absence of VEGF, in atretic follicles. This led to the proposal of a model in which Ang-2, by blocking a constitutive stabilising action of Ang-1, either plays a role in active angiogenesis by destabilising vessels in the presence of VEGF allowing growth factor access and angiogenic action; or in the absence of VEGF, destabilisation of vessel leads to regression as in the atretic follicle (Maisonpierre *et al.*, 1997).

Most evidence of the co-ordinated actions of the angiopoietins and VEGF was accumulated during examinations of mouse embryonic vascular development in specific gene knock-out studies. Expression in the rat ovary suggests that the angiopoietins may also play a critical role in adult ovarian angiogenesis. The corpus luteum is associated with robust angiogenesis, vessel maturation and regression, and so this chapter examines the temporal expression of mRNA for these factors in association with development, maturation, regression and hCG rescue of the human corpus luteum. So far this thesis has emphasised the quantification of luteal angiogenesis by immunocytochemical methods in histological sections, which was shown to be adequate to measure specific angiogenic parameters. Now, because of the availability of archived frozen human luteal tissue, it is possible to quantify the expression of mRNA for these angiogenic factors in the four stages of the human

luteal phase. A 'state of the art' technique has recently become available for the quantification of specific mRNA species using quantitative reverse transcription-polymerase chain reaction (RT-PCR) amplification. This technique, known as Real Time Quantification of RT-PCR, allows measurement of the cDNA produced from each cycle of PCR amplification from the detection of the fluorescence emitted as each strand is synthesised with an associated cleavage of fluorescent quencher. Quantification is based on the cycle number at which the level of emitted fluorescence *i.e.* proportion of cDNA synthesised, rises above a specified threshold in relation to an 18S internal control and a predetermined standard sample, which is known to express the mRNA species of interest. The principles of this technique are further outlined in Chapter 2. Human term placenta was chosen as it is a readily available source of RNA for the angiopoietins, and their Tie-2 receptor (Maisonpierre *et al.*, 1997) as well as VEGF and its Flt-1 and Flk-1/KDR receptors (Clark *et al.*, 1996; Torry and Torry, 1997).

If the postulated roles for the angiopoietins and their co-ordinated action with VEGF in vasculogenesis in the mouse holds true, expression of mRNA species in the corpus luteum should reflect the neovascularisation, stabilisation and regression which has been shown to occur in this tissue (Chapter 3). It is likely that the intense angiogenesis of the developing corpus luteum will be associated with high expression of Ang-2, VEGF and VEGF receptor mRNAs, and that the maturation of the less angiogenic mid-stage corpus luteum will have an associated increase in Ang-1 expression. According to postulated actions of Ang-2, luteal regression is thought to be associated with an increase in Ang-2 and a decline in VEGF mRNA. Human CG rescue of the corpus luteum should demonstrate increases in mRNA for Ang-2, Ang-1, VEGF and VEGF receptors in accordance with the increased angiogenic activity and vessel stabilisation associated with luteal rescue, which was established earlier in the thesis (Chapter 3).

7.2 Materials and Methods

7.2.1 Subjects and tissue collection

Details of patient recruitment and dating of luteal tissue were described in Chapter 2. Corpora lutea were collected by enucleation of the whole gland from the ovary at the time of hysterectomy. The tissue was immediately divided into 4 radial segments. Two segments were snap frozen in liquid nitrogen and stored at –70°C for RNA extraction. Between 4 and 6 corpora lutea were analysed per group.

7.2.2 RNA extraction and DNase treatment of RNA

Total RNA was extracted from small slices of frozen corpora lutea, using Tri-Reagent (Sigma). Details of the extraction procedure can be found in Chapter 2. One microgram of total RNA was DNase-treated in a 10µl reaction containing 1 x reaction buffer (Gibco BRL; 200nM Tris-HCl (pH8.4), 20mM $MgCl_2$, 500mM KCl) 1U of DNase I, and RNase-free H_2O up to 10µl. Samples were incubated for 15 min at room temperature, the DNase was inactivated by the addition of 1µl 25mM EDTA and heating at 65°C for 10 min, then chilled on ice. Samples were then ready for the reverse transcription step of RT-PCR.

7.2.3 Reverse transcription

Complementary DNA synthesis was carried out by reverse transcription of total RNA using the TaqMan reverse transcription reagents (Perkin Elmer) which uses Murine Leukemia Virus Reverse Transcriptase (MuLV-RT). Two hundred nanograms of DNase-treated RNA was reverse transcribed in a 10µl reaction, containing 1 x reaction buffer, 5mM $MgCl_2$, 1mM each dNTPs (dGTP, dATP, dTTP and dCTP), 2.5µM random hexamer primers, 0.2U RNase inhibitor, 0.625U MuLV-RT, and RNase-free H_2O up to 10µl. Enough mixture was made for all samples and all positive and negative controls (outlined below). Reverse transcription was carried out in a PCR Thermal Cycler (Hybaid Ltd., Ashford, Middlesex, UK), during one cycle of 25°C for 1 hour, 48°C for 45 min and 95°C for 5 min. cDNA was then ready for PCR.

7.2.4 Real Time quantitative polymerase chain reaction

Probes and primers for Real Time quantitative PCR were designed from published human sequences to Ang-l, Ang-2, Tie-2, VEGF-A, Flt-1 and KDR using the Primer Express software following the guidelines outlined in Chapter 2. The sequence of each probe and primer set are documented in Appendix B. All primer T_m values were in the range of 58-60°C, and the probe T_m values at 68-70°C. The probe and primers for 18S were designed by Perkin Elmer Applied Biosystems the sequences of which were not made public.

For one 25µl reaction, a PCR cocktail of 12.5µl TaqMan Universal PCR Master Mix (Perkin Elmer; containing AmpliTaq Gold DNA polymerase, AmpErase uracil-N-glycosylase, A, T, C, G dNTPs, $MgCl_2$ and the passive reference ROX (6-carboxy X rhodamine) fluorofore), 300mM forward and reverse primers, 5pmols specific FAM (6-carboxyfluorescein) fluorescent probe, 0.05µM each of 18S forward and reverse primers, 0.2µM 18S VIC fluorescent probe, and 9.525µl RNase-free H_2O was made. Enough cocktail for duplicates of each sample, the reference placental cDNA, the two reverse transcription negatives and a third PCR negative, containing H_2O in place of cDNA template, was prepared. Forty eight microlitres of PCR cocktail was aliquotted into 0.2ml RNase/DNase-free tubes (ABgene, Epsom, Surrey, UK) and 2µl (initially 20ng RNA) of cDNA template added. The tubes were briefly vortexed and centrifuged to collect all components. In an ABI Prism 96-well optical reaction plate (Perkin Elmer) 2 x 24µl of each PCR sample were aliquotted in adjacent wells on the plate. A note of the contents of each well was made. The plate was capped with MicroAmp optical caps (Perkin Elmer) and PCR carried out using ABI Prism 7700 Sequence Detector cycling and detection. PCR conditions consisted of 40 cycles of 50°C for 2 min, 95°C for 10 min 15 sec, and 60°C 1 min.

7.2.5 Positive and negative controls for Real Time RT-PCR

Total RNA from human term placenta was used as a positive control and as the standard, which was used to calculate the relative expression of specific mRNA in all luteal samples. Two reverse transcription negative controls were used for the placental RNA and for a nominated luteal sample. Control 1 contained RNAse-free H_2O in place of MuLV-RT to ensure PCR amplification was not from genomic DNA contamination. Control 2 included RNAse-free H_2O in place of RNA template, to

detect H_2O contamination. A third PCR negative for placental and one luteal RNA was used. This contained RNAse-free H_2O in place of cDNA template. A control without DNA polymerase was not possible as the ready-made Universal Maser Mix contained AmpliTaq DNA polymerase.

7.2.6 Quantification

Quantification is based on the emission of the fluorescent probe for the specific cDNA of interest in relation to an internal 18S control and the nominated standard, in this case placenta. It involves a number of calculations which utilise the C_T values provided by the TaqMan software following PCR, and culminating in the production of a 2^{-ddCT} value for each sample, which is used for statistical analysis. The C_T value is the PCR cycle number (between 1 and 40) at which a statistically significant increase in emission intensity of the reporter from the passive reference is reached, set by a predetermined threshold. The C_T values for the specific mRNA probe (FAM reporter emission) and 18S signal (VIC reporter emission) for each sample was obtained from Sequence Detector Version 1.6.3 software after the 40 PCR cycles. Delta C_T considers the change in C_T of the specific FAM reporter from the 18S VIC signal, this was calculated from subtracting the 18S C_T value from the corresponding sample FAM C_T. The delta C_T for each of the two duplicates for each sample were meaned. The placental standard C_T was subtracted from all delta C_T values to obtain the delta delta C_T value. Messenger RNA expression, relative to the placental standard was calculated from 2^{-ddCT}, which considers the exponential increase in PCR amplification and enhances the differences between samples. The relative mRNA expression was meaned for each group of samples corresponding to the different stages of the luteal phase, and the SEM calculated.

Each of the negative controls had a FAM C_T value > 37 (40 was optimal and in most cases achieved), which was also a minimum of 10 cycles above the highest luteal or placental sample C_T value. An 18S C_T value >35 and also 10 cycles above the highest luteal or placental sample 18S C_T value was acceptable.

2^{-ddCT} values from each stage of the luteal phase and after hCG rescue were analysed for significant variation using a one way analysis of variance with Fisher's

post hoc test, the level of significance being taken as $P<0.05$. The tests were performed using StatView Version 4.0.

7.3 Results

The results reflect quantification from one PCR run. Ideally the average of 3 independent PCR runs should be used for statistical analysis, however, due to the cost of reagents this was not possible. It is worth noting that results from preliminary trials over the luteal stages exhibited comparable trends in expression as the definitive run, which is documented here.

7.3.1 Angiopoietin and Tie-2 mRNA expression

Figure 7.1 suggests a trend from high Ang-1 expression in the early luteal phase to minimal levels in the rescued corpus luteum. However, due to the low number of corpora luteal per stage (n=4-6) and hence the large SEM, particularly in the early luteal group the only significant value was a decrease ($P<0.05$) in Ang-1 mRNA expression from early luteal levels, in the rescued corpus luteum. Similarly for Ang-2 mRNA expression (Fig. 7.2), highest levels were found in the early luteal phase which significantly declined in the rescued corpus luteum. In these results however, there is a trend for expression to increase in the late corpus luteum, although the high SEM values do not make these differences significant. Expression of the common angiopoietin receptor, Tie-2 mRNA (Fig. 7.3) appears greatest in the early luteal phase declining throughout the remainder of the luteal phase and following luteal rescue, although there are no significant differences in level of expression, probably due again to the large SEM values.

7.3.2 VEGF, Flt-1 and KDR mRNA expression

Figure 7.4 demonstrates that VEGF expression is maximal in the early luteal phase and is significantly reduced in the mid- and late corpus luteum. There is a tendency for expression to increase following hCG rescue however this increase is not statistically significant. Similarly, the expression of Flt-1 receptor (Fig. 7.5) and KDR receptor mRNAs (Fig. 7.6) were significantly higher in the early luteal phase than any other stage of the cycle. The same tendency, as for VEGF, for increased VEGF receptor expression in the rescued corpus luteum however, was not apparent.

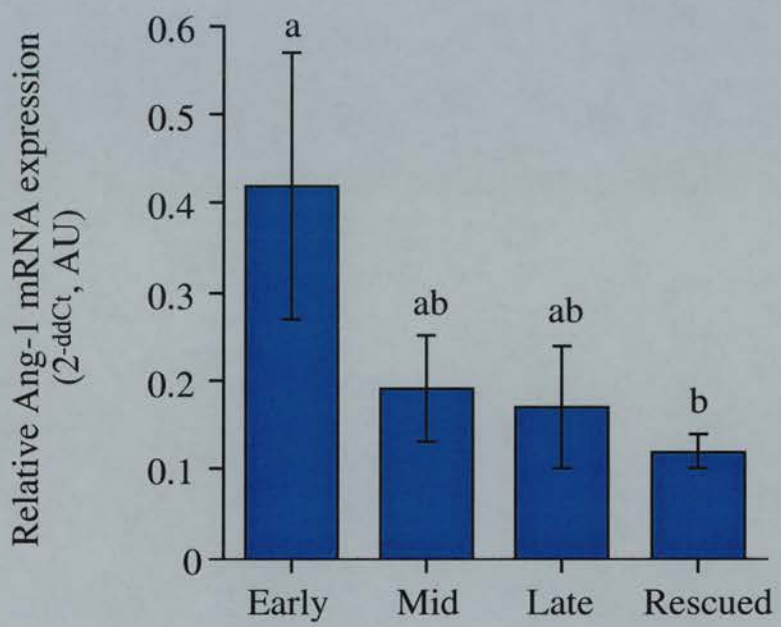

Figure 7.1 Expression of Angiopoietin-1 mRNA in the human corpus luteum

Quantification of Ang-1 mRNA expression during the luteal phase and in hCG rescued human corpora lutea, following Real Time Quantitative RT-PCR. Values are means ± SEM. Different letters denote significant differences between groups, $P<0.05$.

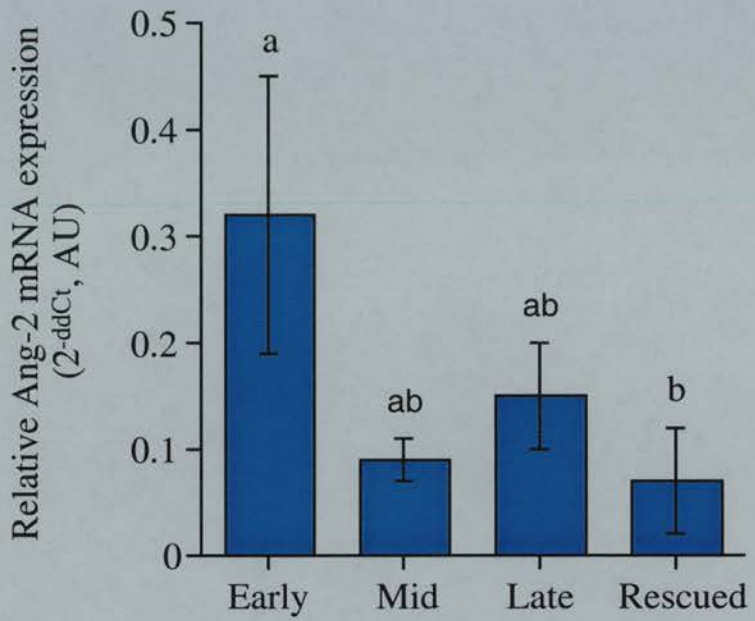

Figure 7.2 Expression of Angiopoietin-2 mRNA in the human corpus luteum

Quantification of Ang-2 mRNA expression during the luteal phase and in hCG rescued human corpora lutea, following Real Time Quantitative RT-PCR. Values are means ± SEM. Different letters denote significant differences between groups, $P<0.05$.

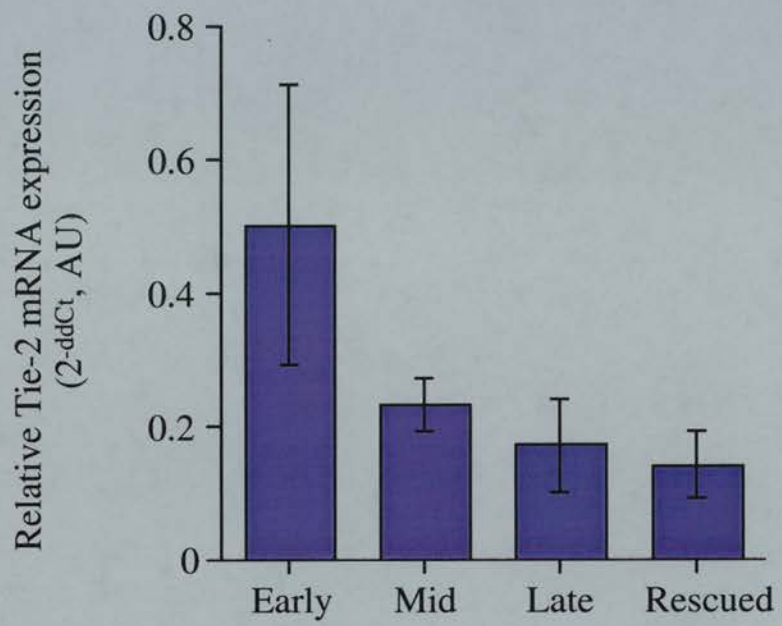

Figure 7.3 Expression of the Angiopoietin receptor, Tie-2 mRNA in the human corpus luteum

Quantification of Tie-2 mRNA expression during the luteal phase and in hCG rescued human corpora lutea, following Real Time Quantitative RT-PCR. Values are means ± SEM. Significant differences between groups were not observed.

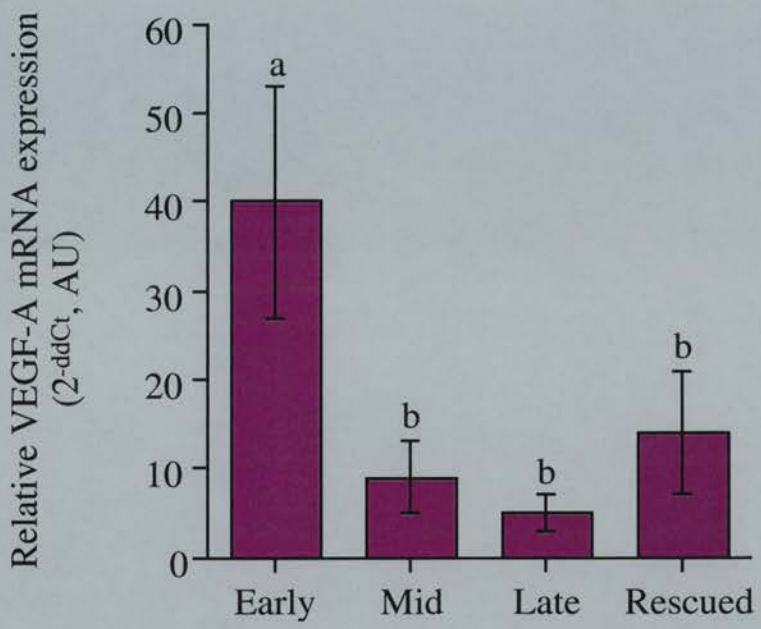

Figure 7.4 Expression of VEGF-A mRNA in the human corpus luteum

Quantification of VEGF mRNA expression during the luteal phase and in hCG rescued human corpora lutea, following Real Time Quantitative RT-PCR. Values are means ± SEM. Different letters denote significant differences between groups, $P<0.05$.

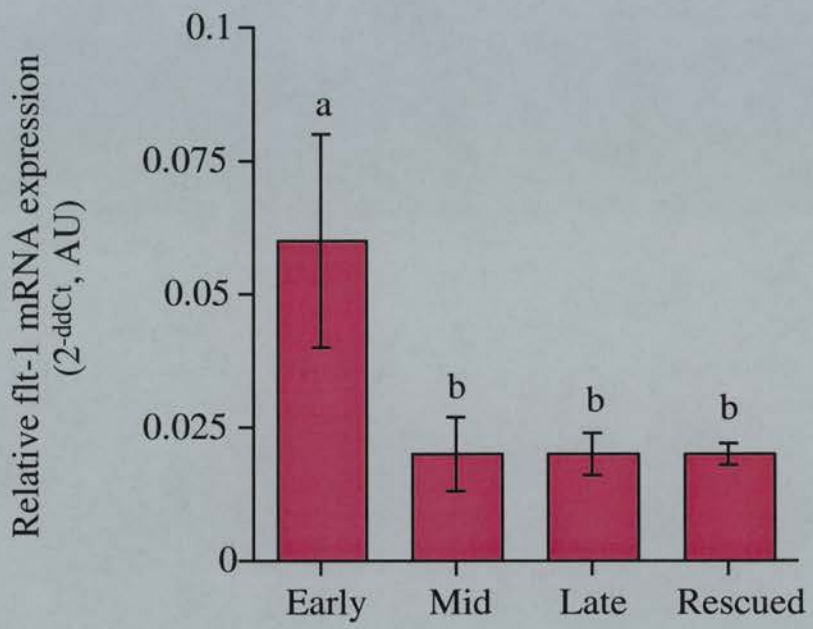

Figure 7.5 Expression of the VEGF receptor, Flt-1 mRNA in the human corpus luteum

Quantification of Flt-1 mRNA expression during the luteal phase and in hCG rescued human corpora lutea, following Real Time Quantitative RT-PCR. Values are means ± SEM. Different letters denote significant differences between groups, $P<0.05$.

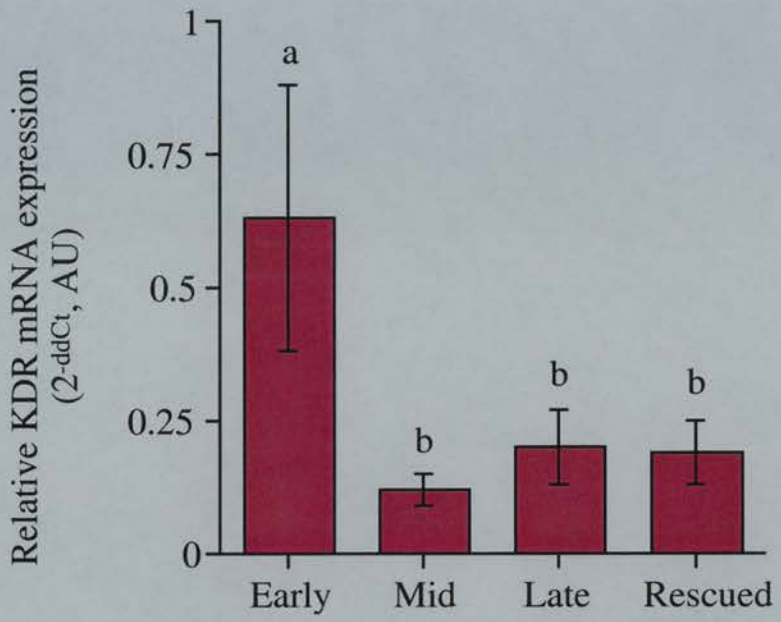

Figure 7.6 Expression of the VEGF receptor, KDR mRNA in the human corpus luteum

Quantification of KDR mRNA expression during the luteal phase and in hCG rescued human corpora lutea, following Real Time Quantitative RT-PCR. Values are means ± SEM. Different letters denote significant differences between groups, $P<0.05$.

7.4 Discussion

This study indicated that the early luteal phase is associated with high levels of mRNA for the Ang-1, Ang-2, their Tie-2 receptor, VEGF and its Flt-1 and KDR receptors, and that there was no significant up regulation of any factor in the corpus luteum at any stage of the luteal phase or in simulated early pregnancy following hCG rescue. The results imply that the angiopoietins and VEGF may modulate the intense angiogenesis associated with the early luteal phase.

High levels of Ang-1 mRNA in the early luteal phase is consistent with the postulated role of this molecule in the recruitment of pericytes and stabilisation of blood vessels. Presumably, translation of this mRNA and protein expression of Ang-1 protein would occur later in the development of the corpus luteum coinciding with the increased pericyte coverage demonstrated in the mid-luteal phase (Chapter 3). Without measuring Ang-1 protein levels this cannot be clarified. In the developing corpus luteum there is an invasion of mature vessels from the thecal layer of the ovulatory follicle, and so high expression of Ang-1 in the early luteal phase could be attributed to continued expression in the theca derived lutein compartment which would be necessary for the maintenance of stability in a proportion of vessels in which intense angiogenesis was not taking place. Nevertheless, postulated roles for Ang-1 in associated angiogenic activities, directly regulating the endothelial cell phenotype have recently been demonstrated. Koblizek *et al.,* (1998), demonstrated that Ang-1 stimulates endothelial cell sprouting *in vitro*, and Ang-1 is chemotactic for cultured endothelial cells (Witzenbilcher *et al.*, 1998), both effects occurring in the absence of accessory cells. This suggests a new role for Ang-1 early in the angiogenic process.

High levels of Ang-1 expression in the early corpus luteum were coincidental with increased Ang-2 expression. Goede *et al.,* (1998) demonstrated that levels of Ang-1 mRNA expression equalled Ang-2 expression in the early bovine corpus luteum. It is believed that Ang-1 is constitutively expressed in the normal vasculature of the adult being present in non-angiogenic tissues (Maisonpierre *et al.*, 1997) and that it is the relative proportions of Ang-2 which dictate the Tie-2 mediated effects. Thus, in the human corpus luteum, the high level of Ang-2 expression in the angiogenic early luteal phase could reflect the postulated role for Ang-2 competitively inhibiting Ang-1 at the level of the Tie-2 receptor causing vessel

destabilisation and allowing access of angiogenic growth factors to susceptible endothelial cells. The associated high level of Tie-2 expression in the early corpus luteum however, provides extra binding sites for both ligands, supporting roles for both Ang-1 and Ang-2 in the intense angiogenesis associated with the developing corpus luteum.

Ang-2 mRNA expression increased in the late luteal phase. Although this was not a significant elevation, it does reflect a role for Ang-2 in the vessel destabilisation and regression associated with this stage. In the absence of VEGF, as demonstrated by low mRNA and protein levels (Chapter 3), the Ang-2 inhibition of Tie-2 phosphorylation and subsequent facilitation of vessel destabilisation is likely to promote the regression of luteal vasculature which has been shown to occur in the late human corpus luteum (Chapter 3). However, there is no evidence from this Chapter to support this hypothesis and so it is not possible to contribute to the debate.

As previously demonstrated (Chapter 3) VEGF protein is highly expressed in the early human corpus luteum correlating with the current findings of high VEGF mRNA expression. Elevated VEGF and Ang-2 levels are consistent with the high angiogenic activity of the early luteal phase, in which VEGF access and subsequent endothelial cell proliferative and migratory actions are likely to be facilitated by the effects of Ang-2 on vessel destabilisation. Simultaneous high expression of both VEGF receptors (Flt-1 and KDR) supports the potent angiogenic action of VEGF at this stage in luteal development, confirming the role of KDR in endothelial cell proliferation and migration, and suggests a previously undefined role for Flt-1 early in the angiogenic process. In the mid-luteal phase, VEGF mRNA expression decreased significantly. This is not consistent with the high levels of VEGF protein as demonstrated by quantitative immunocytochemistry in the human mid-corpus luteum (Chapter 3), however does suggest that VEGF activity could be subject to post-transcriptional regulation. Hazzard *et al.*, (1999b) demonstrated in the rhesus monkey that after the administration of an ovulatory stimulus of hCG, periovulatory follicular fluid VEGF protein concentrations increased dramatically, however VEGF mRNA expression was not altered, signifying translational regulation of VEGF.

There was no significant up-regulation of any factor in the hCG rescued corpus luteum, although there was a tendency for VEGF message to increase as a result of luteal rescue. It has been demonstrated that hCG rescue leads to an increase

VEGF protein expression above mid-luteal values signifying the increased angiogenic activity of this tissue (Chapter 3). The failure to demonstrate a concurrent rise in VEGF mRNA gives further evidence for the translational regulation of VEGF in the primate corpus luteum. Surprisingly, this study demonstrates that the angiopoietins are not involved in the increased angiogenic activity or vessel stabilisation previously demonstrated to occur during luteal rescue (Chapter 3), although translational regulation of these factors cannot be disregarded.

Conversely, a role for Ang-2 during hCG rescue has been indicated by others in our group using quantitative *in situ* hybridisation (Wulff *et al.*, 2000). This study demonstrates that hCG rescue of the human corpus luteum is associated with an up-regulation of Ang-2 and VEGF mRNAs, which correlates with the postulated role of Ang-2 in prolific angiogenesis in the presence of VEGF. This finding supports the results in Chapter 3 which indicate that hCG rescue is associated with increased endothelial cell proliferation, endothelial cell area and VEGF protein expression. The demonstration that expression of VEGF mRNA increased during luteal rescue *in vivo* correlates with the previous finding *in vitro* that expression of VEGF mRNA was up-regulated in cultured human luteinised granulosa cells following CG administration (Neulen *et al.*, 1998). In this study, maximal Tie-2 expression in the early luteal phase is concurrent with elevated Ang-1 and Ang-2 mRNA expression, suggesting that Tie-2 expression is regulated by the availability of its ligands. This was also proposed by Wulff et al., (2000) where rescue of the corpus luteum led to corresponding increases in Ang-2 and Tie-2 mRNA.

It appears that the failure to find elevations in Ang-2, Tie-2 and VEGF mRNA expression during luteal rescue by quantitative RT-PCR, is in contrast to previous studies. The reasons for these discrepancies are possibly due to limitations in the RNA extraction method. Wulff et al., (2000) describe a complex pattern of expression of Ang-2 mRNA in the human corpus luteum. Ang-2 mRNA was strongly expressed in a minority of individual luteal and endothelial cells, found either singly or in clusters, presumably associated to areas of intense angiogenic activity as suggested for the rat corpus luteum (Maisonpierre *et al.*, 1997). Therefore, the extraction of RNA from a small piece of luteal tissue cannot represent the whole structure, in which differential patterns of growth factor expression are present. This notion is supported by the fact that there is a homogeneous expression of VEGF

mRNA throughout the corpus luteum (Wulff *et al.*, 2000) and RT-PCR-quantified expression of VEGF mRNA from total RNA extracted from these small pieces of luteal tissue reflects the *in situ* quantified levels of expression of VEGF mRNA more closely, with an increase, although not significant, during luteal rescue. The large SEM values seen for each group, signify a large variety in levels of expression between samples in one group, and subsequent failure to demonstrate statistically significant differences in expression between groups, which also signifies the heterogeneous nature of the tissue analysed. Results in this study correlated with the trends seen in preliminary data collected from other Real Time quantitative RT-PCR runs, and so discrepancies between these data and previous studies using other techniques appears not to reflect any pitfalls in the RT-PCR quantitative method used, such as inter-run variance. Due to the small differences in expression of the angiopoietins, their Tie –2 receptor, VEGF-A and its flt-1 and KDR receptors, observed between stages of the luteal phase we're uncertain whether the whole luteal mRNA population was represented in the RNA investigated. Therefore, we can conclude that this study demonstrates the importance of mRNA quantification from a large pool of RNA which represents the tissue as a whole.

Chapter 8

General Discussion

This thesis has presented the results of a series of investigations into the control of luteal angiogenesis in the primate and its *in vivo* manipulation in the marmoset monkey. A discussion of the results obtained have been presented in the relevant experimental chapters, and so this section provides an opportunity to summarise the main findings of the thesis, discuss the relative merits of the model used for inhibition of luteal angiogenesis and its clinical implications. In an attempt to clarify unexplained results and to expand the clinical applications of the model, areas for further investigation will be documented throughout the General Discussion.

8.1 The findings of the thesis

At the beginning of this research information concerning primate luteal angiogenesis was limited. A description of the timing of luteal angiogenesis in the primate had recently been described (Christenson and Stouffer, 1996b) demonstrating that luteal development was associated with intense angiogenesis, however, no working model for the analysis of anti-angiogeneic agents had been established. This thesis was designed to investigate the control of angiogenesis in the primate corpus luteum and examine the dependence of luteal function on such angiogenesis by *in vivo* manipulation in the marmoset monkey. A number of important findings have been described. 1) We have demonstrated that luteal angiogenesis can be quantified by measuring specific parameters associated with neovascularisation, such as endothelial cell proliferation, endothelial cell content, growth factor expression, and recruitment of periendothelial support cells for maturation of the newly formed vasculature; and that this can be quantified effectively by immunocytochemical methods. 2) The early luteal phase displays an intense period of angiogenesis which results in the formation of an extensive microvascular network in the mid-luteal phase. Angiogenesis is ongoing in the mid-luteal phase but at a lower level. Luteal regression is associated with a marked decrease in angiogenesis; and hCG rescue, in the human, with a significant increase in angiogenic activity and vessel stabilisation. 3) We have developed a robust model to test anti-angiogenic factors using approaches which target both the intense early luteal angiogenesis and ongoing angiogenesis in the mid-luteal phase. In doing so, we have demonstrated that the intense period of angiogenesis during the early luteal phase in the marmoset is

controlled by gonadotrophin stimulation of luteal steroidogenic cells, growth factors from which are believed to act in a paracrine fashion stimulating endothelial cell migration and proliferation. 4) The angiogenesis inhibitor TNP-470, which prevented normal luteal development and function in the rodent, had no effect on luteal angiogenesis in the marmoset, indicating that caution is needed when extrapolating results from infraprimate species. 5) Finally, and of paramount importance, this thesis reports that luteal angiogenesis is essential for normal luteal function in the marmoset. This research established the fact that luteal angiogenesis is driven primarily by VEGF, the biological activity of which is critical for normal luteal function throughout the active lifespan of the primate corpus luteum.

The use of quantitative immunocytochemistry was demonstrated to be effective in measuring the angiogenic activity of each corpus luteum, and for assessing morphological changes associated with luteal development and effects of treatment. The incorporation of BrdU by proliferating cells in the S phase of the cell cycle was shown to be a robust, reproducible technique, which could serve as the basis for measuring vessel proliferation in subsequent studies. Whilst investigating the possibility of quantifying luteal angiogenesis by immunocytochemical methods it was important to address whether one luteal section would reflect the whole corpus luteum, especially when considering the fact that neovascularisation of this tissue results in a complex web of branching blood vessels, which are not necessarily distributed evenly throughout the gland. It was demonstrated that for measurements of both endothelial cell proliferation and endothelial cell area, one section was representative of the whole gland, and that quantification of angiogenesis in one luteal section in future studies was sufficient to assess the effects of putative inhibitors of angiogenesis.

The techniques developed for quantitative analysis of endothelial cell proliferation and measurements of endothelial cell area in luteal sections, were extended to quantify angiogenic growth factors, such as VEGF, and the degree of vessel maturation as determined by periendothelial support cell contact. In doing so, it was established that pericytes were recruited in the early, intensely angiogenic phase of luteal development, suggesting that they play a dual role, contributing to both the angiogenic activity of the corpus luteum and to vessel maturation and cessation of vessel growth. The roles were determined by the spatial relationship of

pericytes with respect to endothelial cells. This *in vivo* data supports previously reported *in vitro* studies in which the contact of co-cultures of endothelial cells and pericytes determined the stimulatory or inhibitory action of pericytes on endothelial cell growth and migration (Hirschi *et al.*, 1999).

Using the novel information concerning the level of angiogenic activity and expression of VEGF during luteal development in the marmoset, gained in Chapter 3, it was possible to develop a robust model to test the effects of putative angiogenic inhibitors on luteal angiogenesis and function. The first approach was to determine the gonadotrophin support of early luteal intense angiogenesis and mid-luteal ongoing angiogenesis by inhibiting release of the principal luteal gonadotropin, LH, using a GnRH antagonist. This treatment had a profound inhibitory effect on early luteal endothelial cell proliferation and a marked disruptive effect on lutein cell morphology, surprisingly however, a concurrent decrease in establishment of the microvascular tree was not seen. The method of quantification of endothelial cell content per area of luteal tissue may be one explanation for the failure to find a decrease in endothelial cell area following GnRH antagonist treatment. The severe disruption of lutein cell morphology induced by LH withdrawal led to shrinkage of the corpus luteum. To address this problem, a similar approach as used for quantification of endothelial cell content throughout the luteal phase, compensating for a difference in luteal volume, would be necessary. However, because of the loss of lutein cell integrity, the major factor contributing to luteal volume, it was not possible to measure lutein cell area and obtain a conversion factor to measure a correspondingly smaller area of GnRH antagonist-treated tissue. An alternative approach to measure endothelial cell content or luteal volume should therefore be considered, perhaps measuring endothelial cell area per constant number of cell nuclei.

Another surprising effect of GnRH antagonist treatment was the failure to suppress endothelial cell proliferation in the mid-luteal phase although lutein cell morphology was severely compromised. It is possible that other cell types, such as fibroblasts, are proliferating and incorporate BrdU after such damaging treatment, in a similar response as that seen during normal luteolysis when the proportion of fibroblast-like cells is shown to increase. Dual labelling studies with BrdU and a specific fibroblast marker would determine if fibroblast proliferation was induced

after GnRH antagonist treatment in the mid-luteal phase. Another explanation for the failure to demonstrate decreased endothelial cell proliferation after treatment in the mid-luteal phase could be that the control of ongoing angiogenesis at this stage is not dependent on gonadotropin support. The fact that the intense angiogenesis in the early luteal phase is clearly gonadotropin-dependent could suggest a differential stage-dependent regulation of luteal angiogenesis in the marmoset.

The use of GnRH antagonist treatment is limited in the fact that it results in withdrawal of the major driving force of luteal function, and therefore suppresses all aspects of the angiogenic process, which makes it difficult to elucidate individual mechanisms of angiogenic regulation. A more scientific approach was to specifically target the angiogenic process. This led to the use of a synthetic angiogenesis inhibitor, TNP-470, based on a previous study (Klauber *et al.*, 1997) in which TNP-470 , administered subcutaneously, was demonstrated to inhibit luteal development in mice. This compound was also being used in clinical trials as an inhibitor of tumour angiogenesis (Figg *et al.*, 1997; Kudelka *et al.*, 1997; Dezube *et al.*, 1998) and so it was pertinent to investigate possible side effects on female reproduction. The failure of TNP-470 to effect luteal angiogenesis in the marmoset following i.v. injection (Chapter 5; Fraser *et al.*, 1999a), may be due to the different route of administration and/or short half-life of the compound. Clinical trials have shown that all active metabolites of this compound are cleared from the circulation in approximately 2.5 hours (Figg *et al.*, 1997; Bhargava *et al.*, 1999). Variable effects of TNP-470 to reduce tumour growth have been demonstrated in clinical trials (Kudelka *et al.*, 1997; Twardowski and Gradishar, 1997; Dezube *et al.*, 1998), doses were however low, as neurotoxic side effects were apparent. These side effects were completely reversible due to the short half life of the compound and so it was recommended that exploration of prolonged i.v. infusion was warranted (Bhargava *et al.*, 1999). In the marmoset, doses of TNP-470 similar to those used in the Klauber study, on a body weight basis, were administered on the day of ovulation and for 10 days thereafter, with a lack of effect on luteal development. This may be explained by interspecies variability of TNP-470 metabolism (Placidi *et al.*, 1997) or the route of administration. Constant infusion of the drug to marmosets over the 10 day period was not possible as animals would need constant anaesthesia and restraint to prevent

removal of the infusion device and self-harm, although an alternative approach using a subcutaneous or intrauterine releasing system cannot be ruled out.

The concept of targeting luteal angiogenesis was developed further with the specific inhibition of VEGF, which was believed to be a prime regulator of angiogenesis. Targeting specific endogenous angiogenic factors *in vivo* in this way gives an insight into the roles that they play and elucidates the dependence of the system on such factors. Thus, the neutralisation of VEGF proved a powerful tool in the assessment of its role in the regulation of luteal angiogenesis in the marmoset. Inhibition of VEGF activity in both the early and mid-luteal stages demonstrated that VEGF plays a pivotal role in the control of endothelial cell proliferation and establishment of the luteal vasculature. Suppression of neovascularisation in the corpus luteum as a result of VEGF withdrawal demonstrates that luteal angiogenesis is essential for normal luteal function in the primate, as determined by substantial decreases in plasma progesterone concentration in the absence of steroidogenic cell defects.

The decline in plasma progesterone concentrations was initially considered to be solely the result of decreased angiogenic activity and compromised formation of luteal vasculature. However, studies of VEGF inhibition specifically in the mid-luteal phase, resulted in a rapid decrease of plasma progesterone concentration. Since the microvasculature is fully established at this time an effect of angiogenesis inhibition would not be expected to cause such a rapid decline in plasma progesterone concentrations, more likely result in the maintenance of pretreatment levels. This signifies a major role for VEGF in controlling vascular permeability and thus the diffusion of cholesterol precursors to steroidogenic cells and/or progesterone into the circulation. *In vitro* studies suggest that VEGF increases vascular permeability through the Flt-1 receptor and the production of nitric oxide (Murohara *et al.*, 1998), which leads to dilation of endothelial cell tight junctions (Clancy *et al.*, 1997) permitting extravasation. Therefore, further investigation, for example into the effects of VEGF withdrawal on 1) expression of nitric oxide synthase, 2) expression of endothelial gap junction proteins, and 3) endothelial cell-cell connections by ultrastructural analysis, is warranted to determine the role of vascular permeability in relation to the rapid fall in plasma progesterone concentration. It is also conceivable that the treatment could have an inhibitory effect on pituitary LH secretion. A

decrease in permeability of the hypophysial portal vessels at the hypathalomic-pituitary level, may result in suppression of GnRH access to its pituitary receptor and consequential declines in LH pulsatility. However, it has been demonstrated that suppression of LH during the luteal phase results in characteristic and marked changes in the morphology of the lutein cells (Chapter 4; Fraser *et al.,* 1999b; Dickson and Fraser, 2000) that were not observed after VEGF inhibition, indicating that any change in LH secretion would be minor. Decreased as opposed to complete suppression of LH release may not have such a severe effect on lutein cell morphology whilst still compromise the ability of the cell to synthesis and secrete progesterone. LH pulsatility in the luteal phase is low and detection of any small change in plasma LH concentration is unlikely using existing assays and with the sampling frequency employed, although further analysis could be undertaken.

A comparison of the effects of GnRH antagonist treatment and VEGF immunoneutralisation in the early luteal phase demonstrates a greater suppression of endothelial cell proliferation after GnRH antagonist treatment (Figure 8.1) than after VEGF immunoneutralisation. This suggested that growth factors other than VEGF control primate luteal angiogenesis, such as FGF and the angiopoietins. However, subsequent studies undertaken in our laboratory during the last few months, using a truncated soluble Flt-1 receptor demonstrate similar levels of suppression of endothelial cell proliferation as those obtained after GnRH antagonist treatment (Figure 8.1; Wulff *et al.,* 2001). This signifies that the soluble Flt-1 receptor is a more potent inhibitor of VEGF action, perhaps suppressing other members of the VEGF family, and that full VEGF withdrawal was possibly not obtained using the monoclonal antibody. More importantly, it indicates that luteal angiogenesis in the primate is driven almost solely by VEGF and that contributions of other growth factors are likely to be minimal.

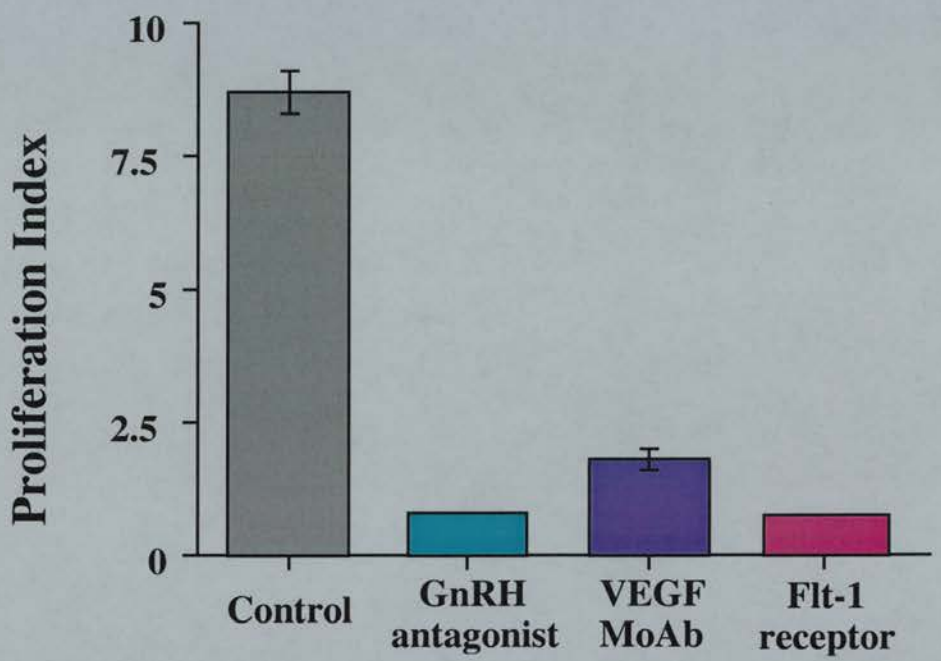

Figure 8.1 The inhibition of Proliferation Index in the marmoset corpus luteum following administration of anti-angiogenic agents

The effect of administration of three anti-angiogenic treatments on luteal endothelial cell proliferation in the marmoset monkey. Note the difference in suppression of PI after GnRH antagonist and anti-VEGF treatment, and the further reduction of PI with truncated soluble Flt-1 receptor as compared to anti-VEGF treatment.

Source: Chapter 4, Chapter 6 and Wulff *et al.*, 2001).

Other studies have demonstrated that VEGF is synthesised by endothelial cells and pericytes in culture (Nomura *et al.*, 1995) and *in vivo* in the bovine corpus luteum (Reynolds and Redmer, 1998). This was not demonstrated in this thesis using an antibody specific to VEGF-A for immunocytochemistry. Yonekura *et al.*, (1999) have demonstrated the expression of VEGF-B, VEGF-C and PlGF mRNA in these vascular cells, and suggest that VEGF related factors produced by endothelial cells and pericytes may have an indirect effect on vessel growth, migration and tube formation in an autocrine or paracrine manner, via the modulation of VEGF-A action. Microvascular cells express plural types of VEGF receptors, such as Flt-1, KDR and Flt-4. Vascular endothelial growth factor-A binds to both Flt-1 and KDR. Platelet derived growth factor and VEGF-B bind to Flt-1. Therefore the presence of high PlGF or VEGF-B may result in masking of Flt-1 in endothelial cells, thereby inhibiting VEGF-A high affinity binding to this receptor. This may in turn allow access of VEGF-A to the low affinity KDR that is abundantly expressed on endothelial cells, in turn stimulating endothelial cell proliferation. Vascular endothelial growth factor-C binds to KDR and Flt-4, thus over production of VEGF-C could decrease the binding of VEGF-A to KDR by competing with VEGF-A and promote Flt-1 binding, and contribution to vascular permeability. The expression of the VEGF-related family of growth factors has not been elucidated in the primate corpus luteum, and their contributions to luteal angiogenesis are unknown. We have demonstrated that VEGF-A can stimulate pericyte recruitment in the early luteal phase however, such recruitment in the mid-luteal phase appears not to be driven by VEGF-A. The stage-specific differences in the control of pericyte recruitment may be a result of differences in the relative expression and actions of other members of the VEGF family. The inter-relationships between VEGF-A and other related factors appear complex, therefore, to increase the understanding of action of VEGF-A in the corpus luteum such studies investigating other VEGF family members are warranted.

Suppression of luteal progesterone production is likely to have adverse effect on endometrial receptivity to an implanting blastocyst. Investigation of expression of progesterone-dependent proteins in the uterus after VEGF withdrawal would address this issue. In the marmoset, endometrial prolactin expression is regulated by progesterone, and prolactin is believed to be essential for endometrial differentiation and ultimately implantation (Dalrymple *et al.*, 2000). A decrease in prolactin levels

in these uterine sections would suggest an indirect effect of VEGF neutralisation, via the suppression of progesterone, on the endometrium. Endometrial quantification of prolactin was however, beyond the scope of this thesis.

This thesis also demonstrated the use of a novel technique, Real Time quantitative RT-PCR, in an investigation to evaluate the expression of angiopoietin and their Tie-2 receptor mRNA in the human corpus luteum. Results using this technique were inconclusive and did not correlate with previous studies from our laboratory (Wulff *et al.*, 2000), due to the fact that extracted RNA did not represent the total luteal population. This research therefore emphasises the need for, and value of multiple techniques which measure both expression of mRNA and protein, using both molecular and histological analysis, to resolve the role of these potential angiogenic factors in the primate corpus luteum.

8.2 The marmoset model for inhibition of luteal angiogenesis

The studies in this thesis utilised the marmoset monkey to examine the dependence of luteal function on angiogenesis, and elucidate the primary factor(s) involved in this process. As a model for the human, the marmoset is not ideal. It is not a mono-ovulatory species, it has a luteal phase length of approximately 20 days as opposed to 14 days in the human, the structure of its corpus luteum differs to that of humans, and the marmoset does not menstruate. However, such invasive investigations of luteal angiogenesis could not be carried out in higher primates. The marmoset has an ovulatory cycle more analogous than any rodent species to that of the human, and so is the most appropriate animal model.

The model of manipulating luteal angiogenesis by targeting specific angiogenic phases of luteal development was designed as a result of extensive research into the angiogenic activity of the corpus luteum (Chapter 3). During the course of this research Ferrara *et al.*, (1998), used truncated soluble Flt-1 receptor to inhibit VEGF activity in a rodent model of hormonally induced ovulation. Despite this being a rodent model which is limited in its relevance to the control of angiogenesis in primates and humans, the timing of treatment casts serious doubt as to whether luteal angiogenesis was specifically targeted. Rats were treated with pregnant mares serum gonadotropin (PMSG), rich in FSH, to initiate follicular

development, then given a bolus of hCG to stimulate ovulation and corpus luteum formation. Truncated soluble Flt-1 receptor was administered twice daily commencing 4-6 hours before PMSG. Treatment of marmosets with truncated soluble receptor, in our laboratory, inhibits follicular development (Wulff *et al.*, unpublished observations). This indicates that, in the study by Ferrara *et al.*, (1998), it was unlikely that luteal angiogenesis was specifically targeted because the timing of treatment probably inhibited normal follicular development which would lead to subnormal corpus luteum formation and function.

The approach taken in this thesis was to inhibit luteal development by specifically timing the administration of treatment to the early luteal phase, that is after ovulation, so any effect on luteal function would be a consequence of inhibition of luteal angiogenesis, not an effect on follicular development. This approach has been successful in elucidating that angiogenesis is essential for normal luteal function, and the role of potential growth factors in luteal angiogenesis by their specific inhibition in the primate. Therefore, this model could be used to examine the effects of other putative endogenous regulators. The recent discovery of differences in expression of the angiopoietins in the human corpus luteum (Wulff *et al.*, 2000) correlating with the known angiogenic activity of the gland indicates a role for these factors in the control or modulation of luteal angiogenesis. There is increasing interest in the scientific world to elucidate the functions of the angiopoietins, and monoclonal antibodies and truncated soluble Tie-2 receptors are being developed at this time. The use of such potential angiopoietin inhibitors in the model created here would be decisive in establishing their contribution to luteal angiogenesis in the primate. The angiopoietins are believed to exert their actions in conjunction with VEGF. Although expression in comparison to VEGF expression has been examined (Chapter 7; Wulff *et al.*, 2000), the dependence of actions of angiopoietins on this primary angiogenic factor has not been established in the primate corpus luteum. It would therefore be justified to evaluate their expression in relationship to VEGF withdrawal after VEGF immunoneutralisation and soluble truncated Flt-1 receptor treatment during the angiogenic stages of the luteal phase.

8.3 Clinical implications of the findings of this thesis

The major function of the corpus luteum is the production of progesterone which results in endometrial receptivity and myometrial quiescence for blastocyst implantation after conception. We have demonstrated that luteal angiogenesis is essential for progesterone production in the primate. Therefore, the strategy to inhibit luteal angiogenesis provides a novel approach to post-ovulatory fertility control. However, a number of scientific questions arise when considering this. 1) Are the effects in ovarian angiogenesis reversible? 2) Is progesterone concentration sufficiently suppressed to prevent the establishment of pregnancy? 3) If not, what would the effects on foetal vasculogenesis be?

Ongoing studies in our laboratory are beginning to answer these questions. Plasma progesterone profiles of animals in which VEGF action was inhibited, demonstrated that after an initial period of plasma progesterone decrease coinciding with treatment, progesterone levels rose to normal values with termination of treatment. This suggests that normal luteal angiogenesis and function was restored, indicating that any effect on follicular development occuring at this time would also be reversible and followed by normal preovulatory development, ovulation and corpus luteum formation. In order to prevent the establishment of pregnancy, further research is needed to investigate the required level of progesterone suppression and the degree of variation between animals. It is possible that the corpus luteum produces an excess of progesterone, and that complete progesterone suppression would be needed to prevent pregnancy in all animals. If this was not achieved it is presumed that the effects of VEGF inhibition on foetal vascularisation would be as detrimental as those seen in murine transgenic models. Therefore the use of angiogenesis inhibition for fertility control demands much more research to ascertain the minimal level of progesterone required to establish pregnancy.

The demonstration that luteal function is dependent on normal luteal angiogenesis not only has implications for new approaches to fertility control but could also lead to treatment of luteal inadequacy which is caused by deficient follicular or luteal angiogenesis.

Tumour growth is dependent on stimulation of new blood vessel growth from the pre-existing vasculature (Folkman and Klagsbrun, 1987) and this dependence on angiogenesis has long been proposed as an attractive therapeutic target. Therefore,

angiogenesis inhibitors are currently being developed primarily for treatment of vascular solid tumours. Anti-angiogenic agents do not kill tumour cells directly, they operate indirectly by inhibiting vascularisation of the tumour and tumour cells die by hypoxia, or from deprivation of endothelial cell-derived survival factors. Inhibition of VEGF has been shown to reduce tumour growth in murine models (Kim *et al.*, 1993) and is currently being tested in clinical trials along with other anti-angiogenic agents which target the pathway at different stages, some of which are shown in Table 8.1. These factors are also likely to have a role in the control of rheumatoid arthritis, retinal neovascularisation and psoriasis in which uncontrollable angiogenesis occurs. The model developed in this thesis could test new generation anti-angiogenic compounds and examine their suitability for further development. Since these inhibitors are being used clinically it is essential that their potential effects on the reproductive system be determined, and the model established here would be highly suitable for such assessment.

Physiological angiogenesis in the corpus luteum is tightly regulated and angiogenic activity decreases with age of the corpus luteum. This could be exploited in a similar model to elucidate endogenous anti-angiogenic factors. In addition, inhibition of these factors or prolonged expression of VEGF could result in continued angiogenic activity. This would serve to assess the relationship between angiogenesis and luteolysis, investigating whether inhibition of vascular regression would prolong the lifespan of the corpus luteum.

The elucidation of pro-angiogenic agents in the primate corpus luteum could have clinical applications in the treatment of conditions which are characterised by decreased vascularisation, such as limb and heart ischaemia. Recent research demonstrates progress in the treatment of such conditions by vascular gene therapy employing recombinant human VEGF DNA (Baumgartner *et al.*, 1998) and local delivery of aFGF, bFGF and VEGF (Thompson *et al.*, 1999).

AGENT	MECHANISM OF ACTION
AG-3340	Metalloproteinase inhibitor
Anti-VEGF monoclonal antibody	**Inhibition of VEGF action**
Batimastat	Metalloproteinase inhibitor
Bay 12-9526	Metalloproteinase inhibitor
Flavopuridol	Protein kinase C inhibitor
Interferon alpha-2a	IP-10 upregulator
Marimastat	Metalloproteinase inhibitor
Neoretna	Metalloproteinase inhibitor
Neovastat	Metalloproteinase inhibitor
Octreotide	Growth factor antagonist
Paclitaxel (Taxol, Docetaxel, Paxane)	Cytotoxic and antiproliferative
Pentosan polysulphate	Growth factor antagonist
PI-88	Growth factor antagonist
Psorvastat	Metalloproteinase inhibitor
Razoxane	Cytotoxic and antiproliferative
SU101	PDGF antagonist
SU5416	VEGF antagonist
Suramin	Growth factor antagonist
Tamoxifen	Cytotoxic and antiproliferative
Tecogalan sodium	Growth factor antagonist
Thalidomide	Unknown
TNP-470 (AGM-1470)	**Numerous**
Vitaxin	Anti-integrin monoclonal antibody

Table 8.1 Anti-angiogenic agents that have entered clinical trials

Source: Clinical Trials Registry, The Angiogenesis Foundation, (Thompson *et al.*, 1999)

Additional research into the potential side effects of inhibition or promotion of angiogenesis is required. Clinical trials have demonstrated unexpected effects of anti-angiogenic agents on the central nervous system (reviewed by Thompson *et al.*, 1999). The discovery that VEGF is a ligand for neuropilin (Soker *et al.*, 1998), a receptor that guides axonal growth, points to links between the control of growth of the microvasculature and the central nervous system. It is therefore appropriate that such effects be explored, and this will depend on the further development of suitable animal models.

8.4 Conclusions

A unique and powerful model has been established to investigate the regulation of luteal angiogenesis in the primate. Using this model, studies reported in this thesis provide compelling evidence that the specific inhibition of luteal angiogenesis severely compromises luteal function. The specific targeting of VEGF has demonstrated that this factor is the major driving force of luteal angiogenesis in the primate. The potential to inhibit angiogenesis in the female reproductive tract should have important implications for clinical practice, but the development of safe and effective strategies will require detailed investigation of suitable animal models, as described in this thesis.

References

References

Abayasekara, D. R. E., Jones, P. M., Persaud, S. J., Michael, A. E. and Flint, A. P. F. (1993) Prostaglandin-F2alpha activates Protein Kinase-C in human ovarian cells. *Mol Cell Endocrinol*, **91**: 51-57

Abdul-Karim, R. W. and Bruce, N. (1973) Blood flow in the ovary and corpus luteum at different stages of gestation in the rabbit. *Fertil Steril*, **24**: 44-47

Abe, J., Zhou, W., Takuwa, N., Taguchi, J., Kurokawa, K., Kumada, M. and Takuwa, Y. (1994) A fumigillin derivative angiogenensis inhibitor, AGM-1470, inhibits activation of cyclin-dependent kinases and phosphorylation of retinoblastoma gene product but not protein tyrosyl phosphorylation or portooncogene expression in vascular endothelial cells. *Cancer Res*, **54**:3407-12

Adams, E. C. and Hertig, A. T. (1969) Studies on the human corpus luteum I. Observations on the ultrastructure of development and regression of the luteal cells during the menstrual cycle. *J Cell Biol*, **41**: 696-715

Adashi, E., Resnick, C., Hernandez, E., Hurwitz, A., Roberts, C., Leroith, D. and Rosenfeld, R. (1991) IGF-1 as an ontraovarian regulator: basic and clinical implications. *Ann NY Acad Sci*, **626**: 161-168

Agudo, S., Zahler, W. and Smith, M. (1984) Effects of PGF2a on the adenylate cyclase and phosphodiesterase activity of ovine corpora lutea. *J Anim Sci*, **58**: 955-962

Albertini, D. and Anderson, E. (1974) The appearance and structure of intercellular connections during the ontogeny of the rabbit ovarian follicle with particular reference to gap junctions. *J Cell Biol*, **63**: 234-250

Amsterdam, A., Koch, Y., Lieberman, M. and Lindner, H. (1975) Distribution of binding sites for human chorionic gonadotripin in the preovulatory follicle of the rat. *J Biol Chem*, **67**: 894-900

Anderson, D. (1926) Lymphatics and blood vessels of the ovary of the sow. *Contrib Embryol*, **17**: 107-123

Antczak, M., Van Blerkom, J. and Clark, A. (1997) A novel mechanism of vascular endothelial growth factor; leptin and transforming growth factor-β2 sequestration in a sub-population of human ovarian follicle cells. *Hum Rep*, 12: 2226-2234

Antonelli-Orlidge, A., Saunders, K., Smith, S. and D'Amore, P. (1989) An activated form of transforming growth factor beta is produced by co-cultures of endothelial cells and pericytes. *Proc Natl Acad Sci USA*, **86**: 4544-4548

Armstrong, D., Goff, A. and Dorrington, J. (1979) Ovarian Follicular Development and Function. In A. Midgley and W. Sadler (eds), Raven Press, New York, p. 169-182.

Asahara, T., Chen, D., Takahashi, T., Fujikawa, K., Kearney, M., Magner, M., Yancopoulos, G. and Isner, J. (1998) Tie2 receptor ligands, angiopoietin-1 and angiopoietin-2, modulate VEGF-induced postnatal neavascularization. *Circ Res*, **83**: 233-240

Augustin, H. G., Braun, K., Telemenakis, I., Modlich, U. and Kuhn, W. (1995) Ovarian angiogenesis: Phenotypic characterization of endothelial cells in a physiological model of blood vessel growth and regression. *Am J Pathol*, **147**: 339-351

Auletta, F., Speroff, L. and Caldwell, B. (1973) Prostaglandin F2-induced steroidogenesis and luteolysis in the primate corpus luteum. *J Clin Endocrinol Metab*, **36**: 405-407

Auletta, F., Kamps, D., Pories, S., Bisset, J. and Gibson, M. (1984) An intra corpus luteum site for the luteolytic action of PGF2a in the rhesus monkey. *Prostaglandins*, **27**: 285-298

Auletta, F. and Flint, A. (1988) Mechanisms controlling corpus luteum function in sheep, cows, non-human primates and women especially in relation to the time of luteolysis. *Endocr Rev*, **9**: 88-105

Ausprunk, D., Falterman, K. and Folkman, J. (1978) The sequence of events in the regression of of corneal capillaries. *Lab Invest*, **38**: 284-294

Azmi, T. I. and O'Shea, J. D. (1984) Mechanism of deletion of endothelial cells during regression of the corpus luteum. *Lab Invest*, **51**: 206-217

Baird, D., Baker, T., McNatty, K. and Neal, P. (1975) Relationship between the secretion of the corpus luteum and the length of the follicular phase of the ovarian cycle. *J Reprod Fertil*, **45**: 611-619

Baird, D., Backstrom, T., McNeilly, A., Smith, S. and Wathen, C. (1984) Effect of enucleation of the corpus luteum at different stages of the luteal phase of the human menstrual cycle on subsequent follicular development. *J Reprod Fertil*, **70**: 615-624

Baird, A. and Ling, N. (1987) Fibroblast growth factors are present in the extracellular matrix produced by endothelial cells in vitro: implications for a role of heparinase-like enzymes in the neovascular response. *Biochem Biophys Res Commun*, **142**: 428-435

Bassett, D. (1943) The changes in the vascular pattern of the ovary of the albino rat during the estrous cycle. *Am J Anat*, **73**: 251-291

Bassett, S., Little-Ihrig, L., Mason, J. and Zeleznik, A. (1991) Expression of messenger ribonucleic acids that encode for 3 beta-hydroxysteroid dehydrogenase and cholesterol-side chain cleavage enzymes throughout the luteal phase of the macaque menstrual cycle. *J Clin Endocrinol Metab*, **72**: 362-366

Baumgartner, I., Pieczek, A., Manor, O., Blair, R., Kearney, M., Walsh, K. and Isner, I. (1998) Constitutive expression of phVEGF165 after intramuscular gene transfer promotes collateral vessels development in patients with critical limb ishaemia. *Circulation*, **97**: 1114-1123

Behrman, H., Aten, R. and Pepperell, J. (1991) Cell-to-cell interactions in luteinization and luteolysis. In S. Hillier (eds), *Ovarian Endocrinology*. Blackwell Scientific, Oxford, p. 190-225.

Behrman, H. R., Endo, T., Aten, R. F. and Musicki, B. (1993) Corpus luteum function and regression. *Reprod Med Rev*, **2**: 153-180

Beling, C., Marcus, S. and Markham, S. (1970) Functional activity of the corpus luteum following hysterectomy. *J Clin Endocrinol Metab*, **30**: 30-39

Bellomo, D., Headrick, J., Silins, G., Paterson, C., Thomas, P., Gartside, M., Mould, A., Cahill, M., Tonks, I., Grimmond, S., Townson, S., *et al.* (2000) Mice lacking the vascular endothelial growth factor-B have smaller hearts, dysfunctional cornary vasculature, and impaired receovery from coronary ischemia. *Circ Res*, **86**: e29-e35

Benjamin, L., Hemo, I. and Keshet, E. (1998) A plasticity window for blood vessel remedolling is defined by pericyte coverage of the preformed endothelail network and is regulated by PDGF-B and VEGF. *Development*, **125**: 1591-1598

Benjamin, L., Golijanin, D., Itin, A., Pode, D. and Keshet, E. (1999) Selective ablation of immature blood vessels in established human tumours follows VEGF withdrawal. *J Clin Invest*, **103**: 159-165

Berges, R. R., Furuya, Y., Remington, L., English, H. F., Jacks, T. and Isaacs, J. T. (1993) Cell proliferation, DNA repair, and p53 function are not required for programmed death of prostatic glandular cells induced by androgen ablation. *Proc Natl Acad Sci USA*, **90**: 8910-8914

Bhargava, P., Marshall, J., Rizvi, N., Dahut, W., Yoe, J., Figuera, M., Phopps, K., Ong, V., Kato, A.,Hawkins, M. (1999) A phase I and pharmokinetic study of TNP-470 administered weekly to patients with advanced cancer. *Clin Cancer Res*, **5**: 1989-1995

Bicknell, R. (1996) Introduction to the endothelial cell. In R. Bicknell (eds), *Endothelial Cell Culture*. University Press, Cambridge, p. 1-6.

Block, E. (1951) Quantitative morphological investigations of the follicular system in women: Variations in the different phases of the sexual cycle. *Acta Endocrinol (kbh)*, **8**: 33-54

Boado, R. and Pardridge, W. (1994) Differential expression of alpha-actin mRNA and immunoreactive protein in brain microvascular pericytes and smooth muscle cells. *J Neurosci Res*, **39**: 430-435

Boulton, R. and Hodgson, H. (1995) Assessing cell proliferation: A methodological review. *Clin Sci*, **88**: 119-130

Bramley, T., Stirling, D., Swanston, I., Menzies, G., McNeilly, A. and Baird, D. (1987) Specific binding sites for GnRH, LH/hCG, LDL, Prolactin and FSH in homogenates of human corpus luteum. II. Concentrations throughout the luteal phase of the menstrual cycle and early pregnancy. *J Endocrinol*, **113**: 317-327

Brem, H. and Folkman, J. (1993) Analysis of experimental antiangiogenic therapy. *J Pedratric Surg*, **28**: 445-451

Brown, J. (1978) Pituitary control of ovarian function - concepts derived from gonadotropin therapy. *Aus NZ J Obstet Gynaecol*, **18**: 46-54

Brown, L., Detman, M., Claffey, K., Nagy, J., Feng, D., Dvorak, A. and Dvorak, H. (1996) Vascular permeability factor/vascular endothelial growth factor; a multifunctional angiogenic cytokine. In I. Goldber and R. E (eds), *Control of Angiogenesis*. Birkhauser Verlag, Berlin.

Brown, M. and Goldstein, J. (1986) A receptor-mediated pathway for cholesterol homeostasis. *Science*, **232**: 34-47

Burger, H. (1993) Evidence for a feedback role of inhibin in FSH regulation in women. *Hum Reprod*, **S2**: 129-32

Burr, J. and Davies, J. (1951) The vascular system of the rabbit ovary and its relationship to ovulation. *Anat Rec*, **111**: 273-297

Cameron, J. and Stouffer, R. (1982) Gonadotropin receptors of the corpus luteum. I. Characterisation of 125I-labeled human LH and hCG binding to luteal membranes from the rhesus monkey. *Endocrinology*, **110**: 2059-2067

Cao, Y. H., Chen, H., Zhou, L., Chiang, M. K., Anandapte, B., Weatherbee, J. A., Wang, Y. D., Fang, F. Y., Flanagan, J. G.,Tsang, M. L. S. (1996) Heterodimers of placenta growth factor vascular endothelial growth factor - Endothelial activity, tumor cell expression, and high affinity binding to Flk-1/KDR. *J Biol Chem*, **271**: 3154-3162

Carlson, J., Wu, X. and Sawanda, M. (1993) Oxygen radicals and the control of ovarian corpus luteum function. *Free Radical Biol*, **14**: 78-84

Carmeliet, P., Ferreira, V., Breier, G., Pollefeyt, S., Kieckens, L., Gertsenstein, M., Fahrig, M., Vandenhoeck, A., Harpal, K., Eberhardt, C., C, D., et al. (1996) Abnormal blood vessel development and lethality in embryos lacking a single VEGF allele. *Nature*, **380**: 435-439

Carr, B., MacDonald, P. and Simpson, E. (1982) The role of lipoproteins in the regulation of progesterone secretion by the human corpus luteum. *Fertil Steril*, **38**: 303-311

Castracane, V., Moore, G. and Shaikh, A. (1979) Ovarian function of hysterectomised Maccaca fuscicularis. *Biol Reprod*, **20**: 462-472

Chaffin, C. and Stouffer, R. (1999) Expression of matrix metalloproteinase and their tissue inhibitor mRNAs in macaque periovulatory granulosa cells; time course and steroid regulation. *Biol Reprod*, **61**: 14-21

Channing, C. (1970) Influences of the in vivo and in vitro hormonal environment upon luteinisation of granulosa cells in tissue culture. *Rec Prog Horm Res*, **26**: 589-622

Charpin, C., Devictor, B., Bergeret, D., Andrac, L., Boulat, J., Horschowski, N., Lavaut, M. and Piana, L. (1995) CD31 quantitative immunocytochemical assays in breast carcinomas. Correlation with current prognostic factors. *Am J Clin Pathol*, **103**: 443-448

Chomczynski, P. and Sacchi, N. (1987) Single-step method of RNA isolation by acid guanidium thiocynate-phenol-chloroform extraction. *Anal Biochem*, **162**: 156-159

Christenson, L. K. and Stouffer, R. L. (1996a) Isolation and culture of microvascular endothelial cells from the primate corpus luteum. *Biol Reprod*, **55**: 1397-1404

Christenson, L. K. and Stouffer, R. L. (1996b) Proliferation of microvascular endothelial cells in the primate corpus luteum during the menstrual cycle and simulated early pregnancy. *Endocrinology*, **137**: 367-374

Christenson, L. K. and Stouffer, R. L. (1997) Follicle-stimulating hormone and luteinizing hormone/chorionic gonadotropin stimulation of vascular endothelial growth factor production by macaque granulosa cells from pre- and periovulatory follicles. *J Clin Endocrinol Metab*, **82**: 2135-2142

Clancy, R., Rediske, J., Tang, X., Nijher, N., Frenkel, S., Philips, M. and Abramson, S. (1997) Outside-in signaling in the chondrocyte. Nitric oxide disrupts fibronectin-induced assembly of a subplasmalemmal actin/rho A/focal adhesion kinase signaling complex. *J Clin Invest*, **100**: 1789-1796

Clapp, C., Martial, J., Guzman, R., Rentier-Delrue, F. and Weiner, R. (1993) The 16 kDa N-terminal fragment of human prolactin is a potent inhibitor of angiogenesis. *Endocrinology*, **133**: 1292-1299

Clark (1900) The origin, development and degeneration of the blood vessels of the human ovary. *John Hopkins Hospital Report*, **9**: 593-676

Clark, D. E., Smith, S. K., Sharkey, A. M. and Charnock-Jones, D. S. (1996) Localization of VEGF and expression of its receptors flt and KDR in human placenta throughout pregnancy. *Hum Reprod*, **11**: 1090-1098

Clarke, I. (1996) The Hypathalamo-Pituitary Axis. In S. Hillier, H. Kitchener and J. Neilson (eds), *Scientific Essentials of Reproductive Medicine*. WB Saunders Company Ltd., p 120-132.

Corner, G. (1943) The hormones in human reproduction. University Press, Princeton.

Corner, G. (1956) The histological dating of the human corpus luteum of menstruation. *Am J Anat*, **98**: 377-401

Cretton-Scott, E., Placidi, L., McClure, H., Anderson, D. and Sommadossi, J. (1996) Pharmacokinetics and metabolism of O-(choroacetyl-carbomol) fumagillol (TNP-470, AGM-1470) in rhesus monkeys. *Cancer Chemother Pharmocol*, **38**: 117-122

Crisp, T. and Channing, C. (1972) Fine structural events correlated with progestin secretion during the luteinisation of rhesus monkey granulosa cells in culture. *Biol Reprod*, **7**: 55-72

Crocker, D., Murad, T. and Greer, J. (1970) Role of the pericyte in wound healing. An ultrastructural study. *Exp Mol Pathol*, **13**: 51-65

Csapo, A., Pulkkinen, M. and Wiest, W. (1973) Effects of luteectomy and progesterone replacement therapy in early pregnancy patients. *Am J Obstet Gynecol*, **115**: 759-765

Cummings, A. and Yochim, J. (1984) Differentiation of the uterus in preparation for gestation: a model for the action of progesterone. *J Theor Biol*, **106**: 353-374

Dalrymple, A. and Jabbour, H. (2000) Localization and signalin gof the prolactin receptor in the uterus of the common marmoset monkey. *J Clin Endocrinol Metab*, **85**: 1711-1718

D'Amore, P. and Smith, S. (1993) Growth factor effects on cells of the vascular wall: a survey. *Growth Factors*, **8**: 61-75

Darland, D. and D'Amore, P. (1999) Blood vessel maturation: vascular development comes of age. *J Clin Invest*, **103**: 157-158

Davies, B., Brown, P., East, N., Crimmin, N. and Balkwill, F. (1993) A synthetic matrix metalloproteinase inhibitor decreases tumor burden and prolongs the survival of mice bearing human ovarian carcinoma xenografts. *Cancer Res*, **53**: 2087-2091

Davis, S., Aldrich, T., Jones, P., Acheson, A., Compton, D., Jain, V., Ryan, T., Bruno, J., Radziejewski, C., Masonpierre, P.,Yancopoulos, G. (1996) Isolation of angiopoietin-1, a ligand for the Tie-2 receptor, by secretion trap expression cloning. *Cell*, **87**: 1161-1169

Dawood, M. and Khan-Dawood, F. (1986) Human ovarian oxytocin; its source and relationship to steroid hormones. *Am J Obstet Gynecol*, **154**: 756-763

Deghenghi, R., Boutignon, F., Wüthrich, P. and Lenaerts, V. (1993) Antarelix (EP 24332) a novel water soluble LHRH antagonist. *Biomed Pharmacother*, **47**: 107-110

Denekamp, J. (1984) Vasculature as a target for tumour therapy. In F. Hammersmith and O. Hudlicka (eds), *Progress in Applied Microcirculation*. Karger, Basel, p. 28-38.

Dezube, B., Von Roenn, J., Holden-Wiltse, J., Cheung, T., Remick, S., Cooley, T., Moore, J., Sommadossi, J., Shriver, S., Suckow, C.,Gill, P. (1998) Fumagillin analog in the treatment of Kapsi's sarcoma: a phase 1 AIDS clinical trial group study. AIDS clinicla trial group no. 215 team. *J Clin Oncol*, **16**: 1444-1449

Dharmarajan, A., Bruce, N. and Meyer, G. (1985) Quantitative ultrastructural characteristics relating to transport between luteal cell cytoplasm and blood in the corpus luteum of the pregnant rat. *Am J Anat*, **172**: 87-89

Daiz-Flores, L., Gutierrez, R., Varela, H., Rancel, N. and Valladarea, F. (1991) Microvascular pericytes: a review of their morphological and functional characteristics. *Histol Histopathol,* **6**: 269-286

Dickson, S. and Fraser, H. (2000) Inhibition of early luteal angiogenesis by gonadotropin-releasing hormone antagonist treatment in the primate. *J Clin Endocrinol Metab*, **85**: 2339-2344

Diebold, J., Dopfer, K., Lai, M. and Lohrs, U. (1994) Comparison of differnet monoclonal antibodies for the immunohistochemical assessment of cell proliferation in routine colorectal biopsies. *Scandin J Gastroenterol*, **29**: 47-53

diZerega, G. and Hodgen, G. (1981) Folliculogenesis in the primate ovarian cycle. *Endocr Rev*, **2**: 27-49

Dodge, A., Lu, X. and D'Amore, P. (1993) Density-dependent endothelial cell production of an inhibitor of smooth muscle cell growth. *J Cell Biochem*, **53**: 21-31

Dubourdieu, S., Charbonnel, B., Massai, M., Marraoui, J., Spitz, I. and Bouchard, P. (1991) Suppression of corpus luteum function by the GnRH antagonist Nal Glu: effect of the dose and timing of hCG adminstration. *Fertil Steril*, **56**: 440-445

Duncan, W., Rodger, F. and Illingworth, P. (1998a) The human corpus luteum: reduction in macrophages during simulated maternal recognition of pregnancy. *Hum Reprod*, **13**: 2435-2442

Duncan, W., Illingwoth, P., Young, F. and Fraser, H. (1998b) Induced luteolysis in the primate: rapid loss of luteinizing hormone receptors. *Hum Reprod*, **13**: 2532-2540

Einspanier, A., Ivell, R., Hodges, J. K. and Rune, G. (1994) Oxytocin gene expression and oxytocin immunoactivity in the ovary of the common marmoset monkey (Callithrix jacchus). *Biol Reprod*, **50**: 1216-1222

Ellinwood, W., Norman, R. and Spies, H. (1984) Changing frequency of pulsatile LH and progesterone secretion during the luteal phase of the menstrual cycle of rhesus monkeys. *Biol Reprod*, **31**: 714-722

Engerman, R. L., Pfaffenbach, D. and Davis, M. D. (1967) Cell turnover of capillaries. *Lab Invest*, **17**: 738-743

Erickson, G. (1997) Defining Apoptosis: Players and Systems. *J Soc Gynecol Invest*, **4**: 219-228

Espey, L. (1980) Ovulation as an inflammatory process - a hypothesis. *Biol Reprod*, **22**: 73-106

Fan, T.-P. D., Jaggar, R. and Bicknell, R. (1995) Controlling the vasculature: angiogenesis, anti-angiogenesis and vascular targeting of gene therapy. *TIPS*, **16**: 57-66

Farin, C. E., Moeller, C. L., Sawyer, H. R., Gamboni, F. and Niswender, G. D. (1986) Morphometric analysis of cell types in the ovine corpus luteum throughout the estrous cycle. *Biol Reprod*, **35**: 1299-1308

Ferenczy, A., Bertrand, G. and Gelfand, M. (1979) Proliferation kinetics of human endometrium during the normal menstrual cycle. *Am J Obs Gynecol*, **133**: 859-867

Ferrara, N., Clapp, C. and Weiner, R. (1991) The 16 kDa fragment of prolactin specifically inhibits basal of FGF-stimulated growth fo capillary endothelial cells. *Endocrinology*, **129**: 896-900

Ferrara, N., Carver-Moore, K., Chen, H., Dowd, M., Lu, L., O'Shea, K., Powell-Braxton, L., Hillan, K. and Moore, M. (1996) Heterozygous embryonic lethality induced by target inactivation of the VEGF gene. *Nature*, **380**: 439-443

Ferrara, N. and Davis-Smyth, T. (1997) The biology of vascular endothelial growth factor. *Endocr Rev*, **18**: 4-25

Ferrara, N., Chen, N., Davis-Smyth, T., Gerber, H., Ngyun, T. and Peers, D. (1998) Vascular endothelial growth factor is essential for corpus luteum angiogenensis. *Nat Med*, **4**: 336-3340

Ferrell, C. (1989) Placental regulation of fetal growth. In D. Campion, G. Hausman and R. Martin (eds), *Animal Growth Regulation*. Plenum, New York, p. 1-19.

Figg, W., Pluda, J., Lush, R., Saville, M., Wyvill, K., Reed, E. and Yarchoan, R. (1997) The pharmokinetics of TNP-470, a new angiogenesis inhibitor. *Pharmacotherapy*, **17**: 91-97

Filicori, M., Butler, J. and Crowley, W. J. (1984) Neuroendocrine regulation of the corpus luteum in the human. *J Clin Invest*, **73**: 1638-1647

Findlay, J. (1986) Angiogenensis in reproductive tissues. *J Endocrinol*, **111**: 357-366

Findlay, J. (1993) An update on the roles of inhibin, activin, and follistatin as local regulators of folliculogenesis. *Biol Reprod*, **48**: 15-23

Fisch, B., Margara, R., Wintston, R. and Hillier, S. (1989) Cellular basis of luteal steroidogenesis in the human ovary. *J Endocrinol*, **122**: 303-311

Folkman, J. (1985) Tumour angiogenensis. *Adv Cancer Res*, **43**: 175-203

Folkman, J. and Klagsbrun, M. (1987) Angiogenic factors. *Science*, **235**: 442-447

Folkman, J., Klagsbrun, M., Sasse, J., Wadzinski, M., Ingber, D. and Vlodavsky, I. (1988) A heparin-binding angiogenic protein - bFGF - is stored within the basement membrane. *Am J Pathol*, **130**: 393-400

Folkman, J. (1992) Angiogenesis in female reproductive organs. In N. Alexander and C. d'Arcangues (eds), *Steroid Hormones and Uterine Bleeding*. AAAS Press, Washington DC, p. 143-155.

Folkman, J. and Shing, Y. (1992) Angiogenesis. *J Biol Chem*, **126**: 10931-10934

Folkman, J. and D'Amore, P. (1996) Blood vessel formation: What is its molecular basis? *Cell*, **87**: 1153-1156

Fong, G., Rossant, J., Gertsenstein, M. and Breitman, M. (1995) Role of the Flt-1 receptor tyrosine kinase in regulating the assembly of the vascular endothelium. *Nature*, **376**: 66-70

Fotsis, T., Pepper, M., Adlercreutz, H., Fleischmann, G., Hase, T., Montesano, R. and L, S. (1993) Genistein, a dietary-derived inhibitor of in vitro angiogenesis. *Proc Natl Acad Sci USA*, **90**: 2690-2694

Fox, S., Leek, R., Bliss, J., Mansi, J. and al, e. (1997) Association of tumour angiogenesis with bonemarrow micrometastases in breast cancer patients. *J Natl Cancer Instit*, **89**: 1044-1049

Fraser, H., Abbott, M., Laird, N., McNeilly, A., Nestor, J. J. and Vickery, B. (1986) Effects of an LH releasing hormone antagonist on the secretion of LH, FSH, prolactin and ovarian steroids at different stages of the luteal phsae in the stumptailed macaque. *J Endocrinol*, **111**: 83-90

Fraser, H., Nestor, J. J. and Vickery, B. (1987) Suppression of luteal function by a LH-RH antagonist during the early luteal phase in the stump-tailed macaque monkey and the effescts of subsequent administration of hCG. *Endocrinology*, **121**: 612-618

Fraser, H., Lunn, S., Cowen, G. and Illingworth, P. (1995) Induced luteal regression in the primate: Evidence for apoptosis and changes in c-myc protein. *J Endocrinol*, **147**: 131-137

Fraser, H., Lunn, S., Kim, H. and Erickson, E. (1998) Insulin-like growth factor binding protein-3 mRNA expression in endothelial cells of the primate corpus luteum. *Hum Reprod*, **12**: 2180-2185

Fraser, H., Dickson, S., Morris, K., Erickson, G. and Lunn, S. (1999a) The effect of the angiogenesis inhibitor TNP-470 on luteal establishment and function in the primate. *Hum Reprod*, **14**: 2054-2060

Fraser, H., Lunn, S., Harrison, DJ., and Kerr, J. (1999b) Luteal regression in the primate: Different forms of cell death during natural and GnRH antagonist or prostaglandin analog-induced luteaolysis. *Biol Reprod*, **61**: 1468-1479

Fraser, H., Dickson, S., Lunn, S., Wulff, C., Morris, K., Carroll, V. and Bicknell, R. (2000) Suppression of luteal angiogenesis in the primate after neutralisation of vascular endothelial cell growth factor. *Endocrinology*, **141**: 995-1000

Gaede, S., Sholley, M. and Quattropani, S. (1985) Endothelial mitosis during the initial stages of corpus luteum neovascularisation in the cycling adult rat. *Am J Anat*, **172**: 173-180

Gale, N. and Yancopoulos, G. (1999) Growth factors acting via endothelial cell-specific receptor tyrosine kinases:VEGFs angiopoietins and ephrins in vascular development. *Genes Develop*, **13**: 1055-1066

Garverick, H., Smith, M., Elmore, R., Morehouse, G., Agudo, S. and Zahler, W. (1985) Changes and interrelationships among luteal LH receptors, adenylate cyclase activity and phosphodiesterase activity during the bovine estrous cycle. *J Anim Sci*, **61**: 216-223

Gasparini, G., Bonoldi, E., Viale, G., Verderio, P., Boracchi, P., Panizzoni, G., Radaelli, U., Di Bacco, A., Guglielmi, R. and Bevilacqua, P. (1996) Prognostic and predictive value of tumour angiogenensis in ovarian carcinomas. *Intl J Cancer*, **69**: 205-211

Gaytan, F., Morales, C., Bellido, C., Aguilar, E. and Sanchezcriado, J. E. (1996) Proliferative activity in the different ovarian compartments in cycling rats estimated by the 5- bromodeoxyuridine technique. *Biol Reprod*, **54**: 1356-1365

Gaytan, F., Morales, C., Garcia-pardo, L., Reymundo, C., Bellido, C. and Sanchez-Criado, J. (1998) Macrophages, cell proliferation and cell death in the human menstrual corpus luteum. *Biol Reprod*, **59**: 417-425

Gemzell, C. (1965) Induction of ovulation with human gonadotropins. *Rec Prog Horm Res*, **21**: 179-204

Gerdes, J., Lemke, H., Baisch, H., Wacker, H., Schwab, U. and Stein, H. (1984) Cell cycle analysis of a cell proliferation-associated human nuclear antigen defined by the monoclonal antibody Ki67. *J Immunol*, **133**: 1710-1715

Giatromanolaki, A., Koukourakis, M., O'Byrne, K., Fox, S., Whitehouse, R., Talbot, D., Harris, A. and Gatter, K. (1996) Prognostic value angiogenesis in operable non-small lung cell cancer. *J Pathol*, **179**: 80-88

Girsh, E., Milvae, R., Wang, W., Milvae, R. and Meidan, R. (1996a) Effect of endothelin-1 on bovine luteal cell function: role of PGF2alpha-induced antisteroidogenic action. *Endocrinology*, **137**: 1306-1312

Girsh, E., Wang, W., Mamluk, R., Arditi, F., Friedman, A., Milvae, R. and Meidan, R. (1996b) Regulation of endothelin-1 in the bovine corpus luteum: elevation by PGF2 alpha. *Endocrinology*, **137**: 5191-5196

Goede, V., Schmidt, T., Kimmina, S., Kozian, D. and Augustin, H. (1998) Analysis of blood vessel maturation processes during cyclic ovarian angiogenesis. *Lab Invest*, **78**: 1385-1394

Goldenberg, R., Powell, R., Rosen, S. and Ross, G. (1976) Ovarian morphology in women anosmia and hypogonadotropic hypogonadism. *Am J Obstet Gynecol*, **126**: 91-94

Goodman, A., Nixon, W., Johnson, D. and Hodgen, G. (1977) Regulation of folliculogenesis in the cycling rhesus monkey; selection of the dominant follicle. *Endocrinology*, **100**: 155-161

Goodman, A. and Hodgen, G. (1983) The ovarian triad of the primate menstrual cycle. *Rec Prog Horm Res*, **39**: 1-73

Gordon, J. D., Mesiano, S., Zaloudek, C. J. and Jaffe, R. B. (1996) Vascular endothelial growth factor localization in human ovary and fallopian tubes: Possible role in reproductive function and ovarian cyst formation. *J Clin Endocrinol Metab*, **81**: 353-359

Gore, B., Caldwell, B. and Speroff, L. (1973) Estrogen-induced human luteolysis. *J Clin Endocrinol Metab*, **36**: 615-617

Gospodarowicz, D. and Thakral, K. (1978) Production of a corpus luteum angiogenic factor responsible for proliferation of capillaries and neovascularisation of the corpus luteum. *Proc Natl Acad Sci USA*, **75**: 847-851

Gospodarowicz, D., Cheng, J., Lui, G. and Bohlen, P. (1985) Corpus luteum angiogenic factor is related to FGF. *Endocrinology*, **117**: 2283-2291

Gougeon, A. (1981) Rate of follicular growth in the human ovary. In R. Rolland, E. von Hall, S. Hillier, K. McNatty and J. Shoemaker (eds), *Follicular Maturation and Ovulation. Proceedings of the IV Reiner deGraaf Symposium.* Excerpta Medica, Princeton, p. 155-163.

Gougeon, A. and Lefevre, B. (1983) Evolution of the largest healthy and atretic follicles during the human menstrual cycle. *J Reprod Fertil*, **69**: 497-502

Gougeon, A. (1986) Dynamics of follicular growth in the human: a model from preliminary results. *Hum Reprod*, **1**: 81-87

Gougeon, A. (1996) Regulation of ovarian follicular development in primates: Facts and hypotheses. *Endocr Rev*, **17**: 121-155

Graham, R. and Karnovsky, M. (1966) The early stages of absorption of injected horse radish peroxidase in the proximal tubules of mouse kidney. Ultrastructural cytochemistry by a new technique. *J Histochem*, **14**: 291-302

Grazul-Bilska, A. T., Redmer, D. A., Killilea, S. D., Kraft, K. C. and Reynolds, L. P. (1992) Production of mitogenic factor(s) by ovine corpora lutea throughout the estrous cycle. *Endocrinology*, **130**: 3625-3632

Grazul-Bilska, A. T., Redmer, D. A., Killilea, S. D., Zheng, J. and Reynolds, L. P. (1993) Initial characterization of endothelial mitogens by bovine corpora lutea from the estrous cycle. *Biochem Cell Biol*, **71**: 270-277

Grazul-Bilska, A., Redmer, D., Killilea, S. and Reynolds, L. (1995) Characterization of mitogenic factors produced by ovine corpora lutea of early pregnancy. *Growth Factors*, **12**: 131-144

Grazul-Bilska, A., Redmer, D. and Reynolds, L. (1997) Cellular interactions in the corpus luteum. *Sem Reprod Endocrinol*, **15**: 383-393

Groome, N., O'Brien, M., Illingworth, P., Pai, R., Mather, J., Priddle, J. and McNeilly, A. (1995) Inhibin B in a major circulating form of inhibin in men and women. *Abstracts of the 77th Annual Meeting of the Endocrine Society*, **OR41-6**: 103

Hamberger, L., Hahlin, M. and Lindblom, B. (1987) The role of prostaglandins and catecholamines for human corpus luteum function. In R. Stouffer (eds), *The Primate Ovary*. Plenum Press, New York and London, p. 191-205.

Hanahan, D. and Folkman, J. (1996) Patterns and emerging mechanisms of the angiogenic switch during tumorigenesis. *Cell*, **86**: 353-364

Harding, R., Hulme, M., Lunn, S., Henderson, C. and Aitken, R. (1982) Plasma progesterone levels throughout the ovarian cycle of the common marmoset (Callithrix jacchus). *J Med Primatol*, **11**: 43-51

Harlow, C., Shaw, H., Hillier, S. and Hodges, J. (1988) Factors influencing FSH-induced steroidogenesis in marmoset granulosa cells: Effects of androgens at all stages of follicular development. *Endocrinology*, **122**: 2780-2787

Hartman, C. and Corner, G. (1947) Removal of the corpus luteum and of the ovaries of the femlae monkey during pregnancy: Observations and cautions. *Anat Rec*, **98**: 539-546

Hawkins, D., Belfiore, C., Kile, J. and Niswender, G. (1993) Regulation of mRNA encoding 3 beta HSD in the ovine corpus luteum. *Biol Reprod*, **48**: 1185-1190

Hazzard, T., Christenson, L. and Stouffer, R. (1999a) Changes in expression of VEGF and Ang-1 in the primate corpus luteum during the menstrual cycle. *Biol Reprod*, **60 (Suppl. 1)**: 179

Hazzard, T., Molskness, T., Chaffin, C. and Stouffer, R. (1999b) VEGF and angiopoietin regulation by gonadotropin and steroids in macaque granulosa cells during the peri-ovulatory interval. *Mol Hum Reprod*, **5**: 1115-1121

Hearn, J., Abbott, D., Chambers, P., Hodges, J. and Lunn, S. (1978) Use of the common marmoset, Callithrix jacchus, in reproductive research. *Primates Med*, **10**: 40-49

Hearn, J. (1983) The common marmoset. In J. Hearn (eds), *Reproduction in New World Primates*. MTP Press, Lancaster, UK, p. 181-216.

Hernandez, E. R., Hurwitz, A., Vera, A., Pellicer, A., Adashi, E. Y., Leroith, D. and Roberts, C. T. J. (1992) Expression of the genes encoding the insulin-like growth factors and their receptors in the human ovary. *J Clin Endocrinol Metab*, **74**: 419-425

Hertig, A. (1935) Angiogenesis in the human chorion and in the primary placenta of the Macaque monkey. *Contrib Embryol Carnegie Inst*, **25**: 37-82

Hillier, S. G. (1981) Regulation of follicular oestrogen biosynthesis: a survey of current concepts. *J Endocrinol*, **89**: 3P-18P

Hillier, S. G., Reichert, L. J. and van Hall, E. (1981) Control of preovulatory follicular oestrogen synthesis in the human ovary. *J Clin Endocrinol Metab*, **52**: 847-856

Hillier, S. G. and Wickings, E. (1985) Cellular aspects of corpus luteum function. In S. Jeffcoate (eds), *The Luteal Phase*. Wiley, London, p. 1-23.

Hillier, S. G. (1991) Paracrine control of follicular estrogen synthesis. *Sem Reprod Endocrinol*, **9**: 332-340

Hillier, S. G., Whitelaw, P. F. and Smyth, C. D. (1994) Follicular Oestrogen Synthesis - The Two-Cell, Two- Gonadotrophin Model Revisited. *Mol Cell Endocrinol*, **100**: 51-54

Hillier, S. G., Wickings, E., Illingworth, P., Yong, E., Reichert, L. J., Baird, D. and McNeilly, A. (1991) Control of immunoreactive inhibin production by human granulosa cells. *Clin Endocrinol*, **35**: 71-78

Hirschi, K. and D'Amore, P. (1996) Pericytes in the microvasculature. *Cardiovasc Res*, **32**: 687-698

Hirschi, K., Rohovsky, S. and D'Amore, P. (1998) PDGF, TGF-beta, and heterotypic cell-cell interactions mediate endothelial cell-induced recruitment of 10T1/2 cells and their differentiation to a smooth muscle fate. *J Cell Biol*, **141**: 805-814

Hirschi, K., Rohovsky, S., Beck, L., SR, S. and D'Amore, P. (1999) Endothelial cells modulate the proliferation of mural cell precursors via platlet-derived growth factor-BB and heterotypic cell contact. *Circ Res*, **84**: 298-305

Hirshfield, A. (1984) Continuous [3H] thymidine infusion: a method for the study of follicular dynamics. *Biol Reprod*, **30**: 485-491

Hobson, B. and Denekamp, J. (1984) Endothelial proliferation in tumours and normal tissues: continuous labeling studies. *Br J Cancer*, **49**: 405-413

Hodges, J., Green, D., Cottingham, P., Sauer, M., Edwards, C. and Lightman, S. (1988) Induction of luteal regression in the marmoset monkey (Callithrix jacchus) with human chorionic gonadotropin-releasing hormone antagonist and effects on subsequent follicular development. *J Reprod Fertil*, **82**: 743-752

Holash, J., Wiegand, S. and Yancopoulos, G. (1999) New model of tumour angiogenesis: dynamic balance between vessel regression and growth mediated by angiopoietins and VEGF. *Oncogene*, **18**: 5356-5362

Hollingsworth, H., Kohn, E., Steinberg, S., Rothenberg, M. and Merino, M. (1995) Tunour angiogenesis in advanced stage ovarian carinoma. *Am J Pathol*, **147**: 33-41

Holmgren, L., Glaser, A., Pfeifer-Ohlsson, S. and Ohlsson, R. (1991) Angiogenensis during human extra-embryonic development involved the spatiotemporal control of PDGF ligand and receptor gene expression. *Development*, **113**: 749-754

Holmgren, L., O'Reilly, M. S. and Folkman, J. (1995) Dormancy of micrometastases: balanced proliferation and apoptosis in the presence of angiogenesis suppression. *Nat Med*, **1**: 149-153

Homandberg, G., Willimas, J., Grant, D., Schumacher, B. and Eisenstein, R. (1985) Heparin-binding fragments of fibronectin are potent inhibitors of endothelial cell growth. *Am J Pathol*, **120**: 327-332

Horak, E., Leek, R., LeJune, S., Stuart, N., Grenall, M., Stepniewska, K. and Harris, A. (1992) Agiogenesis assessed by platelt adhesion molecular antibodies as indicator of node metastases and survival in breast cancer. *Lancet*, **340**: 1120-1124

Hornsby, P. and Crivello, J. (1983a) The role of lipid peroxidation and biological antioxidants in the function of the adrenal cortex. I. A background revies. *Mol Cell Endocrinol*, **30**: 1-20

Hornsby, P. and Crivello, J. (1983b) The role of lipid peroxidation and biological antioxidants in the function of the adrenal cortex. II. *Mol Cell Endocrinol*, **30**: 123-147

Hu, D. and Fan, T.-P. (1995) Suppression of a VEGF-induced angiogenesis by the protein tyrosine kinase inhibitor, lavendustin A. *Br J Pharmacol*, **114**: 262-268

Huang, S., Minassian, H. and More, J. (1976) Application of immunofluorescent staining in paraffin sections improved by trypsin digestion. *Lab Invest*, **35**: 383-390

Huggins, J., Pelton, J. and Miller, R. (1993) The structure and specificity of endothelin receptors; their importance in physiology and medicine. *Pharmacol Therol*, **59**: 55-123

Hurwitz, A. and Adashi, E. (1992) Ovarian follicular atresia as an apoptotic process: a paradigm for programmed cell death in endocrine tissues. *Mol Cell Endocrinol*, **84**: C19-C23

Hutchison, J. and Zeleznik, A. (1984) The rhesus monkey corpus luteum is dependent on pituitary gonadotropin secretion throughout the luteal phase of the menstrual cycle. *Endocrinology*, **115**: 1780-1786

Hutchison, J., Nelson, P. and Zeleznik, A. (1986) Effects of different gonadotropin pulse frequencies on corpus luteum function during the mentrual cycle of rhesus monkeys. *Ebdocrinology*, **119**: 1964-1971

Illingworth, P., Reddi, K., Smith, K. and Baird, D. (1990) Pharmalogical "rescue" of the corpus luteum results in increased inhibin production. *Clin Endocrinol*, **33**: 323-332

Ingber, D. and Folkman, J. (1989) Mechanochemical switching between growth and differentiation during fibroblastic growth factor-stimulated angiogenensis invitro: Role of extracellular matrix. *J Cell Biol*, **109**: 317-330

Ingber, D. (1990) Fibronectin controls capillary endothelial cell growth as based on its ability to modulate cell shape. *Proc Natl Acad Sci USA*, **87**: 3579-3583

Ingber, D., Fujita, T., Kishimoto, S., Sudo, K., Kanamaru, T., Brem, H. and Folkman, J. (1990) Synthetic analogues of fumagillin that inhibit angiogenesis ans suppress tumour growth. *Nature*, **348**: 555-557

Jablonka-Shariff, A., Grazul-Bilska, A. T., Redmer, D. A. and Reynolds, L. P. (1993) Growth and Cellular Proliferation of Ovine Corpora Lutea Throughout the Estrous Cycle. *Endocrinology*, **133**: 1871-1879

Johnson, M. C., Devoto, L., Retamales, I., Kohen, P., Troncoso, J. L. and Aguilera, G. (1996) Localization of insulin-like growth factor (IGF-I) and IGF- I receptor expression in human corpora lutea: Role on estradiol secretion. *FertilSteril*, **65**: 489-494

Joukov, V., Pajusola, K., Kaipainen, A., Chilov, D., Lahtinen, I., Kukk, E., Saksele, O., Kalkkinen, N. and Alito, K. (1996) A novel vascular endothelial growth factor, VEGF-C is a ligand for the Flt4 receptor (VEGFR-3) and KDR (VEGFR-2) receptor tyrosine kinase. *EMBO J*, **15**: 1751

Juengel, J. L., Meberg, B. M., Turzillo, A. M., Nett, T. M. and Niswender, G. D. (1995) Hormonal regulation of messenger ribonucleic acid encoding steroidogenic acute regulatory protein in ovine corpora lutea. *Endocrinology*, **136**: 5423-5429

Kamat, B. R., Brown, L. F., Manseau, E. J., Senger, D. R. and Dvorak, H. F. (1995) Expression of vascular permeability factor/vascular endothelial growth factor by human granulosa and theca lutein cells. *Am J Pathol*, **146**: 157-165

Karsch, F., Krey, L., Weick, R., Dierschke, D. and Knobil, E. (1973) Functional luteolysis in the rhesus monkey: The role of estrogen. *Endocrinology*, **92**: 1148-1152

Kendall, R. and Thomas, K. (1993) Inhibition of vascular endothelial growth factor anctivity by an endogenously encoded soluble receptor. *Prc Natl Acad Sci USA*, **90**: 10705-10709

Kerr, J., Wyllie, A. and Currie, A. (1972) Apoptosis: a basic biological phenomenon with wide-ranging implications in tissue kinetics. *Br J Cancer*, **26**: 239-257

Khan-Dawood, F., Kanu, E. and Dawood, M. (1993) Baboon corpus luteum: presence of oxytocin receptors. *Biol Reprod*, **49**: 262-266

Khan-Dawood, F., Yang, J. and Dawood, Y. (1996) Expression of gap junction protein connexin-43 in human and baboon corpus luteum. *J Clin Endocrinol Metab*, **81**: 835-842

Kim, K., Winer, J. and Armanini, M. (1993) Inhibition of VEGF-induced angiogenesis suppresses tumour growth in vivo. *Nature*, **362**: 841-844

Klagsbrun, M. and D'Amore, P. A. (1991) Regulators of angiogenesis. *Ann Rev Physiol*, **53**: 217-239

Klagsbrun and D'Amore, P. (1996) Vascular endothelial growth factor and its receptors. *Cytokine Growth Factor Rev*, **7**: 259-270

Klauber, N., Rohan, R. M., Flynn, E. and D'Amato, R. J. (1997) Critical components of the female reproductive pathway are suppressed by the angiogenesis inhibitor AGM-1470. *Nat Med*, **3**: 443-446

Knickerbocker, J., Wiltbank, M. and Niswender, G. (1988) Mechanisms of luteolysis in domestic livestock. *Domest Anim Endocrinol*, **5**: 91-107

Knobil, E., Kostyo, J. and Greep, R. (1959) Production of ovulation in the hypophysectomized rhesus monkey. *Endocrinology*, **65**: 487-493

Knobil, E., Plant, T., Wildt, L., Belchetz, P. and Marshall, G. (1980) Control of the rhesus monkey menstrual cycle: permissive role of hypothalamic gonadotropin releasing hormone. *Science*, **207**: 1371-1373

Koblizek, T., Weiss, C., Yancopoulos, G., Deutsch, U. and Risau, W. (1998) Angiopoietin-1 induces sprouting angiogenesis *in vitro*. *Current Biol*, **8**: 529-532

Koering, M. J. (1969) Cyclic changes in ovarian morphology during the menstrual cycle in *Macaca mulatta*. *Am J Anat*, **126**: 73-101

Koos, R. (1986) Stimulation of endothelial cell proliferation by rat granulosa cell-conditioned medium. *Endocrinology*, **119**: 481-489

Kraehenbuhl, J. and Jamieson, J. (1974) Localisation of intracellular antigens by immunoelectron microscopy. *Int Rev Experiment Pathol*, **13**: 1-53

Ku, D., Jaleski, J., Liu, S. and Brock, T. (1993) Vascular endothelial growth factor induces EDRF-dependent relaxation in coronary arteries. *Am J Physiol*, **265**: H586-H592

Kudelka, A., Levy, T., Verschraegren, C., Edwards, C., Piamsomboon, S., Termrungruanglert, W., Freedman, R., Kaplan, A., Kieback, D., Meyers, C., Jaeckle, K., *et al.* (1997) A phase I study of TNP-470 administered to patients with advanced squamous cell cancer of the cervix. *Clin Cancer Res*, **3**: 1501-1505

Kukk, E., Lymboussaki, T., Kaipanen, A., Jeltsch, M., Joukov, V. and Alitalo, K. (1996) VEGF-C receptor binding, and pattern of expressionwith VEGFR-3 suggests a role in lymphatic vascular development. *Development*, **122**: 3829-3837

Kusaka, M., Sudo, K., Fujita, T., Marui, S., Itoh, F., Ingber, D. and Filkman, J. (1991) Potent anti-angiogenic action of AGM-1470: comparison to the fumagillin parent. *Biochem Biophys Res Commun*, **174**: 1070-1076

LaPolt, P. S., Tilly, J. L., Aihara, T., Nishimori, K. and Hsueh, A. J. W. (1992) Gonadotropin-induced up- and down-regulation of ovarian follicle-stimulating hormone (FSH) receptor gene expression in immature rats: effects of pregnant mares serum gonadotropin, human chorionic gonadotropin, and recombinant FSH. *Endocrinology*, **130**: 1289-1295

Lapthorn, A. J., Harris, D. C., Littlejohn, A., Lustbader, J. W., Canfield, R. E., Morgan, F. J. and Isaacs, N. W. (1994) Crystal structure of human chorionic gonadotropin. *Nature*, **369**: 455-461

Lakowicz, J. (1983) Energy transfer. In (eds), *Principals of Fluorescent Spectroscopy*. Plenum Press, New York, p. 303-339.

Le Beux, Y. and Willemot, J. (1978) Actin- and myosin-like filaments in rat brain pericytes. *Anat Rec*, **190**: 811-26

Le Nestour, E., Marraoui, J., Lahlou, N., Roger, M., de Ziegler, D. and Bouchard, P. (1993) Role of estradiol in the rise in follicle-stimulating hormone levels during the luteal-follicular transition. *J Clin Endocrinol Metab*, **77**: 439-442

Lehr, H., Van der Loos, C., Teeling, P. and Gown, A. (1999) Complete chromogen separation and analysis in double immunohistochemistry staining using Photoshop-based image analysis. *J Histochem Cytochem*, **47**: 119-125

Lei, Z. M., Chegini, N. and Rao, C. V. (1991) Quantitative cell composition of human and bovine corpora lutea from various reproductive states. *Biol Reprod*, **44**: 1148-1156

Lenton, E. and Woodward, A. (1988) The endocrinology of conception cycles and implantation in women. *J Reprod Fertil Suppl*, **36**: 1-15

Leung, D., Cachianes, G., Kuang, W., Goeddel, D. and Ferrara, N. (1989) Vascular endothelial growth factor is a secreted angiogenic mitogen. *Science*, **246**: 1306-1309

Leyendecker, G., Wildt, L. and Hansmann, M. (1980) Pregnancies following chronic intermittent (pulsatile) adminstration of GnRH by means of a portable pump - a new approach to infertility in hypothalamic amenorrhea. *J Clin Endocrinol Metab*, **51**: 1214-1216

Li, T., Rogers, A., Dockery, P., Lenton, E. and Cooke, I. (1988) A new method of histological dating of human endometrium in the luteal phase. *Fertil Steril*, **50**: 52-60

Lin, D., Sugawara, T., Strauss, J., Clark, B., Stocco, D., Saenger, P., Rogol, A. and Miller, W. (1995) Role of steroidogenic acute regulatory protein in adrenal and gonadal steroidogenesis. *Science*, **267**: 1828-1831

Magoffin, D. A. and Erickson, G. F. (1994) Control Systems of Theca-Interstitial Cells. In J. Findlay (eds), *Molecular Biology of the Female Reporductive System*. Academic Press, London, p. 39-66.

Maione, T., Gray, G., Human, A. and Sharpe, R. (1991) Inhibition of tumor growth in mice by an analogue of platelet factor 4 that lacks affinity for heparin and retains potent angiostatic activity. *Cancer Res*, **51**: 2077-2083

Mais, V., Kazer, R., Cetel, N., Rivier, J., Vale, W. and Yen, S. (1986) The dependency of folliculogenesis and corpus luteum function on pulsatile gonadotropin secretion in cycling women using a gonadotropin-relasing hormone antagonist as a probe. *J Clin Endocrinol Metab*, **62**: 1250-1255

Maisonpierre, P. C., Suri, C., Jones, P. F., Bartunkova, S., Wiegand, S. J., Radziejewski, C., Compton, D., McLain, J., Aldrich, T. H., Papadopoulos, N., Daly, T. J., *et al.* (1997) Angiopoietin-2, a natural antagonist for Tie2 that disrupts in vivo angiogenesis. *Science*, **277**: 55-60

Mandarino, L., Sundarraj, N., Finlayson, J. and Hassell, J. (1993) Regulation of fibronectin and laminin synthesis by retinal capillary endothelial cells and pericytes in vitro. *Exp Eye Res*, **57**: 609-621

Marshall, J. C., Dalkin, A., Haisenleder, D., Paul, S., Ortolano, G. and Kelch, R. (1991) Gonadotropin-releasing hormone pulses: regulators of gonadotropin synthesis and ovulatory cycles. *Rec Prog Horm Res*, **47**: 155-189

Maslar, I., Powers-Craddock, P. and Ansbacher, R. (1986) Decidual prolactin production by organ cultures of human endometrium: effects of continuous and intermittent progesterone treatment. *Biol Reprod*, **34**: 741-750

Mason, H., Margara, R., Winston, R., Seppala, M., Koistinen, R. and Franks, S. (1993) IGF-1 inhibits production of IGFBP-1 while stimulating estradiol secretion in granulosa cells from normal and polycystic human ovaries. *J Clin Endocrinol Metab*, **76**: 1275-1279

McClure, N., MacPherson, A. M., Healy, D. L., Wreford, N. and Rogers, P. A. W. (1994) An immunohistochemical study of the vascularization of the human Graafian follicle. *Hum Reprod*, **9**: 1401-1405

McCracken, J., Custer, E. and Lamasa, J. (1999) Luteolysis: a neuroendocrine-mediated event. *Physiol Rev*, **79**: 263-323

McGadey, J. (1970) A tetrazolium method for non-specific alkaline phosphatases. *Histochemie*, **23**: 180-184

McGuire, W., Juengel, J. and Niswender, G. (1994) Protein kinase C second messenger system mediated the anti-steroidogenic effects of PGF2alpha in the ovine corpus luteum in vivo. *Biol Reprod*, **51**: 800-806

McLachlan, R., Robertson, D., Healy, D., deKrester, D. and Burger, H. (1986) Plasma inhibin levels during gonadotropin induced ovarian hyperstimulation for IVF: A new index of follicular function? *Lancet*, **1**: 1233-1234

McNatty, K., Baird, D., Bolton, A., Chamber, P., Corker, C. and McLean, H. (1976) Concentrations of oestrogens and androgens in human ovarian venous plasma throughout the menstrual cycle. *J Endocrinol*, **71**: 77-85

McNeilly, A., Kerin, J., Swanston, I., Bramley, T. and Baird, D. (1980) Changes in the binding of hCG/LH, FSH and prolactin to human corpora lutea during the menstrual cycle and pregnancy. *J Endocrinol*, **87**: 315-325

Meegdes, B., Ingenhoes, R., Peeters, L. and Exalto, N. (1988) Early pregnancy wastage; relationship between chorionic vascularisaiton and embryonic development. *Fertil Steril*, **49**: 216-220

Meschia, G. (1983) Circulation to female reproductive organs. In J. Shepher and F. Abboud (eds), *Handbook of Physiology*. American physiological society, Washington DC, p. 241-269.

Meyer, G. and McGeachie, J. (1988) Angiogenesis in the developing corpus luteum of pregnant rats: a stereologic and autoradiographic study. *Anat Rec*, **222**: 18-25

Michael, A. E. and Webley, G. E. (1993) Roles of Cyclic AMP and Inositol Phosphates in the Luteolytic Action of Cloprostenol, a Prostaglandin F2- alpha Analogue, in Marmoset Monkeys (Callithrix-Jacchus). *J Reprod Fertil*, **97**: 425-431

Michael, A., Abayasekara, D. and Webley, G. (1994) Cellular Mechanisms of Luteolysis. *Mol Cell Endocrinol*, **99**: R1-R9

Miller, W. (1988) Molecular biology of steroid hormone synthesis. *Endocrine Rev*, **9**: 295-318

Milvae, R. and Hansel, W. (1985) Inhibition of bovine luteal function by indomethacin. *J Anim Sci*, **60**: 528-531

Milvae, R., Alila, H. and Hansel, W. (1986) Involvement of lipoxygenase products of arachidonic acid metabolism in bovine luteal function. *Biol Reprod*, **35**: 1210-1215

Modlich, U., Kaup, F. J. and Augustin, H. G. (1996) Cyclic angiogenesis and blood vessel regression in the ovary: Blood vessel regression during luteolysis involves endothelial cell detachment and vessel occlusion. *Lab Invest*, **74**: 771-780

Montesano, R., Vassalli, J., Baird, A., Guillemin, R. and Orci, L. (1986) Basic fibroblastic growth factor induced angiogenensis in vitro. *Proc Natl Acad Sci USA*, **83**: 7297-7301

Moor, R. and Seamark, R. (1986) Cell signaling, permeability and microvasculatory changes during antral follicle development in mammals. *J Dairy Sci*, **69**: 927-943

Moudgal, N., MacDonald, J. and Greep, R. (1971) Effect of hCG anti-serum on ovulation and corpus luteum formation in the monkey, (Macaca fascicularis). *J Clin Endocrinol*, **32**: 579-581

Murdoch, W. (1987) Treatment of sheep with PGF2 alpha enhances production of a luteal chemoattractant for eosinophils. *Am J Reprod Immunol*, **15**: 52-56

Murdoch, W., Steadman, L. and Belden, E. (1988) Immunoregulation of luteolysis. *Med Hypoth*, **27**: 197-199

Murohara, T., Horowitz, J., Silver, M., Tsurumi, Y., Chen, D., Sullivan, A. and Isner, J. (1998) VEGF/VPF enhances vascular permeability via nitric oxide and prostacyclin. *Circulation*, **97**: 99-107

Myamoto, A., Volutzow, H. and Schams, D. (1993) Acute actions of PGF2alpha, PGFE2, and PGI2, in myocardialyzed bovine corpus luteum in vitro. *Biol Reprod*, **49**: 423-430

Negoescu, A., Guillermet, C., Lorimer, P., Brambilla, E. and Labat-Moleur, F. (1998) Importance of DNA-fragmentation in apoptosis with regard to TUNEL specificity. *Biomed Pharmacother*, **52**: 252-258

Nehls, V. and Drenckhahn, D. (1991) Heterogeneity of microvascular pericytes for smooth muscle type alpha-actin. *J Cell Biol*, **113**: 147-154

Nehls, V., Denzer, K. and Detlev, D. (1992) Pericyte invovlement in capillary sprouting in situ. *Cell Tissue Res*, **270**: 469-474

Neil, J., Johansson, E. and Knobil, E. (1969) Failure of hysterectomy to influence the normal patteren of cyclic progesterone secretion in the rhesus monkey. *Endocrinology*, **84**: 464-465

Neulen, J., Yan, Z. P., Raczek, S., Weindel, K., Keck, C., Weich, H. A., Marme, D. and Breckwoldt, M. (1995) Human chorionic gonadotropin-dependent expression of vascular endothelial growth factor/vascular permeability factor in human granulosa cells: Importance in ovarian hyperstimulation syndrome. *J Clin Endocrinol Metab*, **80**: 1967-1971

Neulen, J., Raczek, S., Pogorzelski, M., Grunwald, K., Yeo, T., Dvorak, H., Weich, H. and Breckwoldt, M. (1998) Secretion of VEGF/VPF from human luteinised granulosa cells is hCG dependent. *Mol Hum Reprod*, **4**: 203-206

Nicosia, R. and Villaschi, S. (1995) Rat aortic smooth muscle cells become pericytes during angiogenensis in vitro. *Lab Invest*, **73**: 658-666

Nicosia, S., Diaz, J., Nicosia, R., Saunders, B. and Murocacho, C. (1995) Cell proliferation and apoptosis during development and aging of the rabbit corpus luteum. *Ann Clin Lab Sci*, **25**: 143-157

Niswender, G., Reimers, T., Diekman, M. and Nett, T. (1976) Blood flow: a mediator of ovarian function. *Biol Reprod*, **14**: 64-81

Niswender, G., Juengel, J., Mcguire, W., Belfiore, C. and Wiltbank, M. (1994) Luteal Function - The Estrous Cycle and Early Pregnancy. *Biol Reprod*, **50**: 239-247

Niswender, G. and Nett, T. (1994) Corpus Luteum and Its Control in Infraprimate Species. In E. Knobil and J. Neill (eds), *Physiology of Reproduction,.2*. Raven Press, New York, p. 781-816.

Niswender, G., Juengel, J., Silva, P., Rollyson, M. and McIntush, E. (2000) Mechanisms controlling the function and life span of the corpus luteum. *Physiol Rev*, **80**: 1-29

Nomura, M., Yamagishi, S. I., Harada, S. I., Hayashi, Y., Yamashima, T., Yamashita, J. and Yamamoto, H. (1995) Possible participation of autocrine and paracrine vascular endothelial growth factors in hypoxia-induced proliferation of endothelial cells and pericytes. *J Biol Chem*, **270**: 28316-28324

O'Reilly, M., Holmgren, L., Shing, Y., Chen, C., Rosenthal, R., Moses, M., Lane, W., Cao, Y., Sagem, E. and Folkman, J. (1994) Angiostatin: a novel angiogenesis inhibitor that mediated the suppression of metastases by a Lewis lung carcinoma. *Cell*, **79**: 315-328

O'Reilly, M., Boehm, T., Shing, Y., Fukai, N., Vasios, G., Lane, W., Flynn, E., Birkhead, J., Olsen, B. and Folkman, J. (1997) Endostatin: an endogenous inhibitor of angiogenesis and tumour growth. *Cell*, **88**: 277-285

O'Shea, J., Nightingale, M. and Chamley, W. (1977) Changes in small blood vessels during cyclical luteal regression in sheep. *Biol Reprod*, **17**: 162-177

O'Shea, J., Rodgers, R. and Wright, P. (1986) Cellular composition of the sheep corpus luteum in the mid and late luteal phases of the estrous cycle. *J Reprod Fertil*, **76**: 685-691

Ohno, Y. and Mori, T. (1985) Correlation between progesterone and plasminogen activator in rat ovaries during the ovulatory process. *Acta Obst Gynaecol Jpn*, **37**: 247-256

Ohtani, M., Kobayashi, S., Miyamoto, A., Hayashi, K. and Fukui, Y. (1998) Real-time relationships between intraluteal and plasma concentrations of endothelin, oxytocin, and progesterone during PGF2alpha-induced luteolysis in the cow. *Biol Reprod*, **58**: 103-108

Olofsson, B., Pajusola, K., Voneuler, G., Chilov, D., Alitalo, K. and Eriksson, U. (1996) Genomic organization of the mouse and human genes for vascular endothelial growth factor B (VEGF-B) and characterization of a second splice isoform. *J Biol Chem*, **271**: 19310-19317

Olson, T., Mohanraj, D., Roy, S. and Ramakrishnan, S. (1997) Targeting the tumor vasculature: inhibition of tumor growth by a vascular endothelial growth factor -toxin conjugate. *Int J Cancer*, **73**: 865-870

Orre, M., Lotfi-Miri, M., Mamers, P. and Rogers, P. (1998) Increased microvessel density in mucinous compared with malignant serous and benign tumours of the ovary. *Brit J Cancer*, **77**: 2204-2209

Otani, N., Minami, S., Yamoto, M., Shikone, T., Otani, H., Nishiyama, R., Otani, T. and Nakano, R. (1999) The VEGF/fms-like tyrosine kinase system in human ovary during the mesntrual cycle and early pregnancy. *J Clin Endocrinol Metab*, **84**: 3845-3851

Papapetropoulos, A., Garcia-Cardena, G., Dengler, T., Maisonpierre, P., Yancopoulos, G. and Sessa, W. (1999) Direct actions of Ang-1 on human endothelium: evidence for network stabilisation, cell survival, and interaction with other angiogenic growth factors. *Lab Invest*, **79**: 213-223

Park, J., Chen, H., Winer, J., Houck, K. and Ferrara, N. (1994) Placental growth factor: potentiation of vascular endothelial growth factor bioactivity, in vitro and in vivo, and high affinity binding to Flt-1 but not Flk-1/KDR. *J Biol Chem*, **269**: 25646-25654

Pepper, M., Ferrara, N., Orci, L and Montesano, R. (1991) VEGF induces plasminogen activators and plasminogen activator inhibitor type 1 in microvascular endothelial cells. *Biochem Biophys Res Commun*, **181**: 902-908

Pescador, N., Soumano, K., Stocco, D., Price, C. and Murphy, B. (1996) Steroidogenic acute regulatory protein in bovine corpora lutea. *Biol Reprod*, **55**: 485-491

Peters, H., Byskov, A., Himelstein-Braw, R. and Faber, M. (1975) Follicular growth: the basic event in the mouse and human ovary. *J Reprod Fertil*, **45**: 559-566

Pharriss, B., Cornette, J. and Gutknecht, G. (1970) Vascular control of luteal steroidogenesis. *J Reprod Fertil Suppl*, **10**: 97-103

Phelouzat, M., Laforge, T., Quadri, R., Arbogast, A. and Proust, J. (1996) Chemiluminescent detection of apoptotic DNA: A qualitative and quantitative method. *Bio Bechniques*, **21**: 214-216

Phillips, G., Stone, A., Jones, B., Schultz, J., Whitehad, R. and Knighton, D. (1994) Vascular endothelial growth factor (rhVEGF165) stimulates direct angiogensis in the rabbit cornea. *In vivo*, **8**: 961-965

Phillips, H., Hains, J., Leung, D. and Ferrara, N. (1990) Vascular endothelial growth factor is expressed in rat corpus luteum. *Endocrinology*, **127**: 965-967

Placidi, L., Cretton-Scott, E., De Sousa, G., Rahmani, R., Placidi, M. and Sommadossi, J.-P. (1997) Interspecies variability of TNP-470 metabolism, using primary monkey, rat, and dog cultured hepatocytes. *Drug Metab Dispos*, **25**: 94-99

Plouet, J., Schilling, J. and Goaspadarowicz, D. (1989) Isolation and charcterization of of a newly identified endothelial cell mitogen produced by AtT20 cells. *EMBO J*, **8**: 3801-3806

Plouet, J. and Maukadiri, H. (1990) Characterization of the receptor to vasculotropin on bovine adrenal cortex-derived capillary endothelial cells. *J Biol Chem*, **265**: 22071-22074

Poole, J. and Coffin, J. (1989) Vasculogenesis and angiogenensis - two distinct morphogenetic mechanisms establish embryonic vascular pattern. *J Exp Zool*, **251**: 224-231

Puri, M., Rossant, J., Alitalo, K., Berstein, A. and Partanen, J. (1995) The receptor tyrosine kinase Tie is required for integrity and survival of vascular endothelial cells. *EMBO J*, **14**: 5884-91

Ravindranath, N., Little-Ihrig, L., Phillips, H. S., Ferrara, N. and Zeleznik, A. J. (1992a) Vascular endothelial growth factor messenger ribonucleic acid expression in the primate ovary. *Endocrinology*, **131**: 254-260

Ravindranath, N., Little-Irhig, L., Benyo, D. and Zeleznik, A. (1992b) Role of LH in the expression of cholesterol side chain cleavage cytochrome P450 and 3-beta hydroxysteroid dehydrogenase mRNAs in the primate corpus luteum. *Endocrinology*, **131**: 2065-2070

Redmer, D. A., Grazul, A. T., Kirsch, J. D. and Reynolds, L. P. (1988) Angiogenic activity of bovine corpora lutea at several stages of luteal development. *J Reprod Fertil*, **82**: 627-634

Redmer, D. A. and Reynolds, L. P. (1996) Angiogenesis in the ovary. *Rev Reprod*, **1**: 182-192

Reynolds, L. (1986) Utero-ovarian interactions during early pregnancy: role of conceptus-induced vasodilation. *J Anim Sci*, **62 (Suppl.2)**: 47-61

Reynolds, L. P., Killilea, S. D. and Redmer, D. A. (1992) Angiogenesis in the female reproductive system. *FASEB J*, **6**: 886-892

Reynolds, L. and Redmer, D. (1995) Utero-placental vascular development and placental function. *J Anim Sci*, **73**: 1839-1851

Reynolds, L. and Redmer, D. (1998) Expression of the angiogenic factors, basic fibroblastic growth factor and vascular endothelail growth factor, in the ovary. *J Anim Sci*, **76**: 1671-1681

Reynolds, L. P., Grazul-Bilska, A. T., Killilea, S. D. and Redmer, D. A. (1994) Mitogenic factors of corpora lutea. *Prog Growth Fact Res*, **5**: 159-175

Reynolds, L., Grazul-Bilska, A. and Redmer, D. (2000) Angiogenesis in the corpus luteum. *Endocrine*, **12**: 1-9

Rhodin, J. and Fujita, H. (1989) Capillary growth in mesentary of normal young rats. Inatravital video and electron microscope analyses. *J Submicrosc Cytol Pathol*, **21**: 1-34

Richards, J. (1994) Hormonal control of gene expression in the ovary. *Endocr Rev*, **15**: 725-751

Riley, J. and Behrman, H. (1991) Oxygen radicals and reactive oxygen species in reproduction. *Proc Soc Exp Biol Med*, **198**: 781-791

Risau, W. (1991) Embryonic angiogenensis factors. *Pharmacol Ther*, **51**: 371-376

Rodger, F. E., Young, F. M., Fraser, H. M. and Illingworth, P. J. (1997) Endothelial cell proliferation follows the mid-cycle luteinizing hormone surge, but not human chorionic gonadotrophin rescue, in the human corpus luteum. *Hum Reprod*, **12**: 1723-1729

Rogers, P., Lederman, F. and Taylor, N. (1998) Endometrial microvascular growth in normal and dysfunctional states. *Hum Reprod Upd*, **4**: 503-508

Rothchild, I. (1981) Regulation of the mammalian corpus luteum. *Rec Prog Horm Res*, **37**: 183-198

Rueda, B., Tilly, K., Hansen, T., Hoyer, P. and Tilly, J. (1995) Expression of superoxide dismutase, catalase and glutathione peroxidase in the bovine corpus luteum: evidence supporting a role for oxidative stress in luteolysis. *Endocrine*, **3**: 227-232

Sabattini, E., Gerdes, J., Gherlinzoni, F., Poggi, S., Zucchini, L., Melilli, G., Grigioni, F., Del Vecchio, M., Leoncini, L. and Falini, B. (1993) Comparison between the monoclonal antibodies Ki67 and PC10 in 124 malignant lymphomas. *J Pathol*, **169**: 397-403

San Roman, G. and Magoffin, D. (1992) Insulin-like growth factor binding-proteins in ovarian follicles from women with polycystic ovarian disease: Cellular source and levels in follicular fluid. *J Clin Endocrinol Metab*, **75**: 1010-1016

Sato, T., Tozawa, Y., Deutsch, U., Wolburg-Buchholz, K., Fujiwara, Y., Gendron-Maguire, M., Gridley, T., Wolburg, H., Risau, W. and Qin, Y. (1995) Distinct roles of the receptor tyrosin kinases Tie-1 and Tie-2 in blood vessel formation. *Nature*, **376**: 70-74

Sato, Y., Hamanaka, R., Ono, J., Kuwano, M., Rifkin, D. and Takaki, R. (1991) The stimulatory effect of PDGF on vascular smooth muscle cell migration is mediated by the induction of endogenous basic FGF. *Biochem Biophys Res Commum*, **174**: 1260-1266

Sawyer, H. R., Niswender, K. D., Braden, T. D. and Niswender, G. D. (1990) Nuclear changes in ovine luteal cells in response to $PGF_{2\alpha}$. *Dom Anim Endocrinol*, **7**: 229-238

Schoell, W., Pieber, D., Reich, O., Lahousen, M., Janieck, M., Guecer, F. and Winter, R. (1997) Tumour angiogenesis as a prognostic factor in ovarian carcinoma. *Cancer*, **80**: 2257-2262

Schor, A. and Schor, S. (1983) Tumour angiogenensis. *J Pathol*, **141**: 385-413

Schwartzman, R. A. and Cidlowski, J. A. (1993) Apoptosis - The Biochemistry and Molecular Biology of Programmed Cell Death. *Endocrine Rev*, **14**: 133-151

Segaloff, D. L. and Ascoli, M. (1993) The Lutropin/Choriogonadotropin Receptor ... 4 Years Later. *Endocrine Rev*, **14**: 324-347

Senger, D., Galli, S., Dvorak, A., Perruzzi, C., Harvey, V. and Dvorak, H. (1983) Tumor cells secrete a vascular permeability factor that promotes accumulation of ascites fluid. *Science*, **219**: 983-985

Shalaby, F., Rossant, J., Yamaguchi, T., Gertsenstein, M., Wu, X., Breitman, M. and Schuh, A. (1995) Failure of blood-island formation and vasculogenesis in Flk-1 deficient mice. *Nature*, **376**: 62-66

Shi, S., Key, M. and Kalra, K. (1991) Antigen retrieval in formalin-fixed paraffin-embedded tissues: an enhancement method for immunohistochemical staining based on microwave oven heating of sections. *Histochem Cytochem*, **39**: 741-748

Shikone, T., Yamoto, M., Kokawa, K., Yamashita, K., Nishimori, K. and Nakano, R. (1996) Apoptosis of human corpora lutea during cyclic luteal regression and early pregnancy. *J Clin Endocrinol Metab*, **81**: 2376-2380

Shweiki, D., Itin, A., Stouffer, D. and Keshet, E. (1992) Vascular endothelial growth factor induced by hypoxia may mediate hypoxia initiated angiogenensis. *Nature*, **359**: 843-845

Simmons, D. L., Satterthwaite, A. B., Tenen, D. G. and Seed, B. (1992) Molecular cloning of a cDNA encoding CD34, a sialomucin of human hematopoietic stem cells. *J Immunol,* **148**: 267-271

Skalli, O., Pelte, M. F., Peclet, M. C., Gabbiani, G., Gugliotta, P., Bussolati, G. Ravazzola, M. and Orci, L. (1989) Alpha-smooth muscle actin, a differnetiation marker of smooth muscle cells, is present in microfilamentous bundles of pericytes. *J Histochem Cytochem,* **37**: 315-321

Skinner, M. and Parrott, J. (1994) Growth Factor-Mediated Cell - Cell Interactions in the Ovary. In J. Findlay (eds), *Molecular Biology of the Female Reproductive System*. Academic Press, London, p. 67-82.

Skobe, M., Rockwell, P., Goldstein, N., Vosseler, S. and Fusenig, N. E. (1997) Halting angiogenesis suppresses carcinoma cell invasion. *Nat Med*, **3**: 1222-1227

Smith, K. B., Lunn, S. F. and Fraser, H. M. (1990) Inhibin secretion during the ovulatory cycle and pregnancy in the common marmoset monkey. *J Endocrinol*, **126**: 489-495

Soker, S., Takashima, S., Miao, H., Neufeld, G. and Klagsbrun, M. (1998) Neuropilin-1 is expressed by endothelial and tumour cells and is an isoform-specific receptor for vascular endothelial growth factor. *Cell*, **92**: 735-745

Soto, E., Silavin, S., Tureck, R. and Strauss, J. I. (1984) Stimulation of progesterone synthesis in luteinised human granulosa cells by human chorionic gonadotrophin and 8-bromo-adenosine 3', 5'-monophosphate: The effect of low density lipoproteins. *J Clin Enodocrinol Metab*, **58**: 831-837

Stein, I., Itin, A., Einat, P., Skaliter, R., Grossman, Z. and Keshet, E. (1998) Translation of vascular endothelial grwoth factor mRNA by internal ribosome entry: implications for translation under hypoxia. *Mol Cell Biol*, **18**: 3112-9

Stevens, A. and Wilson, I. (1996) The haematoxylins and eosins. In J. Bancroft and A. Stevens (eds), *Theory and Practice of Histological Techniques*. Churchill Livingstone, New York, p. 99-112.

Stevens, V., Xu, T. and Lambeth, J. (1993) Cholsterol trafficking in steroidogenic cells: reversible cyclohaximide-dependent accumulation of cholesterol in a presteroidogenic pool. *Eur J Biol Chem*, **216**: 557-563

Stouffer, R., Nixon, W., Gulyas, B. and Hodgen, G. (1977) Gonadotropin-sensitive progesterone production by rhesus monkey luteal cells in vitro: A function of age of the corpus luteum during the menstrual cycle. *Endocrinology*, **100**: 506-512

Stouffer, R. (1996) Corpus luteum formation and demise. In Adashi, E., Rock, J. and Rasenwaks, Z (eds), *Reproductive Endocrinology, Surgery and Technology*. Lippincott-Raven Publishers, Philadelphia, p. 251-270.

Strinden, S. and Shapiro, S. (1983) Progesterone-altered secretory proteins from cultured human endometrium. *Endocrinology*, **112**: 862-870

Summers, P., Wennink, J. and Hodges, J. (1985) Cloprostenol-induced luteolysis in the marmoset monkey (Callithrix jacchus). *J Reprod Fertil*, **73**: 133-138

Suri, C., Jones, P., Patan, S., Bartunkova, S., Maisonpierre, P., Davis, S., Sato, T. and Yancopoulos, G. (1996) Requisite role of angiopoietin-1, a ligand for the TIE2 receptor, during embryonic angiogenesis. *Cell*, **87**: 1171-1180

Takebayashi, Y., Akiyama, S.-i., Yamada, K., Akiba, S. and Aikou, T. (1996) Angiogenesis as an unfavorable prognostic factor in human colorectal carcinoma. *Cancer*, **78**: 226-231

Tamura, H. and Greenwald, G. S. (1987) Angiogenesis and its hormonal control in the corpus luteum of the pregnant rat. *Biol Reprod*, **36**: 1149-1154

Tan, G., Tweedale, R. and Biggs, J. (1982a) Effects of oxytocin in the bovine corpus luteum of early pregnancy. *J Reprod Fertil*, **66**: 75-78

Tan, G., Tweedale, R. and Biggs, J. (1982b) Oxytocin may play a role in the control of the corpus luteum. *J Endocrinol*, **95**: 65-70

Teasdale, F. (1976) Numerical density of nuclei in the sheep placenta. *Anat Rec*, **185**: 181-196

Thompson, W., Li, W. and Maragoudakis, M. (1999) The clinical manipulation of angiogenesis: Pathology, side effects, surprises, and opportunities with novel human therapies. *J Pathol*, **187**: 503-510

Tian, X., Berndston, A. and Fortune, J. (1994) Changes in levels of mRNA for cytochrome P450 side chain cleavage and 3beta HSD during PGF2alpha-induced luteolysis in cattle. *Biol Reprod*, **50**: 349-356

Tilly, J. (1997) Apoptosis and the ovary: a fashionable trend or food for thought. *Fertil Steril*, **67**: 226-228

Tilton, R., Kilo, C. and Williamson, J. (1979) Pericyte-endothelial relationships in cardiac and skeletal muscle capillaries. *Microvasc Res*, **18**: 325-335

Tjugum, J., Dennefors, B. and Norstrom, A. (1984) Influence of progesterone, androstenedione and oestradiol-17 beta on the incorporation of [3H] proline in the human follicular wall. *Acta Endocrinol (Copenh)*, **105**: 552-557

Torii, R., Abbott, D. and Nigi, H. (1996) Morphological changes of the ovary and hormonal changes through the ovarian cycle of the common marmoset (Callithrix jacchus). *Primates*, **37**: 49-56

Torry, D. and Torry, R. (1997) Angiogenesis and the expression of VEGF in the endometrium and placenta. *Am J Reprod Immunol*, **37**: 21-29

Tsafriri, A. and Dekel, N. (1994) Molecular Mechanisms in Ovulation. In J. Findlay (eds), *Molecular Biology of the Female Reproductive System*. Academic Press, London, p. 207-258.

Tsukada, K., Matsushima, T. and Yamanaka, N. (1996) Neovascularization of the corpus luteum of rats during the estrus cycle. *Pathol Int*, **46**: 408-416

Tureck, R. and Strauss, J. I. (1982) Progesterone synthesis by luteinised granulosa cells in culture: The role of de novo sterole synthesis and lipoprotein-carried sterol. *J Clin Endocrinol Metab*, **54**: 367-373

Twardowski, P. and Gradishar, W. (1997) Clinical trials of antiangiogenic agents. *Curr Opin Oncol*, **9**: 584-589

Unemori, E., Ferrara, N., Bauer, E. and Ameto, E. (1992) VEGF induces interstitial collagnase expression in human endothelial cells. *J Cell Physiol*, **153**: 557-562

Vaisman, N., Gospodarowicz, D. and Neufeld, G. (1990) Characterization of the receptors for vascular endothelial growth factor. *J Biol Chem*, **265**: 19461-19466

van Wagenen, G. and Simpson, M. (1973) Postnantal development of the ovary in *Homo sapiens* and *Macaca mulatta* and experimental induction of ovulation in the macaque. Yale University Press, New Haven, p.

Vande Wiele, R., Bogumil, J., Dyrenfurth, I., Ferin, M., Jewelewicz, R., Warren, M., Rizkallah, T. and Mikhail, G. (1970) Mechanisms regulating the menstrual cycle in women. *Rec Prog Horm Res*, **26**: 63-103

Vega, M. and Devoto, L. (1997) Autocrine/paracrine regulation of normal human corpus luteum development. *Semin Reprod Endocrinol*, **15**: 353-362

Vikkula, M., Boon, L., Carraway, K., Calvert, J., Diamonti, A., Goumnerov, B., Pasyk, K., Marchuk, D., Warman, M., Cantley, L., Mulliken, J., et al. (1996) Vascular dysmorphogenesis caused by an activating mutation in the receptor tyrosine kinase TIE2. *Cell*, **87**: 1181-1890

Walker, N., Harmon, B., Gobe, G. and Kerr, J. (1988) Patterns of cell death. *Meth Achiev Exp Pathol*, **13**: 18-54

Wallow, I. and Burnside, B. (1980) Actin filaments in retinal pericytes and endothelial cells. *Invest Opthalmol Vis Sci*, **19**: 1433-41

Webley, G., Richardson, M., Summers, P., Given, A. and Hearn, J. (1989) Changing resposiveness of luteal cells of the marmoset monkey (Callithrix jacchus) to luteotropic and luteolytic agents dring normal and conception cycles. *J Reprod Fertil*, **87**: 301-310

Webley, G. E., Richardson, M. C., Smith, C. A., Masson, G. M. and Hearn, J. P. (1990) Size distribution of luteal cells from pregnant and non-pregnant marmoset monkeys and a comparison of the morphology of marmoset luteal cells with those from the human corpus luteum. *J Reprod Fertil*, **90**: 427-437

Webley, G., Hodges, J., Given, A. and Hearn, J. (1991) Comparison of the luteolytic action of GnRH antagonist and cloprostenol, and the ability of hCG and melatonin to override their luteolytic effects in the marmoset monkey. *J Endocrinol*, **128**: 121-129

Wehenberg, U. and Rune, G. (2000) Spontaneous luteinisation of marmoset antral follicles in vitro. *Mol Hum Reprod*, **6**: 504-509

Westermark, B., Siegbahn, A., Heldin, C. and Claesson-Welsh, L. (1990) B-type receptor for platelet derived growth factor mediated a chemotactic response by means of ligand-induced activation of the receptor protein tyrosine kinase. *Proc Natl Acad Sci USA*, **87**: 128-132

Whitelaw, P. F., Smyth, C. D., Howles, C. M. and Hillier, S. G. (1992) Cell-specific expression of aromatase and LH receptor mRNAs in the rat ovary. *J Mol Endocrinol*, **9**: 309-312

Wiltbank, M. C., Belfiore, C. J. and Niswender, G. D. (1993) Steroidogenic enzyme activity after acute activation of protein kinase (PK) A and PKC in ovine small and large luteal cells. *Mol Cell Endocrinol*, **97**: 1-7

Witzenbilcher, B., Maisonpierre, P., Jones, P., Yancopoulos, G. and Isner, J. (1998) Chemotactic proerties of Ang-1 and Ang-2, ligands for the endothelial-specific tyrosine kinase Tie-2. *J Biol Chem*, **273**: 18514-18521

Wolf, H. and Dittrich, K. (1992) Detection of PCNA in diangonstic histopathology. *J Histochem Cytochem*, **40**: 1269-1273

Wulff, C., Wilson, H., Largue, P., Duncan, W., Armstrong, D. and Fraser, H. (2000) Angiogenesis in the human corpus luteum: Localisation and changes in angiopoietins, Tie-2 and vascular endothelial growth factor messenger ribonucleic acid. *J Clin Endocrinol Metab*, 85:4302-4309

Wulff, C., Wilson, H., Rudge, J., Weigand, S., Lunn, S. and Fraser, H. (2001) Luteal angiogenesis: prevention and intervention by treatment with vascular endothelial growth factor trap A40. *J Clin Endocrinol Metab*, In press.

Wyllie, A., Kerr, J. and Currie, A. (1980) Cell death: The significance of apoptosis. *Int Rev Cytol*, **68**: 251-306

Yamada, Y., Nezu, J., Shimane, M. and Hirata, Y. (1997) Molecular cloning of a novel vascular endothelial growth factor, VEGF-D. *Genomics*, **42**: 483-488

Yamagishi, S., Kobayashi, K. and Yamamoto, H. (1993) Vascular pericytes not only regulate growth, but also preserve prostacyclin-producing ability and protect against lipid peroxide-injury of co-cultured endothelial cells. *Biochem Biophys Res Commun*, **190**: 418-425

Yamagishi, S., Yonekura, H., Yamamoto, Y., Fujimori, H., Sakurai, S., Yanaka, N. and Yamamoto, H. (1999) Vascular endothelial growth factor acts as a pericyte mitogen under hypoxic conditions. *Lab Invest*, **79**: 501-509

Yan, Z., Weich, H., Bernart, W., Breckwolt, N. and Neulen, J. (1993) VEGF mRNA expression in luteinized human granulosa cells in vitro. *J Clin Endocrinol Metab*, **77**: 1723-1725

Yan, Z., Neulen, J., Raczek, S., Weuich, H., Grunwald, K. and Breckwolt, M. (1998) VEGF/VPF production by luteinized human granulosa cells in vitro: a paracrine signal in corpus luteum formation. *Gynecol Endocrinol*, **12**: 149-153

Yonekura, H., Sakurai, S., Lui, X., Migita, H., Wang, H., Yamagishi, S., Nomura, M., Abedin, M., Unoki, H., Yamamoto, Y. and Yamamoto, H. (1999) Placenta growth factor and VEGF-B and C expression in microvascular endothelial cells and pericytes. *J Biol Chem*, **274**: 35172-35178

Yong, E., Baird, D. and Hillier, S. (1992a) Mediation of gonadotropin-stimulated growth and differentiation of human granulosa cells by adenosine 3', 5'-monophosphate: one molecule two messages. *Clin Endocrinol*, **37**: 51-58

Yong, E., Baird, D. and Hillier, S. (1992b) Transduction of the gonadotropin effects on human granulosa cells by cyclic AMP; One molecule, two messages. In N. Sjoberg, L. Hamberger, P. Janson, C. Owman and H. Coelingh Bennink (eds), *Local Regulation of Ovarian Function*. Parthenon Publshing Corp., Carnforth, UK, p. 123-130.

Yong, E. L., Hillier, S. G., Turner, M., Baird, D. T., Ng, S. C., Bongso, A. and Ratnam, S. S. (1994) Differential Regulation of Cholesterol Side-Chain Cleavage (P450Scc) and Aromatase (P450Arom) Enzyme mRNA Expression by Gonadotrophins and Cyclic AMP in Human Granulosa Cells. *J Mol Endocrinol*, **12**: 239-249

Young, F. M., Illingworth, P. J., Lunn, S. F., Harrison, D. J. and Fraser, H. M. (1997) Cell death during luteal regression in the marmoset monkey *(Callithrix jacchus). J Reprod Fertil*, **111**: 109-119

Young, F. (1999) Luteal regression in the marmoset monkey. PhD Thesis. University of Edinburgh.

Young, F., Rodger, F., Illingworth, P. and Fraser, H. (2000) Cell proliferation and vascular morphology in the marmoset corpus luteum. *Hum Reprod*, **15**: 557-566

Yuan, W. and Giudice, L. C. (1997) Programmed cell death in the human ovary is a function of follicle and corpus luteum status. *J Clin Endocrinol Metab*, **82**: 3148-3155

Zeleznik, A., Midgley, A. J. and Reichert, L. J. (1974) Granulosa cell maturation in the rat: increased binding of human chorionic gonadotropinfollowing treatment with FSH in vivo. *Endocrinology*, **95**: 818-825

Zeleznik, A. and Resko, J. (1980) Proesterone does not inhibit gonadotropin-induced follicular maturation in the female rhesus monkey. *Endocrinology*, **106**: 1820-1826

Zeleznik, A. (1981) Premature elevation of sytemic estradiol reduces serum levels of FSH and lengthens the follicular phase of the menstrual phase in rhesus monkeys. *Endocrinology*, **109**: 352-355

Zeleznik, A., Schuler, H. and Reichert, L. J. (1981) Gonadotropin-binding sites in the rhesus monkey ovary: Role of the vasculature in the selective distribution of human chorionic gonadotropin to the preovulatory follicle. *Endocrinology*, **109**: 356-362

Zeleznik, A., Hutchison, J. and Schuler, H. (1985) Interference with the gonadotropin suppressing actions of estradiol in macaques overrides the selection of a single preovulatory follicle. *Endocrinology*, **117**: 991-999

Zeleznik, A. and Kubik, C. (1986) Ovarian responses in macaques to pulsatile infusion of FSH and LH : Increased sensitivity of the maturing follicle to FSH. *Endocrinology*, **119**: 2025-2032

Zeleznik, A. J. and Benyo, D. F. (1994) Control of Follicular Development, Corpus Luteum Function, and the Recognition of Pregnancy in Higher Primates. In (eds), *Physiology of Reproduction*. Raven Press Ltd., New York, p. 751-782.

Zeleznik, A. and Hillier, S. (1996) The ovary: endocrine function. In S. Hillier, H. Kitchener and J. Neilson (eds), *Scientific Essentials of Reproductive Medicine*. WB Saunders Company Ltd., p 133-146.

Zelinski-Wooten, M. B., Hutchison, J. S., Chandrasekher, Y. A., Wolf, D. P. and Stouffer, R. L. (1992) Administration of human luteinizing hormone (hLH) to macaques after follicular development: further titration of LH surge requirements for ovulatory changes in primate follicles. *J Clin Endocrinol Metab*, **75**: 502-507

Zheng, J., Redmer, D. A. and Reynolds, L. P. (1993) Vascular developments and heparin-binding growth factors in the bovine corpus luteum at several stages of the estrous cycle. *Biol Reprod*, **49**: 1177-1189

Zheng, J., Fricke, P. M., Reynolds, L. P. and Redmer, D. A. (1994) Evaluation of growth, cell proliferation, and cell death in bovine corpora lutea throughout the estrous cycle. *Biol Reprod*, **51**: 623-632

Ziche, M., Maglione, D., Ribatti, D., Morbidelli, L., Lago, C., Battisti, M., Paoletti, I. and Barra, A. (1997) Placental growth factor-1 is chemotactic, mitogenic and angiogenic. *Lab Invest*, **76**: 517-531

Zimmerman, T. (1987) Factor VIII/ von Willebrand Factor. Structure and function. *Ann NY Acad Sci*, **509**: 53-59

Appendices

Appendix A: VEGF-A Riboprobe Sequence for *In Situ* Hybridisation

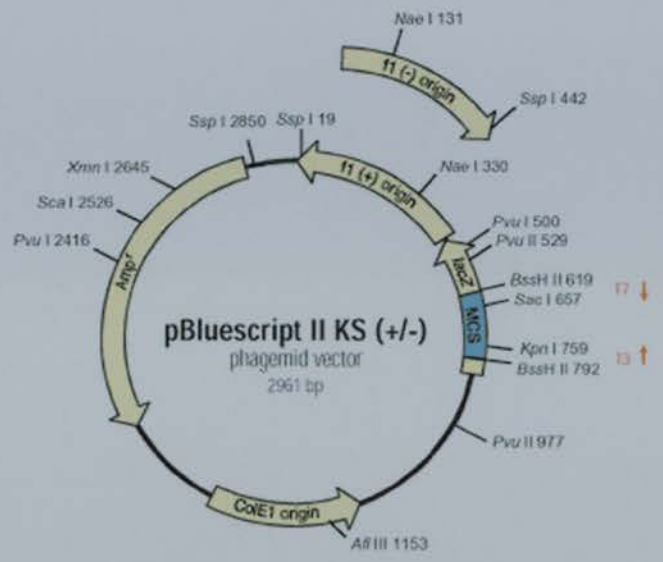

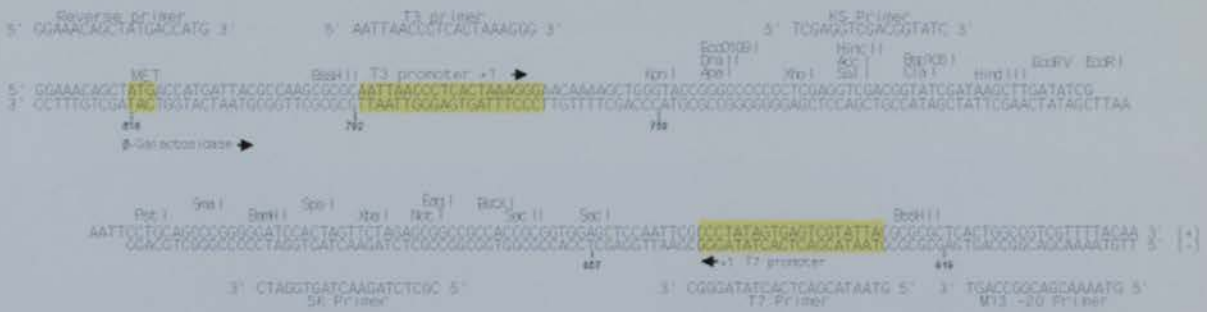

Sequence of the plasmid insert which was specific for all isoforms of VEGF-A

ATGAACTTTC TGCTGTCTTG GGTGCATTGG AGCCTTGCCT TGCTGCTCTA
CCTCCACCAT GCCAAGTGGT CCCAGGCTGC ACCCATGGCA GAAGGAGGAG
GGCAGAATCA TCACGAAGTG GTGAAGTTCA TGGATGTCTA TCAGCGCAGC
TACTGCCATC CAATCGAGAC CCTGGTGGAC ATCTTCCAGG AGTACCCTGA
TGAGATCGAG TACATCTTCA AGCCATCCTG TGTGCCCCTG ATGCGATGCG
GGGGCTGCTG CAATGACGAG GGCCTGGAGT GTGTGCCCAC TGAGGAGTCC
AACATCACCA TGCAGATTAT GCGGATCAAA CCTCACCAAG GCCAGCACAT
AGGAGAGATG AGCTTCCTAC AGCACAACAA ATGTGAATGC AGACCAAAGA
AAGATAGAGC AAGACAAGAA AAATGTGACA AGCCGAGGCG GTGAGCCGGG
CAGGAGGAAG GAGCCTCCCT CAGGGTTTCG GGAACCAGAT CTCTCACCAG
GAAAGACTGA TACAGAACGA TCGATACAGA AACCACGCTG CCGCCACCAC
ACCATCACCA TCGACAGAAC AGTCCTTA

The insert was ligated into the plasmid at the Xba 1 site. The anti-sense riboprobe was synthesised using Xho 1 digestion for plasmid linearisation and T7 RNA polymerase. The sense probe was synthesised using Not 1 and T3.

Appendix B: Probes and Primer Sequences for Quantitative RT-PCR

Ang1

Ang1-Forward primer
CTTGTGGCCCCTCCAATCTA

Ang1-Reverse primer
TAGTGCCACT TTATCCCATT CAGTT

Ang1-Probe on reverse strand
TGGTTTTGTC CCGCAGTATA GAACATTCCA T

Designed from sequence according to the PubMed entrez nucleotide Accession No.:
NM_001146
Length of amplicon: 82bp

Ang2

Ang2- Forward primer
GCCGCTCGAATACGATGACT

Ang2- Reverse primer
ATTAGCCACTGAGTGTTGTTTTCCA

Ang2- FAM labelled probe on reverse strand
TTCTCCAGCACTTGCAGCCTCTGCA

Designed from sequence according to the PubMed entrez nucleotide Accession No.:
NM_001147
Length of amplicon: 77bp

Tie 2

Tie 2- Forward primer
CTTATTTCTGTGAAGGGCGAGTTC

Tie 2- Reverse primer
ATAGTTAAAGTAGCTGGTAGGAAGGAAGCT

Tie 2- FAM labelled probe on reverse strand
TCATGGTTCGTATCCTGATTGCCTCTCCT

Designed from sequence according to the PubMed entrez nucleotide Accession No.:
NM_000459
Length of amplicon: 96bp

VEGF

VEGF- Forward primer
TACCTCCACCATGCCAAGTG

VEGF- Reverse primer
TAGCTGCGCTGATAGACATCCA

VEGF- FAM labelled probe on reverse strand
ACTTCGTGATGATTCTGCCCTCCTCCTT

Designed from sequence according to the PubMed entrez nucleotide Accession No.: E15157
Length of amplicon: 103bp
Recognises all isoforms of VEGF-A, **not** PlGF, VEGF B, C, or D

VEGF Receptor flt

Flt- Forward primer
ATGTGCCAAATGGGTTTCATGT

Flt- Reverse primer
ACTTGTTAACTGTGCAAGACAGTTTCA

Flt- FAM labelled probe on reverse strand
CTCTCCTTCCGTCGGCATTTTTTCCAA

Designed from sequence according to the PubMed entrez nucleotide Accession No.: NM_002019
Length of amplicon: 85bp

VEGF Receptor KDR

KDR- Forward primer
TTACAGCTTCCAAGTGGCTAAGG

KDR- Reverse primer
ATTTTAACCACGTTCTTCTCCGATAA

KDR- FAM labelled probe on forward strand
CTTGGCA TCGCGAAAGT GTATCCACA

Designed from sequence according to the PubMed entrez nucleotide Accession No.: AF063658
Length of amplicon: 110bp

Appendix C: Papers published

Human Reproduction vol.14 no.8 pp.2054–2060, 1999

The effect of the angiogenesis inhibitor TNP-470 on luteal establishment and function in the primate

H.M.Fraser[1,3], S.E.Dickson[1], K.D.Morris[1], G.F.Erickson[2] and S.F.Lunn[1]

[1]MRC Reproductive Biology Unit, Centre for Reproductive Biology, 37 Chalmers Street, Edinburgh EH3 9ET, UK and [2]Department of Reproductive Medicine, University of California at San Diego, USA

[3]To whom correspondence should be addressed

Angiogenesis during luteal development is probably essential for normal lutein cell function. Since the angiogenesis inhibitor TNP-470 inhibits pregnancy in mice, the current study investigated its effects on the establishment and function of the primate corpus luteum. Regularly ovulating macaques were treated with TNP-470 (6 mg/kg), i.v. in three doses, 48 h apart. Serum progesterone concentrations, as indicators of treatment effect, were normal in four macaques where treatment commenced at the onset of the ovulatory progesterone rise, and in five of eight in which treatment commenced a few days before ovulation. In the other three the normal progesterone rise was absent. To investigate the direct effect on luteal angiogenesis of a daily dose over a longer period, four marmosets received 18 mg/kg/day of TNP-470 i.v. for 9 days starting at ovulation. On day 10, luteal cell proliferation was determined by nuclear bromodeoxyuridine incorporation. Luteal microvasculature was examined using immunocytochemical factor VIII staining, and endothelial cell and luteal function assessed by in-situ hybridization of insulin-like growth factor binding protein-3 mRNA and plasma progesterone concentrations respectively. None of these parameters were affected by the TNP-470 treatment. The results show that, with the treatment regimens employed, TNP-470 had no significant effect on the expression of the differentiated state of the primate corpus luteum.

Key words: endothelial cells/factor VIII/IGFBP-3/monkey/proliferation

Introduction

The corpus luteum is essential for the establishment of pregnancy through the production of progesterone from the lutein cells. Intense angiogenesis occurs during early luteal development (Rodger *et al.*, 1997) and it is believed that the angiogenesis is critical for the transport of hormonal precursors of progesterone to, and progesterone from, the lutein cells (Redmer and Reynolds, 1996). Recently, the importance of angiogenesis in the establishment of the rat corpus luteum has been shown by studies in which the process has been inhibited by blocking the action of vascular endothelial growth factor (Ferrara *et al.*, 1998). Further studies in mice have shown that the angiogenesis inhibitor, TNP-470, which acts on endothelial cells at a number of sites in the angiogenic pathway (Abe *et al.*, 1994), inhibits luteal development and prevents pregnancy by interfering with the process of decidualization and placental and yolk sac formation (Klauber *et al.*, 1997). It has been suggested that the corpus luteum could be a target for fertility regulation by virtue of its susceptibility to anti-angiogenic agents (Klauber *et al.*, 1997; Ferrara *et al.*, 1998). The mechanisms which regulate luteal function in rodents and primates are markedly different and in the non-fertile cycle of the rodent the corpus luteum is active for less than a day, while that of many primates is functional for 2 weeks prior to its regression (Behrman *et al.*, 1993). The aim of this study was to investigate the effects of TNP-470 on the primate corpus luteum. The information gleaned from this primate model should be useful to the projected clinical use of this compound.

The study was designed to investigate the effects of TNP-470 on angiogenesis at the time of transformation of the pre-ovulatory follicle into the functional corpus luteum. Two species of non-human primate were employed. First, stump-tailed macaques were investigated to allow detailed analysis of the endocrinology in response to TNP-470 treatment. We chose this species because we have previously established its clinical relevance with respect to manipulation of the menstrual cycle in studies using gonadotrophin releasing hormone analogues (Fraser *et al.*, 1997) and on the physiology of inhibin (Fraser *et al.*, 1999). In addition, we investigated the effects of TNP-470 in the marmoset monkey in which we have built up considerable information on the cellular and molecular control of luteal function (e.g. Young *et al.*, 1997; Duncan *et al.*, 1998; Fraser *et al.*, 1998). The establishment and function of the corpus luteum was determined by measuring circulating progesterone concentrations in both species. Cellular responses were studied in the marmoset by determining the number of mitotic cells, following bromodeoxyuridine (BrdU) administration as a marker, by examining the establishment of the microvascular network using factor VIII staining to identify endothelial cells, and by studying the capacity of the endothelial cells to express insulin-like growth factor-binding protein-3 (IGFBP-3) messenger ribonucleic acid (mRNA) which we have shown previously to be a marker for healthy endothelial cells in the marmoset corpus luteum (Fraser *et al.*, 1998).

Materials and methods

Animals

Adult female stump-tailed macaques weighing 10–13 kg were captive bred and housed as described previously (Fraser *et al.*, 1999) in a unit opened in 1996. Daily vaginal swabs were taken to detect the pattern of menstrual bleeding and the first day of menstruation was designated day 1 of the cycle. Blood samples were collected by femoral venepuncture without anaesthesia. All the animals in the study had regular ovulatory cycles as determined from menstrual pattern monitored for 6 months prior to the study and serum concentrations of oestradiol-17β and progesterone in blood samples obtained three times per week during the cycle prior to treatment.

Common marmoset monkeys were housed in cages in rooms at a temperature of 22.5°C, exposed to the same lighting conditions as described above. The animals were fed daily with a selection of fruit, SDS Mazuri (E) primate diet pellets, and high protein porridge with multivitamin supplements three times per week. Adult females having a body weight of approximately 350 g, with regular ovulatory cycles, were housed together with a younger sister or prepubertal female in cages measuring 1.15 m in height, 1.1 m in depth and 0.6 m wide. Each contained larch branches and a nest box with the floor of the cage filled with wood chippings to allow foraging. Blood samples were collected three times per week by femoral venepuncture without anaesthesia to confirm normal ovulatory cycles. Plasma was stored at –20°C until required for assay. Criteria for the occurrence of ovulation and normal luteal phase length (18–22 days) were based on determination of plasma progesterone concentrations as described previously (Smith *et al.*, 1990).

Treatments

The experiments were carried out in accordance with the Animals (Scientific Procedures) Act, 1986. TNP-470 (*O*-chloroacetylcarbamoyl fumagillol, also known as AGM-1470), has been administered to patients with Kaposi's sarcoma at doses ranging from 10–70 mg/m^2 given by i.v. infusion over a period of 1 h once per week (Dezube *et al.*, 1998). The current clinical schedule is of 60 mg/m^2 TNP-470 administered by i.v. infusion over a period of 1 h three times per week (Dezube *et al.*, 1998). In an attempt to ensure effective treatment, it was decided to administer 120 mg/m^2 to the primates, calculated according to a published formula (Du Bois and Du Bois, 1916). On a dose/kg basis, for a woman weighing 56 kg, the total daily dose would be 96 mg, i.e. 1.7 mg/kg. For the macaques, a dose of between 60 and 84 mg was used, equivalent to 6 mg/kg. Seven stump-tailed macaques, with regular ovulatory menstrual cycles, were treated with TNP-470 dissolved in 5% dextrose at a concentration of 4 mg/ml immediately before use. On three occasions 2 days apart, starting around the time of predicted ovulation, the macaques received a total volume of between 15–21 ml, depending upon body weight, administered by slow i.v. injection in two separate doses 1 h apart. A second experiment was undertaken in which five macaques were given the same treatment, commencing 4 days prior to expected ovulation, a period covering final pre-ovulatory development.

Since the final results in macaques indicated an absence of effect of treatment on luteal function, it was decided to investigate the susceptibility of the primate corpus luteum to an increased (daily) dose of TNP-470 over a longer time period (10 days) and, to investigate the possibility that angiogenesis could be inhibited in the absence of an effect on progesterone secretion, a further experiment was undertaken using the marmoset. To synchronize timing of ovulation during the treatment cycle, eight animals were treated with 1 μg prostaglandin $F_{2\alpha}$ analogue (Planate®; Coopers Animal Health Ltd, Crewe, Cheshire, UK) i.m., during the mid- to late luteal phase of the pre-treatment cycle to induce luteolysis. This treatment is normally followed by ovulation 10–12 days later (Summers *et al.*, 1985). Four marmosets were treated with TNP-470 starting 11 days post-prostaglandin, the day of anticipated ovulation, at a dose of 18 mg/kg/day (equivalent to 120 mg/m^2), by slow i.v. injection. This treatment was repeated for a further 9 days: the remaining four controls were treated with vehicle following the same schedule.

On day 10 after commencement of TNP-470, each marmoset received by slow i.v. infusion, 20 mg BrdU (Boehringer Mannheim, Essex, UK) in saline. One hour later, the animals were sedated using 100 μl ketamine hydrochloride (Parke-Davis Veterinary, Pontypool, Gwent, UK) i.m. and euthanased with an i.v. injection of 400 μl sodium pentobarbitone (Euthetal®; Rhone Merieux, Ireland). Ovaries were removed rapidly, weighed, and fixed immediately in 4% paraformaldehyde for 24 h. After fixation, the corpora lutea of the cycle were identified macroscopically, the ovaries were bisected as closely as possible through the centre of the corpora lutea, and the tissues dehydrated and embedded in paraffin.

Hormone assays

Circulating progesterone and oestradiol concentrations were measured as described previously for the stump-tailed macaque (Fraser and Sandow, 1985; Fraser *et al.*, 1997) and marmoset (Smith *et al.*, 1990).

Immunocytochemistry

Tissue sections (5 μm) were cut onto Tespa-coated (Sigma, Poole, Dorset, UK) slides for immunocytochemistry and morphological examination. Sections were stained with haematoxylin and eosin and examined for morphological features of apoptosis as described previously (Young *et al.*, 1997). Localization of factor VIII as a marker for endothelial cells was determined by immunocytochemistry as described for the human corpus luteum (Rodger *et al.*, 1997) except that visualization was with nitro blue tetrazolium (NBT) in buffer (100 mol/l Tris pH 9.5, 100 mol/l NaCl and 50 mol/l $MgCl_2$). These sections were not counterstained, so that quantitative image analysis could be performed, the corpora lutea being identified from the haematoxylin and eosin-stained sections. Factor VIII immunostaining was quantified using the Image Pro-Plus 3.0® (Media Cybernetics, Silver Spring, MD, USA) image analysis program. Sections were examined at ×400 magnification. The image was converted to grey scale and the area of dark objects on a white background was counted at a threshold of 70. For each corpus luteum, six randomly chosen areas, each of 27 860 μm^2, were analysed and their mean taken as being representative for that animal. Differences between groups were determined using a two tailed unpaired *t*-test, $P < 0.05$ being taken as the level of significance.

Proliferating cells were visualized in ovarian sections using a mouse monoclonal antibody to BrdU (Boehringer Mannheim). Sections were dewaxed in histoclear and rehydrated in decreasing concentrations of industrial methylated spirits. Antigen retrieval was accomplished by microwaving sections for 4×5 min in 0.01 M citrate buffer. Using Sequenza racks (Life Sciences International, Hampshire, UK), sections were treated for 30 min with normal rabbit serum block (NRS; Dako, High Wycombe, Bucks, UK), then incubated in mouse monoclonal anti-BrdU (3 μg/ml in TBS) at 4°C, overnight. Control sections were treated with mouse IgG (Vector Laboratories, Peterborough, UK) (3 μg/ml in TBS) in place of primary antibody. Secondary antibody, rabbit anti-mouse (26 μg/ml in blocking serum), was applied for 30 min at room temperature. BrdU binding was visualized using mouse APAAP (1 μg/ml in blocking serum) incubation for 30 min, and the NBT detection system (Boehringer Mannheim). Sections were briefly counterstained with haematoxylin and mounted for analysis. Cell proliferation was assessed by counting the number of BrdU positive

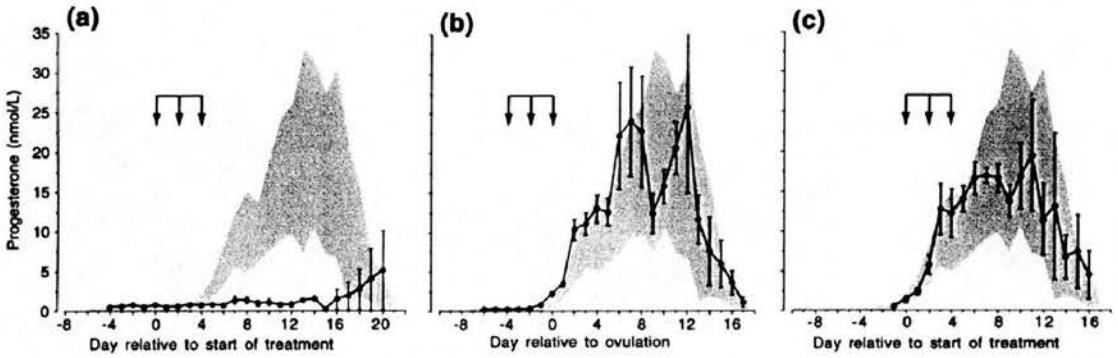

Figure 1. Serum progesterone concentrations in macaques treated with TNP-470 (vertical arrows, 6 mg/kg body weight) starting (**a**) during the follicular phase of the menstrual cycle in which luteal function was not detected (n = 3), (**b**) during the follicular phase of the menstrual cycle in which luteal function appeared normal (n = 5) and (**c**) during the ovulatory period/early luteal phase of the menstrual cycle in which luteal function appeared normal (n = 4). The shaded area represents the mean ± SD for 18 control cycles (taken from Fraser *et al.*, 1997).

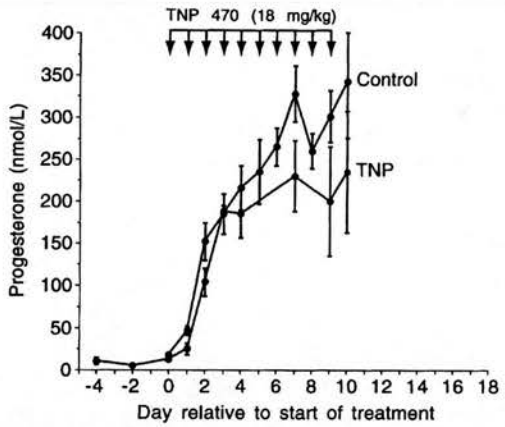

Figure 2. Plasma progesterone concentrations in control marmosets and in those treated daily with TNP-470 (arrows) starting on the day of expected ovulation (n = 4 per group). Values are means ± SEM.

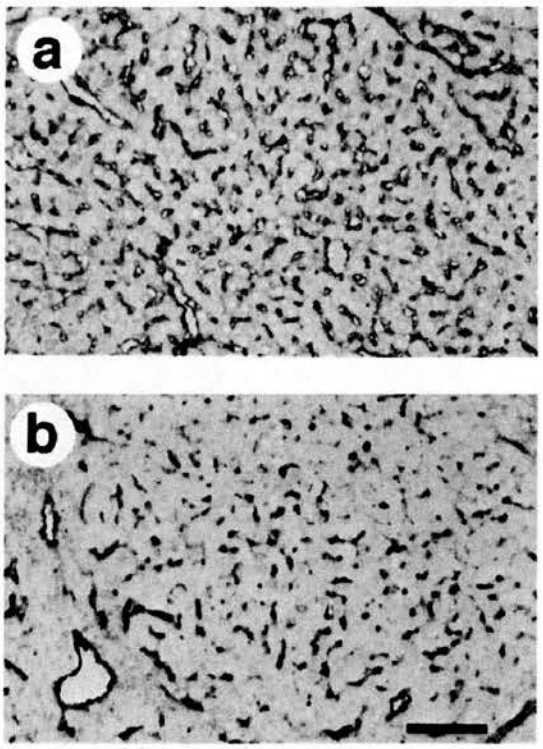

Figure 3. Factor VIII localization in the corpus luteum of (**a**) a control and (**b**) a TNP-470 treated marmoset. In both examples staining of endothelial cells forming the microvessels and a proportion of endothelial cells forming capillaries can be observed (bar = 200 μm).

cells in six randomly chosen fields per corpus luteum and expressed as a mean percentage of the total cells in these fields. Differences between groups were determined using a two tailed unpaired t-test, $P < 0.05$ being taken as the level of significance.

In-situ hybridization

Paraffin sections (5 μm) were mounted onto poly-L-lysine coated glass slides for IGFBP-3 mRNA localization undertaken by in-situ hybridization as described previously (Fraser *et al.*, 1998). In addition to the ovaries from control and treated animals, ovaries from follicular phase marmosets known to contain spontaneously regressing corpora lutea were included in the same run. Following hybridization with antisense (two slides per ovary) and sense probes, and washing, dry slides were dipped in Kodak NTB-2® liquid emulsion (Eastman Kodak, Rochester, NY, USA) and exposed for 3.5 weeks at 4°C in light-tight slide boxes. Slides were developed with D-19 developer (Eastman Kodak) for 3.5 min at 4°C, fixed, and the sense and one antisense stained with haematoxylin (Richard-Allan, Richland, MI, USA), while the remaining antisense slide was stained with both haematoxylin and eosin to allow a more reliable identification of cell type. Identified endothelial cells that were not associated with a perceptible vascular lumen were classified as capillary endothelial cells: when a lumen was evident, they were classified as microvessels and included venules and arterioles. The localization of expression to microvessels, capillaries and lutein cells of the corpora lutea was scored as follows: no expression above tissue background –, low expression +, moderate expression ++, high expression +++.

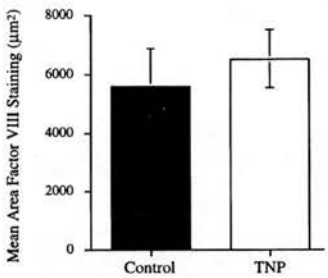

Figure 4. Quantification of factor VIII immunostaining in control and TNP-470 treated marmoset corpora lutea. Data are means ± SEM.

Results

In the first experiment, retrospective analysis indicated that TNP-470 treatment had begun at, or immediately after, ovulation in four of the seven macaques and no effects on serum progesterone were recorded. In these animals, the treatment had commenced when serum oestradiol concentrations had reached pre-ovulatory values (>400 pmol/l) or shortly afterwards. In the other three macaques treatment had commenced prior to ovulation when oestradiol concentrations were <400 pmol/l. In one of these animals, ovulation occurred at the expected time (as demonstrated by normal luteal phase progesterone concentrations), while in the other two animals such a progesterone rise did not occur. This suggested an absence of effect of TNP-470 on luteal function, but indicated that follicle development may be susceptible to such treatment. To study this possibility, a second experiment was performed in which treatment was initiated during the mid-follicular phase: however, ovulation occurred in four of the five macaques as determined by serum oestradiol and progesterone levels. For the purpose of analysis, the results from both experiments were combined according to whether treatment had begun during the follicular phase and was associated with absence of ovulation (Figure 1a, $n = 3$), normal serum progesterone (Figure 1b, $n = 5$), or had commenced at the time of ovulation (Figure 1c, $n = 4$).

In the marmoset, plasma progesterone concentrations (Figure 2) and numbers of corpora lutea were similar in control and treated animals. The presence of corpora lutea was evident in both control and treated animals by gross observation. Study of ovarian sections revealed the presence of similar numbers of recently formed corpora lutea (control: 2,2,3,3; treated: 2,2,3,4). The development of the microvasculature of the corpus luteum was confirmed in the control marmosets by an extensive network of microvessel and capillary staining for factor VIII and this was also evident in the TNP-470 treated animals (Figure 3). Quantification of factor VIII immunostaining showed no significant difference associated with treatment (Figure 4).

BrdU staining indicating proliferating cells was readily observed in all corpora lutea. In the marmoset differences between theca and granuolosa derived lutein cells were not readily apparent (Webley *et al.*, 1990), both types of hormone producing cells having a large spherical or polyhedral nucleus and abundant cytoplasm (Figure 5a). Although dual staining

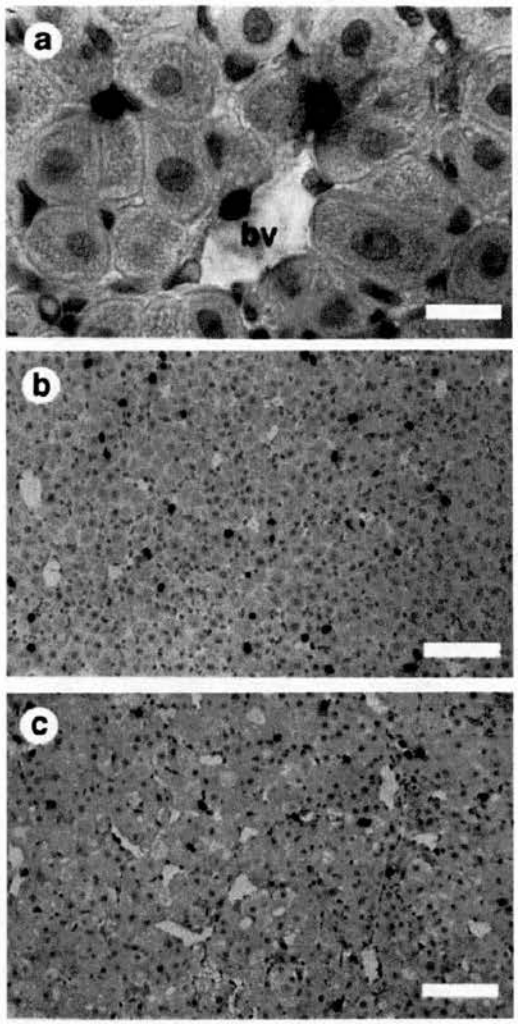

Figure 5. Bromodeoxyuridine (BrdU) incorporation (dark staining nuclei) into endothelial cells of microvessels and capillaries of corpora lutea from control and TNP-470 treated marmosets. **(a)** High power photomicrograph showing the large hormone producing cells with abundant cytoplasm, round nucleus and absence of BrdU staining. Note the microvessel located centrally composed of endothelial cells with little cytoplasm and elongate nuclei. Note the presence of dark BrdU proliferating cells associated with the blood vessel and in endothelial cells of capillaries distributed between the hormone producing cells (bar = 25 μm). **(b, c)** Low power micrographs showing the general distribution of BrdU staining in **(a)** a control, and **(c)** a TNP-470 treated marmoset (bar = 100 μm).

experiments were not performed, it was clear that none of the hormone-producing cells had incorporated BrdU. Incorporation was restricted to some cells surrounding the luminal microvessels and in those whose appearance was consistent with capillary endothelial cells. BrdU staining in these cells was evident in all corpora lutea from control and treated marmosets (Figure 5). Proliferation index showed there was no significant difference between the groups (Figure 6). Examination of sections stained with haematoxylin and eosin by an observer

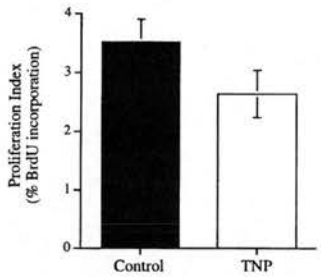

Figure 6. The proliferation index in corpora lutea from control and TNP-470 treated marmoset corpora lutea. Data are means ± SEM.

with expertise in identification of apoptotic cells as described previously (Young *et al.*, 1997) revealed a virtual absence of apoptosis in both groups.

In mid-luteal control ovaries, IGFBP-3 mRNA was strongly expressed in the endothelial cells lining microvessels and in a small number of capillaries within the corpora lutea (Figure 7). In the TNP-470 treated animals, a similar pattern of IGFBP-3 mRNA expression was observed in all corpora lutea. As expected, the regressing corpora lutea in normal follicular phase ovaries exhibited only a low level of expression in a few microvessels (not shown). Hybridization with the IGFBP-3 cRNA sense probe showed no signal above background, underlining the specificity of hybridization using the mRNA antisense probe (not shown).

Discussion

The results show that short-term treatment with TNP-470 had little or no detectable effect on the development and function of the primate corpus luteum of either the stump-tailed macaque or the marmoset monkey. When TNP-470 was administered at the time of expected ovulation, the function of the corpus luteum and duration of the luteal phase, as assessed by circulating progesterone concentrations, was normal. From the oestradiol data in the first experiment in macaques, there was an indication that initiation of treatment at a time when follicular development was less advanced than expected led to suppression of ovulation, but when this was investigated in a second experiment in which treatment was initiated during the late follicular phase, four out of five animals had normal progesterone profiles. Thus, of the 12 cycles studied with TNP-470, nine resulted in normal luteal function while the expected rise in progesterone failed to occur in three animals. Perhaps the simplest explanation of this result is that these three animals were destined to have anovular cycles irrespective of treatment. Alternatively, it is possible that TNP-470 had a marginal effect upon angiogenesis and/or follicular development at this dose. With respect to the former, one could speculate that angiogenesis was being inhibited to some degree, but that luteal function was not uniformly affected.

With respect to timing and duration of treatment, the experiment was designed to target the intense angiogenesis which occurs in the corpus luteum during the early stages of development (Christenson and Stouffer, 1996; Rodger *et al.*, 1997). Accordingly, treatment was started at the time of

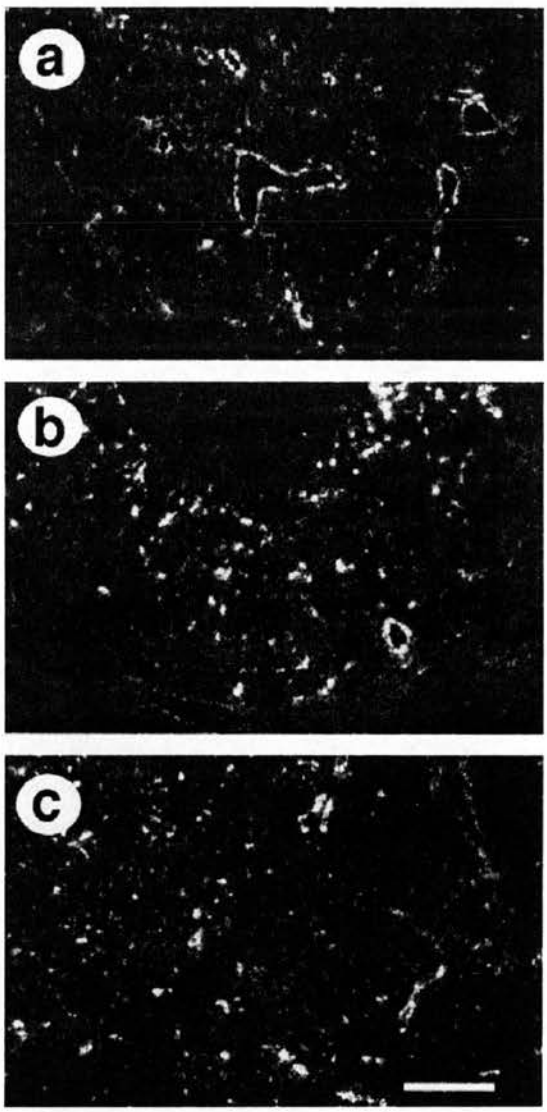

Figure 7. Insulin-like growth factor binding protein (IGFBP)-3 mRNA expression in the corpus luteum from (**a**) control, (**b**) and (**c**) TNP-470-treated animals. Each depicts expression in the microvessels while isolated grain clusters indicate expression in capillary endothelial cells. Note the absence of detectable differences in the level and pattern of IGFBP-3 mRNA expression after treatment (bar = 100 μm).

predicted ovulation and covered the period of the early luteal phase in the macaque and was extended to the mid-luteal phase in the marmoset. The studies in the marmoset allowed the investigation of the effects of a more frequent and prolonged dose schedule of TNP-470 and the examination of its potential consequences on cell proliferation and the luteal vasculature. Progesterone secretion was not impaired and the number of corpora lutea formed was normal. Furthermore, staining for factor VIII illustrated the establishment of the luteal vascular tree despite treatment with the putative angiogenesis inhibitor. As expected, BrdU incorporation demonstrated a high level of

proliferation of endothelial cells during the mid-luteal phase and this too was unaffected by treatment with TNP-470. Finally, expression of IGFBP-3 mRNA, which we have previously shown to be a marker for endothelial cells in the functioning corpus luteum of the marmoset and human (Fraser *et al.*, 1998), was also unchanged. Collectively, these results suggest that TNP-470 does not have negative effects on the structure and function of the normal corpus luteum of the marmoset, in contrast to the findings in the mouse (Klauber *et al.*, 1997). At this early stage of experiments to inhibit angiogenesis in the primate corpus luteum, we are forced to conclude that the differences between the present results and those in the mouse may reflect inter-species variance, and/or differential susceptibility to the anti-angiogenic effect of TNP-470.

The latter possibility could arise from the dose of TNP-470 employed in the present study being insufficient to prevent luteal angiogenesis, or the route of administration being suboptimal. The clinical dose of TNP-470 is 60 mg/m^2 administered by 1 h i.v. infusion three times per week (Dezube *et al.*, 1998). The dose chosen for the macaques was twice that with respect to surface area and 3.5 times that of the human dose when expressed on a drug weight to body weight ratio. Also, a dose of 6 mg/kg by 1 h infusion in macaques was anti-angiogenic with respect to suppression of ocular angiogenesis (J. Folkman and M. O'Reilly, personal communication). The stump-tailed macaques used in the present study were treated using two i.v. injections 1 h apart, rather than by infusion over 1 h, because this enabled the treatment to be administered without surgical intervention or sedation. Studies in the mouse employed the s.c. route at a dose of 30 mg/kg every second day. The marmosets in the present study were treated with 18 mg/kg daily, so approaching the murine dose. It should be noted that TNP-470 is metabolized very rapidly and that its pharmacodynamic properties are incompletely understood (Cretton-Scott *et al.*, 1996). Thus, differences in the pattern of exposure to the drug may result from the different routes of administration. However, at present, a preparation of TNP-470 that can be administered by the s.c. route to larger animals and humans is not available.

This is the first report of an attempt to block angiogenesis in the primate corpus luteum. Although inhibitory effects were not observed, we believe that the approach used to study angiogenesis in the marmoset will be of value to future experiments on the effects of angiogenesis inhibitors on luteal function in the primate. BrdU incorporation proved an accurate method of identifying proliferating cells in the corpus luteum. This technique has been used previously to quantify luteal proliferation in the sheep (Jablonka-Shariff *et al.*, 1993) and rat (Gaytan *et al.*, 1996) but, to our knowledge, this is the first report of its use with respect to the primate ovary. The high level of proliferation during the mid-luteal phase in the marmoset agrees with results using the proliferation marker Ki67 in the rhesus monkey and human (Christenson and Stouffer, 1996; Rodger *et al.*, 1997). The localization of IGFBP-3 mRNA in the marmoset ovary confirms and extends our recent observation that production of this mRNA is associated with the functioning corpus luteum in the primate (Fraser *et al.*, 1998), and contrasts with the situation in the rodent where its expression is temporally associated with luteolysis (Erickson *et al.*, 1993). This binding protein is likely to be of importance in the modulation of IGF activity within the corpus luteum. The observation that the expression of the IGFBP-3 mRNA is associated with the endothelial cells of the functioning corpus luteum only, also indicates a role yet to be defined in endothelial cell proliferation and survival.

The potential of using angiogenesis inhibitors as anti-fertility agents is currently generating considerable interest (Klauber *et al.*, 1997; Ferrara *et al.*, 1998). Furthermore, while they are being developed primarily for treatment of vascular solid tumours, they are also likely to find a role in control of rheumatoid arthritis, retinal neovascularization and psoriasis (Folkman, 1995). It is essential, therefore, that their potential effects upon the reproductive system and its function in such patients be determined. However, the current results show that with the treatment regimens employed, TNP-470 has no significant effect on the expression of the differentiated state of the primate corpus luteum.

Acknowledgements

We thank TAP Holdings, Deerfield, IL, USA, for the gift of TNP-470 and their staff for their help during the course of this project, Dr R.J. D'Amato and Dr J. Folkman for helpful discussions with respect to experimental design, the staff of our Primate Unit for animal management, M. Millar and P. Largue for expert support with histology and F. Pitt and I. Swanston for radioimmunoassays.

References

Abe, J., Zhou, W., Takuwa, N. *et al.* (1994) A fumagillin derivative angiogenesis inhibitor, AGM-1470, inhibits activation of cyclin-dependent kinases and phosphorylation of retinoblastoma gene product but not protein tyrosyl phosphorylation or protooncogene expression in vascular endothelial cells. *Cancer Res.*, **54**, 3407–3412.

Behrman, H.R., Endo, T., Aten, R.F. *et al.* (1993) Corpus luteum function and regression. *Reprod. Med. Rev.*, **2**, 153–180.

Christenson, L.K. and Stouffer, R. L. (1996) Proliferation of microvascular endothelial cells in the primate corpus luteum during the menstrual cycle and simulated early pregnancy. *Endocrinology*, **137**, 367–374.

Cretton-Scott, E., Placidi, L., McClure, H. *et al.* (1996) Pharmacokinetics and metabolism of O-(chloroacetyl–carbamoyl) fumagillol (TNP-470, AGM-1470) in rhesus monkeys. *Cancer Chemother. Pharmacol.*, **38**, 117–122.

Du Bois, D., and Du Bois, E.F. (1916) Clinical calorimetry X. A formula to estimate the approximate surface area if height and weight be known. *Arch. Int. Med.*, **17**, 863–871.

Dezube, B.J., Von Roenn, J.H., Holden-Wiltse, J. *et al.* (1998) Fumagillin analog in the treatment of Kaposi's sarcoma: a phase 1 AIDS clinical trial group study. AIDS clinical trial group no. 215 team. *J. Clin. Oncol.*, **16**, 1444–1449.

Duncan, W.C. Illingworth, P.J., Young, F.M. and Fraser, H.M. (1998) Induced luteolysis in the primate: rapid loss of luteinizing hormone receptors. *Hum. Reprod.*, **13**, 2532–2540.

Erickson, G.F., Natatani, A., Ling, N. *et al.* (1993) Insulin-like growth factor binding protein-3 gene expression is restricted to involuting corpora lutea in rat ovaries. *Endocrinology*, **133**, 1147–1157.

Ferrara, N., Chen, H., Davis-Smyth, T. *et al.* (1998) Vascular endothelial growth factor is essential for corpus luteum angiogenesis. *Nature Med.*, **4**, 336–340.

Folkman, J. (1995) Angiogenesis in cancer, vascular, rheumatoid and other disease. *Nature Med.*, **1**, 27–31.

Fraser, H.M. and Sandow, J. (1985) Suppression of follicular maturation by infusion of a luteinizing hormone-releasing hormone agonist starting during the late luteal phase in the stump-tailed macaque monkey. *J. Clin. Endocrinol. Metab.*, **60**, 579–584.

Fraser, H.M., Lunn, S.F., Morris, K.D. *et al.* (1997) Initiation of high dose GnRH antagonist treatment during the late follicular phase in the macaque abolishes luteal function irrespective of effects upon the LH surge. *Hum. Reprod.*, **12**, 101–106.

Fraser, H.M., Lunn, S.F., Kim, H. *et al.* (1998) Insulin-like growth factor binding protein-3 (IGFBP-3) mRNA in the endothelial cells of the primate corpus luteum. *Hum. Reprod.*, **13**, 2180–2185.

Fraser, H.M., Groome, N.P. and McNeilly, A.S. (1999) FSH-inhibin B interactions during the follicular phase of the primate menstrual cycle revealed by GnRH antagonist and anti-estrogen treatment. *J. Clin. Endocrinol. Metab.*, **84**, 1365–1369.

Gaytan, F., Morales, C., Bellido, C. *et al.* (1996) Proliferative activity in the different ovarian compartments in cycling rats estimated by the 5-bromodeoxyuridine technique. *Biol. Reprod.*, **54**, 1356–1365.

Jablonka-Shariff, A., Grazul-Bilska, A.T., Redmer, D.A. *et al.* (1993) Growth and cellular proliferation of ovine corpora lutea throughout the estrous cycle. *Endocrinology*, **133**, 1871–1879.

Klauber, N., Rohan, R.M., Flynn, E. *et al.* (1997) Critical components of the female reproductive pathway are suppressed by the angiogenesis inhibitor AGM-1470. *Nature Med.*, **3**, 443–446.

Redmer, D.A. and Reynolds, L.P. (1996) Angiogenesis in the ovary. *Rev. Reprod.*, **1**, 182–192.

Rodger, F.E., Young, F.M., Fraser, H.M. *et al.* (1997) Endothelial cell proliferation follows the mid-cycle luteinizing hormone surge, but not human chorionic gonadotrophin rescue, in the human corpus luteum. *Hum. Reprod.*, **12**, 1723–1729.

Smith, K.B., Lunn, S.F. and Fraser, H.M. (1990) Inhibin secretion during the ovulatory cycle and pregnancy in the common marmoset monkey. *J. Endocrinology*, **126**, 489–495.

Summers, P.M., Wennink, J. and Hodges, J.K. (1985) Cloprostenol-induced luteolysis in the marmoset monkey (Callithrix jacchus). *J. Reprod. Fertil.*, **73**, 133–138.

Webley, G.E., Richardson, M.C., Smith, C.A. *et al.* (1990) Size distribution of luteal cells from pregnant and non-pregnant marmoset monkeys and a comparison of the morphology of marmoset luteal cells with those from the human corpus luteum. *J. Reprod. Fertil.*, **90**, 427–437.

Young, F.M., Illingworth, P.J., Lunn, S.F. *et al.* (1997) Cell death during luteal regression in the marmoset monkey (Callithrix jacchus). *J. Reprod. Fertil.*, **111**, 109–119.

Received on November 4, 1998; accepted on April 8, 1999

0013-7227/00/$03.00/0
Endocrinology

Vol. 141, No. 3
Printed in U.S.A.

Suppression of Luteal Angiogenesis in the Primate after Neutralization of Vascular Endothelial Growth Factor*

HAMISH M. FRASER, SARAH E. DICKSON, STEPHEN F. LUNN, CHRISTINE WULFF, KEITH D. MORRIS, VERONICA A. CARROLL, AND ROY BICKNELL

Medical Research Council Reproductive Biology Unit, Center for Reproductive Biology (H.M.F., S.E.D., S.F.L., C.W., K.D.M.), Edinburgh, United Kingdom EH3 9ET; the Department of Cancer Medicine, Imperial College School of Medicine, Hammersmith Campus (V.A.C.), London, United Kingdom W12 0NN; and Molecular Angiogenesis Laboratories, Imperial Cancer Research Fund, Institute of Molecular Medicine, John Radcliffe Hospital (R.B.), Oxford, United Kingdom OX3 9DS

ABSTRACT

Manipulation of angiogenesis may have a profound effect on female reproductive function, but this has not yet been demonstrated by direct experiment in species with ovulatory cycles similar to those in women. To investigate whether angiogenesis could be inhibited in the primate corpus luteum, and the consequences of such inhibition on luteal function, marmosets were treated with an antibody to vascular endothelial growth factor (VEGF). Treatment commenced at the time of ovulation and was continued for 3 days (early luteal group) or 10 days (midluteal group). Bromodeoxyuridine was used to label proliferating cells, being administered 1 h before collecting ovaries from control and treated animals in the early or midluteal phase. Ovarian sections were stained using an antibody to bromodeoxyuridine, and a proliferation index was obtained; endothelial cell quantification was performed using factor VIII as an endothelial cell marker. Intense proliferation in the early luteal phase was suppressed by anti-VEGF treatment. This resulted in blockade of development of the normally extensive capillary bed, as in the animals treated until the mid-luteal phase the numbers of endothelial cells were reduced. The hormone-producing cells remained largely unaltered in the posttreatment corpus luteum, although the presence of lipid accumulation, and small pockets of cells showing basophilia and nuclear condensation were observed. Significantly, luteal function, as judged by secretion of progesterone, was markedly compromised by the treatment, being reduced by 60% in comparison with controls. It is concluded that VEGF-mediated angiogenesis is an essential component of luteal function in primates and therefore has the potential to be regulated. (*Endocrinology* **141:** 995–1000, 2000)

IT IS ESTABLISHED that inhibition of angiogenesis by broad spectrum or systematic targeting (1–4) of the angiogenic pathway can have suppressive effects on tumor growth. However, comparatively little is known about the effect of inhibition of the highly active physiological angiogenesis that occurs in the reproductive tissues: the ovary, uterus, and placenta. The corpus luteum is essential for the establishment of pregnancy through the production of progesterone from lutein cells. Active angiogenesis occurs during early luteal development. It is believed that this angiogenesis is critical for establishment of the vasculature essential for transport of hormonal precursors of progesterone to and progesterone from the lutein cells (5). The role of angiogenesis in the rodent ovary has been addressed (6, 7), but the mechanisms that regulate luteal function in rodents and primates are markedly different (8). Our finding of the failure of TNP-470 to affect luteal function in Old World or New World primates (9) emphasizes the need for caution in extrapolating results from the rodent, in which this angiogenesis inhibitor prevented pregnancy (7). Thus, an effect of inhibition of angiogenesis on female reproductive function has not yet been demonstrated by direct experiment in species with ovulatory cycles similar to those in women.

The aim of this study was to investigate the effects of immunoneutralization of vascular endothelial growth factor (VEGF) on the marmoset corpus luteum of the normal cycle as a means of exploring the role of angiogenesis in luteal function of the primate. VEGF has been shown to be expressed in the corpus luteum of the human and nonhuman primate and is therefore a likely candidate for targeting (10–12).

Materials and Methods

VEGF antibody

Mouse monoclonal anti-VEGF, VG76e, was raised by immunization with recombinant human VEGF-189. The pET146 expression plasmid was used to enable affinity purification of *Escherichia coli*-expressed recombinant protein. The antibody was produced from hybridomas grown in culture, and a highly purified preparation was obtained using protein A-Sepharose columns. Hybridomas were screened by Western blotting of VEGF-189. Using recombinant proteins, it was demonstrated that VG76e recognizes the 121, 165, and 189 isoforms of VEGF.

VG76e was shown to be a blocking antibody by its inhibition of the growth stimulatory activity of VEGF on human umbilical vein endothelial cells (HUVEC), a gift from Prof. B. R. Binder, Vienna University (Vienna, Austria). The cells were cultured in medium 199 (Sigma, Poole, UK) with 20% heat-inactivated FBS (Sigma), 100 IU/ml penicillin/100 μg/ml streptomycin (Life Technologies, Inc., Paisley, UK), 250 ng/mL fungizone (Life Technologies, Inc.), 2 mM glutamine (Life Technologies, Inc.), 5 IU/ml heparin (Sigma), and 50 μg/ml endothelial cell growth supplement (ECGS) (Technoclone, Inc., Vienna, Austria). HUVEC (3×10^3) at passage 5 were plated in complete medium in 96-well plates and

Received October 8, 1999.

Address all correspondence and requests for reprints to: Dr. H. M. Fraser, Medical Research Council, Reproductive Biology Unit, Center for Reproductive Biology, 37 Chalmers Street, Edinburgh, United Kingdom EH3 9EW. E-mail: h.fraser@ed-rbu.mrc.ac.uk.

* This work was supported by Deutsche Forschungsgemeinschaft for financial support (to C.W.).

allowed to attach overnight. Growth was arrested by incubation with 100 μl reduced growth medium (medium 199 containing the supplements described above without ECGS and 2% FBS) for 24 h. Human VEGF (10 ng/ml; R&D Systems, Abingdon, UK) was added to wells with various concentrations of the anti-VEGF antibody (VG76e), a positive control anti-VEGF blocking antibody 2C3 (a gift from Prof. P. Thorpe, ME Medical Center, Portland, ME), or a negative control (mouse IgG, Sigma). Control wells received medium with or without VEGF. After 3 days of incubation, cell number was quantified colorometrically by the addition of 20 μl Cell Titer 96 Aqueous One Solution Cell Proliferation Assay (Promega Corp., Southampton, UK) at 492 and 620 nm reference filter. Background absorbance was determined with substrate alone and subtracted from all wells. Cell growth was calculated by subtracting absorbance in wells with cells grown without VEGF.

Animals

Common marmoset monkeys *(Callithrix jacchus)* were housed in cages in rooms at a temperature of 22.5 C as described previously (9). Adult females with a body weight of approximately 350 g, with regular ovulatory cycles, were housed together with a younger sister or prepubertal female. Blood samples were collected three times per week by femoral venipuncture without anesthesia, and plasma was stored at −20 C until required for progesterone assay to confirm normal ovulatory cycles. Criteria for the occurrence of ovulation and normal luteal phase length (18–22 days) were based on determination of plasma progesterone concentrations as described previously (13).

Treatment

The experiments were carried out in accordance with the Animals (Scientific Procedures) Act, 1986. To synchronize timing of ovulation during the treatment cycle, animals were treated with 1 μg $PGF_{2\alpha}$ analog (Planate, Coopers Animal Health Ltd., Crewe, UK), im, during the mid- to late luteal phase of the pretreatment cycle to induce luteolysis. This treatment is normally followed by ovulation 10 days later (14). Four marmosets were treated with VEGF antibody at a concentration of 2.7 mg/ml starting 10 days after PG, *i.e.* the day of anticipated ovulation (luteal phase day 0), at a dose of 2 mg followed by 1 mg on days 1 and 2 (early luteal group). Four controls were treated with the same dose of mouse γ-globulin (Sigma) following the same schedule.

Treatment was extended to the midluteal phase in an additional six marmosets; additional injections of 1 mg anti-VEGF were administered on days 3, 5, 7, and 9, with six animals receiving mouse γ-globulin as controls (midluteal group). All treatments were given by slow iv injection.

Ovaries were obtained the day after final treatment, luteal day 3 or 10, after the animals had received 20 mg bromodeoxyuridine (BrdU: Roche Molecular Biochemicals, Essex, UK) in saline by slow iv injection. One hour later, the animals were sedated using 100 μl ketamine hydrochloride (Parke-Davis Veterinary, Pontypool, UK), im, and killed with an iv injection of 400 μl Euthetal (sodium pentobarbitone, Rhone Merieux, Harlow, Essex, UK). Ovaries were removed immediately, weighed, fixed in 4% paraformaldehyde for 24 h, dehydrated, and embedded in paraffin. In addition, a small portion of a representative corpus luteum was placed in 3% glutaraldehyde in 0.1 M cacodylate buffer, pH 7.3. These specimens were fixed for 2 h, rinsed in the same buffer, postfixed in buffered 2% osmium tetroxide for 2 h, and embedded in Araldite after dehydration in ethyl alcohol. Semithin (1 μm) sections were stained with toluidine blue for light microscope analysis. When the midluteal group was examined, it was apparent that the density of the lutein cells was increased after treatment. To quantify this change, paraffin sections were stained with hematoxylin and eosin, and lutein cell density was determined in 12 corpora lutea/group.

The establishment and function of the corpus luteum were determined by measuring plasma progesterone concentrations in daily blood plasma samples as described previously (13). Only marmosets in which treatment was started at the time of presumptive ovulation (13) (plasma progesterone having reached >30 nmol/liter and found retrospectively to be sustained at luteal phase values) were included in the study. Analysis of differences in plasma progesterone concentrations was performed by repeated measures ANOVA followed by *post-hoc* Fisher's protected least significant difference test (when a significant interaction was found).

Immunocytochemistry

Cellular responses were studied by determining the number of mitotic cells, after BrdU administration as a marker, and by examining the establishment of the microvascular network using factor VIII staining to identify endothelial cells. Tissue sections (5 μm) were cut onto Tespa-coated (Sigma) slides for immunocytochemistry and morphological examination. Sections were stained with hematoxylin and eosin and examined for morphological features of apoptosis as described previously (15). Localization of factor VIII was determined by immunocytochemistry as described previously (16); visualization was performed with nitro blue tetrazolium. These sections were not counterstained, so that quantitative image analysis could be performed; the corpora lutea were identified from the hematoxylin- and eosin-stained sections. Immunostaining for factor VIII to compare control and treated animals was carried out in separate runs for the early and midluteal groups. Factor VIII immunostaining was quantified using the Image Pro-Plus 3.0 (Media Cybernetics, Silver Spring, MD) image analysis program. Four to six randomly chosen areas of 13.3×10^4 μm^2 for the early luteal sections, and 5.3×10^4 μm^2 for the larger midluteal sections were studied; in total, these areas covered approximately two thirds of each corpus luteum. The captured gray scale image was thresholded and converted to a binary image, and the factor VIII-positive area was quantified. The mean of these areas per corpus luteum was taken as representative for that animal.

Proliferating cells were visualized in ovarian sections using a mouse monoclonal antibody to BrdU (Roche Molecular Biochemicals) as described previously (9). Cell proliferation was assessed by counting the number of BrdU-positive cells in six randomly chosen fields of 62,500 μm^2/corpus luteum and expressed as a mean percentage of the total cells in these fields. For factor VIII quantification, proliferation index, ovarian weight, and luteal cell numbers, differences between groups were determined using a two-tailed unpaired *t* test; $P < 0.05$ was taken as the level of significance.

Results

Neutralizing antibody

The endothelial cell growth assay demonstrated that the monoclonal antibody to human VEGF (VG76e) inhibited

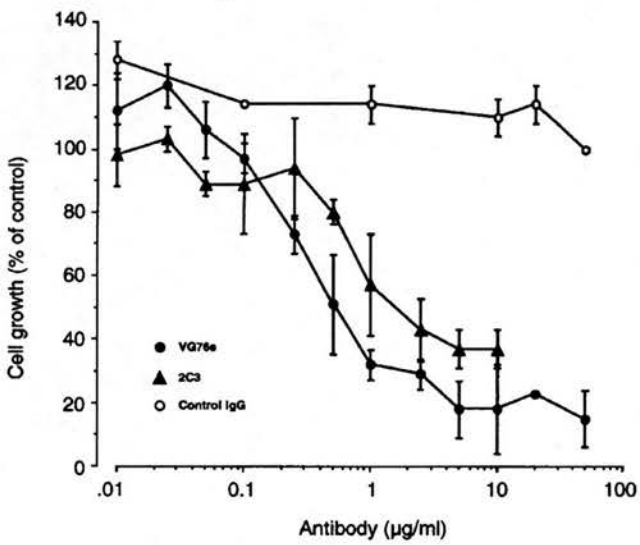

FIG. 1. Effect of VEGF antibody, VG76e, on VEGF-mediated HUVEC growth. Results are given as a percentage of the control value, where cells were grown in the presence of VEGF alone. Results show the mean ± SD of three independent experiments for VG76e and two experiments for positive control VEGF antibody, 2C3, and control IgG. Both VEGF antibodies exhibited a marked inhibitory effect on VEGF-stimulated proliferation of HUVECs. A negative control antibody of irrelevant specificity had no effect on endothelial cell growth.

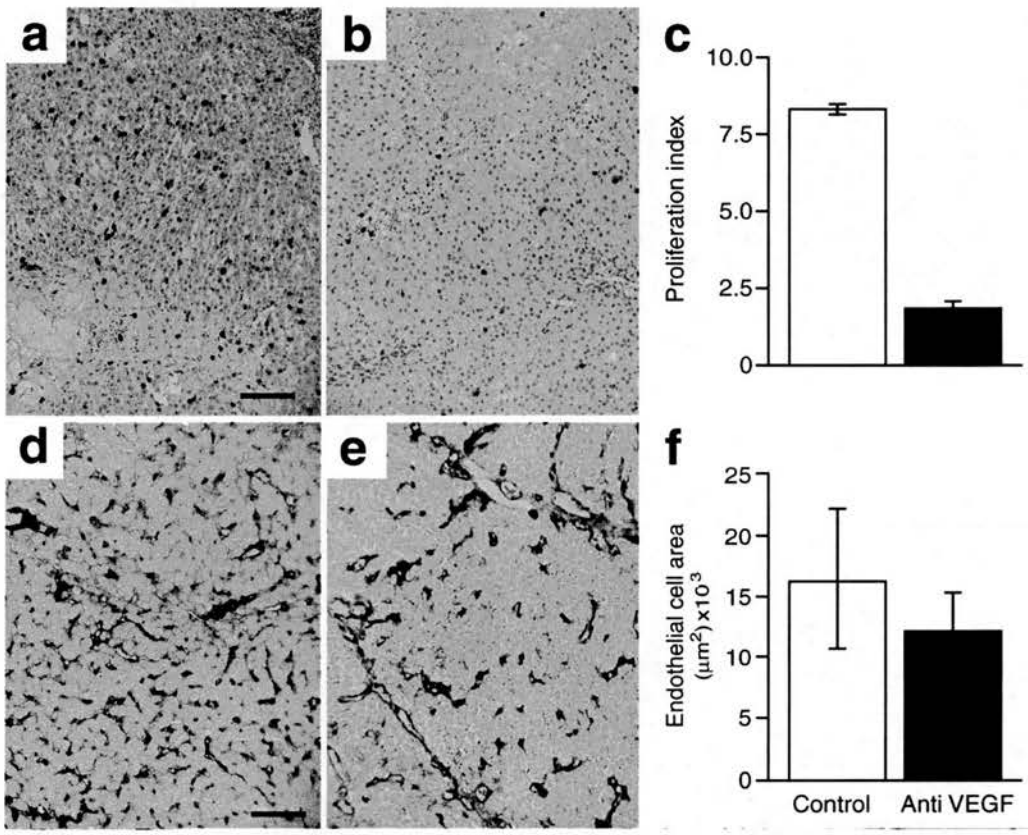

FIG. 2. Low power photomicrographs of early luteal phase marmoset corpora lutea showing the general distribution of BrdU incorporation (dark-staining nuclei) into endothelial cells of microvessels and capillaries in controls, showing high incorporation (a) and reduced incorporation (b) after anti-VEGF treatment. c, The proliferation index in corpora lutea from early luteal phase control (*open bar*) and anti-VEGF-treated (*closed bar*) marmoset corpora lutea. Values from treated animals were significantly lower ($P < 0.01$) than those in controls. d and e, Factor VIII localization (dark staining) in the endothelial cells of microvessels and capillaries of corpora lutea from control and anti-VEGF-treated marmosets, respectively. *Scale bar*, 100 μm. f, Quantification of factor VIII immunostaining in control (*open bar*) and anti-VEGF-treated (*closed bar*) marmoset corpora lutea. There was no significant difference between the groups. Data are the mean ± SEM.

VEGF-stimulated HUVEC growth in a dose-dependent manner (Fig. 1). These results indicate that VG76e is a blocking antibody that inhibits the growth stimulatory activity of VEGF.

Cell proliferation and endothelial cell area

Treatment with anti-VEGF during the early luteal phase did not prevent the formation of clearly identifiable corpora lutea, and ovarian sections revealed the presence of recently formed corpora lutea in all control and treated marmosets. BrdU staining of proliferating cells was readily observed in all corpora lutea (Fig. 2a). It was clear that few (if any) of the hormone-producing cells had incorporated BrdU; positive staining was restricted to some cells surrounding the luminal microvessels and others whose appearance was consistent with that of capillary endothelial cells. We have shown previously that cells incorporating BrdU have the location and morphological appearance of endothelial cells (9). In addition, colocalization studies have demonstrated that more than 80% proliferating cells stain with endothelial cell markers (17). Proliferation was high within the corpora lutea from control marmosets and was markedly reduced by anti-VEGF treatment (Fig. 2b), as confirmed by the decreased proliferation index (Fig. 2c). Factor VIII immunostaining demonstrated the initiation of the development of the microvasculature in control corpora lutea (Fig. 2d), but although there was an indication of reduced capillary number associated with anti-VEGF treatment (Fig. 2e), quantification of factor VIII immunostaining showed no significant difference at this time (Fig. 2f).

In the midluteal phase group, treatment with anti-VEGF from day of ovulation again did not prevent formation of the fresh corpora lutea. In corpora lutea from control animals, the numbers of proliferating cells had declined, as expected by this stage of the luteal phase (Fig. 3a). Some proliferation was also evident in all the corpora lutea from the anti-VEGF-treated marmosets (Fig. 3b), and the proliferation index showed no significant treatment differences (Fig. 3c). However, whereas in control corpora lutea staining for factor VIII revealed that a fully developed microvasculature had been established (Fig. 3d), treatment with anti-VEGF resulted in corpora lutea with a much lower degree of vascularization and the absence of an extensive capillary bed, similar to that observed in the early luteal phase (Fig. 3e). Quantification of

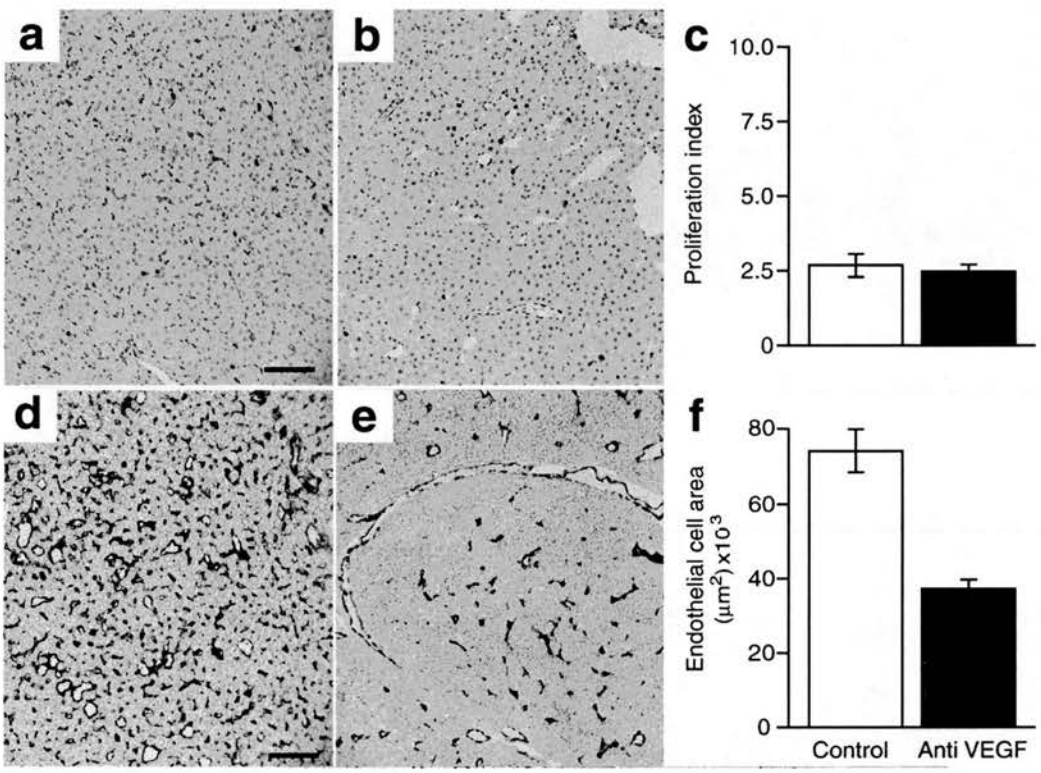

FIG. 3. Low power photomicrographs of midluteal phase marmoset corpora lutea showing the general distribution of BrdU incorporation (dark-staining nuclei) into endothelial cells of microvessels and capillaries in controls (a) and similar incorporation after anti-VEGF treatment (b). c, The proliferation index in corpora lutea from midluteal phase control (*open bar*) and anti-VEGF-treated (*closed bar*) marmoset corpora lutea. There was no significant difference between the groups. d, Factor VIII localization (dark staining) in the endothelial cells of microvessels and capillaries of corpora lutea in a control corpus luteum. e, Reduced staining, especially for incidence of capillary endothelial cells, after anti-VEGF treatment. *Scale bar*, 100 μm. f, Quantification of factor VIII immunostaining in control (*open bar*) and anti-VEGF-treated (*closed bar*) marmoset corpora lutea. Data are the mean ± SEM. Values from treated animals were significantly lower ($P < 0.001$) than those in controls.

factor VIII immunostaining showed a marked suppression of endothelial cell area associated with treatment (Fig. 3f).

Morphology

The weights of the ovaries of the early and midluteal control animals were similar, as were those of both treated groups. However, comparison of the combined weights of the controls (215 ± 11 mg) with those of the treated animals (158 ± 14 mg) revealed a significant reduction ($P < 0.005$) after anti-VEGF. Examination of sections stained with hematoxylin and eosin by two observers with expertise in identification of apoptotic cells, as described previously (15), revealed a virtual absence of apoptosis in both groups. Semithin sections stained with toluidine blue showed that the most prominent features in the control corpora lutea collected during the midluteal phase were the large polyhedral lutein cells, characterized by circular nuclei in cross-section with a nucleolus and large cytoplasmic volume (Fig. 4). Within the cytoplasm were mitochondria and lysosomes together with occasional, less basophilic inclusions typical of lipid droplets. In some tissue sections a few lutein cells showed varying degrees of basophilia, although it was not possible to determine whether cytoplasmic density was correlated with distinct differences in organelle or inclusion content. The lutein cells were supported by connective tissue, including fibroblasts, and there was an extensive blood supply characterized by the occurrence of endothelial cell nuclei and numerous lumina, often containing erythrocytes. In the corpora lutea from the midluteal anti-VEGF-treated marmosets, lutein cells appeared more densely packed (Fig. 4b), with a closer contact with neighboring lutein cells. Quantification of lutein cell number showed that numbers of lutein cells per area were significantly greater ($P < 0.001$) in the treated group (103.8± 5.5, for controls *vs.* 79.2 ± 3 after anti-VEGF). In addition, numerous clusters of basophilic cells, presumably lutein, were present principally in the central area of the corpus luteum. Higher magnification revealed that although the majority of the lutein cells had retained their integrity, they exhibited an increased occurrence of lipid droplets in the peripheral zone of the cytoplasm identified by their gray coloration and homogeneous appearance (Fig. 4d).

Progesterone

Plasma progesterone concentrations were reduced ($P < 0.001$) by anti-VEGF treatment to approximately 40% of the normal values in both the early luteal (data not shown) and midluteal treatments (Fig. 5).

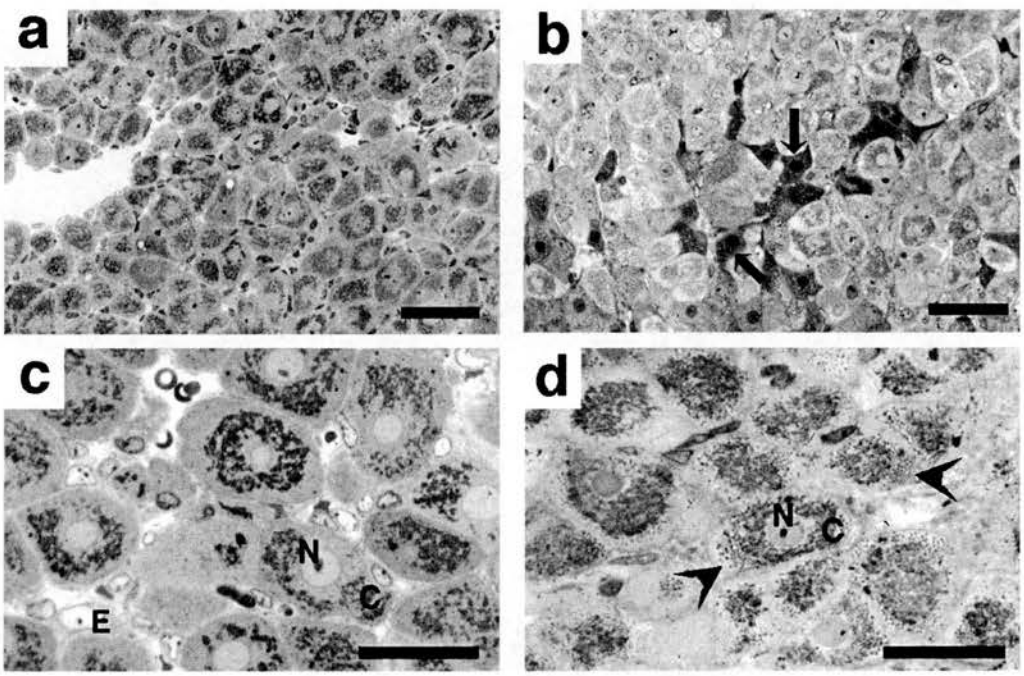

FIG. 4. Photomicrographs of toluidine blue-stained corpora lutea to show the appearance of hormone-producing lutein cells in the midluteal corpus luteum of control (a) and anti-VEGF-treated (b) marmosets. Note how the lutein cells of the treated animal are more closely packed, and the cluster of densely stained cells (*arrows*) presumably of luteal origin. *Scale bars*, 50 μm. Higher magnification of a control corpus luteum (c) shows the appearance of the lutein cell nucleus (N) and cytoplasm (C), with each cell being in contact with an endothelial cell (E). In the anti-VEGF corpus luteum (d) the lutein cells have maintained their integrity, but contain numerous lipid droplets (*gray* staining, *arrowhead*) in the peripheral zone. *Scale bars*, 20 μm.

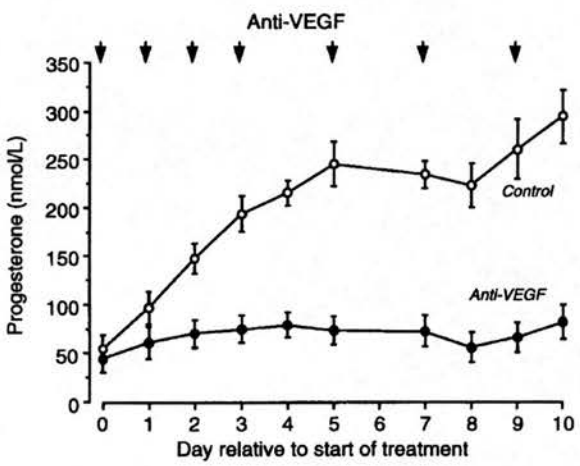

FIG. 5. Plasma progesterone concentrations in control (○) and anti-VEGF-treated marmosets (●). Treatment started on the day of expected ovulation and is associated with a significant suppression ($P < 0.001$). Values are the mean ± SEM (n = 6/group).

Discussion

This is the first report of the successful inhibition of angiogenesis in the primate corpus luteum. To our knowledge, this is the first time physiological angiogenesis has been successfully targeted in a primate species. The high level of endothelial cell proliferation during the early luteal phase in the marmoset, with decreased levels of proliferation during the midluteal phase, agrees with studies using the proliferation marker Ki67 in the rhesus monkey (18) and human (16). We have shown that it is this intense angiogenesis in the early luteal phase that is susceptible to VEGF inhibition, as evidenced by the marked decrease in BrdU incorporation in the marmosets treated with antibody during the early luteal phase. An effect on endothelial cell area was not initially apparent after this short term treatment, but by the midluteal phase, this parameter was markedly inhibited in anti-VEGF-treated corpora lutea as a consequence of the inhibition of endothelial cell proliferation during the intense period of angiogenesis. Although larger blood vessels were established by the midluteal phase in treated animals, there was a marked overall reduction in the number of endothelial cells, suggesting the establishment of early luteal vasculature (possibly from preexisting vessels) and its survival through the midluteal phase, but indicating blockade of development of the normally extensive capillary bed. The absence of an effect on cell proliferation in the midluteal animals treated with anti-VEGF was surprising. However, by this stage, proliferation in controls has been much reduced over that seen during the early luteal phase, and this midluteal proliferation suggests that the rate is maintained either by low levels of VEGF that remain as a result of incomplete neutralization or has resulted from the action of other angiogenic factors in the corpus luteum.

The absence of marked morphological change in the lutein cells after treatment contrasts with observations on the characteristic effects of withdrawal of the tropic factor, LH, which

we have described recently (17, 19). Such treatment also results in inhibition of early luteal angiogenesis, but this is secondary to the destruction of the lutein cells, in which it is assumed most of the principal angiogenic factors are produced (10–12, 17). The observed changes in the structure of the corpus luteum after neutralization of VEGF are likely to result from the specific inhibition of angiogenesis. The increased density of the lutein cells results primarily from the dearth of capillaries, whereas the occurrence of aggregates of subsets of lutein cells with more densely stained nuclei and cytoplasm, found principally in the central area of the corpus luteum, suggests a premature onset of cell death, an observation that would be compatible with a failure of blood vessel development to deliver essential survival factors. The increased presence of lipid droplets is more difficult to explain, but suggests either a lack of tropic hormone stimulus for steroid hormone release or a failure of the normal secretory process. The accumulation of lipid is often associated with the onset of degenerative change in steroid-producing cells, including the early stages of luteolysis in the marmoset (19). Despite the absence of major structural effects within lutein cells, secretion of the principal steroidal hormonal product of these cells is reduced by 60%. The most likely explanation for these findings is that the reduction in development of the microvasculature deprives the lutein cells of both the low density lipoprotein precursors necessary for progesterone production and the transport system for efficient release of their products into the bloodstream. Some effects of the treatment could also be related to an inhibition of the vascular permeability properties of VEGF, although this was not studied specifically. It is also conceivable that the treatment could have an inhibitory effect on pituitary LH secretion. However, we have recently shown that suppression of LH during the luteal phase results in characteristic and marked changes in the morphology of the lutein cells (19) that were not observed in this study, indicating that any change in LH secretion would be minor, making detection of any change unlikely using existing assays and with the sampling frequency employed.

The present results are in agreement with a recent report in the immature rat in which VEGF was inhibited while follicle development and multiple ovulations were induced by PMSG and hCG, respectively (6). However, in the rat model, as VEGF antagonist treatment was initiated before the onset of follicular hyperstimulation, it was not possible to dissociate the luteal inhibition from the consequences of inhibition of angiogenesis in the developing follicle.

Because angiogenesis inhibitors are currently being developed primarily for treatment of vascular solid tumors and are also likely to have a role in the control of rheumatoid arthritis, retinal neovascularization, and psoriasis it is essential that their potential effects on the reproductive system and its function be determined. In addition, the potential of using such inhibitors as antifertility agents is currently generating considerable interest. However, it is unlikely that all angiogenesis inhibitors identified in studies using nonprimate species will influence fertility, as shown by our findings in the marmoset, in which TNP-470 was administered in a protocol similar to that used in the present study but had no inhibitory effect on luteal angiogenesis (9).

As we have shown that luteal inadequacy is associated with inhibition of angiogenesis, this suggests that the clinical incidence of these conditions may in part be the result of defects in the angiogenic process. They may therefore prove to be amenable to treatment with angiogenic growth factors such as VEGF. The potential to inhibit angiogenesis in the female reproductive tract should have important implications for clinical practice, but the development of safe and effective strategies will require detailed investigation of suitable animal models, as described in this study. Finally, manipulation of VEGF in this fashion should provide a novel approach to investigate the precise physiological role of VEGF in ovarian angiogenesis.

Acknowledgments

We thank the staff of our Primate Unit for animal care; M. Millar, S. MacPherson, and P. Largue for expert support with histology; and F. Pitt and I. Swanston for RIAs.

References

1. **Kim KJ, Winer J, Armanini M** 1993 Inhibition of vascular endothelial growth factor-induced angiogenesis suppresses tumor growth *in vivo*. Nature 362:841–844
2. **Olson TA, Mohanraj D, Roy, Ramakrishnan S** 1997 Targeting of the tumor vasculature: inhibition of tumor growth by a vascular endothelial growth factor (VEGF)-toxin conjugate. Int J Cancer 73:865–870
3. **O'Reilly MS., Boehm T, Shing Y, Fukai N, Vasios G, et al** 1997 Endostation: an endogenous inhibitor of angiogenesis and tumor growth. Cell 88:277–285
4. **Skobe M, Rockwell P, Goldstein N, Vosseler S, Fusenig NE** 1997 Halting angiogenesis suppresses carcinoma cell invasion. Nat Med 3:1222–1227
5. **Redmer DA, Reynolds LP** 1996 Angiogenesis in the ovary. Rev Reprod 1:182–192
6. **Ferrara N, Chen H, Davis-Smyth T, Hans-Peter G, Nguyen T-N, et al** 1998 Vascular endothelial growth factor is essential for corpus luteum angiogenesis. Nat Med 4:336–340
7. **Klauber N, Rohan RM, Flynn E, D'Amato RJ** 1997 Critical components of the female reproductive pathway are suppressed by the angiogenesis inhibitor AGM-1470. Nat Med 3:443–446
8. **McCracken JA, Custer, EE, Lamasa JC** 1999 Luteolysis: a neuroendocrine-mediated event. Physiol Rev 79:263–323
9. **Fraser HM, Dickson SE, Morris KD, Erickson GF, Lunn SF** 1999 The effect of the angiogenesis inhibitor TNP-470 on luteal establishment and function in the primate. Hum Reprod 14:2054–2060
10. **Ravindranath N, Little-Ihrig L, Phillips H, Ferrara N, Zeleznik AJ** 1992 Vascular endothelial growth factor messenger ribonucleic acid expression in the primate ovary. Endocrinology 131:254–260
11. **Kamat BR, Brown LF, Manseau EJ, Senger DR, Dvorak HF** 1995 Expression of vascular permeability factor/vascular endothelial growth factor by human granulosa and theca lutein cells. Am J Pathol 146:157–165
12. **Gordon JD, Mesiano S, Zaloudek CJ, Jaffe RB** 1996 Vascular endothelial growth factor localization in human ovary and fallopian tubes: possible role in reproductive function and ovarian cyst formation. J Clin Endocrinol Metab 81:353–359
13. **Smith KB, Lunn SF, Fraser HM** 1990 Inhibin secretion during the ovulatory cycle and pregnancy in the common marmoset monkey. J Endocrinol 126:489–495
14. **Summers PM, Wennink J, Hodges JK** 1985 Cloprostenol-induced luteolysis in the marmoset monkey (*Callithrix jacchus*). J Reprod Fertil 73:133–138
15. **Young FM, Illingworth PJ, Lunn SF, Harrison DJ, Fraser HM** 1997 Cell death during luteal regression in the marmoset monkey *(Callithrix jacchus)*. J Reprod Fertil 111:109–119
16. **Rodger FE, Young FM, Fraser HM, Illingworth PJ** 1997 Endothelial cell proliferation follows the mid-cycle luteinizing hormone surge, but not human chorionic gonadotrophin rescue, in the human corpus luteum. Hum Reprod 12:1723–1729
17. **Dickson SE, Fraser HM,** Inhibition of early luteal angiogenesis by gonadotropin-releasing hormone antagonist treatment in the primate. J Clin Endocrinol Metab, in press
18. **Christenson LK, Stouffer RL** 1996 Proliferation of microvascular endothelial cells in the primate corpus luteum during the menstrual cycle and simulated early pregnancy. Endocrinology 137:367–374
19. **Fraser HM, Lunn SF, Harrison DJ, Kerr JB** 1999 Luteal regression in the primate: different forms of cell death during natural luteolysis and after GnRH antagonist or prostaglandin treatment. Biol Reprod 61:1468–1479

0021-972X/00/$03.00/0
The Journal of Clinical Endocrinology & Metabolism

Vol. 85, No. 6
Printed in U.S.A.

Inhibition of Early Luteal Angiogenesis by Gonadotropin-Releasing Hormone Antagonist Treatment in the Primate

SARAH E. DICKSON AND HAMISH M. FRASER

Medical Research Council Human Reproductive Sciences Unit, Centre for Reproductive Biology, Edinburgh, EH3 9ET, United Kingdom

ABSTRACT

Angiogenesis during luteal development is essential for normal lutein cell function, but the control of this process and the relationships between the steroidogenic and endothelial cells have still to be elucidated. The aim of this study was to: 1) quantify endothelial cell proliferation throughout the luteal phase of the marmoset ovulatory cycle; 2) determine the effect of gonadotropin withdrawal using GnRH antagonist treatment on the early luteal phase angiogenesis peak; and 3) describe the resultant morphological changes in the corpus luteum (CL). Ovaries were collected during the early, mid-, and late luteal phase, and changes in angiogenic activity were determined by quantification of bromodeoxyuridine incorporation. Animals were treated with a GnRH antagonist, on luteal days 1 and 2, and ovaries were collected on day 3. A proliferation index was obtained by counting the number of bromodeoxyuridine immunopositive cells in luteal sections. Cell proliferation was maximal in the early luteal phase and fell significantly in the mid- and late CL. GnRH antagonist treatment reduced the early luteal phase proliferation peak by 90%, suppressed plasma progesterone, and severely disrupted lutein cell morphology. These results demonstrate that the intense angiogenesis in the early primate CL is dependent on gonadotropin stimulation of lutein cells. (*J Clin Endocrinol Metab* **85**: 2339–2344, 2000)

THE CORPUS luteum (CL) is formed subsequent to follicular development and rupture of the preovulatory follicle at ovulation (1). It is well established that LH is the major luteotrophic factor regulating the function of the primate CL. Withdrawal of LH by GnRH antagonist administration results in luteolysis of the CL in the Old World primate (2), New World primate (3), and women (4), as reflected by decreased plasma progesterone levels.

Luteinization is accompanied by prolific angiogenesis, which is essential for normal CL function. During the establishment of the CL, vascularization of the granulosa cell layer takes place as the basement membrane, which in the follicle separated the avascular granulosa from the highly vascularized theca, undergoes loss of integrity. The increased blood supply provides luteal steroidogenic (lutein) cells with oxygen, nutrients, and substrates for progesterone and growth factor biosynthesis, and it facilitates removal of end products of metabolism. The growth of new blood vessels can be monitored by measuring endothelial cell proliferation. Proliferation studies in the human (5, 6), nonhuman primate (7), ovine (8), and bovine (9) show peak levels at the early stages of luteal development, whereas CL regression is associated with a decreased proliferative rate.

Regulation of angiogenesis is controlled by endothelial growth factors, which regulate cell-cell interactions. Most attention has focused on vascular endothelial growth factor (VEGF). It has been shown that neutralization of VEGF in the rat (10) and marmoset monkey (11) blocks both luteal angiogenesis and progesterone production. In most tissues, VEGF is stimulated by hypoxia; but in the endocrine system, the tropic hormones are likely to play a role. A relationship between gonadotropin stimulation of cultured luteinized granulosa cells and VEGF production *in vitro* has been established (12–15). In turn, addition of VEGF to isolated macaque luteal endothelial cells stimulates proliferation (16). However, the *in vivo* connection between gonadotropic stimulation of lutein cells and angiogenesis has not been demonstrated. In this study, endothelial cell proliferation in the CL throughout the luteal phase of the ovulatory cycle of the marmoset was evaluated. The most intense phase of angiogenesis was subsequently targeted for the effects of gonadotropin withdrawal by treatment with GnRH antagonist. Assessment of treatment effects was based on examination of luteal endothelial cell proliferation and morphology of the lutein cells.

Materials and Methods

Animals and treatments

Marmoset monkeys (*Calithrix jacchus*) were housed as described previously (17), and procedures were carried out in accordance with the *Animals (Scientific Procedures) Act, 1986*. Blood samples were collected by femoral venepuncture, three times per week, without anesthesia. Ovulatory cycles were monitored by RIA of plasma progesterone, as previously described (18). The day of ovulation (day 0 of the luteal phase) was taken as the day on which progesterone concentration rose above 30 nmol/L when followed by a sustained increase, characteristic of the luteal phase.

Ovaries were collected from animals in the early (luteal days 2–4), mid-(days 8–10), and late (days 16–20) luteal phase of the ovulatory cycle (n = 5 animals per group). Twenty milligrams of bromodeoxyuridine (BrdU; Roche Molecular Biochemicals, Sussex, UK), dissolved in 500 μl physiological saline, was administered iv, 1 h before tissue collection, to label proliferating cells in the S phase of the cell cycle, via

Received July 22, 1999. Revision received February 9, 2000. Accepted February 21, 2000.

Address correspondence and requests for reprints to: Sarah E. Dickson, Medical Research Council Human Reproductive Sciences Unit, Centre for Reproductive Biology, 37 Chalmers Street, Edinburgh, EH3 9ET, United Kingdom. E-mail: s.dickson@ed-rbu.mrc.ac.uk.

incorporation into DNA. This allowed changes in endothelial cell proliferation throughout the luteal phase of the ovulatory cycle to be determined; and, because the early luteal phase exhibited most intense angiogenesis, this period was selected for targeting with GnRH antagonist to investigate the gonadotropin dependence of early luteal primate angiogenesis.

The animals to receive GnRH antagonist treatment and early luteal control animals were given 1 μg PG $F_{2\alpha}$ analog (Planate; Coopers Animal Health Ltd., Crewe, Cheshire, UK) im, in the mid- to late luteal phase of the pretreatment cycle, to induce luteolysis and synchronize subsequent ovulation, which was presumed to occur 10 days after PG treatment (luteal day 0) (19). Blood samples were collected three times per week, then daily from the day of presumed ovulation, and the animals were subsequently treated with either 1 mg/kg sc. GnRH antagonist, Antarelix (20) or vehicle on luteal days 1 and 2 (n = 4). Ovaries were collected on day 3, as previously described (21), 1 h after administration of BrdU to animals in both control and treatment groups. Ovaries were fixed immediately in 4% paraformaldehyde for paraffin-embedding, and a small piece of CL was fixed in 3% glutaraldehyde in 0.1 mol/L cacodylate buffer, pH 7.3, for araldite resin embedding.

Immunocytochemistry

Paraffin-embedded ovarian sections (5 μm) were mounted onto TESPA (Sigma, Dorset, UK) coated glass slides and dried at 50 C overnight. Fluorescent and colorimetric colocalization of BrdU (Roche Molecular Biochemicals) and the endothelial cell marker, von Willebrand Factor VIII-associated antigen (Factor VIII; DAKO Corp., Cambridge, UK) was carried out on early and mid-luteal ovarian tissue. Sections were dewaxed in Histoclear (National Diagnostics, Hull, UK), rehydrated in descending concentrations of industrial methylated spirits, and washed in distilled water. Antigen retrieval was performed by microwaving (750W) slides on full power in 0.01 mol/L citrate buffer, pH6, for 4 sessions of 5 min. A constant volume of buffer was kept by addition of warm distilled H_2O after each 5 min of microwaving. The slides remained in hot buffer for a further 20 min and were washed in PBS (0.01 mol/L PBS, pH 7.4, containing 2.7 mmol/L KCl, 0.137 mol/L NaCl). The following procedures, with the exception of immunostaining development, were carried out in Sequenza racks (Life Sciences International, Hampshire, UK). Sections were treated for 30 min, at room temperature, with normal goat serum, diluted 1:5 in PBS + 0.25 g BSA [normal goat serum (NGS) diluted 1:5 in PBS + 0.25 g BSA], followed by dual incubation in rabbit polyclonal anti-Factor VIII (22.8 μg/mL in NGS), and mouse monoclonal anti-BrdU (6.6 μg/mL in NGS) at 4 C, overnight. Immunolocalization was undertaken using anti-rabbit FITC conjugate (diluted 1:50 in NGS, Sigma F-6005) and anti-mouse TRITC conjugate (diluted 1:50 in NGS, Sigma T-5393) dual incubation for 45 min at room temperature. The U-MWIBA and U-MWG filters on the Olympus Corp. AX70 Provis fluorescent microscope were used to visualize FITC-stained Factor VIII positive cells, and TRITC-stained BrdU positive cells, respectively.

The occurrence of erythrocyte autofluorescence masked BrdU staining in most sections, and this prevented quantification of endothelial cell proliferation in the majority of CL. To circumvent this problem, a colorimetric approach was also used for analysis. Endogenous peroxidase activity was quenched with a 30-min incubation in 3% hydrogen peroxide in methanol, at room temperature. Microwaving and NGS [diluted in Tris-buffered saline (TBS) (pH 7.4), containing 50 mmol/L Tris-HCl, 150 mmol/L NaCl] blocking was performed as before. Sections were incubated with anti-Factor VIII (28.8 μg/mL in TBS) alone at 4 C, overnight. Immunolocalization was detected with the mouse EnVision system (DAKO Corp.), according to the guidelines of the manufacturer. For BrdU colocalization, nonspecific binding was blocked with normal rabbit serum in TBS (NRS). Sections were incubated in mouse monoclonal anti-BrdU (3.3 μg/mL, in TBS) at 4 C, overnight, or for 2 h at room temperature. Rabbit anti-mouse (DAKO Corp., 26.6 μg/mL in NRS), was applied for 30 min at room temperature. BrdU binding was visualized using mouse APAAP (DAKO Corp., 1 μg/mL in NRS) incubation for 30 min, and the Fast Blue detection system (1 mg Fast Blue BB salt, per 1 mL Fast Blue buffer, containing 20 mg naphthol AS-MX Phosphate, 2 mL dimethylformamide, and 98 mL 0.1 mol/L Tris (pH 8.2), all from Sigma). The reaction was stopped with distilled water, and the slides were very lightly counterstained with hematoxylin and mounted with Permafluor aqueous mounting medium (Coulter Electronics, Bedfordshire, UK).

The procedure for BrdU immunostaining alone to determine changes in cell proliferation throughout the cycle and after treatment was carried out as described previously (17). In this case the NBT (nitro-blue tetrazolium, Roche Molecular Biochemicals) detection method was used, and intense counterstaining was needed.

To examine the effect of GnRH antagonist treatment on CL morphology, treated and control sections were stained with toluidine blue (BDH, Poole, Dorset, UK). Araldite, resin-embedded, 1-μm sections were incubated in toluidine blue at 70 C for 8 min, dried, and examined under the light microscope.

Labeling index and statistical analysis

Manual counting procedures were used to calculate the percentage of proliferating endothelial cells for each CL. Quantification was performed blind on both fluorescent sections and those stained using the colorimetric approach. Both early and mid-luteal phase, left and right ovaries for each animal were examined for appropriately aged CL. Data from all CL fulfilling these criteria were collected for subsequent analysis. Six randomly chosen fields per CL, at ×400 magnification, were analyzed using a grid overlay. The number of proliferating endothelial cells was expressed as a percentage of proliferating cells, *i.e.* (number of dual stained cells/total number of BrdU positive cells) × 100.

The proliferation index (PI) was calculated in a similar manner. Ovaries throughout the luteal phase of the cycle were stained with anti-BrdU only. The number of positive BrdU cells was expressed as a percentage of total number of cells per graticule field, *i.e.* (number of BrdU positive cells/total cells) × 100. Representative sections were also quantified by a second individual. The PIs obtained correlated highly ($r = 0.97$, $P < 0.001$).

PI and plasma progesterone data throughout the luteal phase of the cycle were analyzed using Fisher's protected least-significant difference ANOVA test, at 5% significance. The effects of GnRH antagonist treatment on PI and plasma progesterone levels, as compared with controls, were determined using a two-tailed, unpaired *t* test, with a 95% confidence interval. Both tests were performed using Statview version 4.0.

Results

PI and plasma progesterone throughout the cycle

Figure 1 depicts the CL PI and plasma progesterone concentration throughout the luteal phase of the marmoset ovulatory cycle. Peak cell proliferation was observed in the early luteal phase CL and declined markedly ($P < 0.001$, as compared with early levels) in the mid- and late CL. The 2.5-fold decrease in PI from the mid- to late CL was also significant ($P < 0.05$). Plasma progesterone concentration increased ($P < 0.01$) from early luteal levels, to peak in the mid-luteal phase, subsequently decreasing ($P < 0.01$) from mid- to late luteal phase.

Immunolocalization of BrdU and Factor VIII antibodies

Figure 2 shows fluorescent colocalization of Factor VIII and BrdU. Fig. 2a demonstrates the green cytoplasmic immunostaining for Factor VIII, and Fig. 2b shows red nuclear fluorescent staining for BrdU in the same section. Fig. 2c illustrates colocalization of Factor VIII and BrdU by overlaying 2a and 2b. From quantification of this and the colorimetric method of dual staining, the mean percentage Factor VIII and BrdU colocalization in the early CL was 84.6 ± 0.9 (mean ± SEM); and in the mid-CL, 84.4 ± 1.3 (n = 4 per group).

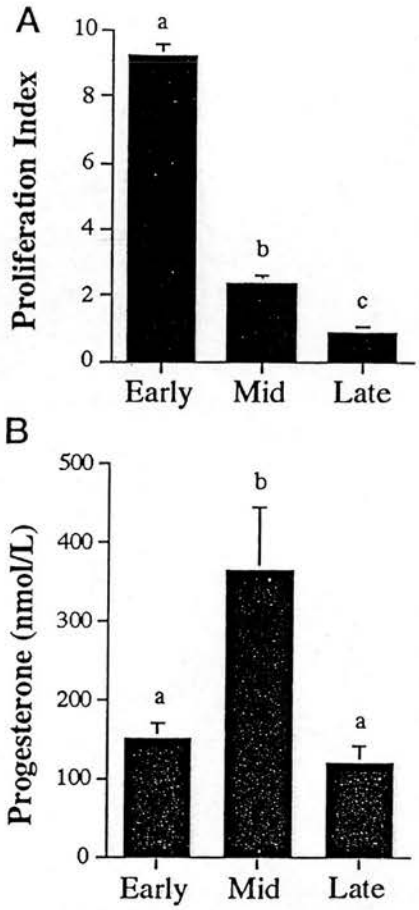

FIG. 1. A, Cell proliferation in the marmoset CL; B, plasma progesterone concentration throughout the luteal phase of the ovulatory cycle. Values are means ± SEM. Different letters denote significant differences between categories, $P < 0.05$.

GnRH antagonist treatment

An elevation of plasma progesterone was observed before treatment in all animals and confirmed by the identification of recently formed CL in control and GnRH antagonist-treated animals. Fig. 2, d–f, shows a comparison of BrdU immunolocalization and PI in an early luteal control CL and an Antarelix-treated CL. BrdU positive staining (*dark nuclei*) and hematoxylin staining (*pale nuclei*) are obvious. A significant decrease ($P < 0.001$) in PI is seen in CL from the Antarelix-treated group of animals, as compared with the early luteal controls. Clusters of densely stained nucleic fragments, characteristic of apoptotic cell death, were apparent in the Antarelix-treated CL (Fig. 2e).

Figure 2, g and h, shows toluidine blue-stained sections of an early control CL and an Antarelix-treated CL. There is a significant effect on lutein cell morphology in the treated CL, as compared with controls. The lutein cells of the early control CL appear normal for this species, with distinct cell margins, and well formed nuclei containing a single nucleolus contained in an abundant cytoplasm, typical of a steroidogenic lutein cell. This contrasts with the appearance of the CL after GnRH antagonist treatment. Here, the CL shows disorganization, and the lutein cells show much-less-clearly defined margins. In addition, there is evidence of lipid accumulation and the occurrence of dense bodies. Typical apoptotic bodies were not observed. Recognizable lutein cells are smaller than in the control tissue, even those in which the nucleus remains intact. Finally, GnRH antagonist treatment was associated with a marked reduction ($P < 0.001$) in plasma progesterone concentration, to follicular phase levels (Fig. 2i).

Discussion

This study has established, for the first time *in vivo*, that the intense angiogenesis in the primate CL associated with the early luteal phase is dependent on gonadotropin support. Over 80% of proliferating cells in the marmoset CL are endothelial cells; and thus, it is reasonable to consider cell proliferation in the CL, based on the PI from single BrdU immunostaining, as being reflective of endothelial cell proliferation. There is evidence that there is little or no proliferation of fully differentiated primate lutein cells (7), which implies that the remaining BrdU positive cells in the CL are most likely fibroblasts, infiltrating macrophages, or endothelial support cells, such as pericytes.

The quantification of endothelial cell proliferation throughout the luteal phase, using the so-called gold standard BrdU technique, shows peak endothelial cell proliferation in the early CL, which had significantly decreased by the mid- and late stages of luteal development. The results agree with studies evaluating cell proliferation in corpora lutea from other species (6–9, 22). The intense proliferation in the early luteal phase leads to increased vascularization during luteinization and CL establishment. By the mid-luteal stage, it is thought that the majority of steroidogenic cells are in contact with at least one capillary (9, 22). Peak plasma progesterone concentrations in the mid-luteal phase correlate with the presence of an extensive capillary network in the CL, for optimal delivery of progesterone precursors to, and progesterone from, the cell. Decreased endothelial cell proliferation in the late luteal phase CL coincides with the observed fall in plasma progesterone concentration and luteal regression (22).

GnRH antagonist treatment was employed to examine the role of gonadotropin dependence of the intense angiogenesis associated with the early luteal phase. In the marmoset, direct effects of GnRH antagonist treatment on the CL are unlikely (23), so the treatment is presumed to be a consequence of pituitary withdrawal of LH, as described previously in the marmoset (3), macaque (2), and human (4) luteal phase. Deprivation of gonadotropin support to steroidogenic cells reduced endothelial cell proliferation by 90%, and plasma progesterone concentration by 95%, demonstrating the dependence of early luteal angiogenesis and function on gonadotropin support.

Light microscopy of toluidine blue-stained sections revealed a severe disruption of normal steroidogenic cell morphology in the GnRH antagonist-treated CL, when compared with early luteal controls. Accumulation of lipid, appearance of densely staining bodies, and the absence of distinct cell margins were obvious after treatment. There was evidence of fragmented nuclei, characteristic of apoptosis, in hematoxylin-stained CL from treated marmosets. However,

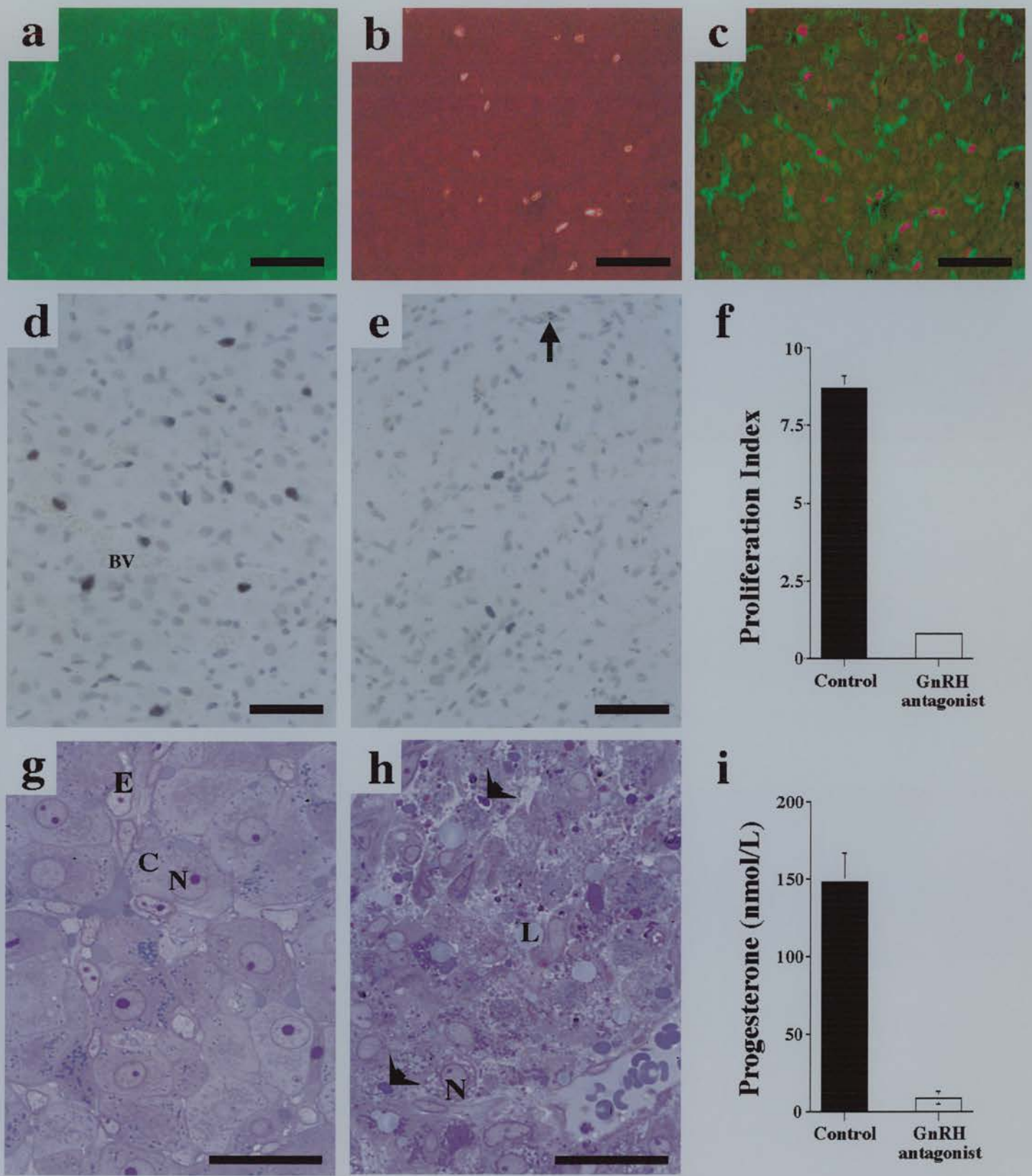

FIG. 2 Fluorescent colocalization of Factor VIII and bromodeoxyuridine (BrdU), and effect of GnRH antagonist treatment on proliferation index (PI), cell morphology and progesterone output.(a-c) Fluorescent immunocytochemical localization of (a) endothelial cell marker, Factor VIII; (b) proliferation marker, BrdU; and (c) colocalization of the two, in an early CL. Note that most BrdU positive cells are also Factor VIII positive. (d-f) Immunocytochemical localization of BrdU in (d) an early control CL and (e) the CL of a GnRH antagonist treated marmoset at the same stage of the cycle. Note the marked reduction in BrdU incorporation and cellular disruption afer treatment. Note also, the presence of the blood vessel (BV), and possible apoptotic body indicated by the arrow. (f) The effect of GnRH antagonist treatment on PI (% BrdU incorporation). Values are means ± sem, $p<0.001$.(g-i) Toluidine blue stained sections of early control CL and (h) a CL after GnRH antagonist treatment. Note the healthy appearence of steroidogenic cells with abundant cytoplasm (C), clear nuclei with nucleoli (N) and probable endothelial cells (E) in the control CL. After treatment the cellular integrity is severely disrupted and dense bodies indicated by the arrow heads, lipid droplets (L), and some intact nuclei (N) are present. (i) The effect of GnRH antagonist treatment on plasma progesterone concentration. Values are means ± sem, $p<0.001$. Scale bars = 50µm.

analysis of semi-thin sections indicated widespread cell death by a process other than apoptosis, as also suggested previously (24, 25); and because ultrastructural studies of GnRH antagonist-induced luteolysis in the marmoset do not indicate widespread cell degeneration via apoptosis (26), it is difficult to ascertain the method of luteal cell death seen in this study. It is clear, however, that the extent of luteal cell disruption was such that steroidogenic cell function was significantly impaired, preventing secretion of progesterone and, most likely, other factors involved in normal CL function.

Early luteal phase administration of GnRH antagonist to macaques (27) and women results in suppression of progesterone secretion and a marked reduction, in response to exogenous hCG administered in the mid-luteal phase (4, 27). Here, we show that administration of GnRH antagonist in the early luteal phase causes a severe disruption of steroidogenic cell morphology and angiogenesis, thus providing an explanation, at the cellular level, for the effects of GnRH antagonist treatment seen previously.

It is tempting to suggest that the adverse effect of GnRH antagonist treatment on early luteal angiogenesis is predominantly a consequence of decreased VEGF production from the dysmorphic steroidogenic cells of the developing CL. VEGF is a secreted angiogenic mitogen (28), specific for endothelial cell receptors (29, 30). Both VEGF messenger RNA (mRNA) and its transcribed protein have been localized to the granulosa and theca lutein cells of the human CL (31, 32). Cultured human (12, 13) and macaque (14, 15) luteinized granulosa cell VEGF expression has been shown to be upregulated by gonadotropins *in vitro*. In preliminary investigations, using immunocytochemistry to determine changes in VEGF in the CL after GnRH antagonist treatment, we did not observe a decrease in immunostaining (unpublished observation). Hypoxia-induced VEGF production; the presence of residual, nonactive, or metabolized VEGF; or nonspecific staining by lutein cell debris in the treated CL may explain the unexpected failure to demonstrate decreased VEGF. Angiogenesis is a multistep process involving a number of angiogenic growth factors, degradation of the extracellular matrix by matrix metalloproteinases, and cell-cell interactions. Neutralization of VEGF in the marmoset, over the same time period, reduces endothelial cell proliferation by 80%, as compared with control levels (11), a significantly greater suppression is demonstrated after GnRH antagonist treatment in this study. This suggests that the reduction in luteal angiogenesis seen here is most probably a consequence of a decrease in other angiogenic factors in addition to VEGF, and/or by a breakdown in endothelial-steroidogenic cell interactions after disruption of lutein cell morphology as caused by treatment. The reduction in local progesterone concentration may also act to reduce angiogenesis. Progesterone is thought to have a local action in the periovulatory follicle, to regulate expression of modulators of the angiogenic process, such as matrix metalloproteinase-1 and its tissue inhibitor (33), implying a role in angiogenesis in the early CL.

The potential of manipulation of angiogenesis in the human reproductive tract is currently generating considerable interest (10, 11, 17), and it will be important to elucidate fully the mechanisms regulating the physiological process in suitable primate models. The current results establish that the intense angiogenesis associated with the formation of the CL, and necessary for normal luteal function, is almost exclusively dependent on normal gonadotropin support.

Acknowledgments

We are grateful to K. Morris and staff for animal management; Dr. R. Deghengi (Europeptides) for the gift of Antarelix; Dr. S. F. Lunn and Dr. C. Wulff for critical evaluation of the manuscript and assistance with photography and morphological analysis; M. Millar, S. MacPherson, and P. Largue for histological support; H. Wilson for assistance with PI quantification; and F. Pitt and I. Swanston for progesterone assay.

References

1. **Zeleznik AJ, Benyo DF.** 1994 Control of follicular development, corpus luteum function, and the recognition of pregnancy in higher primates. In: Knobil E, Neill JD, eds. Physiology of reproduction. Vol 2. New York: Raven Press; 751–782.
2. **Fraser HM, Abbott M, Laird NC,** et al. 1986 Effects of an LH-releasing hormone antagonist on the secretion of LH, FSH, prolactin and ovarian steroids at different stages of the luteal phase in the stump-tailed macaque (Macaca arctoides). J Endocrinol. 111:83–90.
3. **Webley GE, Hodges JK, Given A, Hearn JP.** 1991 Comparison of the luteolytic action of gonadotrophin-releasing hormone antagonist and cloprostenol, and the ability of human chorionic gonadotrophin and melatonin to override their luteolytic effects in the marmoset monkey. J Endocrinol. 128:121–129.
4. **Dubourdieu S, Charbonnel B, Massai M, et al.** 1991 Suppression of corpus luteum function by the gonadotropin releasing hormone antagonist Nal Glu: effect of the dose and timing of human chorionic gonadotropin administration. Fertil Steril. 56:440–445.
5. **Rodger FE, Young FM, Fraser HM, Illingworth PJ.** 1997 Endothelial cell proliferation follows the mid-cycle luteinizing hormone surge, but not human chorionic gonadotrophin rescue, in the human corpus luteum. Hum Reprod. 12:1723–1729.
6. **Gaytan F, Morales C, Garcia-Pardo L, et al.** 1998 Macrophages, cell proliferation, and cell death in the human menstrual corpus luteum. Biol Reprod. 59:417–425.
7. **Christenson LK, Stouffer RL.** 1996 Proliferation of microvascular endothelial cells in the primate corpus luteum during the menstrual cycle and simulated early pregnancy. Endocrinology. 137:367–374.
8. **Jablonka-Shariff A, Grazul-Bilska AT, Redmer DA, Reynolds LP.** 1993 Growth and cellular proliferation of ovine corpora lutea throughout the estrous cycle. Endocrinology. 133:1871–1879.
9. **Zheng J, Fricke PM, Reynolds LP, Redmer DA.** 1994 Evaluation of growth, cell proliferation, and cell death in bovine corpora lutea throughout the estrous cycle. Biol Reprod. 51:623–632.
10. **Ferrara N, Chen H, Davis-Smyth T, et al.** 1998 Vascular endothelial growth factor is essential for corpus luteum angiogenesis. Nat Med. 4:336–340.
11. **Fraser HM, Dickson SE, Lunn SF, et al.** 2000 Suppression of luteal angiogenesis in the primate by neutralization of vascular endothelial growth factor. Endocrinology. 141:995–1000.
12. **Neulen J, Raczek S, Pogorzelski M, et al.** 1998 Secretion of vascular endothelial growth factor/vascular permeability factor from human luteinized granulosa cells is human chorionic gonadotrophin dependent. Mol Hum Reprod. 4:203–206.
13. **Yan Z, Neulen J, Raczek S, et al.** 1998 Secretion of vascular endothelial growth factor (VEGF) permeability factor (VPF) production by luteinized human granulosa cells *in vitro*; a paracrine signal in corpus luteum formation. Gynecol Endocrinol. 12:149–153.
14. **Christenson LK, Stouffer RL.** 1997 Follicle-stimulating hormone and luteinizing hormone/chorionic gonadotropin stimulation of vascular endothelial growth factor production by macaque granulosa cells from pre- and periovulatory follicles. J Clin Endocrinol Metab. 82:2135–2142.
15. **Hazzard T, Molskness T, Chaffin C, Stouffer R.** 1999 Vascular endothelial growth factor (VEGF) and angiopoietin regulation by gonadotrophin and steroids in macaque granulosa cells during the peri-ovulatory interval. Mol Hum Reprod. 5:1115–1121.
16. **Christenson LK, Stouffer RL.** 1996 Isolation and culture of microvascular endothelial cells from the primate corpus luteum. Biol Reprod. 55:1397–1404.
17. **Fraser HM, Dickson SE, Morris KD, Erickson GF, Lunn SF.** 1999 The effects of the angiogenesis inhibitor TNP-470 on luteal establishment and function in the primate. Hum Reprod. 14:2054–2060.
18. **Smith KB, Lunn SF, Fraser HM.** 1990 Inhibin secretion during the ovulatory cycle and pregnancy in the common marmoset monkey. J Endocrinol. 126:489–495.

19. **Summers PM, Wennink J, Hodges JK.** 1985 Cloprostenol-induced luteolysis in the marmoset monkey (*Callithrix jacchus*). J Reprod Fertil. 73:133–138.
20. **Deghenghi R, Boutignon F, Wüthrich P, Lenaerts V.** 1993 Antarelix (EP 24332) a novel water soluble LHRH antagonist. Biomed Pharmacother. 47:107–110.
21. **Fraser HM, Lunn SF, Kim H, Erickson GF.** 1998 Insulin-like growth factor binding protein-3 (IGFBP-3) mRNA in the endothelial cells of the primate corpus luteum. Hum Reprod. 13:2180–2185.
22. **Reynolds LP, Killilea SD, Redmer DA.** 1992 Angiogenesis in the female reproductive system. FASEB J. 6:886–892.
23. **Fraser HM, Sellar RE, Illingworth PJ, Eidne KA.** 1996 GnRH receptor mRNA expression by *in situ* hybridization in the primate pituitary and ovary. Mol Hum Reprod. 2:117–121.
24. **Fraser HM, Lunn SF, Cowen GM, Illingworth PJ.** 1995 Induced luteal regression in the primate: evidence for apoptosis and changes in c-myc protein. J Endocrinol.147:131–137.
25. **Young FM, Illingworth PJ, Lunn SF, Harrison DJ, Fraser HM.** 1997 Cell death during luteal regression in the marmoset monkey *(Callithrix jacchus)*. J Reprod Fertil. 111:109–119.
26. **Fraser HM, Lunn SF, Harrison DJ, Kerr JB.** 1999 Luteal regression in the primate: different forms of cell death during natural and gonadotropin-releasing hormone antagonist or prostaglandin analogue-induced luteolysis. Biol Reprod. 61:1468–1479.
27. **Fraser HM, Nestor Jr JJ, Vickery BH.** 1987 Suppression of luteal function by a luteinizing hormone-releasing hormone antagonist during the early luteal phase in the stump-tailed macaque monkey and the effects of subsequent administration of human chorionic gonadotropin. Endocrinology. 121:612–618.
28. **Leung D, Cachianes G, Kuang W, Goeddel D, Ferrara N.** 1989 Vascular endothelial growth factor is a secreted angiogenic mitogen. Science. 246:1306–1309.
29. **Vaisman N, Gospodarowicz D, Neufeld G.** 1990 Characterization of the receptors for vascular endothelial growth factor. J Biol Chem. 265:19461–19466.
30. **Plouet J, Moukadiri H.** 1990 Characterization of the receptor to vasculotropin on bovine adrenal cortex-derived capillary endothelial cells. J Biol Chem. 265:22071–22074.
31. **Kamat BR, Brown LF, Manseau EJ, Senger DR, Dvorak HF.** 1995 Expression of vascular permeability factor/vascular endothelial growth factor by human granulosa and theca lutein cells. Am J Pathol. 146:157–165.
32. **Otani N, Sawako M, Yamoto M, et al.** 1999 The vascular endothelial growth factor/*fms*-like tyrosine kinase system in human ovary during the menstrual cycle and early pregnancy. J Clin Endocrinol Metab. 84:3845–3851.
33. **Chaffin C, Stouffer R.** 1999 Expression of matrix metalloproteinase and their tissue inhibitor messenger ribonucleic acids in macaque periovulatory granulosa cells: time course and steroid regulation. Biol Reprod. 61:14–21.

Mid-luteal angiogenesis and function in the primate is dependent on vascular endothelial growth factor

S E Dickson, R Bicknell[1] and H M Fraser

MRC Human Reproductive Sciences Unit, Centre for Reproductive Biology, 37 Chalmers Street, Edinburgh EH3 9ET, UK

[1]Molecular Angiogenesis Laboratories, Imperial Cancer Research Fund, Institute of Molecular Medicine, John Radcliffe Hospital, Oxford OX3 9DS, UK

(Requests for offprints should be addressed to H M Fraser, MRC Human Reproductive Sciences Unit, Centre for Reproductive Biology, 37 Chalmers Street, Edinburgh EH3 9ET, UK; E-mail: h.fraser@hrsu.mrc.ac.uk)

Abstract

Vascular endothelial growth factor (VEGF) is essential for the angiogenesis required for the formation of the corpus luteum; however, its role in ongoing luteal angiogenesis and in the maintenance of the established vascular network is unknown. The aim of this study was to determine whether VEGF inhibition could intervene in ongoing luteal angiogenesis using immunoneutralisation of VEGF starting in the mid-luteal phase. In addition, the effects on endothelial cell survival and the recruitment of peri-endothelial support cells were examined. Treatment with a monoclonal antibody to VEGF, or mouse gamma globulin for control animals, commenced on day 7 after ovulation and continued for 3 days. Bromodeoxyuridine (BrdU), used to label proliferating cells to obtain a proliferation index, was administered one hour before collecting ovaries from control and treated animals. Ovarian sections were stained using antibodies to BrdU, the endothelial cell marker, CD31, the pericyte marker, alpha-smooth muscle actin, and 3′ end DNA fragments as a marker for apoptosis. VEGF immunoneutralisation significantly suppressed endothelial cell proliferation and the area occupied by endothelial cells while increasing pericyte coverage and the incidence of endothelial cell apoptosis. Luteal function was markedly compromised by anti-VEGF treatment as judged by a 50% reduction in plasma progesterone concentration. It is concluded that ongoing angiogenesis in the mid-luteal phase is primarily driven by VEGF, and that a proportion of endothelial cells of the mid-luteal phase vasculature are dependent on VEGF support.

Journal of Endocrinology (2001) **168,** 409–416

Introduction

Formation of the primate corpus luteum (CL) is accompanied by prolific angiogenesis in the early luteal phase, and throughout the life span of the CL angiogenesis continues at a lower rate until the late luteal phase when endothelial cell proliferation decreases further (Jablonka-Shariff *et al.* 1993, Rodger *et al.* 1997, Dickson & Fraser 2000). The angiogenic process is regulated by a number of growth factors, degradation of the extracellular matrix and cell–cell interactions. One growth factor primarily involved is vascular endothelial growth factor (VEGF).

The importance of VEGF in the onset of luteal angiogenesis has been demonstrated by specific VEGF neutralisation in the rat (Ferrara *et al.* 1998) and the marmoset monkey (Fraser *et al.* 2000) which resulted in suppression of endothelial cell proliferation, restricted development of the microvascular tree and decreased progesterone production. These studies have solely addressed *prevention* of angiogenesis by targeting the early luteal phase just before the onset of angiogenesis (see Fig. 1) (Dickson & Fraser 2000, Fraser *et al.* 2000). Surprisingly, while immunoneutralisation of VEGF for the first 3 days of the luteal phase markedly suppressed angiogenesis, extending treatment to 10 days post ovulation failed to affect mid-luteal cell proliferation (Fraser *et al.* 2000). It is possible that endothelial cell proliferation was unaffected at this stage as a result of (1) induction of a compensatory effect from other growth factors after chronic inhibition of VEGF, (2) an immune response against the mouse monoclonal antibody or (3) the possibility that VEGF was not involved in stimulating endothelial cell proliferation during this period. In the light of this observation the current study investigated the role of VEGF specifically during the mid-luteal phase to determine whether VEGF inhibition would *intervene* in ongoing luteal angiogenesis.

First, using quantitative immunocytochemistry we established that VEGF was present in high amounts during the mid-luteal phase. We then investigated whether it was possible to intervene in the already established angiogenic process by administering anti-VEGF treatment for 3 days in the mid-luteal phase and examining the effects on angiogenesis and luteal function.

0022–0795/01/0168–409

Previous studies on the effects of withdrawal of VEGF in other angiogenic-dependent systems report the requirement of VEGF for the survival of immature endothelial cells. For example, in human prostate cancer the loss of VEGF as a result of androgen ablation therapy leads to selective apoptosis of endothelial cells in vessels devoid of periendothelial support cells (Benjamin *et al.* 1999). To investigate whether endothelial cells of the primate CL may be susceptible to withdrawal of VEGF, we determined the incidence of apoptosis after anti-VEGF treatment. Finally, to assess the relationship of periendothelial support cells to endothelial cell survival, the area of pericyte coverage in control CL and after anti-VEGF treatment was quantified.

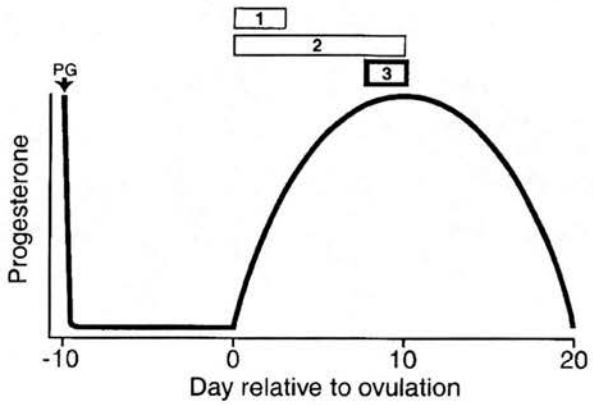

Figure 1 Schematic diagram showing the different treatment regimes (1, 2 and 3) with VEGF monoclonal antibody designed to determine whether inhibition of angiogenic factors can *prevent* angiogenesis (regimes 1 and 2) or intervene once the process is underway (regime 3). The approach used in the current study was to *intervene* in the already established angiogenic process by administering a 3-day treatment with VEGF monoclonal antibody in the mid-luteal phase according to regime 3. PG, prostaglandin $F_{2\alpha}$ analogue.

Materials and Methods

Animals and treatments

Marmoset monkeys (*Calithrix jacchus*) were housed as described previously (Fraser *et al.* 1999*a*) and procedures were carried out in accordance with the Animals (Scientific Procedures) Act 1986. Blood samples were collected by femoral venepuncture three times per week without anaesthesia. Ovulatory cycles were monitored by radioimmunoassay of plasma progesterone as previously described (Smith *et al.* 1990). The day of ovulation (day 0 of the luteal phase) was taken as the day on which progesterone concentration rose above 30 nmol/l when followed by a sustained increase, characteristic of the luteal phase.

Ovaries collected from animals in the early (luteal days 2–4), mid- (days 8–10) and late (days 16–20) luteal phase of the ovulatory cycle ($n=4$–5 animals per group) for previous studies (Fraser *et al.* 1999*a*,*b*, Dickson & Fraser 2000) were used for immunocytochemical localisation and quantification of VEGF protein.

The mid-luteal phase was targeted for anti-VEGF treatment to determine whether luteal angiogenesis could be prevented at the stage when high levels of VEGF are present, as seen by VEGF immunolocalisation throughout the luteal phase of the marmoset ovulatory cycle.

Animals were given 1 μg prostaglandin $F_{2\alpha}$ analogue (Planate; Coopers Animal Health Ltd, Crewe, Cheshire, UK) i.m. in the mid- to late luteal phase of the pre-treatment cycle to induce luteolysis and to synchronise subsequent ovulation which was presumed to occur 10 days after prostaglandin treatment (luteal day 0) (Fig. 1) (Summers *et al.* 1985). Blood samples were collected every second day, then daily from the first day of treatment. The properties of the VEGF monoclonal antibody have been described previously (Fraser *et al.* 2000). Four animals were subsequently treated with 2 mg VEGF monoclonal antibody on luteal day 7 and 1 mg on luteal days 8 and 9, and four control animals were given equivalent doses of mouse gamma globulin (Fig. 1). Ovaries were collected on day 10 as previously described by Fraser *et al.* (1998), 1 h after administration of 20 mg bromodeoxyuridine (BrdU; Boehringer Mannheim, Lewes, East Sussex, UK) dissolved in 500 μl physiological saline, to label proliferating cells in the S phase of the cell cycle. Ovaries were fixed immediately in 4% paraformaldehyde in 0·01 M PBS (phosphate-buffered saline, pH 7·4, containing 2·7 mM KCl, 0·137 M NaCl) for paraffin-embedding.

Immunocytochemistry

Paraffin-embedded ovarian sections (5 μm) were mounted onto TESPA- (Sigma, Poole, Dorset, UK) coated glass slides and dried at 50 °C overnight. To carry out immunocytochemistry for VEGF, sections were dewaxed in Histoclear (National Diagnostics, Aylesbury, Bucks, UK), rehydrated in descending concentrations of industrial methylated spirits and washed in distilled water. VEGF antigen was retrieved by pressure cooking slides on full power in 3 M glycine, 0·1% EDTA buffer, pH 3·5, for 5 min. The slides remained in hot buffer for a further 20 min and were washed in TBS (0·05 M Tris–buffered saline, pH 7·4, containing 50 mM Tris–HCl, 150 mM NaCl). Endogenous peroxidase activity was quenched with a 30-min incubation in 3% hydrogen peroxide in methanol at room temperature. The following procedures, with the exception of immunostaining development, were carried out in Sequenza racks (Shandon Scientific Ltd, Runcorn, Cheshire, UK). To block endogenous biotin, sections were incubated in avidin (Vector Laboratories, Burlingame, CA, USA) at a concentration of 8 drops/ml normal swine serum (NSS, 1:5 dilution in TBS+0·25 g bovine serum albumin), followed by a 20-min incubation

in biotin (Vector Laboratories) in TBS (8 drops/ml). Rabbit polyclonal VEGF antibody (2 μg/ml pre-diluted in NSS, Santa Cruz Biotechnology, Santa Cruz, CA, USA) was added and sections were incubated at 4 °C overnight. Negative controls were incubated in primary antibody pre-absorbed with VEGF peptide in 1:5 ratio of VEGF antibody:blocking peptide (Santa Cruz). Immunolocalisation was undertaken using the rabbit EnVision kit (Dako Ltd, Cambridge, Cambs, UK) according to the guidelines of the manufacturer.

BrdU immunocytochemistry was carried out using a monoclonal antibody (Boehringer Mannheim) as previously described (Fraser *et al.* 2000). Immunocytochemistry for the endothelial cell marker, CD31 (Dako Ltd), and the pericyte marker, alpha-smooth muscle actin (SMA; Dako Ltd), were performed using monoclonal antibodies (20·5 μg/ml in TBS and 4·3 μg/ml in TBS respectively) and the same method as for BrdU immunostaining.

Apoptosis was detected by 3′ end labelling as previously described in the marmoset CL (Young *et al.* 1997), with modifications according to Sharpe *et al.* (1998). An additional proteinase K digestion step was performed after dewaxing and rehydrating the sections. Slides were incubated for 6 min at room temperature in 20 μg/ml proteinase K in buffer containing 0·05 M Tris, pH 8, 0·05 M EDTA, pH 8, in distilled H_2O. After blocking of endogenous peroxidase activity, it was necessary to block endogenous biotin using the avidin-biotin block in PBS as above.

Analysis

A BrdU proliferation index (PI) was obtained as previously described (Dickson & Fraser 2000). Endothelial cell and pericyte areas were quantified in at least 6 randomly chosen areas of $5·3 \times 10^4$ μm^2 (approximately two thirds of each CL) as described by Fraser *et al.* (2000) for the endothelial cell marker, Factor VIII. The area of VEGF immunostaining was measured using Photoshop version 5·0 according to the method of Otani *et al.* (1999). Statistical analysis of VEGF immunostaining throughout

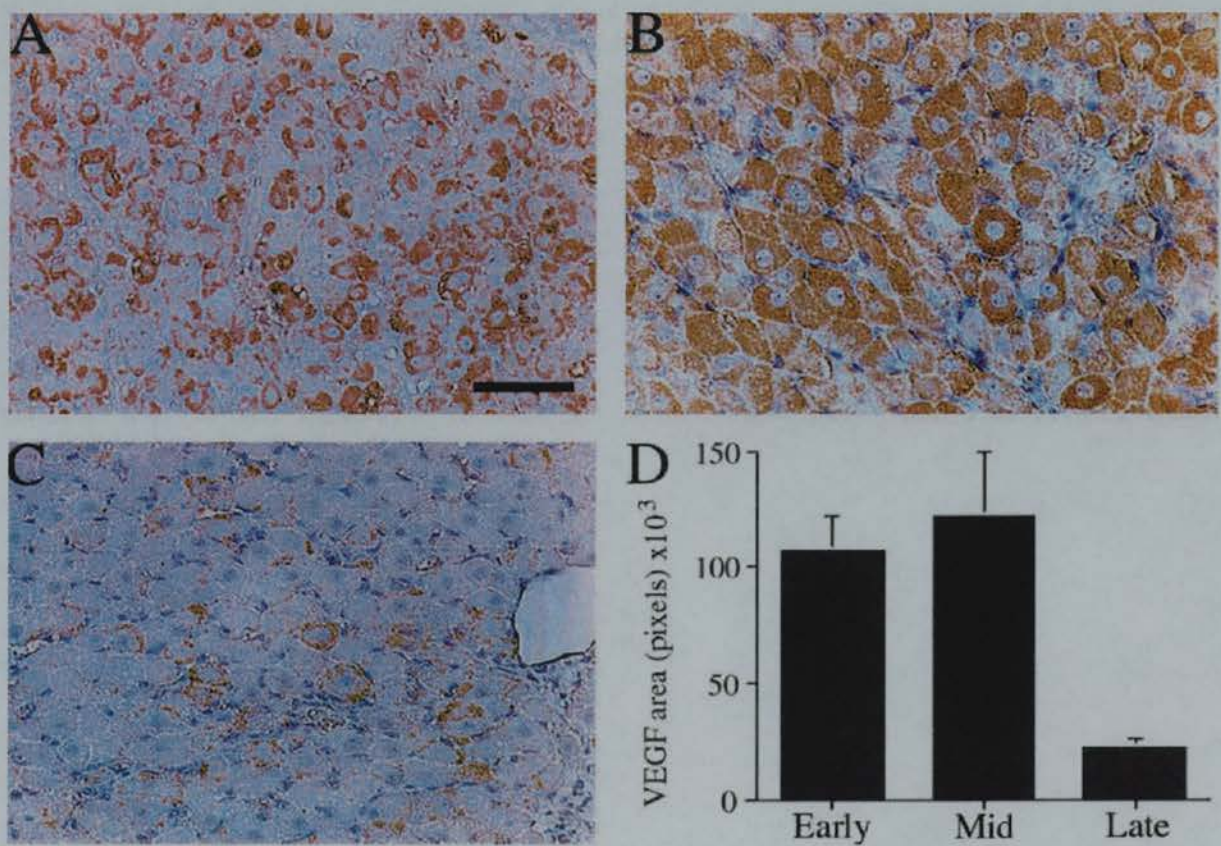

Figure 2 Photomicrographs of marmoset corpora lutea showing VEGF localisation (brown staining cytoplasm) in (A) an early luteal phase corpus luteum, (B) a mid-luteal phase corpus luteum and (C) a late luteal phase corpus luteum. Bar represents 50 μm. (D) Quantification of the area of VEGF immunostaining in the marmoset corpus luteum throughout the luteal phase of the ovulatory cycle. Early and mid-luteal values are significantly higher ($P=0·04$ and $P=0·02$ respectively) than the late luteal value. Data are means ± S.E.M.

the ovulatory cycle was carried out using a factorial one-way analysis of variance (ANOVA) with Fisher's PLSD (protected least significant difference) post-hoc test at 5% significance. The effects of anti-VEGF treatment on PI, endothelial cell and pericyte areas, apoptotic index and VEGF immunostaining, as compared with controls, were determined using separate two-tailed, unpaired *t*-tests, with 95% confidence intervals. Serum progesterone concentrations were analysed using a repeated measures ANOVA with Fisher's PLSD post-hoc test at 5% significance. All tests were performed using Statview version 4·0.

Results

VEGF immunocytochemistry throughout the cycle

Figure 2 illustrates the localisation and quantification of VEGF immunostaining in the CL during the early, mid- and late luteal phase. Early luteal sections show intense, punctate VEGF staining in the cytoplasm of lutein cells (Fig. 2A) which becomes more uniform and widespread in the mid-luteal phase CL (Fig. 2B). Staining was absent from recognisable endothelial cells. In the late luteal phase CL, VEGF staining was markedly reduced (Fig. 2C). Quantification confirmed a high area of staining in the early and mid-luteal phase which declined markedly in the late luteal phase CL, as compared with early and mid-luteal levels ($P=0·04$ and $P=0·02$ respectively) (Fig. 2D).

BrdU, CD31 and SMA immunocytochemistry

Figure 3 shows comparisons of BrdU incorporation, CD31 and SMA immunostaining, and their quantification in mid-luteal control and anti-VEGF-treated CL. Moderate BrdU incorporation into endothelial cells was observed in control CL (Fig. 3A) but this was significantly lowered by anti-VEGF treatment (Fig. 3B). This was confirmed by comparing the PI from control and treated groups ($P<0·01$) (Fig. 3C). In the control CL, CD31 immunostaining confirmed the establishment of the microvascular tree demonstrated by numerous blood vessels and capillary endothelial cells being observed in association with each lutein cell (Fig. 3D). In the treated animals, the number of capillaries appeared reduced (Fig. 3E) and quantitative analysis revealed a significant ($P=0·02$) decrease in endothelial cell area after treatment (Fig. 3F). The converse was apparent for SMA immunostaining. In control sections, pericytes were mostly found aggregated in rings surrounding luminal vessels (Fig. 3G), whereas after anti-VEGF treatment single immunopositive cells were also found distributed through the CL (Fig. 3H). Quantification of pericyte area in control sections and after anti-VEGF treatment is shown in Fig. 3I ($P<0·01$).

Apoptotic cell death

Figure 4 demonstrates 3′ end labelling in mid-luteal control and treated sections. One positive apoptotic endothelial cell associated with a blood vessel can be seen in Fig. 4A. The incidence of apoptotic nuclei increased with anti-VEGF treatment as seen in Fig. 4B which shows two positive nuclei probably of endothelial cell origin. Positive apoptotic nuclei remained sparsely distributed, even though anti-VEGF treatment significantly ($P=0·03$) increased the occurrence of apoptosis (Fig. 4C). The incidence of apoptotic cells was measured per CL section as the size of the control and treated CL did not differ significantly. The regular shape of the steroidogenic lutein cells in control CL was retained in the treated CL.

Plasma progesterone concentration

A sustained elevation of plasma progesterone was observed prior to treatment in all animals. After administration of anti-VEGF treatment starting on luteal day 7 there was a marked reduction in plasma progesterone concentrations which had fallen by over 50% by day 10 (Fig. 5) ($P=0·01$).

Discussion

This study has demonstrated for the first time that VEGF is essential for luteal angiogenesis even when the process is already established. Furthermore, inhibition of VEGF at this time suppresses the function of the CL. We have also demonstrated that VEGF appears to have a role in maintenance of the vascular network in the mid-luteal CL as shown by an increase in 3′ end labelling after VEGF withdrawal.

Our findings also show that the expression of VEGF is high not only in the early luteal period of intense angiogenesis, but also in the less prolific mid-luteal phase CL, and is only down regulated after initiation of luteolysis. This agrees with VEGF measurements throughout the life span of the CL in the bovine (Goede *et al.* 1998) and the human CL (Otani *et al.* 1999). In the present study, the deleterious effect of acute removal of VEGF on mid-luteal angiogenesis shows that ongoing mid-luteal angiogenesis is driven primarily by this growth factor. This indicates that the failure to observe an effect on mid-luteal endothelial cell proliferation after chronic withdrawal of VEGF treatment from the time of ovulation (Fraser *et al.* 2000) is a consequence of induction of other growth factors to compensate for the inhibition of VEGF or inactivation of the neutralising antibody by an immune response.

The high mid-luteal expression of VEGF could also reflect some of the non-angiogenic functions of VEGF, such as the regulation of vascular permeability or the mediation of endothelial cell survival as suggested by Goede *et al.* (1998). By the mid-luteal phase, the vasculature is becoming highly developed and progesterone is being maximally secreted. If the effect of anti-VEGF was solely to suppress angiogenesis it might be anticipated that progesterone would be maintained at pretreatment levels,

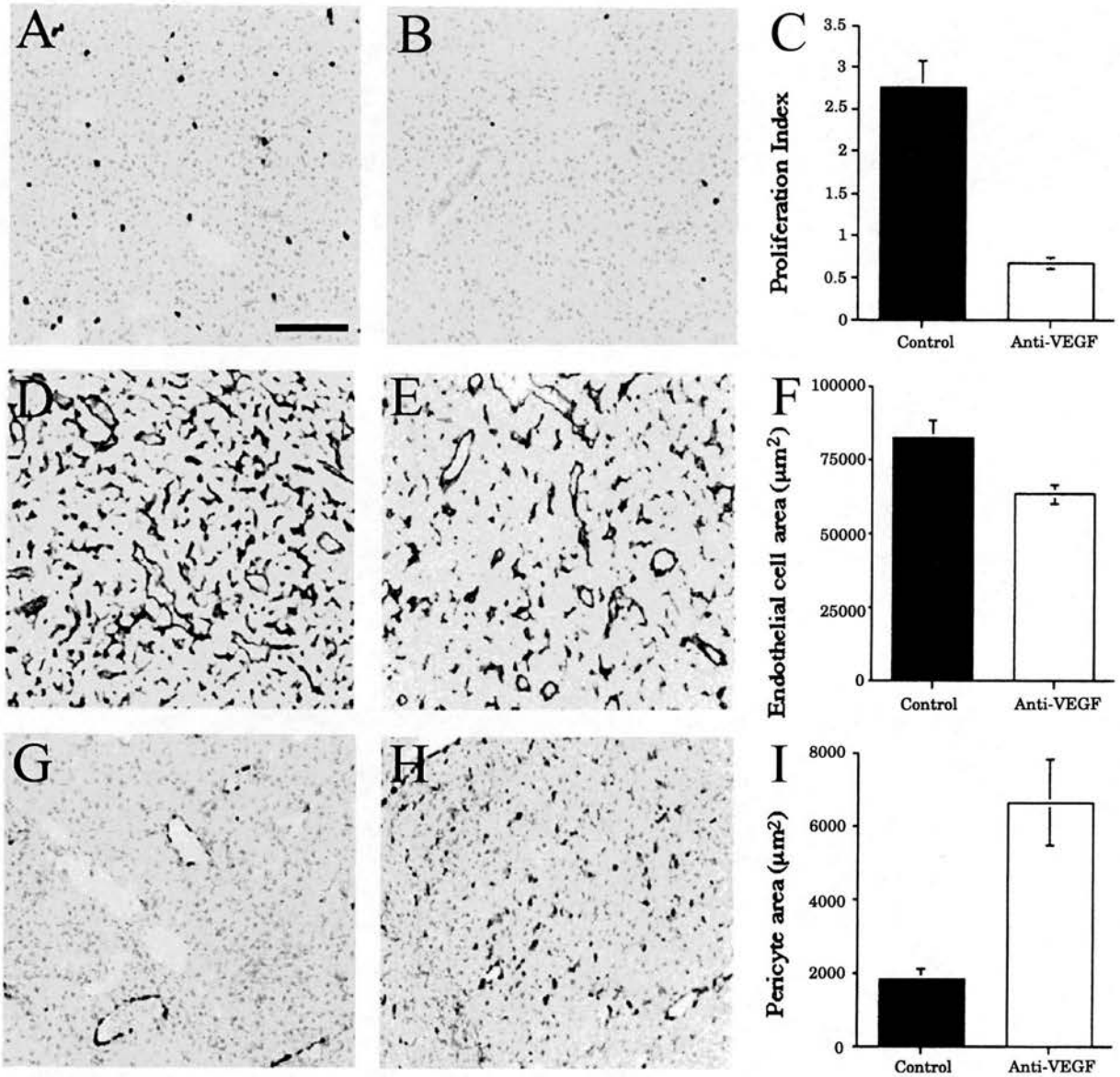

Figure 3 Low power photomicrographs of marmoset corpora lutea showing the general distribution of endothelial cell BrdU incorporation (dark-staining nuclei) in a control section (A) and its reduced incorporation after anti-VEGF treatment (B). (C) The proliferation index in corpora lutea from mid-luteal phase controls (solid bar) and anti-VEGF-treated (open bar) marmoset corpora lutea. Values from treated animals were significantly lower ($P<0{\cdot}01$) than those from controls. (D) CD31 localisation (dark staining) in the endothelial cells of the vascular network in a mid-luteal phase control corpus luteum. (E) Reduced CD31 staining after anti-VEGF treatment. (F) Quantification of CD31 immunostaining in control (solid bar) and anti-VEGF-treated (open bar) marmoset corpora lutea. Values from treated animals were significantly lower ($P=0{\cdot}02$) than those from controls. (G) Smooth muscle actin localisation in pericytes in a control section, and (H) increased smooth muscle actin immunostaining after anti-VEGF treatment. Note that the dark stained cells in control and treated sections are characteristic of perivascular cells, based on the small size and elongated shape; none appears to be of lutein cell origin. (I) Quantification of alpha-smooth muscle staining in control (solid bar) and anti-VEGF-treated (open bar); values from treated animals were significantly ($P=<0{\cdot}01$) higher than those from controls. Data are means ± S.E.M. Bar represents 100 μm.

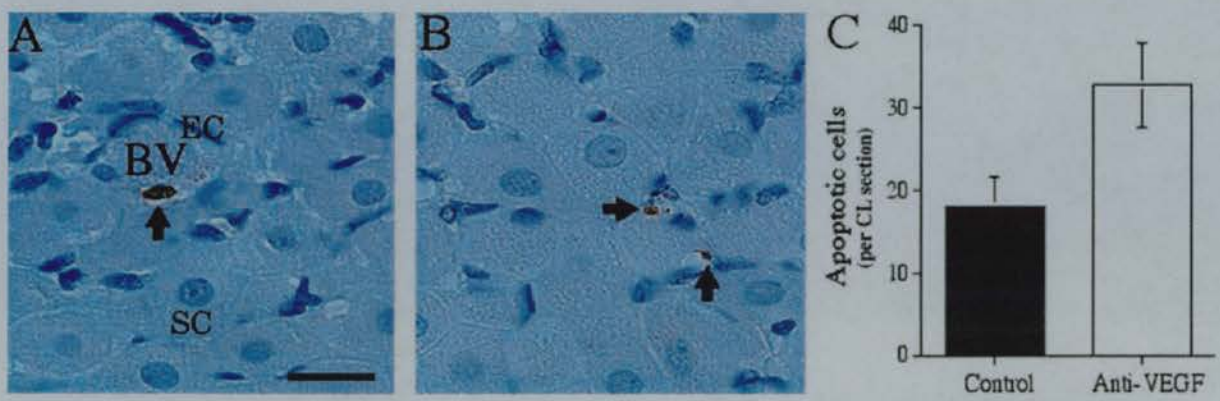

Figure 4 High power photomicrographs of 3′ end labelled apoptotic cells (brown staining) in (A) a mid-luteal phase control marmoset corpus luteum and (B) after anti-VEGF treatment. Note the presence of endothelial cells (EC) surrounding a blood vessel (BV) in the control section, and smaller dark haematoxylin-stained nuclei representing endothelial cells and periendothelial support cells in both control and treated CL. Arrows point to positive apoptotic nuclei assumed to be endothelial cells by their small, elongated form. The morphology of steroidogenic cells (SC) appears unaffected by treatment. (C) Quantification of positive cells in control (solid bar) and treated sections (open bar) shows increased presence of positive nuclei in anti-VEGF-treated sections. Note that values are per corpus luteum section so the incidence of apoptosis even after treatment is very low. Data are means ± S.E.M. Bar represents 20 μm.

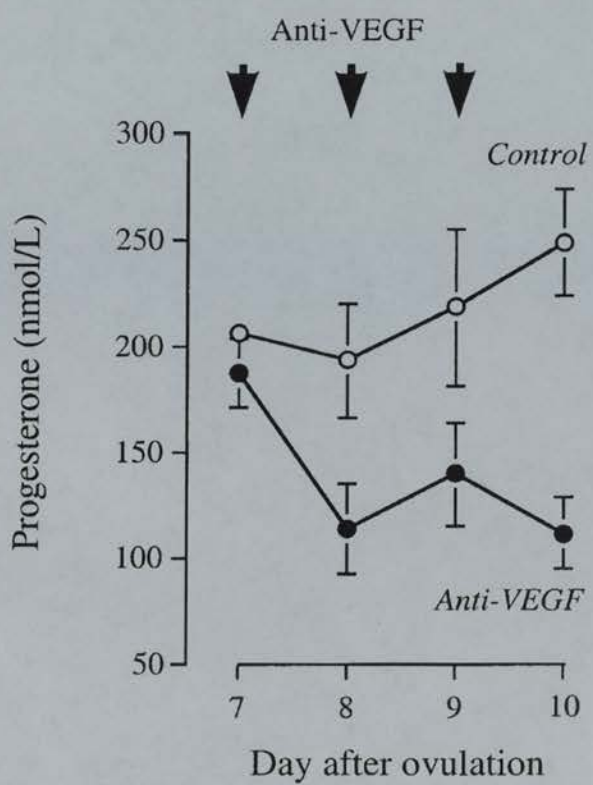

Figure 5 Plasma progesterone concentrations in control (○) and anti-VEGF-treated (●) marmosets. Treatment started on day 7 after ovulation and is associated with a significant suppression ($P=0{\cdot}01$). Data are means ± S.E.M.

at least during the first 1–2 days of treatment. The rapid decline in plasma progesterone concentration seen on the first day of this acute mid-luteal phase anti-VEGF treatment, indicates that in addition to the regulation of ongoing mid-luteal angiogenesis, VEGF also modulates vascular permeability in the CL. An effect on CL vascular permeability could deprive the lutein cells of both the necessary precursors for progesterone production and the efficient release of their products into the bloodstream, which would result in marked reductions in plasma progesterone values.

After anti-VEGF treatment, morphological changes in lutein steroidogenic cells were not apparent. This contrasts with observations on the characteristic effects of withdrawal of the trophic factor, luteinising hormone (LH), which have been described recently (Fraser *et al.* 1999*b*, Dickson & Fraser 2000), suggesting that anti-VEGF treatment does not markedly interfere with pituitary LH secretion.

In this study, we have also observed an increase in pericyte coverage as a result of VEGF withdrawal. Pericytes are believed to be involved in the remodelling process which occurs during blood vessel maturation (reviewed by Darland & D'Amore 1999), a process also thought to take place in the CL (Tsukada *et al.* 1996, Goede *et al.* 1998). Benjamin *et al.* (1999) demonstrated that in both xenografted tumour and primary human tumours, VEGF withdrawal resulted in specific obliteration of immature vessels and that in human prostate cancer loss of VEGF led to selective apoptosis of endothelial cells devoid of periendothelial cells. Mature vessels with associated pericytes are believed to be VEGF

independent (Benjamin *et al.* 1998). It is possible that, in the current study, the increase in apparent apoptosis in endothelial cells after anti-VEGF treatment is a consequence of a lack of VEGF support to susceptible, immature vessels with no associated pericytes. It could follow, therefore, that endothelial cells of more mature vessels with associated pericytes would be VEGF independent and not susceptible to anti-VEGF treatment. Our finding that mid-luteal VEGF withdrawal led to an increase in endothelial cell apoptosis, the occurrence of which was rare, in the presence of extended pericyte coverage suggests that it is the endothelial cells associated with the few remaining immature capillaries which were susceptible to loss of VEGF support. This, in turn, indicates that the reduction in endothelial cell area after anti-VEGF treatment may be a consequence not only of a decreased angiogenic rate, but also of increased endothelial cell death.

Factors involved in the recruitment of pericytes include platelet-derived growth factor-B (reviewed in Darland & D'Amore 1999) and angiopoietin-1 (Davis *et al.* 1996, Maisonpierre *et al.* 1997, Koblizek *et al.* 1998), while transforming growth factor β is thought to regulate pericyte differentiation (Hirschi *et al.* 1999). It remains to be determined whether factors such as angiopoietin-1 may be activated after VEGF inhibition to act as a survival mechanism to 'rescue' existing vessels from the absence of the immature endothelial cell survival factor, VEGF.

In conclusion, this study demonstrates that VEGF is a primary factor controlling angiogenesis and luteal function in the mid-luteal phase. The rapid decline in plasma progesterone after VEGF inhibition suggests that another function of VEGF at this stage may be in the maintenance of vascular permeability. In addition, the increase in endothelial cell apoptosis indicates a role for VEGF in the survival of a proportion of endothelial cells, perhaps those without associated periendothelial support cells. However, further investigation into the role of VEGF in pericyte recruitment is required to further elucidate the processes of blood vessel maturation in the CL. Since the mid-luteal phase is a crucial period in the establishment of early pregnancy and a time at which survival of the luteal vasculature may be important in the 'rescue' of the CL, manipulation of VEGF may have clinical importance with respect to, on the one hand, treatment of early pregnancy loss, and, on the other hand, interruption of pregnancy.

Acknowledgements

We thank the staff of our primate unit for animal care, M Millar and S MacPherson for expert support with histology, and P Hartley and I Swanston for progesterone RIAs.

References

Benjamin LE, Hemo I & Keshet E 1998 A plasticity window for blood vessels remodelling is defined by pericyte coverage of the preformed endothelial network and is regulated by PDGF-B and VEGF. *Development* **125** 1591–1598.

Benjamin LE, Golojanin D, Itin A, Pode D & Keshet E 1999 Selective ablation of immature blood vessels in established human tumors follows vascular endothelial growth factor withdrawal. *Journal of Clinical Investigation* **103** 159–165.

Darland DC & D'Amore PA 1999 Blood vessel maturation: vascular development comes of age. *Journal of Clinical Investigation* **103** 157–158.

Davis S, Aldrich TH, Jones PF, Acheson A, Compton DL, Jain V, Ryan TE, Bruno J, Radziejewski C, Maisonpierre PC & Yancopoulos GD 1996 Isolation of angiopoietin-1, a ligand for the TIE2 receptor, by secretion-trap expression cloning. *Cell* **87** 1161–1169.

Dickson SE & Fraser HM 2000 Inhibition of early luteal angiogenesis by gonadotropin-releasing hormone antagonist treatment in the primate. *Journal of Clinical Endocrinology and Metabolism* **85** 2339–2344.

Ferrara N, Chen H, Davis-Smyth T, Hans-Peter G, Nguyen T-N, Peers D, Chisholm V, Hillan K & Schwall R 1998 Vascular endothelial growth factor is essential for corpus luteum angiogenesis. *Nature Medicine* **4** 336–340.

Fraser HM, Lunn SF, Kim H & Erickson GF 1998 Insulin-like growth factor binding protein-3 (IGFBP-3) mRNA in the endothelial cells of the primate corpus luteum. *Human Reproduction* **13** 2180–2185.

Fraser HM, Dickson SE, Morris KD, Erickson GF & Lunn SF 1999*a* The effects of the angiogenesis inhibitor TNP-470 on luteal establishment and function in the primate. *Human Reproduction* **14** 2054–2060.

Fraser HM, Lunn SF, Harrison DJ & Kerr JB 1999*b* Luteal regression in the primate: different forms of cell death during natural and gonadotropin-releasing hormone antagonist or prostaglandin analogue-induced luteolysis. *Biology of Reproduction* **61** 1468–1479.

Fraser HM, Dickson SE, Lunn SF, Wulff C, Morris KD, Carroll V & Bicknell R 2000 Suppression of luteal angiogenesis in the primate by neutralization of vascular endothelial growth factor. *Endocrinology* **141** 995–1000.

Goede V, Schmidt T, Kimmina S, Kozian D & Augustin HG 1998 Analysis of blood vessel maturation processes during cyclic ovarian angiogenesis. *Laboratory Investigations* **78** 1385–1394.

Hirschi K, Rohovsky S, Beck L, Smith S & D'Amore P 1999 Endothelial cells modulate the proliferation of mural-cell precursors via platelet-derived growth factor-BB and heterotypic cell contact. *Circulation Research* **84** 298–305.

Jablonka-Shariff A, Grazul-Bilska AT, Redmer DA & Reynolds LP 1993 Growth and cellular proliferation of ovine corpora lutea throughout the estrous cycle. *Endocrinology* **133** 1871–1879.

Koblizek TI, Weiss C, Yancopoulos GD, Deutsch U & Risau W 1998 Angiopoietin-1 induces sprouting angiogenesis *in vitro*. *Current Biology* **8** 529–532.

Maisonpierre PC, Suri C, Jones PF, Bartunkova S, Wiegand SJ, Radziejewski C, Compton D, McLain J, Aldrich TH, Papadopoulos N, Daly TJ, Davis S, Sato TN & Yancopoulos GD 1997 Angiopoietin-2, a natural antagonist for Tie2 that disrupts *in vivo* angiogenesis. *Science* **277** 55–60.

Otani N, Sawako M, Yamoto M, Shikone T, Otani H, Nishiyama R, Otani T & Nakano R 1999 The vascular endothelial growth factor/*fms*-like tyrosine kinase system in human ovary during the menstrual cycle and early pregnancy. *Journal of Clinical Endocrinology and Metabolism* **84** 3845–3851.

Rodger FE, Young FM, Fraser HM & Illingworth PJ 1997 Endothelial cell proliferation follows the mid-cycle luteinizing hormone surge, but not human chorionic gonadotrophin rescue, in the human corpus luteum. *Human Reproduction* **12** 1723–1729.

Sharpe RM, Atanassova N, McKinnell C, Parte P, Turner KJ, Fisher JS, Kerr JB, Groome NP, MacPherson S, Millar MR & Saunders PTK 1998 Abnormalities in functional development of the Sertoli cells in rats treated neonatally with diethylstilbestrol: a role for estrogens in Sertoli cell development. *Biology of Reproduction* **59** 1084–1094.

Smith KB, Lunn SF & Fraser HM 1990 Inhibin secretion during the ovulatory cycle and pregnancy in the common marmoset monkey. *Journal of Endocrinology* **126** 489–495.

Summers PM, Wennink J & Hodges JK 1985 Cloprostenol-induced luteolysis in the marmoset monkey (*Callithrix jacchus*). *Journal of Reproduction and Fertility* **73** 133–138.

Tsukada K, Matsushima T & Yamanaka N 1996 Neovascularization of the corpus luteum of rats during the estrous cycle. *Pathology International* **46** 408–416.

Young FM, Illingworth PJ, Lunn SF, Harrison DJ & Fraser HM 1997 Cell death during luteal regression in the marmoset monkey *(Callithrix jacchus)*. *Journal of Reproduction and Fertility* **111** 109–119.

Received 16 October 2000
Accepted 10 November 2000